An investigation into expression of hydrogen sulfide synthesising enzymes in placentas from normal and complicated pregnancies

Fatema Saleh

M.B.Ch.B, MSc.

Submitted in fulfilment of the requirements for the Degree of

Doctor of Philosophy (PhD)

in

Medical Genetics

School of Medicine

College of Medical, Veterinary and Life Science

University of Glasgow

January 2022

Abstract

Hydrogen sulfide (H_2S) has recently attracted substantial interest as an endogenous gaseous signalling molecule. Like nitric oxide (NO) and carbon monoxide (CO), it promotes vasodilation and exhibits cytoprotective and anti-inflammatory properties. It is involved in diverse physiological and pathophysiological processes such as neurogenesis, regulation of blood pressure, atherosclerosis and inflammation. Endogenous H_2S is synthesised predominantly by three enzymes: cystathionine β-synthase (CBS), cystathionine γ-lyase (CSE) and 3-mercaptopyruvate sulfurtransferase (3-MST). Recently, the endogenous production of H_2S in human myometrium and placental tissues and its role in pathophysiology of complicated pregnancies with pre-eclampsia (PE) and fetal growth restriction (FGR) has been studied. In PE, inadequate remodelling of spiral arteries by trophoblasts causes ischemia-reperfusion insult of the placenta which is one source for oxidative stress, and it causes reductions in utero-placental blood flow, often resulting in FGR.

The limited research undertaken to study expression of H_2S synthesising enzymes in anormal and abnormal placental tissues is characterised by contradictory findings in mRNA and protein expressions of these enzymes. All studies used a random placental sampling method which could mask spatial variation in gene expression. Therefore, this study aimed to examine expression of these enzymes using a systematic sampling method in which placental samples were taken from different identified zones of each placenta. The expression of these enzymes was studied at both mRNA and protein levels using quantitative polymerase chain reaction (qPCR) and western blotting techniques. Extensive testing of several anti-CBS and CSE antibodies for western blotting revealed persistent non-specific binding of these antibodies to multiple unidentified proteins in all sample types. Antibodies tested included all those used in the previous studies in western blotting and *in situ* methods. These all showed highly images of CBS and CSE bands and lacked any supplementary data about testing antibodies specificity raising concerns about the previous research findings and identifying another potential source of the lack of consistency in conclusions they reached. CRISPR knockout clones of each protein were generated using two different cell lines to test specificity of these antibodies which confirmed the antibodies did detect proteins of the expected size. This enabled identification the correct CBS and CSE bands to study the expression at protein level in the comparative groups. Additionally, these clones identified isoforms not predicted by gene databases, allowed retrospective specificity testing of *in situ*

procedures used and revealed an intriguing regulation of CBS, CSE by 3-MST which may be of relevance to placenta.

CBS, CSE and 3-MST spatial expressions were examined in normal placentas obtained from women who delivered by caesarean section (CS) and were not in labour, in placentas from women who delivered spontaneously and in placentas from women with complicated pregnancies with PE, FGR and high body mass index (BMI). The study showed that there were significant spatial differences in expression of CSE and 3-MST, with an up-regulation in labour when compared to non-labour group at a particular placental site. Also, the study showed a significant increase in 3-MST mRNA and protein abundances in FGR group compared to control healthy group at the outer placental site. Only CBS and CSE mRNA abundances were significantly increased in PE compared to healthy controls at inner and middle placental sites, respectively. The spatial difference in gene expression in labour or complicated pregnancies at precise zones suggests that there is a controlled spatial change in expression or susceptibility to change which may be due to the vascular biology of the placenta. The physiological and pathological significances of these differences remain to be elucidated but oxidative stress and inflammatory pathway are the common links. Also, the reduction in CBS and CSE protein abundances in absence of 3-MST may suggest that there is a complex of regulatory mechanisms on these enzymes. Taken together, these results suggest that H_2S involves in labour and pathophysiology of PE and FGR. However, further investigations with highly specific antibodies are required especially the data in this study showed significant differences in expression between controls and the targeted groups.

To conclude, the present study highlights the possibility that ordinary placental sampling methods may mask the altered expression of some genes, and therefore, this study represent a further step toward developing a systematic way for sampling in placental research. In addition to this, the present study illustrates how using simple CRISPR knockout technology could help testing specificity of primary antibodies, and presents a real example of how incomplete reporting of antibodies research antibodies compromise the reducibility of research results. Furthermore, it emphasises on full documentation of the experimental procedure describing the data supporting the specificity of antibodies validation to help researchers to collaborate and build on each other's work.

Table of Contents

List of Tables

List of Figures

List of Publications

This work presented in this thesis has resulted in the following poster presentations:

1- Evaluation of the Spatial Regulation of Hydrogen Sulphide Producing Enzymes in the Placenta during Labour presented at ICOG 2017: 19th International Conference on Obstetrics and Gynaecology, February-2017, London, UK.

2- Hydrogen sulphide producing enzymes expression is altered in pre-eclamptic placenta presented at RCOG Annual Academic Meeting, February-2018, London, UK.

Dedication

I would like to dedicate this work to my lovely parents, who supported me throughout my life and studies. This work is also dedicated to my supportive husband, for the encouragement, great patience and understanding, and to my lovely children who gave me the strength and motivation to strive further. I also dedicate this work to my father-in-law, who supported and encouraged me throughout my PhD years.

Acknowledgement

I would like to express my deepest appreciation to my principal supervisor, Dr Andrew Hamilton, who has given me endless support and encouragement. Completion of this work would not have been possible without his suggestions, constrictive criticisms and insightful feedback in addition to his tireless efforts. I would also like to thank my co-supervisor, professor Gordon Ramage, for his support and constrictive advice to improve my work.

I would like to thank, professor Fiona Lyall, for her work in planning the original project and giving me the opportunity to undertake it.

Additional thanks must go to Clare Orange, who prepared the tissue slides and gave some advice regarding staining. I am also very grateful to Jennifer Hay, who patiently scanned hundreds of slides into Slidepath for me to analyse. I am also thankful to Dr Joanne Edwards for teaching me the weighted histoscore method to assess the staining intensity for my slides. I would also like to thank Dr Maribel Verdesoto for teaching me the RT-PCR technique and for her support and friendship.

Deepest thanks are also due to the lab staff in the department of human nutrition at the Royal infirmary, Glasgow for being keen to help always. Special thanks to Graeme Fyffe and Frances Cousins for teaching me IHC technique and for their willingness to help.

I would like to thank the University of Glasgow staff for all the support and help throughout my PhD journey.

A very special thank you goes out to the Ministry of Libya Higher Education and the Libyan Cultural Affairs Bureau for their financial support.

Last but not least, I would like to thank my husband, children and my family in Libya for their understanding, encouragement, endless love, support and patience.

Author's Declaration

I hereby declare that all the work presented in this thesis, unless otherwise indicated, is entirely my own contribution and has not submitted for any other degree at the University of Glasgow or any other institution.

Fatema Saleh

January, 2022.

Definitions/Abbreviations

AdoMet	S-adenosyl-methionine
ANOVA	Analysis of variance
ATF4	Activating transcription factor
ATP	Adenosine triphosphate
β-ME	Beta-Mercaptoethanol
BMI	Body mass index
bp	Base pairs
BSA	Bovine serum albumin
cAMP/PKA	Cyclic adenosine 3′,5′-monophosphate /protein kinase A
Cas	CRISPR-associated nucleases
CAT	Cysteine aminotransferase
CBS	Cystathionine β-synthase
CBSL	Cystathionine β-synthase like
cDNA	Complementary deoxy-ribonucleic acid
CEMACH	The confidential enquiry into maternal and child health
cGMP	Cyclic guanosine monophosphate
CHI	Cycloheximide
CO	Carbon monoxide
CO_2	Carbon dioxide
CRH	Corticotrophin-releasing hormone
CRISPR	Clustered Regulatory Interspaced Short Palindromic Repeats
crRNA	CRISPR RNA
CS	Caesarean section
CSE	Cystathionine γ-lyase
CTH	Cystathionine γ-lyase
C_T	Threshold cycle
CV	Coefficient of variation
DAB	3,3'-Diaminobenzidine Tetrahydrchloride
DAM	Donkey anti-mouse
DAPI	4′,6-diamidino-2-phenylindole
DAR	Donkey anti-rabbit
DNA	Deoxyribonucleic acid
DSBs	Double-stranded breaks
EDTA	Ethylenediaminetetraacetic acid
EGF	Epidermal growth factor
ELC/S	Elective caesarean section
ELISA	Enzyme-linked immunosorbent assay
EMC/S	Emergency caesarean section
eNOS	Endothelial NOS
evCTB	Extravillous trophoblasts
FGR	Fetal growth restriction
g	Grams
GAM	Goat anti-mouse
GAR	Goat anti-rabbit
GC	Guanylyl cyclase
GTEx	Genotype-Tissue Expression
GTP	Guanosine triphosphate
HCG	Human chorionic gonadotropin
HCL	Hydrochloric acid
HDL	High density lipoprotein

HDR	Homology-directed repair
HO	Heme oxygenase
HO-1	Heme oxygenase-1
HO-2	Heme oxygenase-2
H_2O_2	Hydrogen peroxide
HPG	L-homopropargylglycine
hPGH	Human placenta growth hormone
hPL	Human placental lactogen
HRP	Horseradish peroxidase
H_2S	Hydrogen sulfide
ICE	Inference of CRISPR Editing
IF	Immunofluorescence
IgG	Immunoglobulin G
IHC	Immunohistochemistry
IL-6	Interleukin 6
IL-10	Interleukin 10
IL-1β	Interleukin 1 beta
INDELs	Insertions or deletions
iNOS	Inducible NOS
IQR	Interquartile range
K_{ATP}	ATP-sensitive potassium channels
kDa	Kilo Dalton
KO	Knockout
LG	Labour group
LG-PE	Labour group-pre-eclampsia
LH	Luteinizing hormone
LPS	Lipopolysaccharides
MAPK	Mitogen activated protein kinase
Met	Methionine
μg	Microgram
mg	Milligram
mg/L	Milligrams per litre
miRNAs	MicroRNAs
μL	Microlitre
mL	Millilitre
mM	Mili-molar
mmHg	Millimetre of mercury
3MP	3-mercaptopyruvate
mRNA	Messenger ribonucleic acid
3-MST/MPST	3-mercaptopyruvate sulfurtransferase
MTCO1	Mitochondrion cytochrome C oxidase 1
MW	Molecular weight
$NaHCO_3$	Sodium hydrogen carbonate
NaHS	Sodium hydrosulfide
NaOH	Sodium hydroxide
NCBI	The National Centre for Biotechnology Information

ng	Nanogram
NGS	Next-Generation Sequencing
NHEJ	Non-homologus end joining
NLG	Non-labour group
NLG-PE	Non-labour group Pre-eclampsia
NO	Nitric oxide
NTC	No-template control
ORFs	Open reading frames
PAM	Protospacer adjacent motif
PBS	Phosphate buffer saline
PE	Pre-eclampsia
PG	Primigravida
PGH	Placental growth hormone
PlGF	Placental growth factor
PLP	Pyridoxal 5' phosphate
PO_2	Partial pressure of oxygen
PROM	Premature rupture of the membranes
PSCB-puro	Plasmid encoding puromycin resistance
RNA	Ribonucleic acid
ROS	Reactive oxygen species
RT	Reverse transcription
RT-PCR	Real time-polymerase chain reaction
SDS-PAGE	Sodium deodecyl sulfate polyacrylamide gel electrophoresis
sEng	Soluble endoglin
sFlt-1	Soluble fms-like tyrosine kinase receptor-1
sgRNA	Single guide RNA
SMCs	Smooth muscle cells
Sp1	Specificity protein 1
STD	Stock standard solution
SUMO	Small ubiquitin-like modifier
SUMO-1	Small ubiquitin-like modifier-1 protein
SVD	Spontaneous vaginal delivery
TBST	Tris buffer saline tween-20
TGF	Transforming growth factor
TNF-α	Tumour necrosis factor-α
tracrRNA	Trans-activating CRISPR RNA
UP-H_2O	Ultra-pure water
VEGF	Vascular endothelial growth factor
VTE	Venous thromboembolic
WHO	World Health Organisation
WT	Wild-type
Y	Years

Chapter 1   Introduction

There is a growing interest in H_2S as a biological signalling molecule: no longer a smell of the past but now a mediator of the future. It exhibits properties similar to other mediators such as NO and CO and plays important regulatory roles in many organs, cells and tissues as vasodilator, antioxidant and anti-inflammatory. H_2S is synthesised enzymatically through the transsulfuration pathway, and these enzymes are widely distributed in tissues. The endogenous production of H_2S in human myometrium and placental tissues and its role in pathophysiology of complicated pregnancies has recently been gaining attention in placenta research. This thesis provides an overview of placental vascular differentiation and oxidative stress under physiological or pathological conditions, and broadly investigates expression of H_2S synthesising enzymes in normal and abnormal placental tissues, as well as discusses the H_2S synthesis and biological effects.

1.1 Placenta

1.1.1 Overview of the placenta

The placenta is a vital organ that connects the developing fetus to the uterine wall to ensure nutrient uptake, waste removal, and gas exchange between the maternal and fetal circulatory systems. It undergoes rapid growth, differentiation, and maturation. In early pregnancy, the trophoblast cells are essential for implantation and interacting with the maternal uterine environment in order to regulate sufficient blood supply to the implantation site and prevent immune rejection of the semi-allogeneic fetus (Gude et al., 2004). As the pregnancy continues, trophoblast cells develop specialised functions to allow adequate nutrients to be transported to the fetus, as well as to allow disposal of products from it.

Macroscopically, term placenta is a discoid organ in about 90% of cases. Around 10% of cases, however, have abnormal shaped placentas such as placenta succenturiata and placenta membranacea (Benirschke et al., 2012a). Term placenta is about 15 to 20 cm in diameter, and the thickness is around 3 cm at the centre. It weighs on average 500g (Burton et al., 2012). The considerable individual variation in these measurements depends on several factors such as mode of delivery, time of cord clamping and the time between delivery and examination (Bouw et al., 1976).

The placenta consists of two plates or surfaces: the basal plate or the maternal surface that binds the maternal endometrium and the chorionic plate or the fetal surface to which the umbilical cord is attached (Figure 1-1). The maternal surface of the placenta usually appears to have several divisions. This results from degenerative processes that led to separation of the organ from the uterine wall. The fetal surface, facing the amniotic cavity, is glossy in appearance, because of the intact epithelial surface of the amnion. It contains the chorionic vessels that branch out over the placenta and form a star-like pattern network (Benirschke et al., 2012a). The space between the two plates is filled with maternal blood from the endometrial spiral arteries through openings in the basal plate. The placenta is divided by septa created by invagination of the basal plate into 10 to 40 cotyledons (Burton et al., 2012). Each cotyledon is supplied by branches of the umbilical circulation. The umbilical cord is approximately 55-60 cm in length and inserts centrically in most placentas into the chorionic plate. It contains two arteries and one vein (Rampersad et al., 2011). It is usually inserted near the centre of the placenta as a result of the blastocyst orientation during time of implantation.
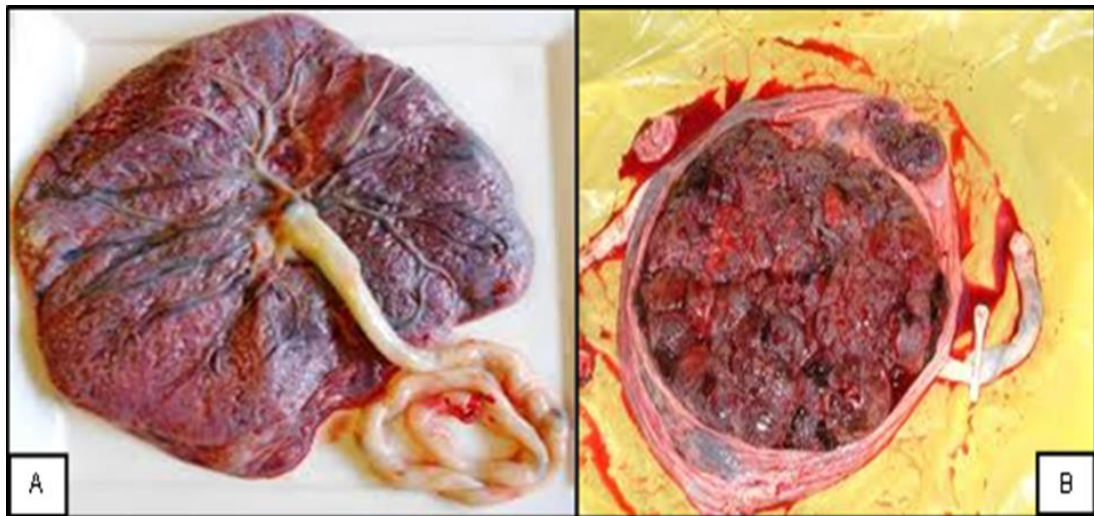
Figure 1-1 The term human placenta. (A) The fetal side of the placenta. The umbilical cord inserts within the chorionic plate. (B) The maternal side which is in contact with uterus and divided into cotyledons. (An original image).

The functional units of the placenta are the chorionic villi within which fetal blood is separated from maternal blood in the surrounding intervillous space by three or four cell layers (placental membrane) (Gude et al., 2004). The fetal component of the placenta comprises a series of elaborately branched villous trees that arise from the inner surface of the chorionic plate and project into the cavity of the placenta. Each villous tree originates from a single-stem villus that undergoes several generations of branching until the functional units of the placenta, the terminal villi, are formed. These villi consist of an epithelial

covering of trophoblast, and a mesodermal core containing branches of the umbilical arteries and tributaries of the umbilical vein (Figure 1-2). The repeated branching of the villous tree results in lobule formation within the placental lobe, and there may be two to three within a single placental lobe (Burton et al., 2012).
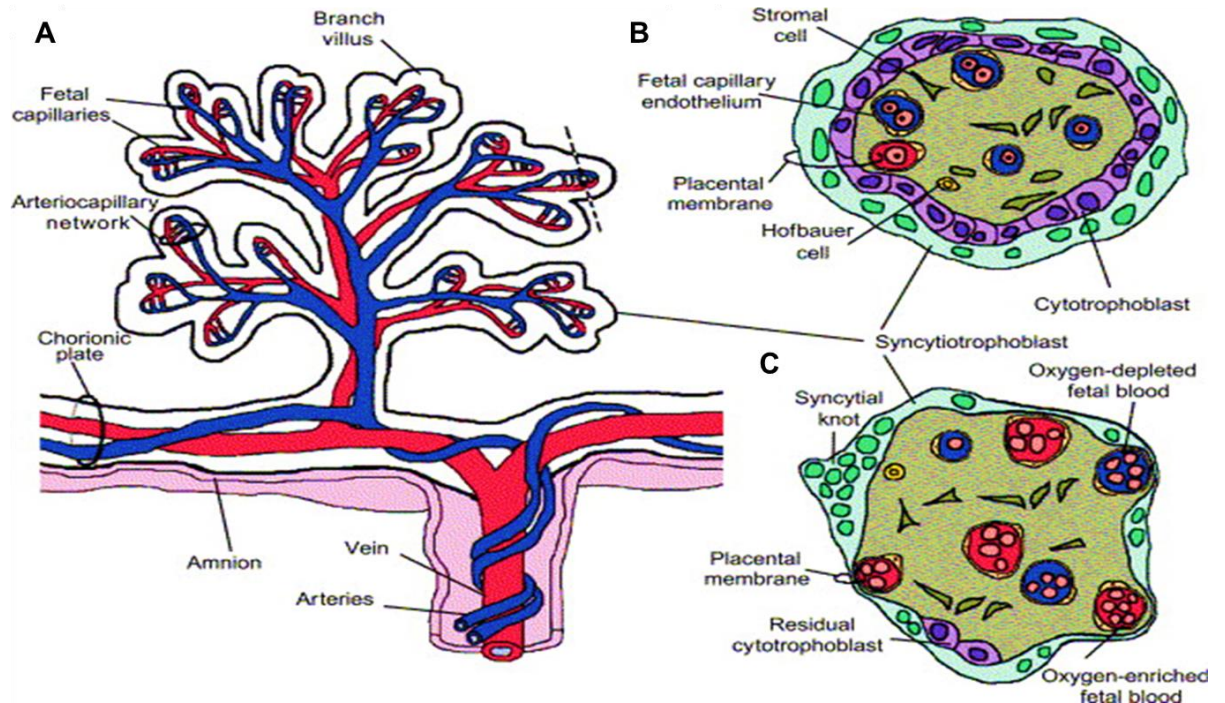
Figure 1-2 The structure of the mature placenta. (A) The fetoplacental circulation. (B) The structure of chorionic villous at 10 weeks. (C) The structure of chorionic villous at full term. The Image modified from Gude et al. (2004).

1.1.2 Development of the placenta

In order to understand the morphological features of the placenta, it is crucial to understand the organ's development. Also, any aberration in the development process may result in complications throughout the pregnancy. The placental development is initiated at the implantation time, when the embryonic pole of the blastocyst establishes contact with the uterine epithelium (Lindhard et al., 2002). After fertilisation of the ovum, it enters the uterine cavity as a morula which rapidly sheds its surrounding zona pellucida and becomes the blastocyst. Implantation of the blastocyst is the key step for the pregnancy to become established. Apposition of the blastocyst, which is the ability of the blastocyst to adhere to the epithelium, is the first step in the implantation, followed by an adhesion step. The apposition of the blastocyst depends on the interaction between receptors on the blastocyst and cell surface receptors at the site of implantation (Lindhard et al., 2002). This interaction is mediated by growth factors, cytokines and adhesion molecules, which are secreted by the blastocyst and the endometrium (Lindhard et al., 2002). The cells in the outer layer of the

blastocyst then proliferate to form the primary trophoblastic cell mass. From this mass, cells infiltrate between those of the endometrial epithelium which in turn degenerates and the trophoblast thus comes into direct contact with the endometrial stroma. This process is called implantation and is complete by the day10 or 11 post conception. An asymmetric group of cells within the blastocyst forms the inner cell mass that develops into fetus and umbilical cord (Benirschke et al., 2012b).

The epithelium of the blastocyst known as trophectoderm is responsible for evolution of the human placenta (Pijnenborg et al., 1980). Differentiation of trophectoderm results in formation of multiple trophoblast cell lines (primary trophoblastic mass) each with different biological activities. In the 6-7th day post-conception the trophoblast forms a peripheral plaque that rapidly differentiates into two layers, an inner layer of cytotrophoblast cells and an outer layer of syncytiotrophoblast cells that begins to penetrate between the endometrial cells. Trophoblastic differentiation into two major cell lines, the syncytiotrophoblast and the invasive trophoblast continues up to the end of the pregnancy (Irving et al., 1995). The syncytiotrophoblast of the chorionic villi is responsible for placental nutrient and gas exchange. It is also responsible for most placental hormones and growth factors production. The second cell line (extravillous) is the invasive pathway which can be defined as interstitial or endovascular trophoblast phenotypes. Post-conception between 10-13 days, a series of intercommunicating clefts, or lacunae, appear in the rapidly enlarging trophoblastic cell mass; these formed due to engulfment of the endometrial capillaries within the trophoblasts. The lacunae soon become a precursor of the intervillous space, and as the maternal vessels are progressively eroded this space becomes filled with maternal blood (Burton et al., 2012).

1.1.3 Development of villus tree

One of the main functions of the placenta is diffusional exchange. The exchange is proportional to the surface area achieved by repeated branching of the villous trees. The villi are tree-like structures formed of outgrowths of trophoblast, proliferating into the intervillous space through process of remodeling and lateral branching. Initially, the primary villi contain an outer layer of multinucleated syncytiotrophoblast and a layer of mononucleated cytotrophoblast. Secondary villi contain also mesenchyme in the core. When the secondary villi are penetrated by fetal vessels, the tertiary villi, mesenchymal villi, are formed (Rampersad et al., 2011). Toward the end of the first trimester the villi begin to differentiate into their principal types. The connections to the chorionic plate become remodeled to form the stem villi, which represent the supporting framework of each villous

tree. These stem villi contain few capillaries so play a little role in placental exchange. After several generations of branching, stem villi give rise to the immature and mature intermediate villi. The mature intermediate villi provide a distributing framework, and terminal villi arise at intervals from their surface. The core of these villi contains arterioles and venules, as well as a significant number of capillaries, allowing a large capacity for exchange (Burton et al., 2012).

1.1.4 Placental blood circulation

The placenta which is a unique vascular organ receives blood supplies from both maternal and fetal circulatory systems. The placental blood flow has two directions; from mother to the placenta (maternal-placental or utero-placental circulation) and from the placenta to the fetus (fetal-placental or fetoplacental circulation (Wang and Zhao, 2010).

1.1.4.1 Utero-placental circulation

Utero-placental circulation begins when the endovascular trophoblasts migrate along the decidual spiral arteries, invade the vessel walls, and form trophoblastic plugs. These trophoblastic plugs obstruct maternal blood flow into the intervillous space and prevent flow until the end of first trimester of pregnancy (10-12 weeks) (Pijnenborg, 1994). Therefore, the maternal-placental circulation is not fully established until the end of the first trimester. The plugs then loosen and permit continuous maternal blood flow into the intervillous space. The maternal blood enters the placenta through the endometrial arteries (spiral arteries) (Figure 1-3), perfuses intervillous spaces, and flows around the villi where exchange of oxygen and nutrients occurs with fetal blood (Wang and Zhao, 2010). The maternal blood then returns to the maternal systemic circulation through the uterine veins (endometrial veins).

1.1.4.2 Fetoplacental circulation

The umbilical cord is the lifeline that connects the fetus to the placenta. It contains one umbilical vein and two umbilical arteries. The umbilical vein carries oxygenated and nutrient-rich blood from the placenta to the fetus, while the umbilical arteries carry deoxygenated blood from the fetus to the placenta (Figure 1-3). Any impairment in the umbilical blood flow results in fetal hypoxia and serious complications. The umbilical vessels branch to form chorionic vessels at the junction of the umbilical cord and the

placenta, and cross the fetal surface of the placenta. In the chorionic plate, the umbilical vessels branch further before they enter into the villi. The umbilical and the chorionic vessels are sensitive to vasodilators, such as angiotensin II and they produce several vasodilators. It has been reported that the endothelium from umbilical vein produce more prostaglandins than the endothelium from the umbilical arteries (Wang and Zhao, 2010). About two thirds of the chorionic vessels form branching networks that supply the cotyledons (fetal capillaries) and the rest of them radiate to the edge of the placenta and down to a network (arteriocapillary venous network or villous capillaries) (Figure 1-3). The villous capillaries are the functional unit of the maternal-fetal exchange. They bring the fetal blood extremely close to the maternal blood but no intermixing between fetal and maternal blood occurs.
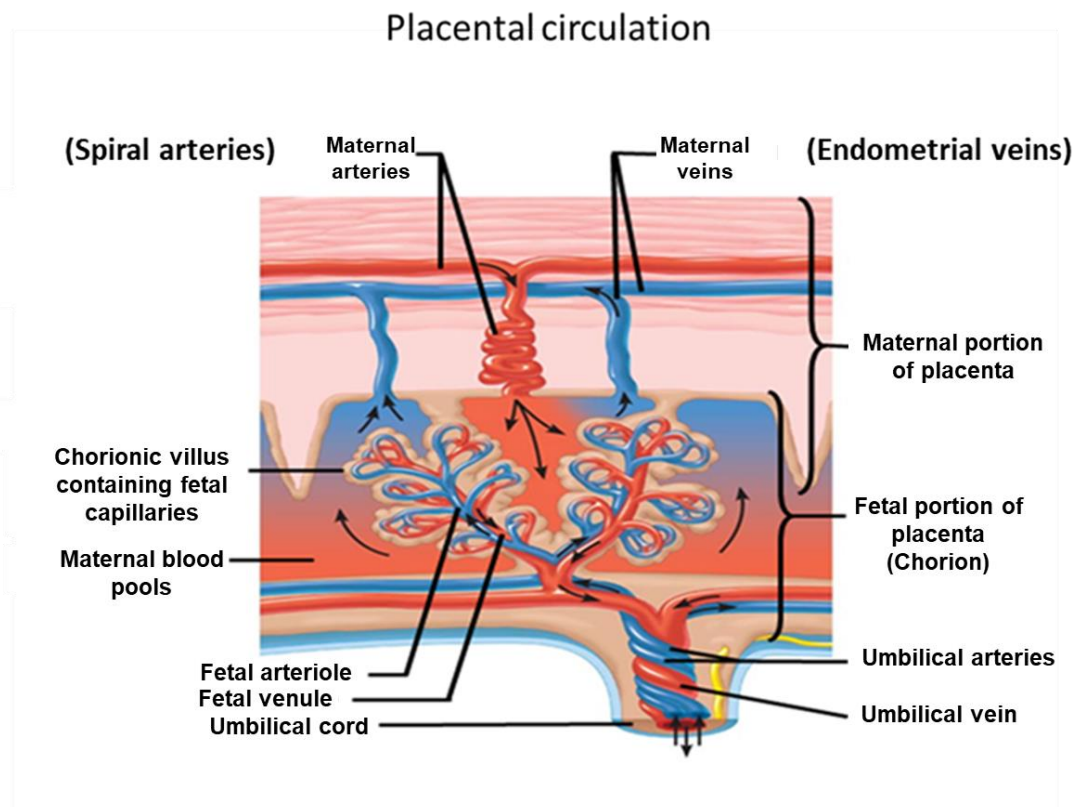
Figure 1-3 Schematic diagram of placental circulation showing fetal and maternal portions of the placenta. The arrows indicate the direction of the blood flow. The red colour means oxygenated blood and the blue colour means deoxygenated blood. The image modified from Murthi et al. (2014).

The blood pressure is about 80–100 mmHg in uterine arteries, 70 mmHg in spiral arteries, and only 10 mmHg within intervillous space. The blood pressure in the umbilical arteries is about 50 mmHg, and it falls to 30 mmHg in the capillaries in the villi. In the umbilical vein the pressure is 20 mmHg. The pressure in the fetal vessels and their villous branches is always greater than that within the intervillous space. This protects the fetal vessels against collapse. Also, the low-resistance of utero-placental vessels and the gradient of blood

pressure between uterine arteries and placental intervillous space allow the maternal blood to perfuse the intervillous space efficiently and effectively. The blood in the intervillous space is therefore completely exchanged two to three times per minute. In general, the spiral arteries are perpendicular to the uterine wall, while the veins are parallel to the uterine wall. This arrangement facilitates closure of the veins during uterine contractions and prevents squeezing of maternal blood from the intervillous space (Wang and Zhao, 2010).

1.1.5 Extravillous trophoblast invasion and the physiological conversion of the spiral arteries

Early in pregnancy cytotrophoblasts begin to proliferate and form cell columns. From these cell columns a subpopulation of trophoblastic cells migrates from the deep surface of the cytotrophoblast shell into the endometrium. These cells are referred to as extravillous trophoblasts (evCTB) because they do not take part in the development of the definitive placenta. Their activities are, however, fundamental to the successful functioning of the placenta, for their presence in the endometrium which is associated with the physiological conversion of the maternal spiral arteries (Burton et al., 2012). From the extravillous trophoblasts the endovascular and interstitial invasive trophoblasts are derived. The interstitial invasive trophoblast migrates through and invades the uterine tissue and anchors the placenta to the uterus, then penetrates the maternal vasculature forming the placenta bed and surrounding the spiral arteries. The endovascular invasive trophoblast migrates to the lumen of maternal uterine spiral arteries (Pijnenborg, 1994). This process is regulated by various cell types including decidua and trophoblast cells, and other diffusible factors such as NO and CO produced by interstitial trophoblasts (Lyall, 2006). It has been estimated that at term there are about 120 spiral arterial entries into the intervillous space (Cunningham et al., 2005)

In the uterine spiral arteries, the trophoblast displaces and replaces the endothelial cell lining and plays a role in the degradation of the muscle and elastic coat which normally maintain the vessel integrity. This process of loosening of the maternal spiral artery, termed conversion, forms a vessel of high capacitance and low resistance in order to meet the demands for sufficient blood flow to the placenta as the pregnancy progresses. This must occur by the end of the first trimester for a healthy pregnancy to continue (Lyall and Belfort, 2007). This process involves mainly the spiral arteries in the centre of the placental bed. The density of the spiral artery invasion decreases towards the placenta margin (Meekins et al., 1994).

Since maternal blood flow through these vessels is limited by the plugs of endovascular trophoblast in early gestation, development of human placenta during the first ten weeks of gestation occurs in a low oxygen environment with a PO_2 measured at <15 mmHg (Rodesch et al., 1992). This low oxygen state alters after 10 weeks' gestation so that the developing villous tree of the chorioallantoic placenta becomes bathed with oxygenated maternal blood from the modified spiral arteries, raising the PO_2 to about 60 mmHg (Jauniaux et al., 2000).

Matijevic et al. (1995) assessed the resistance to blood flow through spiral arteries in the central and peripheral areas of the placental bed to determine if *in vivo* findings are in concordance with histologic observations of cytotrophoblast invasion. They used pulsed Doppler imaging in pregnant women with normal singleton pregnancies at 17-20 weeks. Spiral arteries were visualised in the central and peripheral parts of the placental bed, and blood flow was analysed to calculate the resistance index and the pulsatility index. Matijevic et al. (1995) found that both indices were significantly lower in the centre compared with the periphery. There was no significant difference in the peak systolic velocities between the two areas. Moreover, the analysis showed no significant differences in both indices at the different weeks of gestation in the central and peripheral areas of the placental bed.

The physiological change continues to fade toward the periphery of the placental bed at term, although some arteries in this area undergo physiological transformation. However, any change in the peripheral spiral arteries is likely to be restricted to the decidual segments. Therefore, the histologic data suggest a possible lag phase in which peripheral vessels undergo a restricted physiologic change later than central ones. This is reflected by the significantly higher indices values in the periphery of the placenta compared to the centre. Any continued physiological change in the periphery between 17-20 weeks does not appear to have an important functional effect in decreasing resistance to blood flow.

1.1.6 Defects in extravillous trophoblast invasion

Defects in extravillous trophoblast invasion and failure to establish the maternal circulation correctly, leading to abnormal placental function, are associated with severe pregnancy complications such as preterm birth, FGR and PE. Absence of endovascular trophoblast invasion of myometrial segments of the spiral arteries, characteristic of FGR, results in a high resistance vasculature with persistent smooth muscle histology in the maternal spiral arteries. This lack of transformation predisposes to hypoperfusion, hypoxia, re-perfusion

injury, oxidative stress and, ultimately, to signs of villous tree mal-development in the second half of the pregnancy, all factors associated with FGR (Scifres and Nelson, 2009).

1.1.7 Functions of the placenta

The placenta is a specialised organ that supports the development of the fetus and maintenance of pregnancy. Its functions include nutrition, excretion, immunity and endocrine functions. The perfusion of the intervillous spaces with maternal blood permits the nutrients and oxygen to be transferred from the mother to the fetus, and also allows waste products such as urea, creatinine and carbon dioxide transfer from the fetus to the maternal blood supply. Transfer of nutrient to the fetus occurs via both passive and active transport (Illsley, 2011). Significantly different plasma concentrations of various large molecules are maintained on the maternal and fetal sides of the placental barrier by active transport systems. Adverse pregnancy conditions, such as those involving maternal diabetes or obesity, can cause a rise or decline in levels of nutrient transporters in the placenta, resulting in overgrowth or restricted growth of the fetus.

The placenta also provides protection to the fetus *in utero*. Immunoglobulin G (IgG) antibodies can pass through the placenta, thereby providing protection to the fetus. Transfer of antibodies usually begins as early as the 20th week of gestational age. This passive immunity remains for several months after birth to provide a newborn with a copy of the mother's long-term humoral immunity. Furthermore, the placenta functions as a selective maternal-fetal barrier against transmission of microbes. However, inadequacy in this function may still cause mother-to-child transmission of infectious diseases (Gude et al., 2004).

The placenta is also secretory organ. The syncytial layer of chorionic villi secrets hormones that are important during pregnancy. These include human chorionic gonadotropin (hCG), human placental lactogen (hPL), estrogen, progesterone, human placental growth hormone. The placenta moreover produces oxytocin, inhibin, corticotrophin-releasing hormone (CRH), and prolactin. Many growth factors that promote uterine blood flow and placental development such as vascular endothelial growth factor (VEGF), placental growth factor (PlGF), epidermal growth factor (EGF), and transforming growth factor (TGF) are produced by placenta (McNamara and Kay, 2011).

1.1.8 Oxidative stress in the placenta

It is essential to consider the oxidative stress in the placenta because this helps understand the role of protective pathways mediated via some gaseous molecules. These molecules and their effects will be discussed later in this chapter. Oxidative stress occurs when there is an imbalance in production of reactive oxygen species (ROS) and the ability of the antioxidant defences (Myatt and Cui, 2004). Burton and Jauniaux (2011) define the oxidative stress as "an alteration in the pro-oxidant-antioxidant balance in favour of the former that leads to potential damage". That means the disturbance could happen due to changes on either side of the equilibrium whether an increase in the production of ROS and/or a decrease in the antioxidant capacity (Myatt and Cui, 2004). It may induce a range of cellular responses depending upon the severity of the insult and the compartment in which ROS are generated (Roberts and Hubel, 2009, Burton and Jauniaux, 2011).

The ROS free radicals and non-radical intermediates cause cellular damage by acting on proteins and lipids (Myatt and Cui, 2004). The superoxide anion is the most common oxygen free radical, generated under physiological and pathological conditions. Paradoxically, it is also increased under conditions of hypoxia (Boveris, 1984). There are enzymatic defences against the oxidant attack produced by the placenta including superoxide dismutase, catalase, glutathione and non-enzymatic (vitamins C and E) (Burton and Jauniaux, 2011). The ROS at the homeostatic levels have actions on cell functions including activation of protein kinases and redox-sensitive transcription factor, and have pathological effects on lipid peroxidation, opening of ion channels, DNA oxidation and proteins modification (Burton and Jauniaux, 2011).

Pregnancy itself is a state of oxidative stress where there is an increase in the metabolic activity in placental mitochondria, resulting in production of ROS, mainly superoxide anions. At the same time, there is a reduction in the antioxidant capacity. The placenta also produces other ROS such as NO, CO and peroxynitrite that have effects on placental function including vascular reactivity and proliferation and differentiation of trophoblast. Excessive production of ROS may occur at a certain time during placental development in complicated pregnancies, such as PE and FGR. Peroxynitrite is a powerful pro-oxidant which results from interaction of NO with the excessive superoxide and it has diverse deleterious effects including nitration of tyrosine residuals on proteins thus altering the function (Myatt and Cui, 2004). These well controlled ROS are involved in many essential cellular signalling pathways and induce the expression of physiologically necessary genes. At higher levels,

they can cause damage to biological molecules, resulting in loss of function and even cell death. On the other hand, the major antioxidant systems including the catalase, glutathione, vitamins C and E are present in the placenta (Myatt and Cui, 2004). Oxidative stress also plays a role in the pathophysiology of a whole host of disorders including complication of pregnancy such as miscarriage, PE, premature rupture of the amniotic membrane and FGR (Hempstock et al., 2003, Kokawa et al., 1998).

1.1.9 Sampling of the placenta

Placenta tissue samples may be used for various investigations regarding development of placenta, its biology and pathophysiology. Gene expression studies, that examine the pathophysiology of placental diseases, are one of these investigations and are fundamental to understand placental dysfunction because the identity of any genes/proteins whose expression is changed gives key insights into biochemical and physiological mechanisms underlying the pathological state. Burton and his colleagues in 2014 reported that there are some methodological factors that affect the quality of samples and determine the worth of a study design and for reliability and reducibility of research. Factors regarding collection, processing and storage of placental samples are crucial, and should be taken in account carefully in order to reflect the *in vivo* state and help compare datasets and obtain powerful statistical results. Numerous maternal factors such as age, ethnicity, parity and lifestyle and fetal sex can affect placental physiology, function and pathology (Burton et al., 2014).

Mode of delivery either vaginally or by CS may have an impact on the data obtained. During labour the placenta is subjected to potentially stressful conditions including mechanical compression caused by the uterine contractions and intermittent reduction in the maternal blood supply during contractions. These conditions influence the metabolic profile of the placenta, generation of oxidative and other stresses, gene transcription and activation of signalling pathways (Burton et al., 2014, Yung et al., 2014). Therefore, it would be ideal to conduct placental research on placental tissues delivered by CS whenever possible. Given the activation of stress response pathways, changes in gene expression might be expected as a result of labour. Therefore, standardisation of the collection procedure enables samples to be shared among research groups.

The time interval between delivery and a sample collection is another factor worth considering. Certainly, the placenta is exposed to a period of ischemia after its separation from the uterine wall and delivery. The volume of maternal blood entrapped within the

placenta after delivery has been estimated to meet metabolic requirements for 7-10 minutes as it contains sufficient oxygen but after that time hypoxemia occurs (Bloxam and Bobinski, 1984). Serkova et al. (2003) have concluded that the optimal window for collecting placental samples free from *ex-vivo* ischaemic artefacts is within 10 min after delivery.

Previous research about tissue sampling from the placenta (Mayhew, 2008) found that for placental samples to be worthwhile, they should be taken by an unbiased selection process based on random sampling. One valuable form of random sampling is systematic uniform random sampling in which the first item is chosen randomly, and then a pre-determined pattern decides the sites of other samples. Greater transparency in describing the sampling design used in a study is highly desirable since it will facilitate study repeatability and allow readers to judge better the validity of outcome measures and biomedical conclusions.

1.2 Labour

1.2.1 Definition

Labour is a physiological process through which the fetus, membrane, umbilical cord and placenta are expelled from the uterus. It is a distinctive event in the human (Smith 2007). Normal labour occurs between 37-42 weeks gestation. The duration of labour varies commonly; the first and second stage lasts for 9-18 hours in women giving birth to their first child and 6-13 hours for women who have previously given birth. There are three stages of labour. The first stage of labour begins when the effaced cervix is 3 cm dilated. The second stage begins when the cervix is fully dilated, ending when the baby is born. The period from just after the fetus is expelled until just after the placenta is expelled is called the third stage of labour, which lasts, on average, 10-12 minutes (Martin and Hutchon, 2004). Labour or parturition results from a complex interaction of maternal and fetal factors. A variety of endocrine systems play a role in the maintenance of uterine quiescence and the onset of labour, with its attendant increase in uterine contractility and cervical ripening (Cindrova-Davies et al., 2007).

1.2.2 Labour as an inflammatory response

Previous studies illustrated that inflammatory mediators like cytokines, resulting from infiltration of activated leucocytes into the cervix, placenta and myometrium during labour, participate in initiating the labour process. Recently, there has been considerable evidence

to support the view that during labour, two T- cell sets of memory like T cells such as CD3, CD4 and others were detected in the choriodecidua of term placenta delivered by normal labour (Gomez-Lopez et al., 2013). Many studies have recognised a role for prostaglandins and cytokines in the initiation and maintenance of the uterine contractions during labour (Lee et al., 2010).

1.2.3 Labour and the link with oxidative stress

The uterine contractions happening during labour cause compression of the uterine artery and the latter is associated with intermittent utero-placental perfusion. During oxytocin-induced contractions, a 50% reduction in flow into the intervillous space was found compared to when no contractions occurred. This intermittent perfusion could lead to an ischemia-reperfusion injury to the placenta (Brar et al., 1988). Previous studies demonstrated that during labour, there is an increase in oxygen consumption. Consequently, mitochondrial respiration is increased and electrons produced in the electron transport chain are lost, resulting in production of ROS (Díaz-Castro et al., 2015). Recently some studies have established, using Doppler ultrasound, that there is a linear inverse relationship between intensity of uterine contractions during labour and resistance of the uterine arteries (Brar et al., 1988, Cindrova-Davies et al., 2007).

Labour is also associated with placental alterations in several pathways linked to oxidative stress like inflammatory and apoptotic pathways (Cindrova-Davies et al., 2007). Oxidative stress is related with conversion of xanthine dehydrogenase to xanthine oxidase (XD/XO) a marker of ischemia-reperfusion injury, and the latter has been found to be increased in labouring placentas compared to the non-labouring ones (Many and Roberts, 1997). Additionally, during labour there is a reduction in tissue concentrations of Adenosine triphosphate (ATP), depletion of vitamin C in maternal blood and high glutathione levels in umbilical venous blood compared to the non-labour controls (Bloxam and Bobinski, 1984). The inflammatory response at parturition has been reported as a potent cause of the formation of ROS (Díaz-Castro et al., 2015). Numerous pro-inflammatory mediators including cytokines, interleukin-6 (IL-6) and prostaglandins are produced during labour, which cause formation of ROS and in turn these free radicals re-induce the inflammatory process in a positive feedback loop (Díaz-Castro et al., 2015, Fernandez-Sanchez et al., 2011).

1.2.4 Changes in gene expression in human placenta during labour

Labour is a complex biological process involving interactions of neurological, hormonal, mechanical stretching and inflammatory factors. The labour pain is one of the major causes of the stress perceived by women during labour. It has been shown that uterine contractions and labour pain cause physiological changes in gene expression in maternal and fetal blood, and in placenta during the process of labour (Peng et al., 2011). Cindrova-Davies et al. (2007) suggested that the healthy placenta is subjected to intermittent blood supply during labour, and based on this suggestion the impact of ischemia-reperfusion *in vivo* on placental gene expression and cytokine profile was assessed. They reported that, oxidative and inflammatory stress pathways are imposed by labour and delivery and cause alteration of placental gene expression. The haemodynamic effect of labour might induce many changes in placenta as well. Additionally, in placental tissues, labour increases the expression of genes involved in placental oxidative stress, inflammatory cytokines, angiogenic regulators and apoptosis. Although there is a close association between the placenta and labour, the pattern of gene expression in placenta and how this is influenced by labour or vice versa is complex, and the haemodynamic and endocrine effects of labour on placenta cannot be separated (Patel et al., 2009).

Lee et al. (2010) studied the differences in gene expression profiles of the placenta between women who underwent vaginal delivery and those who underwent elective CS. They performed a microarray analysis to identify the differentially expressed transcripts of genes that may participate in the onset and progression of labour. They found that there was diversity in the expression of 351 genes between the two groups. Also, they found that these genes involved 15 categories including genes involved in stress response, immune response and blood vessel development. These changes in gene expression are likely to be related to initiation of labour, and may have a causative role in labour onset.

1.3 Pre-eclampsia

1.3.1 Definition, epidemiology and clinical features

PE is a disease of pregnancy, affecting about 2-8% of all pregnant women worldwide (Hauth et al., 2000). It is a leading cause of maternal and fetal morbidity and mortality, especially

in developing countries. Hypertensive disorders account for 16% of all maternal deaths in developed countries, 9% of maternal deaths in Africa and Asia, and as many as 26% of maternal deaths in Latin America and the Caribbean (Khan et al., 2006). As a result of a lack of predictive biomarkers and effective pharmaceutical interventions, PE continues to be a serious obstetric complication. FGR and premature delivery are frequent consequences of PE (Tannetta and Sargent, 2013).

Clinically, PE is defined as a new onset of high blood pressure; systolic blood pressure ≥140 mmHg or diastolic blood pressure of ≥ 90 mmHg on at least two occasions 6 hours apart, and significant proteinuria ≥ 300 mg / 24 hours urine collection or two episodes of 1+ protein reading on a dipstick test after 20 weeks of gestation (Tranquilli et al., 2014). It presents as an early-onset PE which usually develops before 34 weeks of gestation or as late-onset which develops at or after 34 weeks of gestation. In terms of severity, late-onset PE is typically a mild to moderate disease with good maternal and perinatal outcomes, whereas an early-onset PE is more often severe with increased risks (Tannetta and Sargent, 2013). PE is frequently a recurrent disorder in subsequent pregnancies. The risk of recurrence is a 7-20% in a subsequent pregnancy (Hernández-Díaz et al., 2009). The risk is influenced by the gestational age of its onset, and increased if women have had two prior pregnancies with PE (Sibai et al., 1991).

Risk factors for PE are various. They are classified into pregnancy specific characteristics and maternal pre-existing conditions. Nulliparity is a strong risk factor. New paternity is also a risk factor and raises the risk in a subsequent pregnancy (Redman, 1991). Hydatidiform mole and multiple gestations are pregnancy related factors, suggesting increased placental mass plays some role (Sibai et al., 2000). Notably, classic cardiovascular risk factors including maternal age > 40 years, insulin resistance, obesity, a systemic inflammation, pre-existing hypertension, diabetes mellitus or renal disease are pre-existing maternal features (Duckitt and Harrington, 2005).

1.3.2 Maternal, fetal and neonatal effects

Maternal morbidity associated with severe PE includes renal failure, cardiac dysfunction, stroke, respiratory compromise, coagulation disorders and liver failure (Mattar and Sibai, 2000). Pregnant women with hypertensive disorders in pregnancy have an increased future risk of cardiovascular diseases and venous thromboembolism (van Walraven et al., 2003). Fetal and neonatal outcomes associated with PE vary around the world. Around 12-25% of

FGR and small-for-gestational-age infants as well as 15-20% of preterm births are outcomes of PE (Duley, 2009). In developing countries, one quarter of stillbirths and neonatal deaths are related to PE (Ngoc et al., 2006).

1.3.3 Pathogenesis of PE

Although the precise cause of PE is unknown, the placenta and maternal inflammatory response play a crucial role in its pathogenesis as discussed below. The placenta is considered to be a key to the pathogenesis of PE. This is shown by the effectiveness of delivery of the placenta in abating the symptoms, as well as the occurrence of this disease in molar pregnancies, indicating the requirement for the placenta and not the fetus for disease development (Powe et al., 2011).

1.3.3.1 Abnormal placentation in pathogenesis of PE

The placenta contains two circulations: fetal via the umbilical vessels and maternal from around 40 spiral arteries supplied by the uterine arteries. The spiral arteries open directly into the intervillous space, which in turn acts as a large arteriovenous shunt. During a healthy pregnancy the distal ends of the spiral arteries lose their smooth muscle and become widely dilated and unresponsive to vasoconstrictive stimuli. Blood then enters the intervillous space in a non-pulsatile manner and under low pressure (Lyall, 2006). This process modifies the quality (well oxygenated blood) but not the quantity of the maternal blood entering the intervillous space at low pressure (Redman, 2011).

In normal pregnancy, during placentation, trophoblasts invade into the endometrium and spiral arteries, resulting in spiral artery dilation. In PE, the trophoblastic invasion is incomplete, leading to inadequate or incomplete spiral artery remodelling (Lyall et al., 2013). The incomplete remodelling causes decreased blood flow and increased thrombosis within the utero-placental vasculature, resulting in placental hypoperfusion (Figure 1-3). Additionally, the myometrial vessels may undergo partial transformation that will lead to intermittent contraction, resulting in intermittent pulses of fully oxygenated arterial blood. The latter leads to fluctuation in oxygen delivery that predisposes the placenta to oxidative stress (Redman, 2011, Roberts and Hubel, 2009) and ischemia-reperfusion injury, which is a feature of PE. Consequently, the ischemic and the poorly perfused placenta releases factors that enter the maternal circulation, causing maternal endothelial dysfunction and maternal immune response activation, leading to the signs of PE (Genbacev et al., 1996).
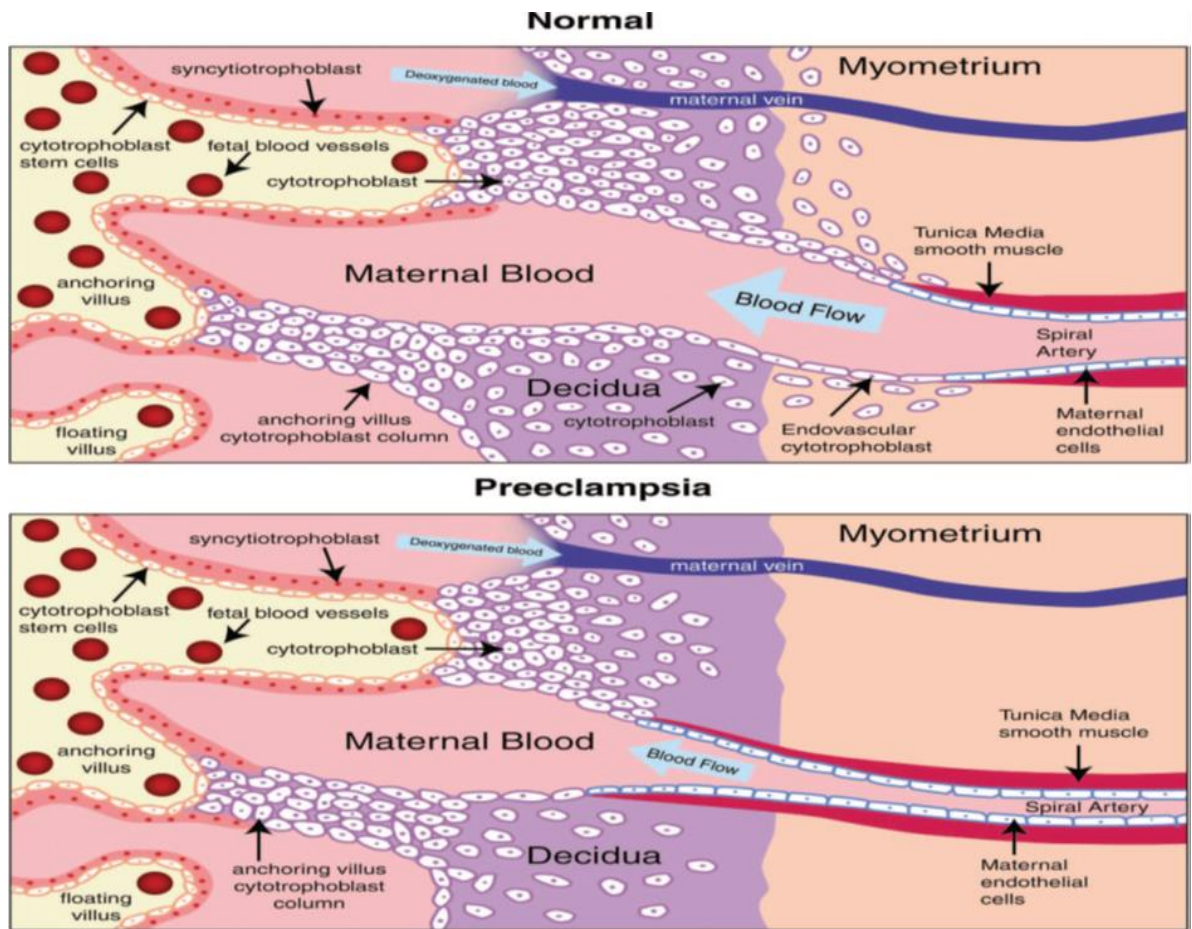
Figure 1-4 Schematic diagram of spiral artery remodelling in normal placental development. Invasive trophoblasts of fetal origin invade the maternal spiral arteries, transforming them from small-calibre resistance vessels to high-calibre capacitance vessels capable of providing placental perfusion adequate to sustain the growing fetus. In PE, trophoblasts fail to adopt an invasive phenotype. Instead, invasion of the spiral arteries is shallow, and they remain small-calibre resistance vessels. The image adapted from Powe et al. (2011).

Thus, several placental and maternal factors have been recently implicated in the pathophysiology of PE. Oxidative stress is apparent both in the placenta and in the maternal circulation. Pre-eclamptic placentas release larger quantities of superoxide and have less antioxidant capacity than normal placentas. The intense oxidative activity overcomes the antioxidant defence (Redman, 2011). The serum from women with PE shows evidence of oxidative modification of protein and lipoprotein particles. In addition, blood levels of antioxidants have been reported to be reduced in women with PE (Powe et al., 2011). Oxidative stress promotes inflammation in various ways. It generates oxidative modified molecules, which are pro-inflammatory, such as oxidised low-density lipoproteins. Also, it may lead to apoptosis, which is a physiological programmed cell death, or necrosis which is a highly pro-inflammatory pathological cell death (Esteve et al., 1999). There are also signs of endoplasmic reticulum stress in the syncytiotrophoblast which has adverse effects on protein synthesis, and oxidative stress in mitochondria alters energy metabolism.

1.3.3.2 Endothelial dysfunction in pathogenesis of PE

During pregnancy, some factors produced by placenta are pro-angiogenic, including VEGF, PlGF, and anti-angiogenic factors such as soluble fms-like tyrosine kinase receptor-1 (sFlt-1) and soluble endoglin (sEng). Normal development of placenta requires a balance of these factors (Maynard et al., 2003). Alteration in angiogenic balance is likely to contribute to the maternal syndrome in PE because of high circulation levels of sFlt-1 and conversely reduced levels of PlGF and VEGF. Additionally, women with PE have less TGF-β caused by increased placental production of soluble TGF-β co-receptor endoglin (sEng). Variations in anti-angiogenic factors in certain target organs such as the kidneys are assumed to lead to endothelial dysfunction and consequently hypertension and proteinuria (Wang et al., 2009).

1.3.3.3 Inflammation in pathogenesis of PE

During normal pregnancy, changes are induced in maternal physiology to accommodate the fetus and the placenta. The systemic inflammatory response is activated and exaggerated in PE. An inappropriate activated inflammatory response is associated with abnormal invasion of trophoblasts, endothelial cell damage and renal dysfunction. Numerous pro-inflammatory factors, for instance tumour necrosis factor-α (TNF-α) and IL-6 are released by the pre-eclamptic placenta (Holwerda et al., 2013). The levels of these factors are significantly higher in PE than normal pregnancy (Vince et al., 1995).

1.3.4 Placental pathology in PE

The placenta in PE may be grossly normal, but may also show pathological findings. These findings are related to chronic ischemia of placenta (Roberts and Post, 2008). Placental infarcts are common, and evidence of acute or chronic abruption may be seen as well. These changes become much worse in early-onset PE. Moreover, decidua arteriolopathy, impaired growth and Tenny-Parker changes (increased surface budding of placental syncytium) are obvious changes in the placenta in PE (Lyall and Belfort, 2007). Tenny-Parker changes include protrusions, containing normal nuclei and section of syncytial bridges, these changes may be a response to the alteration in oxygen content or blood flow to the intervillous space.

1.4   **Fetal growth restriction**

1.4.1 Normal fetal growth

Understanding the dynamics of normal fetal growth is vital in order to identify the pathophysiology of FGR. A complex cascade of processes that require coordination of components within the maternal, placental and fetal parts results in normal fetal growth (Sankaran and Kyle, 2009). Growth of the fetus is regulated at multiple levels and requires successful development of the placental interface and a complex interplay between fetal and maternal compartments. Both endocrine and paracrine signalling between the placenta and the maternal circulation promotes maternal metabolic and cardiovascular adaptations to pregnancy, which result in greater substrate availability and enhanced placental perfusion, thereby supporting placental growth (Baschat et al., 2012).

Maternal physiological changes, including cardiovascular adaptation, ability of the mother to deliver oxygenated blood to the uterine circulation and uterine perfusion, development of placenta vasculature, nutrient transfer through the placenta and fetal adaptation are essential processes for fetal growth. These are controlled by endocrine and genetic factors (Sankaran and Kyle, 2009). When the milestones in fetal, placental and maternal development are met, placental and fetal growth progress normally. The metabolic and vascular maternal adaptations promote a steady and enhanced nutrient delivery to the uterus, and placental transport mechanisms allow for efficient exchange of nutrient and waste (Baschat et al., 2012).

1.4.2 Fetal growth restriction

FGR is a significant cause of perinatal morbidity and mortality (Rasmussen et al., 1999), increasing the risks of adverse health effects throughout life. FGR is not a specific disease, but it is a manifestation of a number of fetal and maternal disorders. It is crucial to distinguish between infants who presented with in utero growth restriction from infants with in utero normal growth but who are constitutionally small, since FGR fetuses undergo fetal adaptations to a pathologic condition, resulting in distinct short- and long-term outcomes.

1.4.2.1 Definition, epidemiology and classification

FGR can be defined as fetal growth less than the 10th percentile for gestational age, however clinically, less than the 3rd percentile is probably a more reliable cut off for associated perinatal morbidity (Lubchenco et al., 1963). Also, FGR is defined as a decline in fetal growth rate that prevents an infant from reaching its complete growth potential. The incidence of FGR is estimated to be around 7% in full-term infants and 16% in preterm infants (Liu et al., 2014). However, this percentage is raised up to 15% of pregnancies when these reports define FGR and small for gestational age as equivalent. FGR remains prevalent in developed countries despite the advances in obstetric care. In most Western societies, placental insufficiency is the major cause of FGR, whereas inadequate maternal nutrition and infections play a greater role in developing nations (Crosby, 1991, Menendez et al., 2000).

 Based on whether the head is involved or not, FGR is classified into symmetric FGR, in which the head is affected, or asymmetric FGR in which the head is spared. Symmetric FGR is considered to be a constitutional event and the fetal growth is impaired during the first or second trimester. It is caused by decreased fetal cellular proliferation of all organs. It occurs in about 20% to 30% of FGR infants (Lin et al., 1991), and it is associated with small weight placentas without pathological findings. In contrast, asymmetric FGR is characterised by a restriction in abdominal growth more than that of the head. It develops when oxygen or substrate supply to the fetus is reduced during the third trimester. It represents 70% to 80% of FGR infants (Lin et al., 1991) and associated with significant placental pathology (Roberts and Post, 2008).

FGR due to placental dysfunction has significant short and long-term influences that may reach into adulthood. Early-onset FGR before 32 weeks gestation shows a specific sequence of responses to placental dysfunction that progress from the arterial circulation to the venous system and finally to biophysical abnormalities. Late-onset FGR presents with subtle Doppler and biophysical abnormalities (Bahado-Singh et al., 1999, Hecher et al., 1992).

1.4.2.2 Aetiology of FGR

There are a number of fetal, placental and maternal factors that are associated with FGR. Placental insufficiency is associated with the majority of FGR cases (Hendrix and Berghella, 2008). A compromised supply of nutrients and oxygen through the placenta to the fetus is

the most common cause of FGR and is presents in 80-90% of FGR cases (Campbell and Dewhurst, 1971, Warkany et al., 1961). This cause could be amendable to preventive and therapeutic management in the future.

Chromosomal disorders and congenital malformations are fetal factors of FGR. These are responsible for about 20% of the growth restricted fetuses. Fetuses with chromosomal abnormalities such as trisomy 13, 18 and 21 often have impaired growth. Additionally, fetuses having autosomal irregularities like deletions often experience in utero growth restriction (Khoury et al., 1988, Snijders et al., 1993). Multiple gestations are associated with FGR (Sassoon et al., 1990, Yinon et al., 2005). Fetal infections during first or second trimester, including cytomegalovirus, malaria, parvovirus, and rubella may lead to early gestation symmetric FGR (Militello et al., 2009). Abnormal placentation, chronic abruption, cord and placental abnormalities and placenta previa are placental factors associated with FGR (Sankaran and Kyle, 2009).

Chronic maternal vascular diseases due to hypertension, diabetes mellitus, renal diseases are associated with FGR (Cunningham et al., 1990, Ounsted et al., 1985). The most profound effect is observed if the hypertension is early-onset, severe, or due to chronic hypertension with superimposed PE. PE causes placental damage that results in utero-placental insufficiency, leading to reduced blood flow to the developing fetus. Consequently, the fetus fails to grow normally. Hypercoagulable maternal conditions such as thrombophilia and antiphospholipid antibody syndrome also inhibit growth either by placental thrombosis formation or by secondary effects of maternal hypertension (Many et al., 2001). Persistent maternal hypoxia due to high altitude, severe pulmonary or cardiac disease and severe chronic anaemia limits oxygen delivery to the fetus and slows fetal growth. However, multigenerational high-altitude residents are protected from the reductions in fetal growth and uterine artery blood flow (Wilson et al., 2007). Additionally, there are some environmental factors that may associate with FGR like smoking, drug use, alcohol and irradiation (Sankaran and Kyle, 2009).

1.4.2.3 FGR outcomes

FGR infants have a high risk of neonatal morbidity and mortality especially if delivered preterm (Bernstein et al., 2000). Neonatal hypoxia either antepartum or intrapartum is a result of oxygen and substrate deprivation. Neonatal hypoglycaemia and hypothermia occur because of decreased liver glycogen and fat stores (Doctor et al., 2001). Neonatal ischemic

encephalopathy and meconium aspiration are other complications of FGR (Barker, 1992). In general, fetal and neonatal complications and outcomes of FGR depend on the primary aetiology and on its severity. The effects of FGR persist beyond the neonatal period and may have profound effects during childhood. These include short stature and long-term neurological outcomes such as cerebral palsy (Blair and Stanley, 1990, Topp et al., 1996)

1.4.2.4 Placental pathophysiology

Gross and microscopic pathological findings on a placenta can be an invaluable tool to determine the pathophysiology leading to FGR. Most FGR placentas are small and weigh less than the 10th percentile for gestational age. Many of them show findings associated with vascular compromise from either maternal side as in hypertensive disorders and in decreased maternal blood flow due to vessel obstruction, or fetal side due to fetal vascular obstructive lesions (Roberts and Post, 2008).

The invasion of extavillous trophoblasts and transformation of the decidual and intra-myometrial portions of uterine spiral arteries are a key aspect of successful placentation as previously described. In FGR, reductions in utero-placental blood flow and variation in intervillous hemodynamics are a result of retained spiral arteries contractility due to inadequate remodelling by trophoblasts (Crocker, 2011). Histopathological studies indicate that there is an association between FGR and characteristic placental injuries including abnormalities of the maternal spiral arteries, fibrin deposition and dysregulated villous vasculogenesis (Crocker, 2011). The mechanisms of these injuries contribute to placental dysfunction that is the main cause of this important clinical condition. Inadequately developed spiral arteries are responsible for the ischemia-reperfusion of the placenta which is one source for oxidative stress (Scifres and Nelson, 2009). During the oxidative stress the ROS are linked with placental tissue injury and trophoblast damage. Beside ROS generation, hypoxia, hypoxia/reoxygenation or both contribute to placental injury through activation of the complement cascade (Hung et al., 2002). According to Yung et al. (2008), FGR placentas exhibit signs of oxidative stress, with reduced protein translation and particular reductions in key signalling pathways. Moreover, the syncytiotrophoblast shows signs of endoplasmic reticulum stress.

In FGR, retained spiral arteries contractility resulting from inadequate remodelling by trophoblasts causes decreases in utero-placental blood flow and causes alterations in intervillous hemodynamics. Pregnancies complicated by severe early-onset forms of PE

and/or FGR typically exhibit increased resistance in the umbilical circulation, with absent or even reversed end-diastolic flow velocity (Geerts and Odendaal, 2007). In the human placenta, the umbilical arteries branch into a series of resistance arteries contained in the distributing stem villi. These arteries eventually supply the capillary network in the terminal villi that are the principal sites of gaseous exchange. In the absence of nerves in the placenta, vasomotor control of the resistance arteries is performed by locally produced vasoactive molecules (Cindrova-Davies et al., 2013) which will be described in section 1.7.

1.5 Ischemia-reperfusion injury as a model for oxidative stress in complicated pregnancies

In early pregnancy oxygen is a controlling factor for trophoblast differentiation (Genbacev et al., 1997). At the end of week 11 of pregnancy blood flow in intervillous space starts and oxygen tension increases from 2% to 8% (Burton et al., 1999). This activates trophoblast invasion of spiral arteries.

During labour there are cycles of normal placental blood flow alternating with periods of ischemia followed by reperfusion. This happens because of the uterine contractions. Previous experiments involving hypoxia-reoxygenation of villous explants *in vitro* have supported this hypothesis demonstrating that ischemia-reperfusion injury can lead to oxidative stress rapidly (Hung et al., 2001). Cindrova-Davies et al. (2007) investigated the same hypothesis taking the advantage of the nature that occurs when healthy placenta is subjected to intermittent blood flow during labour. They suggested impact of hypoxia-reperfusion *in vivo* on placental expression of genes and cytokine profile.

Complications of pregnancies, such as PE and FGR are linked to exposure of placental villi to hypoxia (Newby et al., 2005). In PE and FGR, oxidative stress is an important feature of the placenta. The cause of the oxidative stress is not clear, although ischemia-reperfusion injury is one possible mechanism. The most pertinent predisposing factor for PE is deficient invasion of the endometrium by extravillous cytotrophoblast cells during the first trimester of pregnancy. This results in incomplete conversion of the spiral arteries. Consequently, these vessels display an abnormally high vascular resistance, and are associated with reduced utero-placental perfusion and hypoxia (Lyall, 2006).

Much research has shown that in PE certain pathological changes of the placenta cannot be explained by hypoxia alone. Alternatively, studies by Hung et al. (2001) and Hung et al. (2002) have hypothesised that the retention of vasoreactivity in the incompletely remodelled arteries affects the maternal blood flow to the intervillous space. It becomes more variable than normal, and the constancy of the placental perfusion becomes a more important factor than the absolute rate of blood flow. The placental tissues will become locally hypoxic during periods of vasoconstriction. When the maternal blood flow is re-established there will therefore be a rapid increase in tissue oxygenation. These studies suggested that, due to incomplete remodelling of spiral arteries in PE, the placenta would be exposed to fluctuations in oxygen tension similar to an ischemia-reperfusion injury. Depending on the severity and frequency of these insults, the outcome may range from mild to severe oxidative stress and tissue damages (Hung et al., 2001).

Ischemia-reperfusion injury is now a well-predictable consequence of hypoperfusion in many organs, and it is mediated mainly through the generation of ROS. If the ROS generation exceeds the antioxidant capacity defences then oxidative stress results. The oxidative stress may lead to a damage to lipids, proteins and DNA, leading to cell dysfunction and tissue damage (Hung et al., 2001). Generally, ischemic-reperfusion insult is characterised by oxidant production, leucocyte-endothelial cell adhesion, platelet–leucocyte aggregation, increased microvascular permeability and decreased endothelium-dependent relaxation. Ischemia-reperfusion injury can lead to multi-organ damage and death (Pierro and Eaton, 2004).

A number of studies have shown that the fluctuation in oxygen tensions, caused by incomplete remodeling of spiral arteries in the placenta, are analogous to an ischemia-reperfusion injury. Hypoxia-reoxygenation experiments demonstrated that placental oxidative stress can be induced by an ischemia-reperfusion type insult and, in turn, can alter placental genes and their expression (Cindrova-Davies et al., 2007). Previous studies have investigated the effect of ischemia and re-oxygenation on expression of some important enzymes as HO-1 and HO-2, the CO producers. McCaig and Lyall (2009) tested the hypothesis that expression of HO-1 and or HO-2 in placental villous explants would be altered by an ischemia-reperfusion insult. Human term placental explants were exposed to hypoxia then re-oxygenation at different concentrations: in 5% O2, 20% O2 or repeated cycles of hypoxia-re-oxygenation in 5% O2 or 20% O2. HO protein concentrations were assessed by western blotting. They found that there were no differences in expression of HO-1 and HO-2 with any treatment protocol.

1.6 Maternal Obesity

1.6.1 Background and introduction

Obesity represents a significant health risk in all population. Obesity is a common condition in both developed and developing countries, and the major characteristic is an increase in the fat mass. According to the World Health Organisation (WHO), an abnormal or excessive fat accumulation impairing the health is defined as overweight and obesity (WHO, 2000). Obesity is a chronic multifactorial disease caused by genetic, environmental and behavioural factors that lead to serious health consequences. Obese adults are at a higher risk for cardiovascular and metabolic morbidity, cancer and mortality compared to non-obese individuals with similar characteristics (Kenchaiah et al., 2002). In addition to the physical and emotional costs of this disease, obesity also has important direct and indirect financial costs.

Obesity among women of reproductive age is particularly detrimental, given its high prevalence and short-term and long-term adverse health impacts on both the women themselves and their offspring. Obesity in pregnancy has become one of the most commonly occurring risk factor seen in obstetric practice. Maternal obesity is usually defined as a body mass index (BMI) of 30 kg/m^2 or more at the first antenatal visit. The normal BMI between 18.5 and 24.9 indicates that the women are healthy weight. BMI is a simple index of weight for height, and is calculated by dividing the weight in kilograms by the square of the height in meters (kg/m^2). There are three classes of obesity: class 1 (BMI 30-34.9); class 2 (BMI 35.0-39.9); class 3 or morbid obesity (BMI $\geq$ 40) (NICE,National Institute, 2006).

The prevalence of obesity is increasing in all ethnic and age groups. In England, it has increased markedly since the early 1990s. The prevalence of maternal obesity has also been seen to increase, rising from 9-10% in the early 1990s to 16-19% in the 2000s (Heslehurst et al., 2007). The confidential enquiry into maternal and child health (CEMACH) in the UK reported an increase in female obesity of 10% between 1993 and 2002 (Bowyer, 2008). CEMACH also reported that of all mothers who died during 2000–2002 in the UK, 30% were obese (BMI >30 kg/ m^2) (Lewis et al., 2004). Moreover, their report published in 2007, stated that during the 3 years (2003-2005) more than half of the mothers who died were obese or overweight, and more than 15% of all women who died were morbidly obese

(Lewis et al., 2007). In the United States, the percentage of overweight or obese women has increased by around 60% over the past 30 years (Wang et al., 2008).

1.6.2 Etiological Factors

Obesity is a result of excessive energy consumption compared with the energy expended. Also, increased consumption of fats and sugars and lack of physical activity as in children have been linked with obesity (Gazzaniga and Burns, 1993, Ludwig et al., 2001). The basic hypothesis of the cause of the disease is that some populations may have genes variants that predispose to increased fat storage, and when experiencing periods of starvation, this provided a survival advantage; but under current circumstances, overstocking of fat results in obesity and type 2 diabetes mellitus (Hu et al., 2001). Alternatively, it has been postulated that in the early stages of our evolution, highly effective systems were developed to collect the limited energy available, leading to the appearance of adipose tissue. Changes in lifestyle and diet as well play a role in increasing the number of obese subjects. Another theory for explaining the development of obesity is known as the fetal origin's hypothesis of chronic diseases. This suggests that poor maternal nutrition and poor fetal growth are risk factors for developing chronic diseases that disturb the programming of body structure, physiology, and metabolism (Langley-Evans, 2006).

1.6.3 Complications associated with maternal obesity

Maternal obesity is a risk factor for adverse pregnancy outcomes, with increased morbidity and mortality for both mother and fetus alike both in the short and long-term (Jarvie and Ramsay, 2010). Obese women during pregnancy are at increased risk of gestational diabetes mellitus (Sebire et al., 2001), PE (O'Brien et al., 2003) and venous thromboembolism (Larsen et al., 2007). Several studies have shown an association between the maternal obesity and the gestational hypertension. Two large population-based studies have also shown positive strong associations between the pre-pregnancy BMI and the risk of developing PE (Baeten et al., 2001). Venous thromboembolic (VTE) complications are a leading cause of maternal mortality in the UK and other developed countries (Bourjeily et al., 2010). Obese women have two and half times more risk for developing of VTE compared to lean pregnant women (Knight, 2008). The major two pathways mostly responsible for obesity-induced thrombosis are chronic inflammation (Vandanmagsar et al., 2011) and impaired fibrinolysis (Shimomura et al., 1996).

Obese pregnant women at the time of the birth are at risk of induced labour, instrumental delivery, CS, haemorrhage, anaesthetic complications, wound infections and longer duration of hospital stay (Buhimschi et al., 2004). Babies of obese mothers are also at increased risk of stillbirth (Chu et al., 2007), congenital anomalies (Waller et al., 1994), macrosomia (Ehrenberg et al., 2004) and neonatal death (Kristensen et al., 2005, Naeye, 1990). Intrauterine exposure to maternal obesity is also associated with an increased risk of developing obesity and metabolic disorders in childhood (Boney et al., 2005).

1.6.4 Obesity and PE

Obesity has been described as global epidemic over recent decades. This rising trend has substantial consequences on pregnancy. Elevated BMI is one of the maternal pre-existing features that is associated with PE (Bodnar et al., 2005b). Given the obesity epidemic, this is one of the largest attributable and potentially modified risk factors for PE. Obesity increases the overall risk of PE by approximately 2-3-fold (Bodnar et al., 2005b). Many studies have been conducted to investigate the association between PE and maternal obesity. In the USA, a study of 96801 nulliparous women showed that obese women, with a BMI more than 30 kg/m^2, were 3.3 times more likely to develop PE compared with women with BMI less than 20 kg/m^2 (Baeten et al., 2001). The risk of early and late forms of PE rise progressively with increasing BMI (Bodnar et al., 2007). It is suggested that excessive maternal weight gain during pregnancy is associated with the risk of PE; however, these may partly be a result of the increase in fluid retention that occurs with PE, thereby contributing to higher weight (Fortner et al., 2009).

1.6.5 Potential mechanisms contributing to PE and cardiovascular disease in obese women

Obesity is a risk factor for both PE and cardiovascular disease. Exploring and understanding of the underlying common mechanisms of these links may reveal the pathophysiologic processes leading to PE as well as providing insight into potential targets for therapy. The common features include insulin resistance, inflammation, oxidative stress, increased levels of angiogenic factors and adipokines.

1.6.5.1 Insulin resistance

Two-thirds of overweight individuals have insulin resistance, which is a risk factor for type 2 diabetes and cardiovascular disease (Kaaja, 1998). Insulin resistance is more common in women with PE and can persist for years after a pregnancy complicated with PE, thus increasing cardiovascular risk (Kaaja, 1998, Laivuori et al., 2000). Obesity, hypertension, insulin resistance, dyslipidaemia and impaired glucose tolerance, features of metabolic syndrome, are also observed more commonly in women with PE (Kaaja, 1998, Sattar and Freeman, 2012). In metabolic syndrome, it has been suggested that obesity contributes to hypertension by several mechanisms that include reduction in available NO due to oxidative stress, increase in sympathetic tone and increased release of angiotensinogen by adipose tissue. Dyslipidaemia and the overproduction of free fatty acids released from adipocytes have also been proposed to contribute to oxidative stress and insulin resistance which are clear signs of obesity (Tripathy et al., 2003).

1.6.5.2 Oxidative stress

Oxidative stress is a postulated mechanism linking obesity to many diseases. ROS overproduction and oxidative stress under physiological or pathological conditions result in direct or indirect damage to organs. It is known that oxidative stress is involved in pathological processes such as diabetes, cardiovascular disease, atherogenic processes and obesity (Fernandez-Sanchez et al., 2011). In obesity oxidative stress may be induced and, in turn, it is associated with irregularity in adipokines production, contributing to development of the metabolic syndrome (Esposito et al., 2006). Obesity is associated with oxidative stress, possibly due to increased inflammation and free fatty acids along with the decrease in circulating antioxidants (Wallstrom et al., 2001). In PE, oxidative stress leads to altered endothelial function and vascular dysfunction (Kaaja, 1998). Therefore, oxidative stress may predispose obese women to the development of PE.

1.6.5.3 Inflammation

Inflammation is a shared feature of obesity, cardiovascular disease, and PE. Adipose tissue generates numerous inflammatory mediators that are produced more actively in obese individuals and can alter endothelial function. In obese women there is an elevation in production of C-reactive protein, an inflammatory mediator produced by the liver as well as by adipocytes, which is associated with cardiovascular morbidity (Bodnar et al., 2005a, Wolf

et al., 2001). IL-6 production increases during obesity, cardiovascular disease as well as in insulin resistance, leading to vascular tissue damage (Lowe et al., 2014, Spranger et al., 2003).

1.6.5.4 Angiogenic factors

The balance of circulating angiogenic factors is altered in PE compared with normal pregnancy. Levels of PlGF are lower in women with PE. This is likely due to higher circulating concentrations of soluble Flt-1, an antiangiogenic factor that binds and inactivates PlGF and vascular endothelial growth factor. Previously, it was found that levels of both sFlt-1 and PlGF are lower in obese pregnant women (Mijal et al., 2011). Other studies have shown that higher BMI is associated with higher sFlt-1 concentrations (Faupel-Badger et al., 2011). Although findings are not consistent across studies, the altered angiogenic balance in obesity may have implications in the development of PE.

1.6.5.5 Adipokines

Adipose tissue produces substances such as leptin and adiponectin which affect the metabolism and have an association with cardiovascular diseases. The leptin concentration is elevated in obesity while the concentration of adiponectin is decreased (Vega and Grundy, 2013). In PE there is an increase in the circulating leptin and this correlates with the maternal BMI (Laivuori et al., 2000). The placenta is considered as a major contributor of circulating concentrations of leptin during pregnancy since leptin is also produced by the placenta. In relation to the adiponectin which has insulin sensitising effects, it is reported that it is decreased in obese people and is inversely correlated with the cardiovascular risk. However, it is not clear yet whether the adiponectin concentrations are related to PE or not, as studies have described higher as well as lower concentrations (Mazaki-Tovi et al., 2009).

1.7 Endothelium-dependent vasorelaxant gaseous molecules

Endogenously generated molecules such as NO and CO are involved in the vascular adaptations of normal pregnancy. NO and CO have been shown to have dilator actions in *vitro* (Barber et al., 2001, Myatt, 1992). Accumulating studies suggest that H_2S also exerts significant effects in the adult cardiovascular system, mainly via endothelium-independent vasodilation (Zhao et al., 2001). These gaseous signalling molecules have been considered

as endogenous protective pathways and also hailed as promising molecules with therapeutic potential due to their ability to act as vasodilators (Bir and Kevil, 2013).

The enzyme systems generating these molecules (NO, CO and H_2S) are able to promote placental vasodilatation by regulating placental blood vessel tone *in vivo* and *in vitro* (Ahmed et al., 2000, Myatt et al., 1991, Patel et al., 2009, Wang et al., 2013). It is not surprisingly that these molecules can promote the placental blood flow as their vasodilator effect has been shown in a number of other vascular beds such as cardiovascular and cerebrovascular circulation (Leffler et al., 1999). Abnormalities in gasotransmitters signalling and production are related to diseases like hypertension, atherosclerosis, and inflammation (Wang, 2002). Experimental studies have shown that abnormal production of these molecules is associated with PE (Wang, 2002).

1.7.1 Nitric oxide

NO is a highly reactive gas produced from the amino acid L- arginine by the endothelial nitric oxide synthase (NOS) in several cells including vascular endothelial cells. Endothelial NOS (eNOS) and inducible NOS (iNOS) are two isoforms of NOS. eNOS is produced under normal conditions in endothelial cells. eNOS is stimulated by calcium which is released either in response to the high blood flow (flow-dependent), or in response to receptor stimulator such as acetylcholine or other NO dependent vasodilators (receptor-stimulation dependent). iNOS has minimum activity under normal conditions, whereas it is highly active and over expressed in response to inflammatory reactions by cytokines, interleukins or bacterial endotoxins. NO diffuses freely across the cell membrane to the smooth muscle cells (SMCs) in the tunica media where it stimulates guanylyl cyclase (GC) promoting conversion of guanosine triphosphate (GTP) to cyclic guanosine monophosphate (cGMP). cGMP, is a main second messenger, activates protein kinase, resulting in a decrease in the ca^{++} concentration and relaxation that results in dilation of blood vessels (Klabunde, 2004).

NO is a key signalling molecule for endothelium-dependent regulation of vasculature. Flow dependent and receptor mediated vasodilatation and inhibition of vasoconstrictors such as angiotensin II are important functions of NO. It also has anti-platelet aggregation effect and anti-inflammatory effect that limits up-regulation and adhesion of the leukocytes to the epithelium of blood vessels (Klabunde, 2004). Moreover, it performs other significant functions, including having anticoagulant and antioxidant activity (Klabunde, 2004).

In normal pregnancy, NO contributes to the reduction in vascular resistance and is actively involved in placental development (Demir et al., 2012). During pregnancy, increase of maternal blood volume is not accompanied by an increase in arterial blood pressure for several reasons. NO synthesised by iNOS and eNOS in the placenta and myometrium is thought to induce systemic vascular dilation, compensating the maternal cardiovascular hemodynamics (Sandrim et al., 2008). Human placental syncytiotrophoblast express eNOS but not iNOS (Lyall et al., 1998).

The NO-cGMP pathway has been suggested as a mechanism for relaxation of myometrium during pregnancy, and as a modulator of labour (Sladek et al., 1993, Yallampalli et al., 1994). However, Barber et al. (1999) found that eNOS was detectable on the endothelium of blood vessels in non-pregnant and pregnant myometrium, but no eNOS was detectable on smooth muscle in pregnant and non-pregnant myometrium. Also, iNOS was absent in both pregnant and non-pregnant myometrium. Their findings suggested that NOS is not up-regulated during human pregnancy and therefore is unlikely to be involved in uterine quiescence.

Interestingly, the vasodilator effect of NO in normal pregnancy reflects the possible role of NO in the pathophysiology of PE. However, it is still not clear whether NO levels are altered in PE. Significantly higher expression of eNOS in myometrium and placenta were detected in pre-eclamptic women compared with that in normal pregnant women; however, the expression of iNOS was the same in myometrium and lower in the placenta (Faxen et al., 2001).

1.7.2 Expression of NOS

During early pregnancy the interstitial evCTB invade the uterine endometrium and myometrium, and the endovascular trophoblast migrate in a retrograde direction up the spiral arteries, transforming them into large vessels with low resistance (Goldman-Wohl and Yagel, 2002). These physiological changes are required for a successful pregnancy. Transformation of spiral arteries is thought to result from the loss of musculoelastic structure due to extravillous cytotrophoblast invasion. However, vascular changes have been documented as early as 8 to 10 weeks of gestation before invasion of endovascular cytotrophoblasts in myometrium has occurred (Craven et al., 1998 cited in, Lyall et al., 1999).

Lyall et al. (1999) tested the hypothesis that NOS is expressed by invading extravillous cytotrophoblasts giving these cells the potential to release NO and thus to influence spiral artery transformation, resulting in vasodilatation. The study samples, the placental biopsies, were obtained from normal pregnant women at third trimester and between 8 to 19 weeks of gestation, using transcervical sampling technique. The researchers demonstrated that eNOS was expressed by syncytiotrophoblast and villous endothelial cells whereas extravillous cytotrophoblasts were negative for both eNOS and iNOS. Placental bed examination revealed that spiral artery endothelial cells were positive for eNOS whereas interstitial cells were negative (Lyall et al., 1999). Takizawa et al. (2002) found that NOS expression in the fetal component of placenta was considerably higher at term pregnancy compared to pre-term levels suggesting that NO could have a significant role in maintenance of placental function until birth.

1.7.3 Carbon monoxide

CO is a gaseous molecule synthesised endogenously from the degradation of heme molecules in the endoplasmic reticulum by the heme oxygenase enzyme (HO) (Maines, 1993). The HO exists in two main isoforms, HO-1 and HO-2. HO-1 is widely distributed in the body with high concentrations in the liver and the spleen, while the HO-2 is constitutively expressed at high concentrations in the brain, testis and vascular endothelium. CO stimulates soluble GC, which, in turn, converts GTP to cGMP (Maines, 1993). The products of HO-mediated heme degradation including biliverdin, bilirubin, CO, and ferrous iron regulate vital biological processes such as oxidative stress, inflammation, apoptosis, cell proliferation, fibrosis, and angiogenesis (Dulak et al., 2008). CO mediates protection against ischemia and cell injuries, and inhibits inflammatory responses (Kohmoto et al., 2007). In addition, CO has vasodilatory and anti-apoptotic effects and plays a role in angiogenesis (Brouard et al., 2000). During pregnancy, the HO/CO system is believed to maintain maternal systemic vascular tone.

1.7.4 Expression of CO

HO-1 and CO play an important role in the maintenance of uterine quiescence in human pregnancy (Acevedo and Ahmed, 1998) and also in modulating of the utero-placental circulation (Lyall et al., 2000). Importantly, placental HO is thought to protect the placenta from cellular damage (Ahmed et al., 2000). Linzke et al. (2014) showed that CO is a vital contributor to successful pregnancy through modulating the uterine natural killer cells,

which result in the promotion of the remodelling of maternal spiral arteries. Moreover, reduction in HO expression has been associated with complication of pregnancy such as recurrent miscarriage (Denschlag et al., 2004), FGR and PE (Ahmed et al., 2000).

The expression of HO isoforms in human placenta was investigated by Lyall et al. (2000), who demonstrated that HO-2 immunostaining was prominent in syncytiotrophoblast during the first trimester and decreased at the end of gestation. On the other hand, HO-2 was low in endothelial cells during the first trimester and increased by term. HO-1 immunostaining was generally low in placenta but intense in the placental bed. Moreover, this study found that placental perfusion is significantly increased in a dose dependent manner after administration of HO inhibitors suggesting a role of CO in placental perfusion.

Farina et al. (2008) studied HO-1 mRNA expression in the placenta using chorionic villous samples at 11 weeks and revealed that patients who developed PE later had lower expression than normal pregnant women. Moreover, Nakamura et al. (2009) illustrated that patients with PE had lower levels of HO-1 mRNA in their circulation. Furthermore, Ahmed et al. (2000) and Baum et al. (2000) reported that pre-eclamptic women exhale less CO than those who have normal pregnancy, and suggested that HO/CO has an anti-inflammatory function in pregnancy by inhibiting sFlt-1 and sEng release, thus, loss of its activity initiates inflammatory reaction and the development of PE.

1.8 Hydrogen sulfide

Over the last decade, research into the biology of H_2S has drawn our attention to its importance in many physiological and pathological processes in a wide range of biological systems. Traditionally, it was considered as a toxic gas in the earth's atmosphere. However, it recently has been shown to be synthesised in human and mammalian tissues. H_2S is a water-soluble gas with a repulsive odour, and freely diffuses through membranes (Cuevasanta et al., 2012). Similarly to NO and CO, H_2S is lipophilic and partially dissociates to H^+, HS^-, which subsequently may decompose to H^+ and S^{2-} (Lowicka and Beltowski, 2007). However, the later reaction does not occur *in vivo* at substantial amount as it occurs only at high pH. H_2S is a reducing agent, so it has the ability to reduce the cysteine disulfide bond, thereby changing the conformation and activity of enzymes, channels and receptors (Kimura, 2014). H_2S is detectable in serum and most tissues at a concentration of about 50 μM (Lowicka and Beltowski, 2007).

H$_2$S has been investigated as a signalling molecule, and can be produced endogenously. Many reports showed that H$_2$S synthesising enzymes are expressed in various tissues in mammalian and human body (Whiteman et al., 2011). The production of H$_2$S by mammalian tissues is likely to occur in a slow and constant rate (Abe and Kimura, 1996). Recently, H$_2$S has been demonstrated to be an endogenous gaseous mediator (Whiteman et al., 2011). It forms one of group signalling molecules named gasotransmitters, alongside other gaseous mediators – CO and NO, and was found to mediate many important physiological and pathological pathways. More interestingly, H$_2$S, NO and CO are similar in their properties. They are produced enzymatically, as well as all being small molecules with free permeability across membranes.

1.8.1 Synthesis of H$_2$S

The endogenous production of H$_2$S is attributed to three key enzymes in the L-cysteine and/or homocysteine biosynthesis pathway (Figure 1-4). These enzymes are cystathionine β-synthase (CBS), cystathionine γ-lyase (CSE or CTH) and 3-mercaptopyruvate sulfurtransferase (3-MST/MPST).
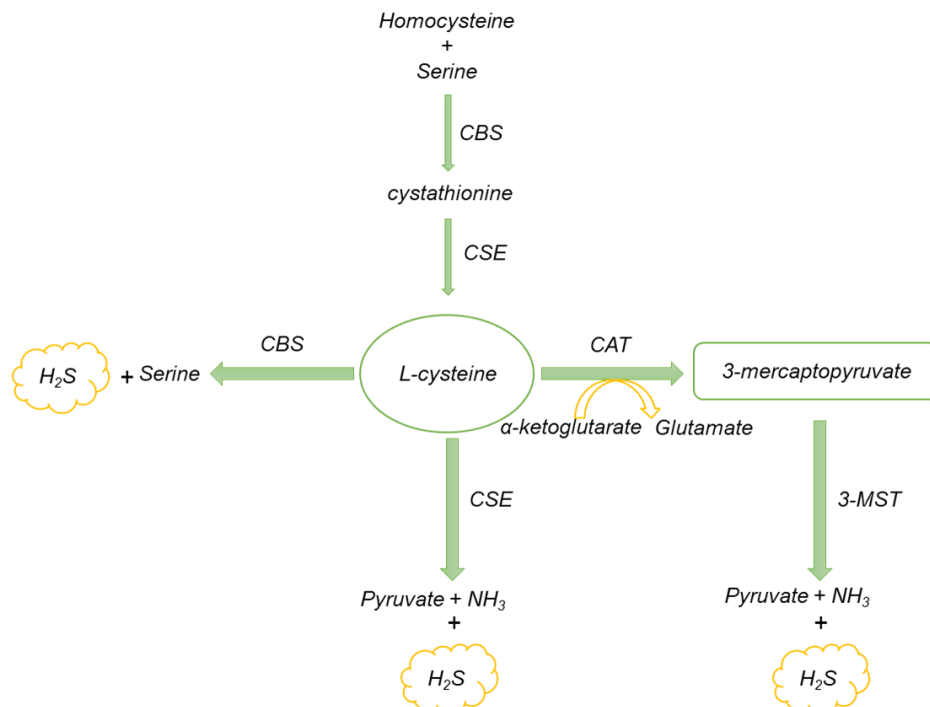
Figure 1-5 Pathways for H$_2$S biosynthesis. The endogenous production of H$_2$S occurs via three pathways; CSE induces conversion of L-cysteine to H$_2$S, pyruvate and ammonia, whereas, CBS converts L-cysteine into H$_2$S and serine. The third pathway occurs in mitochondria where 3-MST synthesises H$_2$S from 3-mercaptopyruvate which results from conversion of L-cysteine via cysteine aminotransferase (CAT) in a reaction dependent on the cofactor α-ketoglutarate. The figure compiled using information from Gemici and Wallace (2015).

1.8.1.1 Cystathionine β-synthase enzyme

CBS enzyme catalyses the first step of the transsulfuration pathway by condensing homocysteine with serine to generate cystathionine, which in turn generates cysteine by CSE. CBS also converts L-cysteine to serine and releases H_2S in this reaction (Ge et al., 2001). It utilises a combination of cystine and homocysteine to generate H_2S however, the mechanisms controlling whether CBS produces cystathionine or H_2S are still unclear. CBS belongs to cysteine synthase family, and its subcellular location is mainly in the cytoplasm, but some is also detected localised in the nucleus (Kabil et al., 2006). The CBS enzyme has a complex domain structure and regulatory mechanism. It is a homotetrameric enzyme formed by four identical of 63 kDa subunits. Each comprises 551 amino acids and binds to cofactors including pyridoxal 5-phosphate (PLP) and heme. Each subunit consists of three structural domains. The catalytic domain binds to the cofactor PLP. The N-terminal domain, which contains about 70 amino acids, binds to heme that functions as a redox-sensitive gas sensor and it is also required for successful protein folding. The C-terminal domain of the protein, which is the regulatory region, contains two CBS motifs that dimerise to form a domain which is responsible for CBS subunits tetramerization, and contains the binding sites for an activator, S-adenosyl-methionine (AdoMet) (Kery et al., 1994). The C-terminal domain is also suggested to play a targeting role for compartment localisation (Bateman, 1997).

1.8.1.2 Cystathionine γ-lyase enzyme

It is also known as γ-cystathionase, cysteine lyase or cysteine desulfhydrase. It is the second enzyme in the transsulfuration pathway. It is a member of the γ-family of PLP-dependent enzymes. CSE catalyses the α, γ-Carbon elimination of cystathionine to produce cysteine, α-oxobutyrate and ammonia (Sun et al., 2009). It also induces conversion of a cysteine to H_2S, pyruvate and ammonia. The CSE is a homotetrameric enzyme with each subunit being 45 kDa, and with the cofactor PLP bound to the active site by Lys[212] to each subunit (Sun et al., 2009). It is located in the cytoplasm, and it is also believed to be the major endogenous source of H_2S in vascular and peripheral tissues as CSE knockout mice have low serum H_2S levels (Yang et al., 2008).

1.8.1.3 Mercaptopyruvate sulfurtransferase enzyme

3-MST has recently demonstrated as a third H_2S producing enzyme, along CAT in neurons (Mikami et al., 2011a), retina (Mikami et al., 2011b), the brain (Tanizawa, 2011) and in the vascular endothelium (Shibuya et al., 2009a). 3-MST is a cysteine catabolising enzyme that exists as either monomer or an inactive disulfide-linked homodimer. It requires endogenous reducing agents as thioredoxin and dihydrolipoic acid to release H_2S (Mikami et al., 2011a), and its optimal activity is achieved under alkaline conditions (Kimura, 2014). 3-MST is non-PLP dependent and uses 3-mrecaptopurvate as substrate. The structure consists of two domains of very similar conformation. However, the sequences of the two domains are very different. 3-MST is primarily localised in the mitochondria as well as in the cytosol (Nagahara et al., 1998), and it consists of 317 amino acids.

H_2S can also be synthesised in mammalian tissues via a non-enzymatic pathway, such as by the reduction of thiols and thiol-containing molecules. In the presence of reducing agents such as glutathione, H_2S can be released in neurons and astrocyte from bound sulfur in persulfides (Ishigami et al., 2009), and can also be produced from polysulfides in red blood cells (Yang et al., 2019). Although non-enzymatic routes for H_2S generation have been identified, it seems likely that the all of the H_2S, which is generated in the body for biological functions, is derived enzymatically (Ishigami et al., 2009).

1.8.2 Metabolism of H_2S

The endogenous H_2S can be metabolised by different routes. In mitochondria the H_2S can be oxidised to thiosulfate, which can be converted to sulfate and excreted by the kidney either in free or conjugated form (Lowicka and Beltowski, 2007). The second pathway of H_2S metabolism is the methylation by thiol S-methyltransferase to methanethiol and dimethylsulfide (Furne et al., 2001). Finally, H_2S may form sulfhemoglobin by binding to methemoglobin (Lowicka and Beltowski, 2007).

1.8.3 Expression of Cystathionine β-synthase, Cystathionine γ-lyase and Mercaptopyruvate sulfurtransferase

The expression of H_2S synthesising enzymes varies between different tissues. CBS is predominantly expressed in cerebellum, brain stem, cerebral cortex and hippocampus, and it generates H_2S acting as a neuromodulator (Abe and Kimura, 1996). The CBS activity in

these tissues is about thirty-fold greater than CSE enzyme. It is considered as a major contributor to cellular production of H_2S in central nervous system (Sun et al., 2009). It is also expressed in the kidney, ileum, liver, pancreatic islets, uterus and placenta (Kimura, 2011). The expression and activity of CSE has been detected at high levels in mesenteric artery, portal vein, aorta and other vascular tissues, and the smooth muscle relaxant effect of H_2S was noted (Hosoki et al., 1997). 3-MST is primarily responsible for H_2S production in central and peripheral nervous systems (Miyamoto et al., 2014). 3-MST is also expressed in a number of tissues with high activity in the proximal tubular epithelium of the kidney, hepatocytes in the liver, heart, lung, and spleen (Nagahara et al., 1998, Shibuya et al., 2009b). In some tissues such as kidney, both enzymes CBS and CSE are expressed and contribute to H_2S synthesis (House et al., 1997), while in others only one enzyme is required. In vasculature and heart, CSE appears to be the main enzyme required for H_2S synthesis (Yang et al., 2008), whereas in brain tissue CBS is predominant enzymatic source of H_2S (Caliendo et al., 2010).

1.8.4 Biological function of H_2S

1.8.4.1 Effects of endogenous H_2S on various tissues and organs

It has been previously confirmed that H_2S has physiological roles in different tissues. It is suggested to be an endogenous neuromodulator in rat brain tissue as it is involved in synaptic transmission (Abe and Kimura, 1996). Recently, great efforts have been made to find out other effects of this gaseous molecule on a number of biological targets. Studies conducted on animals and human have demonstrated that H_2S is involved in various physiological and pathophysiological processes, including diabetes and obesity. It is reported that both endogenous and exogenous H_2S exposure acts on insulin secretion, thereby resulting in changed glucose levels in the peripheral circulations (Yusuf et al., 2005).

In the cardiovascular system H_2S acts as a vasodilator both *in vivo* and *in vitro* and reduces blood pressure *in vivo* through vasodilatation of blood vessels, and relaxation of vascular smooth muscles by opening K_{ATP} channels in vascular SMCs (Lefer, 2007). In many systems, the H_2S effect is mainly mediated by K_{ATP} channels (Lowicka and Beltowski, 2007). In addition, H_2S regulates angiogenesis *in vitro* and *in vivo* under either physiological or pathological conditions, such as ischemia.

During hypoxia, H_2S acts as a protective molecule because of its antioxidant properties (Whiteman et al., 2011). H_2S is a highly reactive molecule, and may easily react with ROS resulting protein and lipid protection from ROS-mediated damage. Also, H_2S may exert antioxidant effect by stimulation of cysteine transport to the cells and enhancement of glutathione synthesis (Kimura and Kimura, 2004).

Furthermore, H_2S participates in glomerular and tubular renal functions and it has been reported that H_2S synthesising enzymes are abundant in kidney, predominantly in renal proximal tubules (Li et al., 2006). In addition to the previous effects, H_2S acts as an anti-inflammatory molecule. Anti-inflammatory and pro- inflammatory effects of H_2S have been reported in different animal models and cultured cells. Experimental studies have shown that H_2S inhibits leukocyte-endothelial cell interactions *in vivo* (Zanardo et al., 2006).

Many studies have demonstrated that H_2S activates K_{ATP} channel, thereby causing relaxation of smooth muscle. Studies of Tang et al. (2005) have suggested that K_{ATP} channel opening is induced by H_2S resulted in vasorelaxation in rat aorta and mesenteric beds. Zhao et al. (2009) found that H_2S donor has dual effects on the spontaneous contraction of gastric smooth muscle in guinea-pig. It inhibits the amplitude of spontaneous contraction at high concentration whereas it induces tonic contractions at low concentration. Also, Teague et al., 2002 showed that sodium hydrosulfide, H_2S donor, relaxed ileum smooth muscle, the thoracic aorta and portal vein in rats.

Although H_2S has biological and physiological functions, it has also been implicated in several pathological states. Studies investigating the effects of H_2S have revealed that the deficiency of H_2S may lead to various pathological changes, such as arterial and pulmonary hypertension, Alzheimer's disease, gastric mucosal injury and liver cirrhosis (Whiteman et al., 2011). However, excessive production of H_2S, by using inorganic H_2S donors may contribute to pathogenesis of inflammatory diseases, septic shock and cerebral stroke (Whiteman et al., 2011).

1.8.4.2 H_2S in the adipose tissue

Adipose acts as a passive reservoir for energy storage, and it has recently been considered as an active metabolic and endocrine tissue (Flier et al., 1987). Adipokines, such as leptin and adiponectin, have been identified as hormones produced by adipocytes (Bing et al., 2004). The CBS and CSE mRNA expression, as well as, CSE protein expression have been

found located in the adipose tissue of rats. Researchers have found a negative correlation between endogenous production of H_2S and adipose glucose uptake *in vivo*, and H_2S decreases basal and insulin-induced glucose uptake in adipocytes *in vitro*, suggesting that H_2S produced by adipose tissues regulates the local insulin sensitivity (Feng et al., 2009). Impaired vascular reactivity has been found in the obese and those with type 2 diabetes (Dubova et al., 2011). Interestingly, investigators have found that the plasma level of H_2S was reduced in patients with obesity and type 2 diabetes, and in animal models of obesity and diabetes. Recently, Whiteman et al. (2010) showed that H_2S level was negatively correlated with measurements of adiposity including waist circumference, waist: hip ratio, BMI and hip circumference.

1.8.4.3 Effects of H_2S on the reproductive system

Previously, H_2S was thought to have damaging effects on female and male reproductive tracts. More recently, the endogenous production of H_2S, as well as the expression of CBS and CSE, has been recognised to occur in the normal state in both male and female reproductive system in different mammalian tissues (Sugiura et al., 2005). The endogenous production of H_2S and its involvement in penile erection has been reported (d'Emmanuele di Villa Bianca et al., 2009). In the female reproductive system, H_2S plays different roles. Both CBS and CSE have also been detected in rabbit vaginal and clitoral cavernosal smooth muscle (Srilatha et al., 2009). According to Yang et al. (2008), CSE knockout mice are fertile and give birth normally. The female offspring of CBS knockout mice have decreased fertility, while male offspring are fertile. These findings point to importance of CBS in female reproductive function (Yang et al., 2008).

Another experimental study has demonstrated that CBS knockout female mice have a reduced number of developed follicles in the ovaries (Guzmán et al., 2006). Additionally, it is revealed that, H_2S has a relaxing effect on different smooth muscles. Since it is generated in the human placenta, it could be involved in sustaining uterine quiescence during pregnancy. Patel et al. (2009) reported expression of CBS and CSE enzymes in rat and human intrauterine tissues, including uterus, fetal membranes and placenta, as well as the production of H_2S by these tissues.

1.8.4.4 Effect of H$_2$S during labour

The smooth muscle relaxant effect of H$_2$S has been reported in myometrium (You et al., 2011). Hu et al. (2011) conducted a study on a human myometrium, and showed that sodium hydrosulfide (NaHS), an H$_2$S donor, inhibits spontaneous myometrial contractions with a decrease in frequency and amplitude of the contraction, and inhibits oxytocin induced contractions but with a decrease in the frequency only. In addition, experiments that focused on therapeutic properties of H$_2$S suggested its use in delaying pain of parturition and inhibiting uterus contractions in difficult deliveries in animals (Hayden et al., 1989).

1.8.4.5 H$_2$S in Pre-eclampsia

H$_2$S has been considered as a vasodilator (Zhao et al., 2001), which protects against cellular damage induced by reperfusion injury (Elrod et al., 2007) and stimulates vascular angiogenesis (Papapetropoulos et al., 2009). Cindrova-Davies et al. (2013) showed for the first time that H$_2$S is a potent vasodilator in the human placenta as it significantly reduced the perfusion pressure and vascular resistance of perfused placenta and that circulating PlGF levels are reduced in women with PE in association with dysregulation of CSE signalling pathway (Wang et al., 2013). H$_2$S is also known as a vasorelaxant and proangiogenic gas. Numerous studies have demonstrated that one of the major contributors to endothelial dysfunction, resulting in hypertension and proteinuria in PE, is increased level of sFlt-1, the soluble secreted form of VEGF receptor (Ahmad and Ahmed, 2004, Chaiworapongsa et al., 2013). However, treatment with NaHS, H$_2$S donor, for 8 days was found to significantly reduce sFlt-1 induced hypertension, proteinuria and glomerular endotheliosis by up-regulating VEGF expression in rats (Holwerda et al., 2014). Additionally, Hu et al. (2015) reported an inhibition in sFlt-1 release in cultured syncytiotrophoblasts by the H$_2$S, donor, NaHS, and precursor L-cysteine.

1.8.5 H$_2$S protects against ischemia-reperfusion injury in different tissues

Several research groups have demonstrated the cytoprotective role of H$_2$S in different tissues. Elrod et al. (2007) tested the hypothesis that H$_2$S improves myocardial function in ischemia-reperfusion injury model. The experimental model was in mice, who were subjected to 30 minutes of left coronary artery ischemia and 24 hours reperfusion. When the H$_2$S donor was administrated, Elrod and his colleagues found a significant reduction in

the size of infarction at time of reperfusion. Also, the over-expression of CSE has been shown to attenuate ischemia-reperfusion injury. The observed protection is associated with reduced myocardial inflammation, preserved mitochondrial structure and function and reduced apoptosis in cells after infarction. Similar findings were reported by Predmore et al. (2012). These results suggest the cytoprotective effect of H_2S during myocardial infarction.

In addition to the cytoprotective role in the cardiovascular system, the role of H_2S as a hepatoprotective has been demonstrated. Chen et al. (2010) investigated the cytoprotective effect of H_2S in rats against induced total hepatic ischemia and reperfusion. In that study, the proposed protective mechanisms were through inhibition of lipid peroxidation and inflammation. The study concluded that H_2S has a protective effect against hepatic ischemia-reperfusion injury and targeting H_2S may present a promising approach against liver injury.

1.9 Justification of the current research project

There is a limited amount of published data on CBS, CSE and 3-MST expression in the human placenta in normal pregnancy as well in PE and FGR (Table 1-1). Also, there is sparse data on their expression in regards to maternal obesity, which is associated with PE. Moreover, relatively little is known about the included subjects and techniques used in some previous studies. For instance, mode of delivery and gestational ages were not clear in all studies. There is also a discrepancy in reported gene expression between different studies which could be due to the difference in gestational ages at delivery or to the use of different techniques for detection. Furthermore, there is a lack of information about the sampling methods, which is important as some placental transcripts differ according to site of samples (Wyatt et al., 2005). Finally, the role of H_2S in pathogenesis of PE and FGR is still unknown; therefore, more analysis and investigation are required in order to provide better understanding to the pathogenesis of complicated pregnancies.

Table 1-1: Previous published studies on expression of H_2S synthesising enzymes in normal and abnormal placentas.

Study	Sample size	Results	comments
You et al., 2011 (CBS and CSE) Myometrium tissues	Non-labour (n=10) v labour group (n=10)	CBS and CSE mRNA levels were significantly decreased in labour group Only CBS protein level was reduced in labour group	Discrepancy between mRNA and Protein levels. Samples were randomly taken
Holwerda et al., 2012 (CBS and CSE) Human placental tissue	Control group (n=9) v early onset PE group (n=10) Control group (n=8) v late onset PE group (n=9).	Only CBS mRNA was decreased in early-onset PE No significant difference in CSE mRNA in early or late-onset PE No significant differences in CBS and CSE protein expression were detected between early and late-onset PE groups and their controls. CBS and CSE protein (not mRNA) levels were decreased in labour controls compared to non-labour controls.	Discrepancy between mRNA and Protein expression. Gestational ages were not matched between controls and PE groups. Samples were randomly taken.
Cidrova-Davies et al., 2013 (CBS and CSE) Human placental tissue	Control group (n=6) FGR group(n=6) PE (normal doppler results) (n=7) PE (abnormal doppler results) (n=6)	CSE protein and mRNA were significantly decreased in FGR and PE with abnormal doppler results. CSE protein level (not mRNA) was increased in PE with normal doppler results No significant difference in CBS protein or mRNA level in FGR or PE	Discrepancy between mRNA and Protein expression. Gestational ages were not matched among groups. Samples were randomly taken.

Wang et al., 2013 (CSE) Human placental tissue	Control (n=14) PE (n=14) Control (n=5) v PE (n=5)	Plasma levels of H_2S, CSE mRNA and CSE Immunoreactivity were decreased in PE.	Three FGR cases in the PE. Samples were randomly taken.
Hu et al., 2015 (CBS and CSE) Human placental tissues	Control group (n=19) PE group (n=18)	CBS and CSE protein levels were significantly decreased in PE	Samples were randomly taken.
Hu et al., 2017 (**3MST**) Human placental tissues	Control group (n=23) PE group (n=19)	No significant difference in 3-MST mRNA and protein expression was detected between control and PE group	Samples were randomly taken
Lu et al., 2017 (CSE) Stem villus arteries explants from FGR placentas	Control group (n=8) FGR group (n=34)	Significant reduction in CSE mRNA and immunostaining CSE protein level positively correlated with contractile smooth muscle protein markers	Samples were randomly taken

1.10 Hypothesis and aims

Little is known about the precise role of H_2S in the placenta or whether it plays a role in labour and complicated pregnancies such as PE and FGR. Also, nothing is known about H_2S synthesising enzymes expression in the placenta of obese women although oxidative and inflammatory stress pathways that have been implicated in labour and complicated pregnancies, are also associated with obesity, and may cause alteration of placental gene expression. Variation in gene expression in different areas of the placenta was previously confirmed by Wyatt et al. (2005). Beside this, a difference in spiral arteries blood flow between the centre and periphery of the placenta (Matijevic et al., 1995) was reported. Recently, H_2S has been demonstrated to be an endogenous gaseous mediator, which promotes vasodilation and exhibits cytoprotective anti-inflammatory properties. As the H_2S pathway has anti-oxidative and anti-inflammatory characteristics, it was hypothesised that placental CBS, CSE and 3-MST expression would alter during labour and in complicated pregnancies. Furthermore, it was also hypothesised that expression of these enzymes would vary at different zones of the placenta.

- The null hypothesis was there is no difference in expression of H_2S synthesising enzymes (CBS, CSE and 3-MST) between healthy and complicated pregnancies across different placental zones.

Therefore, the aims of this thesis were to examine:

1- The spatial CBS, CSE and 3-MST expression in placentas from heathy pregnant women who delivered by CS (non-labour group) and the spatial distribution was assessed by comparing the expression at inner, middle and outer placental zones within individual placentas.

2- The expression of CBS, CSE and 3-MST in placentas from complicated pregnancies with PE and FGR, and correlation of protein and transcripts levels to the placental site (inner, middle and outer).

3- The CBS, CSE and 3-MST expression in placentas from women with high BMI at different placental sites.

4- Whether the mode of delivery either normal or CS has an impact on the CBS, CSE and 3-MST expression. The difference in expression, either at mRNA or protein level was assessed by comparing the inner, middle and outer placental zones of non-labour group with the respective zones of the labour group.

5- Localisation of CBS, CSE and 3-MST proteins within normal placental tissues and placental tissues from complicated pregnancies with PE, FGR and high BMI.

Chapter 2   Materials and methods

2.1 Identifying suitable subjects

Human term placental tissues were collected from pregnant women at the Queen Elizabeth University Hospital, Glasgow. The patient details are shown in Table 2-1, 2-2 and 2-3. The placental samples were collected from:

(1) **Control groups:** Full term pregnant women with uncomplicated pregnancies, who delivered, either by spontaneous vaginal delivery (labour group (LG), n= 6) or by elective CS (non-labour group (NLG), n=6). Normal pregnancy is defined as a pregnancy with no medical complications.

All women in the labour group were delivered spontaneously, and the minimum time taken for labour was minimum 3 hours and the maximum was 8 hours. In the non-labour group, placentas were delivered by elective CS. The CS was performed for obstetric causes, such as previous CS, transverse lie, and breach presentation or on maternal request. All collected placentas were confirmed free of infection by pathology report. These groups had no underlying maternal conditions for instance, hypertension, PE, diabetes or any other medical disorders. There was no fetal pathology such as FGR or fetal anomalies in the control groups.

(2) **PE groups:** Women who had pregnancies complicated with PE, who delivered either vaginally (LG-PE, n=8) or by CS (NLG-PE, n=4). PE is defined as pregnancy induced hypertension (blood pressure $\geq$ 140/90 mmHg) and proteinuria ($\geq$ 300mg/24h) in women who were normotensive prior to pregnancy and had no any underlying renal disease (Brown et al., 2001).

(3) **FGR group:** Women who had pregnancies complicated by FGR. The Royal College of Obstetricians and Gynaecologists in Green-top Guideline No. 31 have defined FGR as "Growth restriction implies a pathological restriction of the genetic growth potential. As a result, growth restricted fetuses may manifest evidence of fetal compromise (abnormal Doppler studies, reduced liquor volume)". The number of samples in this group is (n=6), and they were obtained from severe group with estimated fetal weight less than the 5th percentile.

(4) **Obese group**: According to the National Institute for Health and Clinical Excellence (NICE), 50% of women of childbearing age are overweight (BMI 25.0-29.9 kg/m^2), and 18% are obese at the start of pregnancy. Moreover, the Confidential Enquiry into Maternal and Child health 2007 reported that pregnant women with a BMI greater than 30.0 kg/m^2 are more likely to die than those with a BMI less than 30.0 kg/m^2. Therefore, Obese women who had uncomplicated pregnancies and delivered by elective CS were studied. This group includes samples from women who are obese (their BMI a greater than or equal to 30.0 kg/m^2) (n=13). This group was compared to the control placental samples (n=6) that were collected from women with BMI less than 30kg/m^2.

2.1.1 Exclusion criteria

Pregnant women who were smokers were excluded from all groups. Women with an essential hypertension or diabetes were excluded from all groups. Multiple pregnancy and pregnancies with fetal pathology such as fetal anomalies were excluded from all groups.

2.2 Ethical approval

The ethical approval for this project was performed according to Declaration of Helsinki. The project was approved by the West of Scotland research ethics service (REC reference number 13/WS/0149, IRAS ID 130896). The women who participated in the study were provided with an information sheet to explain what the research is about, before they gave their consents. All information sheets, consent form and ethical approval for this study are shown in Appendix 1. Signed consents were saved in case required for future audit. All the consent was obtained by the department. Placental samples were stored within the Institute of Medical Genetics, University of Glasgow.

Table 2-1: Control patient clinical details. NLG (non-labour group) (n = 6); LG (labour Group) (n = 6); ELC/S (elective caesarean section); EMC/S (emergency caesarean section); SVD (spontaneous vaginal delivery); PG (primigravida); G (refer to the number of pregnancies the woman has had); P (refers to the number of live children from these pregnancies).

Sample	Age	Parity	Smoker	Gestation (weeks/days)	Birth weight (g)	Placenta weight (g)	Mode of delivery	BMI
NLG	26	G3P2	NO	40+3	3809	840	ELC/S	28.5
NLG	36	G2P1	NO	39+1	4220	630	ELC/S	23
NLG	25	G3P1^{+1}	NO	40	5250	980	ELC/S	24.1
NLG	32	G2P1	NO	39	4255	605	ELC/S	27
NLG	32	G2P1	NO	39	3510	716	ELC/S	24.4
NLG	30	G2P1	NO	39 +2	3000	560	ELC/S	26
LG	27	PG	NO	40 +4	4192	585	SVD	24
LG	28	PG	NO	40+2	3646	595	SVD	28
LG	22	PG	NO	41+3	3940	700	EMC/S	34
LG	25	PG	NO	41+3	3310	486	SVD	24
LG	28	G3P2	NO	37+6	3354	636	SVD	26
LG	26	G4P3	NO	41+1	3870	535	SVD	33.9

Table 2-2: PE and FGR patient clinical details. NLG-PE (non-labour pre-eclampsia) (n = 4); LG-PE (labour pre-eclampsia) (n = 8); LG-FGR (labour fetal growth restriction) (n = 6); P0+2 (means 2 miscarriages); FVD refers to forceps' vaginal delivery.

Sample	Age	Parity	Smoker	Gestation (weeks/days)	Birth weight (g)	Placenta weight (g)	Mode of delivery	BMI
NLG-PE	34	G3P2	NO	39	3490	592	ELC/S	27
NLG-PE	33	PG	NO	36+6	2800	450	ELC/S	39
NLG-PE	38	G2P1	NO	39	3736	695	ELC/S	47.2
NLG-PE	29	G2P1	NO	37+3	3210	675	ELC/S	32.2
LG-PE	42	G6P4	NO	36+6	2248	449	EMC/S	29
LG-PE	32	PG	NO	38+1	2812	521	SVD	23
LG-PE	30	PG	NO	28+5	1230	265	EMC/S	29.7
LG-PE	32	PG	NO	38+3	2990	420	EMC/S	21.9
LG-PE	28	PG	NO	40+6	3530	692	SVD	26.7
LG-PE	17	PG	NO	29+2	1260	317	EMC/S	23
LG-PE	20	PG	NO	38+6	3526	800	EMC/S	22.8
LG-PE	27	PG	NO	39+6	3400	480	FVD	28.6

LG-FGR	27	G4P2	NO	37	1880	310	SVD	29
LG-FGR	33	G2P1	NO	35+2	1850	370	EMC/S	34.5
LG-FGR	32	G8P0	NO	37+4	1990	265	EMC/S	39
LG-FGR	23	PG	NO	38+4	2880	427	SVD	22.4
LG-FGR	28	G3P2	NO	37+2	2075	324	EMC/S	20.1
LG-FGR	22	PG	NO	37+6	2368	470	EMC/S	21.3

Table 2-3: BMI patient clinical details. BMI C (control group): BMI less than 30 (n=6). BMI 1 group: BMI is equal to or greater than 30 (n=13).

Sample	Age	Parity	Smoker	Gestation (weeks/days)	Birth weight (g)	Placenta weight (g)	Mode of delivery	BMI
BMI C	26	G3P2	NO	40+3	3809	840	ELC/S	28.5
BMI C	30	G2P1	NO	39 +2	3000	560	ELC/S	26
BMI C	32	G2P1	NO	39	4255	605	ELC/S	27
BMI C	25	G3P1^{+1}	NO	40	5250	980	ELC/S	24.1
BMI C	32	G2P1	NO	39	3510	716	ELC/S	24.4

BMI C	36	G2P1	NO	39+1	4220	630	ELC/S	23
BMI 1	37	PG	NO	38+3	3460	595	ELC/S	33.1
BMI 2	29	G2P1	NO	37+3	3210	675	ELC/S	32.2
BMI 3	43	G4P3	NO	37	3515	750	ELC/S	32.8
BMI 4	25	G2P1	NO	39+5	3770	690	ELC/S	36.7
BMI 5	32	PG	NO	38+5	2740	430	ELC/S	37.9
BMI 6	36	G2P1	NO	39+3	4035	790	ELC/S	35.9
BMI 7	40	G3P2	NA	38+4	4850	940	ELC/S	36.6
BMI 8	29	G3P2	NO	39+3	4015	955	ELC/S	40.3
BMI 9	46	G3P1^{+1}	NO	38	2845	590	ELC/S	42.3
BMI 10	42	G3P2	NO	39+3	3550	685	ELC/S	44.7
BMI 11	38	G2P1	NO	39	3736	695	ELC/S	47.2
BMI 12	25	G3P1^{+1}	NO	38+4	3575	645	ELC/S	49
BMI 13	33	G2P1	NO	39+2	2940	494	ELC/S	52

2.3 Placental sampling methods

The placenta was collected immediately after either normal delivery or CS and washed with tap water to remove blood. The amnion was removed and then the placenta was weighed. All placentas had central cord insertion. The samples were collected according to a systemic sampling method. The placenta was divided by concentric circles into 3 sites (inner, middle and, outer) by taking the measurement from the cord insertion point. Briefly, the inner site is the inner third which is closer to the cord insertion, the outer site is the outer third closes to the periphery of the placenta and the middle is in between. Each zone was divided into quadrants. From each site, full thickness placental samples (about 1cm^3) were taken from the inner, middle and outer zones of the placenta at about 2, 4, 6 cm from the umbilical cord insertion, respectively as illustrated in Figure 2-1. Within each zone four separate samples were obtained representing the four quadrants. In the FGR placentas, there were only two zones (inner and outer) because the placenta was smaller. Within each zone, four separate samples were obtained representing the four quadrants. The samples were immediately flash frozen in liquid nitrogen. The rest of the placenta was transported to the Pathology Department to be examined by a pathologist.
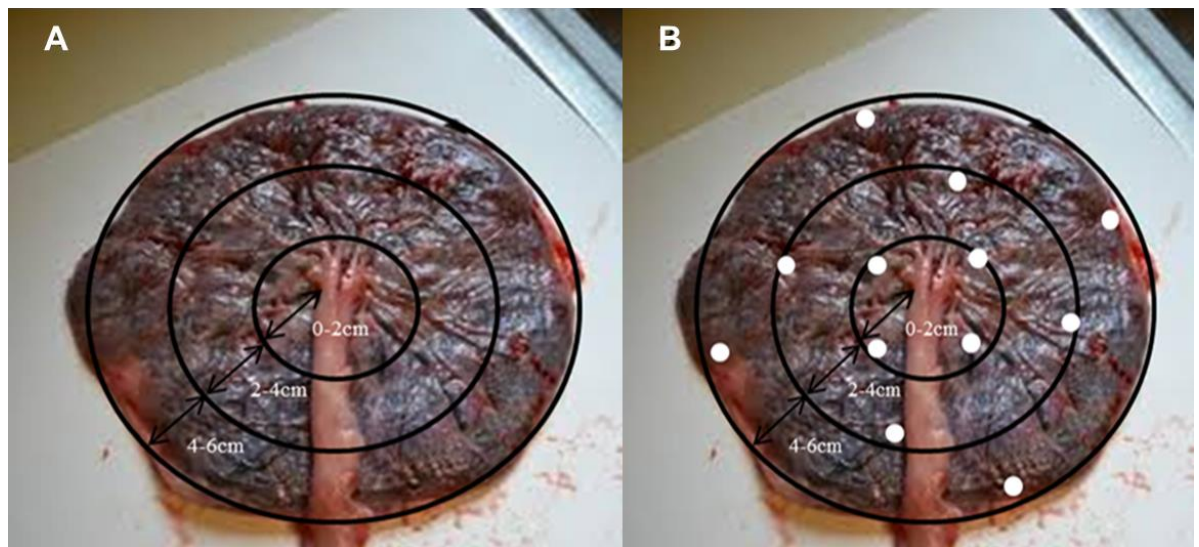
Figure 2-1 The sampling method of placentas. (A) shows how a placenta is divided into three zones. (B) shows areas where samples were taken in each individual placenta.

2.4 Placental collection and processing for protein and mRNA analysis

All equipment used for processing the tissue was cleaned with 70% ethanol to sterilise them before use and a number of labelled cryostat containers equal to the number of samples that would be used for storage of snap frozen samples were put on dry ice to ensure they were

also at a low temperature. Tissue samples were collected according to the systemic sampling method. The obtained samples were washed in phosphate buffered saline (PBS, Sigma-Aldrich, cat.no. P4417-50TAB) three times. The PBS is a solution of one PBS tablet per 100ml Ultra-pure water (UP-H$_2$O). The washed samples then were frozen immediately in liquid nitrogen. Snap frozen tissues were then brought to the laboratory on dry ice and stored at -80C° to be retrieved at the appropriate time for protein extraction, RNA extraction and immunohistochemistry (IHC).

2.5 mRNA expression analysis

2.5.1 RNA extraction from placental tissues and quantification of RNA

2.5.1.1 Extraction of RNA

Snap frozen placental tissues were retrieved from -80°C storage. All equipment was cleaned with RNase ZAP (Sigma-Aldrich, cat. no. R2020-250ML) (cleaning agent for removing RNase) and then with 70% ethanol. RNeasy Midi Kit for soft tissues (Qiagen, cat. no. 75142) was used. The placental tissue was weighed before starting the homogenisation. As determined by previous experiments, the optimum amount of placental tissue was between 150-200 mg.

The weighed placental tissue was placed into suitably sized vessel, which contained 4ml RLT buffer (buffer provided with kit) supplemented with beta-mercaptoethanol (ß-ME) (10 µl ß-ME per 1 ml buffer RLT), for disruption and homogenisation. The tissue was then homogenised using a Rotor-stator homogeniser (Polytron PT1600E, Lucerne, Kinematica) at setting full speed for 3x20 seconds. The tissue lysate was centrifuged at 4000 x g and 25°C for 10 minutes, in order to remove insoluble materials, and then the supernatant (lysate) was carefully transferred to a new 10-15 ml Falcon tube (Sigma-Aldrich, cat. no. Z617849). After that, a volume of 70% ethanol equal to the initial homogenate volume was added to supernatant to optimise subsequent binding of RNA to the silica column, and mixed immediately by shaking vigorously until clear solution was obtained. This solution was applied to an RNeasy column in a 15ml collection tube, and then spun in the centrifuge for 5 minutes at 4000 x g, and the flow-through was then discarded. This was repeated twice until all the mixed supernatant had gone through the column. Then, 4ml of RW1 buffer

(provided in kit) was added to the RNeasy column then spun down in the centrifuge at 4000 x g, 25°C for 5 minutes, and then the flow-through was discarded.

Once completed, to wash the column, 2.5 ml of RPE buffer (provided in the kit) was added to each column which was then spun down in the centrifuge at 4000 x g for 2 minutes. Another 2.5 ml of RPE buffer was added to each spin column then again spun down in the centrifuge at 4000 x g, 25°C for 5 minutes, to dry the RNeasy silica-gel membrane since residual ethanol may interfere with downstream reactions. The RNeasy columns were removed from their original collection tubes and put in new ones (supplied in the kit) to ensure no ethanol in the RPE buffer in the flow through from the last step of centrifugation is present on the spin column.

For RNA elution, 250 µl of RNase-free water was added directly into the membrane of the spin columns and allowed to stand for 1 minute. After this they were spun down in the centrifuge for 3 minutes at 4000 x g and 25°C to collect the RNA eluted from the column, and then this step was repeated twice. Finally, the RNA was aliquoted and stored at -80°C.

2.5.1.2 Quantification of RNA

Once RNA was successfully eluted in RNase free water, the RNA concentration (ng/µl) was measured using a spectrophotometer-NanoDrop® (Thermo Scientific, USA). The absorbance at 260 nm was used to determine the concentration of RNA using the Beer-Lambert equation encoded in the instrument's software. The ratio 260/280 nm gives an indication of RNA purity, a value close to 2 indicates optimal purity.

2.5.2 Reverse transcription (RT) of mRNA (Converting mRNA into cDNA)

RNA cannot serve as a temple for PCR so a reverse transcription reaction is required. The RNA was reverse transcribed into cDNA using reagents from the QuantiTect® Reverse transcription Kit (Qiagen, cat. no. 205311) and GoScript™ reverse transcriptase (Promega, cat. no. A5003) because, in an initial optimisation process (carried out by another student), the quality of cDNA obtained using GoScript™ reverse transcriptase was better than the one obtained using reverse transcriptase of the Qiagen kit.

The QuantiTect® Reverse transcription Kit includes the following: Wipeout buffer, QuantiScript RT buffer, RT primer Mix and RNase free water. Converting mRNA into cDNA was carried out by two steps:

- **Genomic (gDNA) elimination reaction:**

Residual contaminating genomic DNA was eliminated using the Wipeout® buffer (mechanism is undisclosed by the manufacture). 100 ng of RNA in 12 µl was incubated with 2 µl of Wipeout buffer in a thermal cycler (DNA Engine®, Bio-Rad) for 3 minutes at 42°C.

- **Reverse transcript (RT) reaction:**

Once the genomic elimination was completed, 1 µl of GoScript Reverse transcriptase (Promega), 1 µl of RT primer Mix (Qiagen kit) and 4 µl of RT Buffer (Qiagen kit) were added to each tube and PCR tubes were again placed in the thermal cycle for 30 minutes at 42°C and 5 minutes at 95°C (enzyme deactivation). Once the reaction was completed, the newly made cDNA was put into -20°C storage.

2.5.3 Quantitative real time polymerase chain reaction (RT-qPCR)

qPCR was performed using TaqMan human gene expression assays predesigned by Applied Biosystems (Table 2-4) and chosen to maximise the number of RefSeq transcripts recognised. These assays were designed across exon-exon junction to eliminate amplification from residual undegraded genomic DNA. The assay for CBS also detects cystathionine β-synthase like gene (CBSL). This assay detects five CBS mRNA transcript variants (RefSeq (NM)), encoding protein isoform 1 and 2. Also, it detects about 20 predicted mRNA model transcript variants (RefSeq (XM)). The assay for CSE/CTH mRNA also detects the maximum number of transcripts for the CTH gene, and does not detect gene products with similar sequences as predicted by the manufacture. The assay for CTH gene detects all three RefSeq (NM), encoding different isoforms and two 2 RefSeq (XM). The assay for MPST/3-MST gene detects three RefSeq (NM) and 1 RefSeq (XM). NM is referred to known mRNAs that are derived from GenBank cDNA data, and XM is referred to model mRNA sequences that are generated by computational prediction.

All gene expression assays have FAM™ reporter dye at the 5' end of the probe and a non-fluorescent quencher at the 3' end of the probe (TaqMan® MGB probes). TaqMan® MGB

probes and PCR primers have been premixed to a concentration of 5 uM and 18 uM, respectively. All gene expression assays amplicon length were less than 150 base pairs (bp) (endogenous control amplicon length was 171 bp).

All equipment and work bench were cleaned with 70% ethanol before starting this method to eliminate DNA contamination. cDNA was removed from -20°C storage and put on wet ice to thaw. qPCR was performed from reverse transcribed cDNA samples using the quantitative PCR StepOnePlus® machine (applied Biosystems). Briefly, 100 ng of cDNA were diluted 1:5 in RNase-free water (1µl cDNA+ 4µl RNase free water) and then added to a 96-well MicroAmp® Fast Optical Reaction Plate (Applied Biosystems, cat.no. 4346906) with 10 µl of TaqMan Master mix (Applied Biosystems, cat.no. 4369514), 4 µl RNase-free water and 1 µl TaqMan Gene Expression Assay (either gene-specific inventoried assays or endogenous reference assays). The total volume in each well was 20µl. A plastic film or cover (Applied Biosystems, cat.no. 4311971) was placed on the plate after it was set up. The plate was mixed and then centrifuged (4860 g for 90 seconds) to remove any bubbles. Finally, the plate was placed in a RT-PCR StepOnePlus machine and the reactions were run for 50 cycles; initial holding stage at 50°C for 2 minutes and then 95°C for 10 minutes, followed by cycling stage at 95°C for 15 seconds for denaturation and 60°C for 1 minute for annealing and extension.

The samples and the controls were measured in triplicate (technical replicates) to test the reproducibility of the RT-PCR technology (instruments and reagents) and detect outliers. β-actin (Applied Biosystems, cat. no. 4331182 / Hs99999903-m1) was used as an endogenous control for normalising relative expression levels in the different RNA samples. β-actin was chosen because it has previously been demonstrated as a suitable endogenous control in this laboratory. Moreover, Lanoix et al. (2012) found that β-actin is more stably expressed than Glyceraldehyde-3-phosphate dehydrogenase (GAPDH) and α-tubulin in placentas from normal pregnancies and complicated pregnancies with PE. Furthermore, Baek et al. (2008) reported that oxidative stress is a known inducer of GAPDH expression, therefore it is not a suitable for comparison between normal and complicated pregnancies with PE, FGR or gestational diabetes mellitus because placental oxidative stress is a hallmark of these pregnancy complications. UP-H_2O was used as a negative control to test for presence of any contaminating amplifiable DNA. The degree of differential gene expression was measured using the comparative CT methods of Applied Biosystem software® v2.1.

Table 2-4: The TaqMan Gene Expression Assays.

Assay ID	Gene name	Gene symbol	Assay design	Amplicon length
Hs99999903-m1	Actin beta	ACTB	amplicon spans exons and probe does not span exons	171
Hs00163925-m1	Cystathionine-beta-synthase/	CBS	Probe spans exons	59
	Cystathionine-beta-synthase like	CBSL		
Hs00542284-m1	Cystathionine gamma-lyase	CTH	Probe spans exons	110
Hs00560401-m1	Mercaptopyruvate sulfurtransferase	MPST	Probe spans exons	81

Hs means Homo sapiens and m means an assay whose probe spans an exon junction.

2.5.4 qPCR data analysis

Differential gene expressions in samples were quantified using the comparative C_T method ($\Delta\Delta C_T$) as described by Livak and Schmittgen (2001) in which the change in expression of a target gene in one group relative to the control group is calculated after normalising to any differential levels of amplifiable cDNA of and endogenous reference gene whose actual expression level is assumed to be constant.

The endogenous control was β-actin, whose mRNA expressions levels are assumed to be constant in all cell types analysed here. In any sample the known expression of β-actin gene was measured against the unknown expression of a gene of interest. This is performed in order to account for intra sample variation of cDNA quality and quantity. Therefore, the level of expression i.e. C_T of the endogenous control in each sample is measured against the C_T of the gene of interest in each sample. This provides the ΔC_T value. The high ΔC_Ts represent low expression, while highly expressed genes have low ΔC_Ts.

To determine the fold change, first of all, the C_T values for each sample should be normalised to obtain ΔC_T. For each group, the mean C_T of endogenous control β-actin was subtracted from the corresponding mean C_T value of a gene of interest to give ΔC_T (C_T gene of interest - C_T β-actin). Then a $\Delta\Delta C_T$ was obtained by subtracting ΔC_T of sample from the mean ΔC_T of the control group. Finally, due to the exponential nature of PCR, the actual fold change (FC) in expression was determined by raising 2 to the power of the negative value of $\Delta\Delta C_T$ ($2^{-\Delta\Delta C_T}$) for each sample (Amount of target = $2^{-\Delta\Delta C_T}$) (using the TaqMan technology,

the efficiency is assumed to be close to 100% and also the same for each reaction with the same primers/probe (Applied Biosystems 2006). The fold change (FC) of a given gene is measured as a ratio and these raw ratios were then log-transformed, usually $\log_2$. The $\log_2$ FC (the log-transformed values on a liner scale) is calculated and this is expected to give a mean log-ratio of zero and improve the symmetry of data distribution. In order to visualise the differences in gene expression across samples, the $\log_2$ fold change values (normalised and transformed) were calculated and presented as a heat map.

2.6 Placental tissue preparation for protein expression analysis

2.6.1 Homogenisation of placental tissues

2.6.1.1 Buffers used in the homogenisation (1L)

Tris (Sigma-Aldrich, cat.no.93352), EDTA (Sigma-Aldrich, cat.no. E6758), Sucrose (Sigma-Aldrich, cat.no. S9378) and Protease Inhibitor Cocktail (Sigma-Aldrich, cat.no. P8340-5ml) were used.

Homogenisation buffer contained 1L of dH_2O, 25 mM Tris (3.02g), 1 mM ethylenediaminetetraacetic acid (EDTA) (0.4g), and 250 mM sucrose (85.6g). The buffer pH was adjusted to 7.6 with HCl and the buffer was stored at 4ºC. 12.5µl/ml mammalian cell protease inhibitor cocktail (250µl in 20ml of the buffer) was added immediately prior to use on the day of the experiment to prevent proteolysis.

2.6.1.2 Placental tissue homogenisation

An appropriate volume (20ml) of tissue homogenising buffer was added into a sterile universal container, and then 250µl of protease inhibitor cocktail was added to the universal container immediately before use. The prepared homogenising buffer was put on ice at 4ºC. Relevant tissue samples were collected from -80ºC storage and immediately put on dry ice. Mortar and pestle were retrieved, and liquid nitrogen was poured into the mortar to cool down them before use. The sample was added and ground down rapidly to fine powder. After that, the ground tissue was put into the bijous and reweighed without lid to determine the weight of the tissue. The homogenisation buffer was added to the fine powder at a final ratio of 3:1 (v/w). The tissue in buffer samples were homogenised using a rotor-stator homogenizer (Polytron® PT 1600E, Lucerne) at speed "20". For each sample, the homogenisation was carried out in 5 bursts, 10 second each with a minute cooling interval.

Next, the tissue samples in bijous were left on ice, and labelled 15 ml tubes were retrieved to aliquot the tissue lysate into each of them. Placental homogenates were centrifuged at (5000 x g for 10 minutes at 4ºC) to remove debris. The supernatant contained total cytosolic protein was allocated to new labelled 1.5ml Eppendorf tubes and then stored at - 80Cº.

2.6.2 Determination of total protein concentration (Bradford's assay)

The Bradford protein assay was used to quantify total protein concentrations. A stock standard solution (STD) of bovine serum albumin (BSA) (Sigma-Aldrich, cat. no. A 7906-100G) (1mg of BSA per ml of dH_2O) was used to create the standard curve. STD of 10 mg BSA in 10ml UP-H_2O was made and kept in the fridge. A series of standard solutions (STD) were made up at 0, 200, 400, 600, 800 and1000 µg/ml as shown in Table 2-5.

Table 2-5: Standards stock dilution (µg/ml).

STD concentration (µg/ml)	Vol. stock STD (µl)	Vol. of UP-H_2O (µl)
0	n/a	50
200	10	40
400	20	30
600	30	20
800	40	10
1000	50	n/a

For each concentration, an Eppendorf tube was used, and then the UP-H_2O was added first followed by STD solution. The total volume in each tube was 50µl. The placenta protein samples were diluted by 1:7 (56 µl of UP-H_2O and 8 µl of homogenate). For standards and sample assay preparation, a new tube for each STD solution and sample was labelled, and then 10µl of each STD solution or diluted sample was added after mixing by vortexing. Next, 200µl of Bradford's reagent (Sigma-Aldrich, cat. no. B6916-500ML) was added to each tube containing 10µl of standards or samples then all tubes were mixed on vortex and left for 20 minutes. Absorbance at 595nm was then measured for each sample solution using a NanoDrop 1000 spectrophotometer. A standard curve was created of absorbance against different BSA concentrations and this was used to find the concentration of protein samples (Figure 2-2). For a western blot 20-40 µg was used for sample loading.

BSA standard curve

$y = 0.0001x + 0.0023$
$R^2 = 0.996$
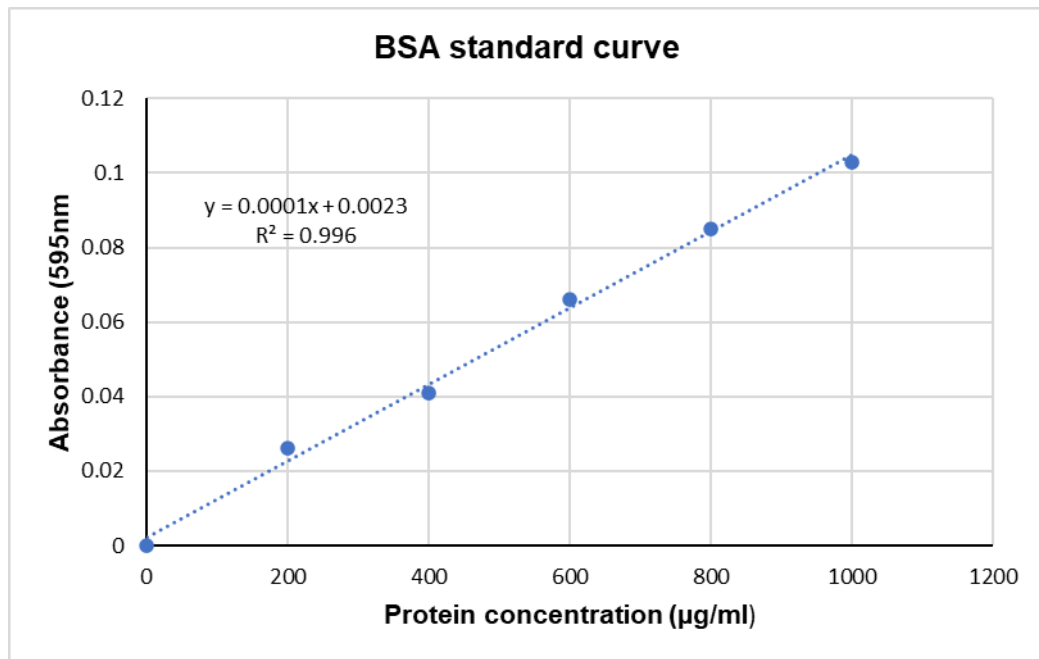
Figure 2-2 BSA standard curve using Bradford assay. A plot of absorbance vs a varying amount of some known concentration of BSA protein; in equation (x) stands for sample concentration and (y) stands for average net absorbance.

2.7 Western blotting (Immunoblot) for protein expression analysis

2.7.1 Samples preparation and gel electrophoresis

2.7.1.1 Sample preparation

Protein lysate samples 20-40 μg were mixed with 4X NuPAGE LDS sample buffer (Invitrogen™, cat.no. NP0007) to a final concentration of 1X with 5% (v/v) β-ME (Sigma-Aldrich, cat. no. M3148) in a final volume of 40 μl, then samples were incubated in water bath at 70 C° for 15 minutes to fully denature proteins and allow protein-detergent complexes to form.

2.7.1.2 Gel electrophoresis

Pre-cast NuPAGE® 4-12% Bis-Tris gels (Invitrogen™, cat. no. NP0321-NP0323) were used. The gels were run in the Invitrogen™ Novex™ XCell™ SureLock™ running system. Prior to sample loading, the comb was removed and the well were flushed with running buffer. Samples were loaded onto the gel with 8 μl SeeBlue Plus 2® Standard Ladder (Invitrogen™, cat. no. LC5925) in 1X MES (2-N-morpholino ethanesulfonic acid) SDS running Buffer (Novex, cat. no. NP0002) then proteins were separated by electrophoresis at 200V for 22 minutes. SeeBlue™ Plus 2 Standard Ladder is a mixture of ten proteins,

generating ten reference bands (198, 98, 62, 49, 38, 28, 17, 14, 6, 3 kDa (Kilo Dalton)). As well as providing size estimation, the ladder served to monitoring progress of electrophoresis, checking transfer efficiency, and for orienting the subsequent immunoblot.

2.7.1.3 Coomassie staining

For total protein visualisation by Coomassie staining, gels were fixed in a solution of 50% methanol (v/v) and 10% glacial acetic acid (v/v) for 1 hour at room temperature with gentle agitation. The gel was then placed in the Coomassie blue solution (0.25% (w/v) of Coomassie blue R-250 in 45% methanol (v/v) and 10% acetic acid (v/v) and incubated for 30 minutes at room temperature with gentle agitation. The gel was destained in a solution of 40% methanol (v/v) and 10% acetic acid (v/v) for 5-6 hours at room temperature with agitation and with replenishment the solution several times until background of the gel was clear.

2.7.2 Transfer of proteins to nitrocellulose membranes

Separated proteins were transferred from the gel onto Whatman® Protran nitrocellulose transfer membranes (Thermo Scientific, cat. no. 88018) as follows. Nitrocellulose transfer membrane, two sheets of Whatman® 3-10 mm filter paper and four sponge pads were pre-soaked in transfer buffer 1X NuPAGE transfer buffer (Novex NuPAGE, cat. no. NP0006-1) supplemented with 10% (v/v) methanol for 10-30 minutes. After electrophoresis, the gel was gently separated from the gel plates and placed on a filter paper and then the nitrocellulose membrane was placed on the top of the gel and "sandwich" of filter paper and sponge pads was assembled. This was inserted into a XCell™ blot module filled with the transfer buffer. The transfer was performed at 30 V for an hour and 30 minutes. Successful and sufficient transfer was indicated by full transfer of SeeBlue Plus 2 protein ladder onto the nitrocellulose membrane and by staining with Ponceau S solution (Sigma-Aldrich, cat. no. P7170). Ponceau S solution was used to ensure the protein transfer and also served as a measure of sample loading. Once done, the nitrocellulose was de-stained in dH$_2$O.

2.7.3 Immuno-detection of proteins

Tris-buffered saline with Tween-20 (TBST) was prepared by adding 1.21 g Tris-base (10 mM), 5.85 g sodium chloride (100 mM) (Sigma-Aldrich, cat. no. S7653), 1 ml of Tween-20 (0.1%) (Sigma-Aldrich, cat. no. P1379-1L). into 1L of dH$_2$O, pH adjusted to 7.6 with 5M HCl.

The Membranes were blocked in 5% (w/v) dried skimmed milk in TBST buffer for an hour at room temperature with gentle agitation. After blocking, the membranes were incubated with the primary antibody of interest, which was diluted in 5% BSA (w/v) in TBST, for 1 hour at room temperature with agitation (3-MST and β-actin) or overnight at 4 °C with agitation (CBS and CSE) (Table 2-6). The membranes were then washed three times, 5 minutes each, in TBST and then incubated for an hour at room temperature with an appropriate horseradish peroxidase (HRP) conjugated anti-immunoglobulin G (IgG) secondary antibody (Table 2-7) diluted in blocking solution with agitation. After that, membranes were washed three times in TBST for 5 minutes each.

Table 2-6: List of primary antibodies for western blotting.

Antibody	company	Catalogue number	Dilution	Host & clonality	Expected size of protein detected
Anti-CBS	Abcam	ab131155	1:1000	Rabbit monoclonal	61 kDa
Anti-CSE	Novusbio	H00001491-M01	1:2000	Mouse monoclonal	45 kDa
Anti-3-MST	Novusbio	NBP1-82617	1:250	Rabbit polyclonal	33 kDa
Anti-β-actin	Abcam	ab8227	1:2000	Rabbit polyclonal	42 kDa
Anti-α-tubulin	Abcam	ab4074	1:2000	Rabbit polyclonal	50 kDa

Table 2-7: List of secondary antibodies.

Antibody	Supplier	Catalogue number	Dilution	conjugate
Donkey anti-rabbit	Abcam	Ab7083	1:3000	HRP
Goat ant-rabbit	Abcam	Ab6721	1:5000	HRP
Goat anti-mouse (1)	Novusbio	NB7511	1:10000	HRP
Goat anti-mouse (2)	Dako	P 0447	1:1000	HRP
Donkey anti-mouse	Abcam	Ab6820	1:10000	HRP

2.7.4 Detection and image analysis

Immunologically reactive proteins were visualised using Pierce™ ECL western blotting substrate (Thermo Scientific, cat. no. 32106) (pre-made) or the "home-made" ECL reagents prepared as shown in Table 2-8. Reagents A and B were mixed in ratio 1:1 immediately

before use and placed on the membranes for a minute. Excess solution was drained off then the membranes were wrapped in Saran wrap. Emitted light was detected using a cooled (-30°C) CCD camera imaging system (LAS-3000 Fuji) and ImageReader LAS-3000 software. The membranes were exposed for appropriate periods of time to obtain the correctly exposed bands that were not saturated (indicated by the device and software). Molecular weight (MW) of proteins was estimated by comparison with prestained coloured markers. The position of these relative to bands obtained by ECL imaging was determined using a ruler visible by both eye and by luminescence positioned beside the membrane during ECL imaging. Band intensities were quantitatively analysed with AIDA analysis software (Fuji).

Table 2-8: Composition of reagents for "home-made" ECL procedure.

Reagent A	Reagent B
1 ml luminol solution (Sigma, cat, no. A8511) (made up to 250 mM in DMSO.	64 µl 30% hydrogen peroxide (H_2O_2)
0.44 ml coumaric acid (Sigma, cat, no. C9008) (made up to 90 mM in DMSO.	10 ml Tris-Hcl, 1M PH 8.5
10 ml Tris-Hcl 1M, PH 8.5	UP-H_2O up to a final volume of 100 ml
UP-H_2O up to a final volume of 100 ml	
Both solutions were kept in 1 ml aliquots and stored at - 80 °C for a longer storage.	

2.7.5 Re-probing of western blots

Stripping buffer (pH 6.7) was prepared by adding tris HCL 4.9 g (62mM), 10 g SDS (2%) and 3.5 ml of β-ME (0.1M) into 500 ml of dH_2O).

Blots were stripped and re-probed with anti-β-actin antibody. Bound primary antibodies were removed from the membranes by placing the membrane in stripping buffer for 1 hour at 60°C with gentle agitation. Blots were then rinsed with distilled water and washed with TBST (3 x 5 minutes each) in mild agitation. To check for successful removal of antibody, ECL detection of any residual HRP signal was carried out and images were taken at the same exposure time used before the stripping process. If there was no detectable signal on the membrane, the membrane then re-blocked and next round of immunodetection was performed, as previously described.

2.8 Cell culture

Two cell lines were used in this project:

1. Human trophoblast-derived choriocarcinoma (BeWo): these cells were obtained from Fiona Jordan at Passage 7 (frozen on 28/04/2004 by (ANW)).

2. Human breast cancer cells (MCF-7): these cells were obtained from Dr Andrew Hamilton, at Passage 25 (frozen on 25/5/2015).

3. Human embryonic kidney cells (HEK293): these cells were obtained from Dr Andrew Hamilton, at Passage 6 (frozen on 25/3/2019).

2.8.1 Cells maintenance, subculturing, freezing and storage

The cells were retrieved from liquid nitrogen storage and incubated at 37°C straight away till fully thawed. The cell suspension was transferred gently into 15ml centrifuge tube and 10 ml of supplemented media were added slowly drop by drop into the tube to slowly dilute the freezing medium. The cells were centrifuged at 1000 x g for 3 minutes and cell pellet was then resuspended with the recommended supplemented growth medium and dispensed into a culture flask. The cells were grown in 25 cm^2 or 75 cm^2 cell culture flask in a humidified atmosphere with 5% CO_2 and 37°C temperature for either routine splits or experimental work. The cells were handled all the time under strict aseptic conditions in a biological safety unit class II laminar flow hood. The media for cultured cells were renewed 3 to 4 times per week. The cells were routinely observed under an inverted microscope at 100x and 400x magnification. Satisfactory growth was indicated by the presence of few floating cells and morphology and doubling time consistent with the literature on that line.

2.8.1.1 The human choriocarcinoma (BeWo) cells

BeWo cells were cultivated in Ham's F-12 Nutrient Mix medium which is already supplemented with 1mM L-glutamine (Gibco, cat. no. 11765-054). The medium was supplemented with 10% (v/v) of FBS (Gibco, cat no. 10270-106) (not heat inactivated) and 1% (v/v) penicillin/ streptomycin (Gibco, cat. no. 15140-122). When BeWo cells in 25 cm^2 cell culture flask had grown and reached confluency (90-100%), they were split by 1:5 dilution for continuation as follows. The culture medium was removed and discarded. The adherent cells were rinsed gently with Dulbecco's Phosphate Buffer Saline 1X (PBS)

(Gibco, cat. no. 14190-094) to remove all traces of serum which contains trypsin inhibitors. Then the cells were trypsinised with 500 µl of 0.05% Trypsin-EDTA 1X solution (Gibco, cat. no. 25300-054), and the flask was placed in the humidified incubator at 37°C and 5% CO_2 for about 5 minutes to detach cells. Hand agitation was used to assist cells detachment and the cells were observed under the microscope until cell layer was fully detached. 10 ml of fresh supplemented medium was added to inhibit the enzyme activity and 1 ml of this cell suspension was added to a new 25 cm^2 culture flask containing 4 ml of the fresh supplemented medium.

2.8.1.2 Female human breast cancer (MCF-7) cells

MCF-7 cells were cultivated in Dulbecco's Modified Eagle Medium- high glucose (DMEM) (Gibco, cat. no. D6546). The medium was supplemented with 2 mM Glutamaine (Sigma, cat. no. G7513), 10% (v/v) of FBS and 1% (v/v) penicillin/ streptomycin. The cells were split twice a week in the same conditions and steps as BeWo cells.

2.8.1.3 Female human embryonic kidney (HEK 293) cells

HEK 293 cells were cultivated in Dulbecco's Modified Eagle Medium- high glucose (DMEM). The medium was supplemented with 2 mM Glutamaine and 10% (v/v) of FBS and 1% (v/v) penicillin/ streptomycin. The cells were split twice a week in the same conditions and steps as BeWo cells.

2.8.1.4 cell culture freezing and storage

Regarding cell culture freezing and storage, cells were routinely grown in corning 75 cm^2 cell culture flasks for freezing. The earlier passage cells were frozen down in Recovery ^{TM} cell culture freezing medium (Gibco, cat. no. 12648-010) when the cells were 90-100 confluent. This was performed through trypsinization of cells with 500 µl of trypsin and neutralisation with 10 ml of the regular growth medium for that line. Then, cells were collected by centrifuging at 1000 x g for 3 minutes. The culture medium was removed and the cells were gently resuspended in 3 ml of recovery freezing medium. Each 1 ml of cell suspension was added into sterile labelled cryogenic vials that were stored at -20°C for about 2 hours, then placed at -80°C overnight, then finally transferred to liquid nitrogen for long term storage.

2.8.2 Preparation of cell lysate from cell culture (protein extraction)

As much as possible, extraction of protein from cell lines was carried out the same way as for protein extracted from placental samples to make comparison of results from these two difference sources more comparable. Cells were grown to 95-100 % confluence on T25 cm^2 flask for total protein isolation. Medium was removed, and cells were washed with ice-cold PBS. The PBS was drained and then 2ml of ice-cold lysis buffer (homogenisation buffer, section 2.6.1.1) supplemented with protease cocktail inhibitors (according to the manufacture recommendation) were added. The adherent cells were scraped off the flask using a cold plastic cell scraper. The cells suspension was gently transferred into a pre-cooled microcentrifuge tube after homogenising with an electric homogeniser at speed 20 for 5 bursts each one is 10 seconds with a minute cool down on wet ice. Lysates were centrifuged at 5000 x g for 10minutes in a 4 °C pre-cooled centrifuge to remove insoluble debris. Protein lysate (supernatant) was transferred to a fresh labelled tube and then samples were stored at -80 °C for later use for protein quantification or loading onto a gel.

2.8.3 Determination of protein concentration

For quantification of the protein in samples, BCA (Bicinchoninic Acid) protein assay was performed using Pierce BCA protein assay kit (Thermo, cat. no. 23225). In BCA assay, the protein is measured at its wavelength maximum of 562nm.

2.8.3.1 Preparation of standards and working reagents

For preparation of diluted (BSA) standards, BSA standard stock in homogenising buffer at 2mg/ml was made up. A set of serially diluted protein standards (0, 50, 125, 250, 500, 1000, 1500, 2000 µg/ml) were prepared as in Table 2-9.

Table 2-9: Dilution scheme for standards (working range: 50-2000 μg/ml).

Standards	Volume of Diluent	Volume and source of BSA (μl)	Final BSA concentration (μg/μl)
A	0	300 of stock	2000
B	125	375 of stock	1500
C	325	325 of stock	1000
D	325	325 of vial C dilution	500
E	325	325 of vial D dilution	250
F	325	325 of vial E dilution	125
G	400	200 of vial F dilution	50
H	400	0	0

The total volume of BCA working reagent required for eight standards and unknow samples (2 replicates for each sample) was prepared by mixing reagent A with reagent B at 50:1 ratio. Then 10μl of each unknown sample and standard were mixed with 200 μl of reagent mix in a 96 wells plate. The plate was covered and incubated in the dark at 37°C for 30 minutes. Absorbance at 562nm was then measured using a NanoDrop 1000 spectrophotometer. The absorbances of diluted protein standards were used to generate a standard curve (Figure 2-3) from which sample protein concentrations were calculated from input absorbance values using the equation for the curve ($Y = mX + C$, $Y = 0.1077X + 0.0004$). Where Y is the absorbance of unknown sample and X is the concentration of unknown sample. Therefore, $X = (Y-C)/m$. Once the protein concentration of each sample had been determined, the samples were frozen at -80 °C for later use.
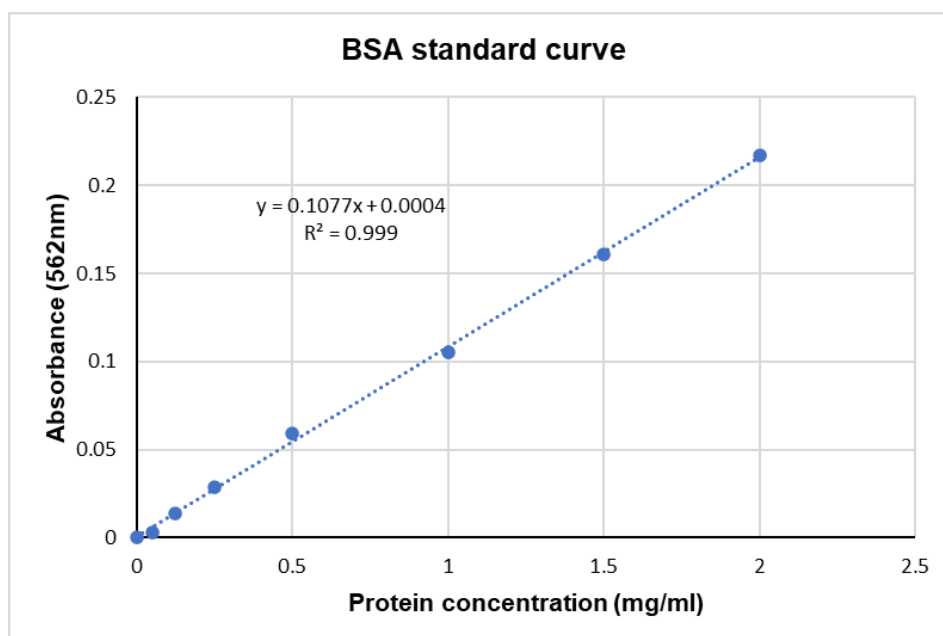
Figure 2-3 BSA standard curve using BCA assay. A plot of absorbance vs a varying amount of some known concentration of BSA protein; in equation (x) stands for sample concentration and (y) stands for average net absorbance.

2.9 CRISPR-Cas9 genome editing

2.9.1 Cloning single guide RNA (sgRNA) into plasmid (Plasmid construction)

Single guide RNA (sgRNA) for CBS, CSE and 3-MST were designed using the CHOPCHOP online tool (section 5.1.2) choosing knockout and Cas9 as selection criteria. The highest ranking sgRNA within as early an exon as possible were chosen to maximise the effect of protein synthesis of gene disruption. The site identified by the tool was the basis for forward oligos. If the first nucleotide was not G, a non-templated G was added for optimal transcription by RNA polymerase III. The reverse strand oligo was designed by creating the reverse complement of the top strand sequence. CACC was added to the 5' end of the forward oligo and AAAC was added to the 5'end of the reverse strand oligo to allow cloning into *Bbs*1 digested recipient plasmid. The forward and reverse oligonucleotides (oligos) were resuspended with UP-H$_2$O according to the manufacture's instruction (Table 2-10) to make a final concentration of 100 µM.

Table 2-10: sgRNA sequences.

Oligo name	Sequence (5' - 3')	µl for 100µm
CBS sg1f	CACCGGCTCGATAATCGTGTCCCC	760
CBS sg1r	AAACGGGGACACGATTATCGAGCC	643
CSE sg1f	CACCGTCCACCACGTTCAAGCAAG	700
CSE sg1r	AAACCTTGCTTGAACGTGGTGGAC	670
3-MST sg 1f	CACCGGCGTCGTAGATCACGACGT	697
3-MST sg1r	AAACACGTCGTGATCTACGACGCC	637

To increase efficiency of ligation, oligonucleotides were 5' phosphorylated: 2 µl of T4 polynucleotide kinase buffer 10X buffer (New England BioLabs, cat. no. M0201S), 2 µl of 10 mM ATP solutions (Thermo Scientific, cat. no. R0441) and 1 µl of T4 polynucleotide kinase (New England BioLabs, cat. no. M0201S) were added to 15 µl of each resuspended oligonucleotide solution. The tubes then were incubated in water bath at 37°C for 30 minutes. Forward and reverse, phosphorylated oligos were then annealed by mixing equal molar amounts, heating up at 65°C for 5 minutes and then slow cooling to room temperature.

pX300-mCherry already digested by *Bbs*1 was provided by Dr Andrew Hamilton. Phosphorylated, annealed oligo pairs were ligated with this as follows. 4 PCR tubes were

labelled for control (no oligos), CBS, CSE and 3-MST. In each tube, 2.5 µl of 1:1000 diluted oligonucleotide (or water for the control), 1 µl (200 ng) of digested plasmid, 1 µl of 5X ligase buffer and 0.5 µl of ligase (5 units) enzyme (New England BioLabs, cat. no. M0202) were added and incubated at room temperature for 1 hour.

2.9.2 Transformation of ligations into E coli

2.9.2.1 Preparation of plates

3.5g of LB broth with agar, microbial growth medium, (Sigma-Aldrich, cat. no. L2897) was dissolved in 100 ml of UP-H$_2$O and boiled in a microwave. After cooling down, ampicillin (50 mg/ml) was added in 1:1000 ratio (100 µl) and then the mixture was poured in 4 petri dishes labelled as a control, CBS, CSE and 3-MST and allowed to solidify.

2.9.2.2 Transformation procedure (bacterial culture)

MAX Efficiency DH5α competent cells (E coli) (Invitrogen, cat. no. 18258012) were retrieved from -80°C storage and thawed on wet ice. 1 µl of each ligation reaction was added to 40 µl of the cell suspension in new pre-chilled labelled four tubes. The cells were incubated on ice for 30 minutes. The tubes were heat pulsed in 42°C water bath for 45 seconds then incubated back on ice for 2 minutes. 360 µl of room temperature S.O.C. medium (Sigma-Aldrich, cat. no. S1797) were added into the tubes and followed by incubation at 37°C for 1 hour with shaking at 225 rpm. Then, 100 µl from each tube were spread on the corresponding LB plate. The plates were incubated overnight at 37°C to allow colonies to develop.

2.9.3 Extraction of plasmids DNAs and purification

2.9.3.1 Miniprep plasmid purification

LB broth was prepared by mixing 2.5 gm of LB broth (Sigma-Aldrich, cat. no. L3022) with 100 ml of dH$_2$O). Colonies from transformation plates were inoculated to 15 ml centrifuge tube containing 5 ml of LB broth medium supplemented with ampicillin (50 mg/ml) and the tubes incubated overnight in a shaking incubator at 37°C. Next day, the bacterial culture tubes were taken from the incubator and poured into new 15 ml centrifuge tubes. The old tubes containing around 500 µl culture were kept on the fridge for use as inoculum if needed. The bacterial culture was harvested by centrifuging at 5000 x g for 5 minutes at 4°C. Solutions P1, P2 and P3 from (QIAGEN Plasmid Midi kit, cat. no. 12143) were used for

resuspension, lysis and neutralisation respectively: the culture supernatant was discarded and the bacterial pellet was resuspended subsequently with 400 µl of buffer P1 (with RNase A added), then 400 µl buffer P2 (Lysis buffer) was added and the solutions mixed by inversion, then 400 µl buffer P3 (neutralisation buffer) was added, the solutions mixed well, incubated on ice for 15 minutes, then centrifuged at 5000 x g and 4°C for 15 minutes. Two pellet layers were seen at this stage. The supernatants (approximately 1.2 ml each) were carefully pipetted and added into microcentrifuge tubes containing 300 µl of 50% polyethylene glycol (MW 8000) and mixed vigorously and left on ice for 30 minutes. After that, the tubes were centrifuged at 16000 x g for 20 minutes and the supernatant was discarded. 150 µl of 70% ethanol were added to wash the pellet, centrifuged at high speed for 5 minutes and the supernatant was discarded. The tubes were then left open at room temperature to dry the ethanol and after that the pellets (plasmid) were resuspended in 50 µl of UP-H$_2$O and kept at -20°C storage.

2.9.3.2 Midiprep plasmid purification

Plasmids were extracted using the Qiagen Midi prep kit according to the manufacturer's instructions. Briefly, clones containing plasmids were grown in conical flasks containing 50 ml LB broth medium supplemented with ampicillin 1:1000 (v/v) overnight at 37°C, transferred into 50 ml centrifuge tubes and cells harvested by centrifuging at 5000 x g for 15 minutes at 4°C. The supernatant was removed and the bacterial pellet was resuspended with 4 ml of kit buffer P1. Then 4 ml of buffer P2 was added and the tubes were mixed gently and incubated at room temperature for 5 minutes to allow lysis of the cells. Then lysates were neutralised and proteins and genomic DNA precipitated by addition of 4 ml of kit buffer P3, incubation on ice for 15 minutes. The tubes were centrifuged at 5000 x g for 10 minutes at 4 °C and the supernatant containing plasmid, degraded RNA and low molecular weight contaminants applied to a Qiagen column that had been pre-equilibrated with 4 ml of buffer QBT (low salt buffer). The supernatant was allowed to enter the column resin by gravity flow and then the column was washed with 2 x 10 ml buffer QC (medium salt buffer) again by gravity flow. The tips were transferred into fresh 50 ml centrifuge tubes and the DNA was eluted from the column with 5 ml buffer QF (high salt buffer). DNA was precipitated from this eluate by addition of 4 ml room temperature isopropanol and incubating tubes on ice for 10 minutes. Plasmid was collected by centrifugation at 16000 x g for 10 minutes at 4°C. The supernatant was discarded and the DNA pellet was washed with 2 ml 70% ethanol and centrifuged again at 16000 x g for 10 minutes. The supernatant was removed. Finally,

the DNA pellet was air-dried for 5-10minutes and re-dissolved in 400 µl of UP-H₂O. The purified plasmid was kept at -20°C.

2.9.4 Restriction digest of Plasmid DNA

Restriction enzyme digestion of the plasmid DNA was carried out in the buffer recommended and supplied by the enzyme manufacturer using no more than 1/10 volume of restriction endonuclease and incubation at 37°C for at least one hour.

2.9.5 Purification of digested plasmids

Purification of the digested plasmid DNA was performed using Pure Link Quick PCR purification kit (Invitrogen, cat. no. k3100-01) according to manufacturer's instructions. Four volumes of the binding buffer B3 supplemented with isopropanol was combined with one volume of the digestion reaction, and mixed well. The mixture was then loaded into Pure Link spin column in a collection tube, centrifuged at 10000 x g for 1 minute at room temperature and the flow through was discarded. The column was reinserted in the collection tube, washed with 650 µl of wash buffer (W1) supplemented with ethanol, centrifuged at 10000 x g for 1 minute. The flow through was discarded and the column was placed in the same collection tube and centrifuged at maximum speed for 2-3 minutes to remove the residual wash buffer. The dried column was inserted in a clean 1.5 tube, 25 µl of elution buffer (E1) added to the centre of the column and incubated at room temperature for 1 minutes to release the DNA bound to the column. Finally, the column was centrifuged at maximum speed for 2-3 minutes to collect the eluted, purified plasmid.

2.9.6 DNA gel electrophoresis, staining and imaging

DNA samples were separated by agarose gel electrophoresis. 0.7% (w/v) agarose gels were prepared by dissolving agarose (Invitrogen, cat. no.10975-035) in 0.5 X TBE buffer (Tris-base, boric acid and EDTA). For gel casting, the solution was poured into Bio-Rad Mini Sub Cell GT agarose gel system with comb inserted to create wells and allowed to set at room temperature. Once set, the comb was removed and the gel was placed in a gel tank containing 0.5 X TBE buffer. DNA samples were mixed with loading solutions. These were 6X Orange G loading dye (0.25% (w/v) Orange dye, 30% (v/v) Glycerol in UP-H₂O) or loading buffer (10 X Blue Juice ᵀᴹ gel loading buffer, Invitrogen, cat. no. 10816015). Gels were run at 150 volts for 20-50 minutes. 5 µl of 1kb DNA ladder (Invitrogen, cat. no. 15615016) was used for sizing double-stranded DNA fragments. Gels were incubated and

stained in 1 µg/ml (1:1000) ethidium bromide in 0.5 X TBE for 20 minutes, then rinsed with water and scanned using Fujifilm FLA-5000 Image Reader. Images obtained were analysed by AIDA analysis software, version 4.13.

2.9.7 Quantification of DNA concentration

DNA concentrations from plasmid preparations, column purified digested plasmid and genomic DNA from culture cells were all measured by absorbance spectrophotometry at 260 nm using a Nano-Drop ND-1000 spectrophotometer. Concentrations in ng/µl were calculated using the Beer-Lambert equation via the instrument's embedded software. The 260/280 ratio determines the purity of DNA where a value of 1.8 is indicative of highly purified DNA. The DNA concentration was calculated using the Beer-Lambert law. Quantification of PCR-amplified, gel-purified DNA for DNA sequencing was performed by comparative densitometry of digital fluorescence images against marker DNA bands of known mass. This was because the ethidium bromide used as gel stain prior to gel purification remains intercalated in the purified DNA and affected accurate quantification by spectrophotometry.

2.9.8 Puromycin concentration for CRISPR selection

Cultured cells were seeded in a 6 well plate for antibiotic treatment. 10 mg/ml puromycin (Sigma-Aldrich, cat.no. P8833) was added to the regular growth medium at different final concentrations (0.25, 0.5, 1, 2, 3µg/ml) into 5 wells and the last well was set as a control (no added Puromycin). The plates were incubated for 5 days during which the cells were observed under an inverted microscope and cell death was monitored as detachment from the plastic surface. Media was renewed with fresh puromycin supplemented media every 2 days. The minimum effective concentration was the one that resulted in complete cell death within 2-3 days.

2.9.9 Transfection of the recombinant plasmid into cultured cells

2.9.9.1 Seeding cells for transfection

One day before transfection, cultured cells (the same passage used for protein expression experiment) at 80-90% confluent in T25 flask were dissociated and seeded into wells of a 6-well plate. Well 1 was set up as a negative control (without plasmid DNA), and the other wells were transfected with the constructed plasmids

2.9.9.2 Transfection of MCF-7 or BeWo cells

Cells grown in a 6-well plate at 70% confluency were transfected using Lipofectamine^{TM} 3000 (Invitrogen, L3000-008). All the transfection was done in 37°C Opt-MEM reduced serum medium (Gibco, cat.no. 31985-062). On the day of transfection, 7.5 µl Lipofectamine 3000 reagent was diluted in 125 µl opti-MEM medium per well. A master mix for 4 or 5 wells was prepared in a microcentrifuge tube.   Microcentrifuge tubes were labelled as a negative control, pCBS sg1, pCSEsg1 and p3-MSTsg1. A master mix of 2 µg/ml DNA plasmid (recombinant plasmid and digested psCB puromycin with ratio of 9:1) and 4 µl P3000 reagent diluted in Opt-MEM medium was prepared in each tube. After that, 125 µl diluted Lipofectamine reagent was added to the diluted DNA (1:1 ratio). The tubes were incubated at room temperature for 10-15 minutes to allow DNA-lipid complex to be formed. Finally, the complexes were added to the corresponding wells, and the plate was swirled gently to ensure homogenous distribution of the complex to the entire well.

The next day of transfection, the transfected cells in each well were passaged down into a 6 wells plate and cultured in selective medium, supplemented DMEM with 1 µg/ml puromycin. The cells were incubated at 37°C and 5% CO_2. The use of the selective medium is continued for 2-3 weeks, with frequent change of medium every 48 hours to remove dead cells and debris, until distinct colonies can be visualised. During the expansion or growth period of the transfected cells, the cells were observed under the microscope. Colonies started growing eight days after the transfection. However, some colonies with few cells number disappeared after few days, and that could be explained by transient transfection. Colonies with a large number of cells were ready to be transferred into another well containing only fresh medium without puromycin.

2.9.9.3 Selection and Isolation of colonies

The growth of surviving transfected cells was monitored over the course of 3 weeks after the transfection. Using an inverted microscope, places of growing colonies were marked. When the colonies became large (more than 80 cells) and distinct, the colonies were picked up using a colony ring and trypsinisation. A sterile colony ring was placed around the colony, 20 µl of trypsin were added, and then the cells were incubated at 37°C for 2 minutes. When the cells are detached from the well surface, about 100 µl of fresh medium were added, and the cells were pipetted and placed into the corresponding well containing non-puromycin medium. When the cells reached a 90-100% confluency, they were transferred into a T25 flask for either protein extraction or continuation.

2.9.10   Protein extraction from transfected cells, protein quantification and western blotting

Transfected cells were collected from each T25 flask. The protein extraction and quantification were performed as in sections 2.8.2 and 2.8.3. Western blotting was performed as in section 2.7.

2.9.11   DNA extraction from cultured cells

Extraction of DNA was performed using PureLink Genomic DNA Mini kit (Invitrogen, cat. no. K1820-01) from cells grown in a T25 flask at 100% confluency. Cells were harvested by scraping in PBS and centrifuged at 1000 x g for 5 minutes at room temperature. Cell pellets were resuspended in 200 µl PBS, 20 µl proteinase K solution and 20 µl RNase A solution from the kit added, the sample mixed well by brief vortexing and then incubated at room temperature for 2 minutes. Then, 200 µl PureLink genomic lysis/binding buffer was added and mixed well to obtain a homogenous solution and the sample incubated at 55°C for 10 minutes to promote protein digestion. After that, 200 µl of 100% ethanol was added to the sample and vortexed for 5 seconds. The sample was then transferred into the PureLink spin column for binding DNA to the silica membrane. The column was centrifuged at 10000 x g for one minute at room temperature. The flow through was discarded and the spin column was placed into a new collection tube. Subsequently, the column was washed with 500 µl wash buffer 1 and then buffer 2, and after each wash the column was centrifuged at 10000 x g for one minute at room temperature. Next, the column was centrifuged at maximum speed for 3minuts at room temperature to remove any traces of ethanol. Then, the spin column was placed in a sterile 1.5 ml microcentrifuge tube, and the DNA was eluted in 200 µl of PureLink Genomic elution buffer. Finally, the column was incubated at room temperature for 3 minutes and centrifuged at maximum speed for 2-3 minutes to recover the DNA solution. The quality of genomic DNA was checked by gel electrophoresis as for plasmid samples (section 2.9.6) and quantified by spectrophotometry as for plasmids (section 2.9.7).

2.9.12   PCR amplification for extracted DNA

DNA oligonucleotides to be used as PCR primers were purchased from Sigma/Merck as lyophilised pellets. All were dissolved in UP-H$_2$O according to the manufacturer's instruction (Table 2-11) to make a final stock concentration of 100 µM and then further to 10 µM as working solutions.

Table 2-11: PCR primers sequences

Oligo name	Sequence (5' - 3')
CBS 5p1	ACATGCGGCTGCAGCTCAG
CBS 3p1	TTGGCCTTGTGCGGGAACC
CBSL 5p1	ACATGCGGCTGCAGCTCAT
CBSL 3p1	TTGGCCTTGTGCGGGAACT
CSE 5p1	CTCTACCTGCGTGCTTTAGCTC
CSE 3p1	GCTCCTTCCAGTCCTGCTTATC
3-MST 5p1	CGCCGCTTTCTTCGACAT
3-MST 3p1	CCGCCATCAAGCAGTGACA

For 20 µl reaction, 10 µl of 2X GoTaq G2 Hot Start Green master mix (Promega, cat. no. M7422), 2 µl forward primer (10 µM), 2 µl reverse primer (10 µM) and 50 ng DNA template were added in a PCR tube. UP-H$_2$O was added to make the final volume 20 µl. Then, PCR tubes were placed in a thermal cycler machine and the reactions were run for 35 cycles: initial denaturing stage at 98°C for 2 minutes, followed by cycling stage at 98°C for 15 seconds for denaturation and 60°C for 15 seconds for annealing and then 72 °C for 15 seconds for extension. The PCR reactions were loaded and run on 0.8% (w/v) agarose gels in 0.5 X TBE as previously mentioned in section 2.10.6 to check for amplification of the correct size of DNA.

2.9.13 Extraction and purification of DNA from gel after electrophoresis

Following the agarose gel electrophoresis and staining, the gel was moved to an open UV box. The desired DNA fragment identified by visual inspection then was excised from the gel with a sterile razor blade. The gel slice was placed in a labelled microfuge tube. The gel slice was weighted by subtracting the weight of the empty tube from the wight of the tube with the gel slice. After that, DNA extraction was carried out, using PureLink quick gel extraction kit (Invitrogen, cat. no. K210012), as follows. Gel solubilization buffer (L3) was added to the excised gel in the tube in 3:1 ratio (v/w; buffer L3: gel piece). Then, the tube with gel slice and buffer was placed in a heat block and incubated at 50°C for 10 minutes. After dissolving of the gel slice, one gel volume of isopropanol was added and mixed well and this solution was loaded onto a quick gel extraction column inside a wash tube. The column then was centrifuged at 12000 x g for 1 minute. The flow-through was

discarded and the column was placed into the wash tube. Next, 500 µl wash buffer containing ethanol was added to the column, and the column was centrifuged at 12000 x g for 1 minute. The flow-through was discarded and the column was centrifuged at maximum speed for 2 minutes. The column was then placed in a sterile 1.5 ml microcentrifuge tube, and the DNA was eluted with 50 µl of elution buffer (E5) by incubation at room temperature for 2 minutes and centrifugation at 12000 x g for 2 minutes to recover the DNA solution. The purified DNA was stored at -20°C.

2.10 Immunofluorescence (IF)

WT BeWo and mutant cells were grown on four-well glass chamber slides (Labtek) to a confluence of 70-90% on the day of the experiment. The media were removed and cells washed with ice-cold PBS buffer three times prior to the further steps. Cells were then permeabilised by incubation on ice for 2 minutes in PBS supplemented with 0.015% digitonin (Sigma-Aldrich, cat. no. D141-500MG) (for staining mitochondrial proteins). After that, the permeabilising solution was removed and the cells were fixed with a 1:10 dilution of 40% formaldehyde solution in PBS for 30 minutes at room temperature. Formaldehyde was freshly prepared each time by depolymerisation of paraformaldehyde at 65°C in 100 mM NaOH. Cells were then washed with PBS three times. Alternatively, in experiments to compare IF with IHC data, the cells grown on slides were fixed in acetone for 15 minutes at room temperature without detergent permeabilisation.

The fixed cells were blocked in PBS with 2.5% (v/v) horse serum (Gibco) for 30 minutes at room temperature on a rocking platform. Then, the fixed cells in some wells were incubated in PBS with 2.5% horse serum and a dilution of primary antibody of interest (Table 2-12) for an hour at room temperature on a rocking platform or overnight at 4°C. The fixed cells in the other wells were used as negative (no-primary antibody) control and incubated in PBS with 2.5% horse serum only. After washing the cells three times with PBS, the cells in all wells were incubated in in PBS with 2.5% horse serum and a dilution of secondary antibody (Table 2-13) for an hour at room temperature on a rocking platform. Finally, the cells were washed with PBS three times and then DNA stained by adding 0.1 µg/ml 4′,6-diamidino-2-phenylindole (DAPI) (Sigma-Aldrich, cat. no. S9542) in PBS for 15 minutes at room temperature followed by further washing in PBS.

Table 2-12: List of primary antibodies used for IF experiments.

Antibody	company	Catalogue number	Dilution	Host & clonality
Anti-CBS	Abcam	ab54883	1:100	Mouse monoclonal
Anti-CSE	Abcam	ab54573	1:200	Mouse monoclonal
Anti-MTCO1	Abcam	ab203912	1:100	Rabbit monoclonal

MTCO1: mitochondrion-encoded cytochrome oxidase 1

Table 2-13: List of secondary antibodies

Antibody	company	Catalogue number	Dilution	conjugate
Donkey anti-rabbit	Life technologies	A21206	1:1000	Alexa Flour-488 labelled
Goat anti-mouse	Abcam	ab150117	1:1000	Alexa Flour-488 labelled

2.11 Fluorescent labelling and imaging of total and mitochondrial translation

WT BeWo and mutant 3-MST (C6) cells were grown on eight-well glass chamber slides (Labtek) to a confluence of 50% on the day of the experiment.

2.11.1 Protein labelling

For protein labelling, Methionine (Met)-free medium, (Sigma-Aldrich, cat. no. D0422) was used after supplementing with 2mM Glutamine and 0.0303 mg/ml (1:200) cysteine and with or without 100 µg/ml Cycloheximide (CHI), a rapid and potent inhibitor of cytoplasmic but not mitochondrial translation. The Met-free medium was pre-warmed to 37°C before use. Prior to labelling, the slide was removed from the incubator and placed on a 37°C block. The existing medium was removed and the cells washed briefly with pre-warmed Met-free medium (+/- CHI). Then, the medium was removed and replaced with pre-warmed Met-free medium (+/- CHI) further supplemented with 1mM L-homopropargylglycine (HPG). All these manipulations were done while the slide was on a 37°C block. After that, the slide was placed back in the humidified CO_2 incubator for 10 minutes.

2.11.2   Cell fixation and click reaction

For fixation, the slide was removed from the incubator and placed on ice and the existing medium was removed and the cells were washed twice with PBS. The cells were permeabilised with 0.015% digitonin in ice-cold CIB buffer for 5 minutes. After permeabilising solution removed, the cells were then fixed with CIB buffer supplemented with a 1:10 dilution of 40% formaldehyde solution for 30 minutes at room temperature. Formaldehyde was freshly prepared each time by depolymerisation of paraformaldehyde at 65°C in 100 mM NaOH. Fixing solution was discarded and the cells were then washed three times with PBS.

For click reaction, the cells were incubated in dark in a solution of 40 µM of copper sulfate ($CuSO_4$), 200 µM BTTAA, 10 µM Picolyl cy3 azide and 5% DMSO for 30 minutes at room temperature (pre-click step), and then ascorbic acid was added in 2 mM final concentration to the solution in each well and cells were incubated in dark for 15 minutes at room temperature. Finally, the solution was removed and the cells were washed with DMSO, and then with PBS. DAPI was used to counter-stain DNA at 0.1 µg/ml in PBS for 15 minutes at room temperature.

2.12 Microscopy data and image analysis

All images were taken using an inverted fluorescence microscope (Olympus X51, Japan), under a 40x objective lens (Olympus Japan, aperture 0.6) provided with five excitation filters. The blue filter was used for DAPI fluorophore (Olympus Japan, U-MNV2) excitation 360-370 nm/emission420 nm. The red filter was used for Cy3 fluorophore (Olympus Japan, U-MN1GA3) excitation 540-550 nm/emission 575-625 nm. The green filter was used for Alexa-488 fluorophores (Olympus Japan, U-MN1BA3) excitation 470-455 nm/emission 510-550 nm. Images were taken under total magnification of 400 X using a digital camera and acquired with the micromanager program at same exposure time for each fluorophore. For display, images taken with the same exposure time were opened with the Image J software (Fiji download) and adjusted to have identical threshold settings. Images were coloured and a scale bar was added again using Image J (Fiji).

For quantification, only images taken with the same filter and exposure time were measured and compared. Areas were selected manually and the mean fluorescence intensity calculated with the Image J measurement tool. The mean background signal was measured from 5

independent selections in each image and subtracted, then the mean fluorescence intensity was determined. To correct for the differences in the cell number and size, the mean fluorescence intensity was normalised to DAPI fluorescence intensity. Then the mean normalised fluorescence intensity, the standard deviation and the p value (t-test) were calculated, and graphs were created using GraphPad Prism software. For mitochondrial translation, six areas were selected from the WT and 3-MST knockout BeWo cells. For each area, the cytoplasmic fluorescence intensity was measured by subtracting the nuclear fluorescence intensity from the total fluorescence intensity in ROI. The mean cytoplasmic fluorescence intensities then were compared between the WT and the 3-MST knockout cells.

2.13 Troubleshooting

Different commercially CBS, CSE, 3-MST and loading controls antibodies were used to detect the intended bands. Different concentrations of both primary and secondary antibodies were used to eliminate multiple and non-specific bands and different blocking protocols were used (Appendix 2).

For 3-MST and β-actin, the optimisation was successful to get a single band at the predicted MW for both of them. However, it was not the case for CBS and CSE antibodies. Every time, the CBS and CSE blots showed multiple bands. Therefore, further experiments were carried out to sort it out. The results of those experiments will be exposed and discussed in chapters 4 and 5.

2.14 Statistical analysis

Statistical analysis was performed using Graph Pad prism 9 software. Unless otherwise stated, the data were analysed using non-parametric tests because most of the time the data were not normally distributed, and also some groups have a small sample size. The significance threshold was set at 0.05. Results are expressed as median and interquartile range unless otherwise stated. To compare the differences in expression between three groups of samples from the same placenta, repeated measures one-way ANOVA (Friedman test) followed by Dunne's post hoc test was used. Comparison between two groups was performed using the Mann Whitney test (two tailed). The strength of the association between two variables was assessed by correlation analysis, Pearson's correlation test, using the SPSS software version 27 (IBM SPSS, IL, USA).

The power of study and the sample size calculation were determined by the first supervisor of this project, Prof. Fiona Lyall in relation to a previous student's study. The calculated sample size required in each of the control and diseased groups was 10. The justification for that calculation was that a previous study conducted by the same research group showed significant changes in the stress gene expression in pregnant women complicated with PE by 1.2-fold more than normal pregnant controls with standard deviation of 0.88. Giving the account to the previous study that in the diseased group the expression difference was 1.25 with the same standard deviation of 0.88 then the sample size of at least 10 pregnant women in each group was required for 80% power (actual power 0.82) to detect a significant difference between the groups.

Chapter 3   mRNA expression analysis by qPCR of hydrogen sulfide producing enzymes in placentas from healthy and complicated pregnancies

3.1 Introduction

As previously stated, there are three enzymatic pathways for the biosynthesis of H_2S which are CBS, CSE, 3-MST, and in order to advance our understanding of the importance of H_2S in placental tissues, it is vital to explore the gene expression and regulation of the key synthesising enzymes.   Gene expression, a multi-stage process, that includes transcription, RNA splicing, translation and post-translational protein modification can be regulated at any of these stages, controlling the ability to deliver a functional protein.

To date, changes in mRNA and/or protein expression of H_2S synthesising enzymes have been identified in a number of cells and tissues and in a variety of different disease states, involving a range of different signalling pathways (Whiteman et al., 2011).   Differential expression of CBS, CSE and 3-MST mRNA and protein in normal tissues have been confirmed by the Genotype-Tissue Expression (GTEx) project (Stelzer et al., 2016), and it has shown that the *CBS* gene is overexpressed in liver and pancreas, the *CSE* is overexpressed in liver and ovary, and *3-MST* is overexpressed in liver.   In many disease states, the expression of these enzymes is both inducible and dynamic.   In diabetes, high glucose significantly reduced CSE mRNA and protein levels in freshly isolated rat pancreatic islets and in the rat pancreatic cell line, INS-1E.   This was mediated by stimulating phosphorylation of the transcription factor specificity protein 1 (SP1) via p38 mitogen-activated protein kinase activation which subsequently led to decreased CSE promoter activity (Zhang et al., 2011).   Wang et al. (2012) have reported an increase in CSE mRNA and protein levels in mammalian cells due to the increase in promoter activity in oxidative stress.   Furthermore, Wu et al. (2010) have demonstrated a significant decrease in CBS mRNA and protein levels in the kidney as a result of the decrease in the binding activity of the Sp1 to promoter region on *CBS* gene in renal ischemia/reperfusion.   In colon cancer, human colon cell line showed a reduction in 3-MST protein level (Ramasamy et al., 2006) whereas, hepatocellular carcinoma cell lines revealed an increase in CSE protein level due to binding of Sp1 to the CSE promoter region (Yin et al., 2012).

The studies described above have led to the suggestion that CBS, CSE and 3-MST may express differentially in complicated pregnancies, and so an examination of the pattern of expression in healthy and complicated pregnancies is warranted. This chapter describes the analysis of CBS, CSE and 3-MST mRNA by qPCR. Results for each are presented together, therefore a brief overview of each gene is provided first.

3.1.1 Cystathionine β-synthase gene

CBS gene is a protein coding gene located on chromosome 21 (21q22.3) (Whiteman et al., 2011). Additional names for this gene include beta-thionase, cysteine synthase and serine sulfhydrase. The human *CBS* gene spans over 30 kilobases and consists of 23 exons ranging in size from 42 to 209 bp (Kraus et al., 1998). The CBS polypeptide is encoded by exons 1-14 and 16. Defects or mutations in this CBS gene can cause CBS deficiency which can lead to the most common form of homocystinuria (Kraus et al., 1998). Mutations in the *CBS* gene disrupt the function of CBS, preventing homocysteine from being used properly. As a result, this amino acid and toxic byproducts substances accumulate in the blood, and some of the excess homocysteine is excreted in urine. There are more than 150 mutations in the *CBS* gene that cause homocystinuria. Most of these mutations change single amino acids in CBS. The most common mutation substitutes the amino acid threonine for the amino acid isoleucine at position 278 in the enzyme. Another common mutation, which is the most frequent cause of homocystinuria in the Irish population, replaces the amino acid glycine with the amino acid serine at position 307 (Kraus et al., 1999).

The human *CBS* gene encodes multiple mRNAs differing in their 5′ regions. Two transcripts appear to be the most abundant isoforms and are found in a range of adult and fetal tissues, predominantly in cerebellum, liver, and pancreas. The other three transcripts are relatively rare (Bao et al., 1998). Although the *CBS* gene encodes several mRNAs, function of H_2S production by these different mRNAs has not been well studied (Whiteman et al., 2011). Interestingly, according to the human gene database, there is a duplication of the *CBS* gene on chromosome 21 named as cystathionine beta-synthase like (*CBSL*) gene. CBS was originally identified as the gene encoding CBS, and CBSL encode identical protein.

3.1.2 Cystathionine γ-lyase gene

CTH/CSE gene encodes the CSE enzyme which is involved in transsulfuration pathway for biosynthesis of cysteine from methionine. It is located on chromosome 1 (1p31.1) (GeneCards). It consists of 13 exons, and alternative splicing of this gene results in three

transcript variants encoding different isoforms of the enzyme. Variant 1 encodes the longest isoform 1 of this protein. Variants 2 and 3 each lack a different exon in the coding region compared to variant 1, resulting in shorter protein isoforms 2 and 3, respectively (Levonen et al., 2000, Lu et al., 1992). Although Levonen et al. (2000) has suggested the shorter (truncated) isoform to be inactive, they did not examine its contribution in H_2S production. Mutations in *CSE* that decrease the activity of CSE are associated with cystathioninuria, a disease condition characterised by accumulation of cystathionine in blood, tissue and urine. Also, it is associated with mental retardation (Sun et al., 2009)

3.1.3 Mercaptopyruvate sulfurtransferase gene

MPST/3-MST is a protein coding gene located on chromosome 22 (22q12.3). It has also additional names such as 3- mercaptopyruvate sulfurtransferase and human liver rhodanese (The National Centre for Biotechnology Information, NCBI). The human *3-MST* gene consists of five exons, and there are five splice variants encoding protein isoforms 1 and 2. Deficiency in 3-MST activity has been implicated in a rare inheritable disorder known as mercaptolactate-cysteine disulfiduria (MCDU) (Hannestad et al., 1981). It is an autosomal recessive metabolic disorder, characterised with severe mental retardation and increased susceptibility to infection.

3.1.4 Regulation of hydrogen sulfide producing enzymes at transcriptional level

Precise control of H_2S synthesis is critical for maintenance of cellular function, therefore, its main synthesising enzymes are regulated at multiple levels. CBS and CSE are regulated at transcriptional and post-translational levels. Unlike CBS and CSE, the activity of which is regulated for the most part by binding of other factors, 3-MST activity is probably regulated intrinsically by its redox state (will be discussed in chapter 6).

3.1.4.1 Regulation of CBS

The human *CBS* gene is transcriptionally regulated by two promoter regions designated -1a and -1b (Bao et al., 1998). The major promoter-1b is down-regulated by insulin and growth arrest due to nutrient depletion and the induction of differentiation. In contrast, it is up-regulated by glucocorticoids, glycogen and methionine. Enokido et al. (2005) reported that growth/differentiation factors such as EGF, TGF-α, cAMP and dexamethasone induced CBS protein expression in mouse astrocytes. The *CBS*-1b promoter is regulated in a redox-

sensitive fashion by synergistic interactions between Sp1 and nuclear factor-Y (NF-Y), a histone-like CCAAT-binding trimer, and Sp1 and specificity protein 3 (Sp3). The dominant and indispensable role of Sp1in regulating both GC-rich CBS promoters may allow tissue-specific repression by Kruppel-like factors (Ge et al., 2001, Kraus et al., 1998). Sp1-like proteins and Kruppel-like factors are highly related redox-sensitive zinc-finger proteins that are important components of the eukaryotic cellular transcriptional machinery. Then, hypoxia up-regulated *CBS* expression at transcriptional level via hypoxia induced factor (HIF-1) (Teng et al., 2013).

3.1.4.2 Regulation of CSE

CSE is a highly inducible gene and it is regulated in response to a wide variety of stimuli ranging from oxidative stress, endoplasmic reticulum stress, and inflammation to nutrient deprivation. *CSE* is induced by oxidative stress where the CSE promoter contains a binding site for the master regulator of oxidative stress response, nuclear factor erythroid 2 (Martín et al., 2007). Moreover, *CSE* expression is over-regulated in response to endoplasmic reticulum stress in a mechanism dependent on the activating transcription factor 4 (ATF4), a protein which is expressed as a part of the unfolded protein response to alleviate stress damage (Harding et al., 2003).

Also, *CSE* expression is up-regulated in response to inflammation, when stimulation of macrophage with TNF-α and lipopolysaccharide, a potent activator, leads to increased association of Sp1 with the CSE promoter. This leads to elevated H_2S production which acts by sulfhydration of the p65 subunit of the anti-apoptotic transcription factor, nuclear factor-κB promoting its binding to promoters of anti-apoptotic genes (Sen et al., 2012).

Another stress stimulus that results in up-regulation of *CSE* expression and H_2S production is amino acid starvation due to nutrient restriction. This involves binding ATF4 to the CSE promoter and also to promoters of other amino acid biosynthetic and transport genes (Harding et al., 2003). Since ATF4 controls expression of genes responsible for amino acid metabolism and redox status, ATF4 might, by increasing glutathione synthesis through the transsulfuration pathway, be a key cellular survival factor. It has been reported that the absence of ATF4 in mouse embryonic fibroblasts resulted in a substantial fall in glutathione levels due to down-regulation of *CSE* expression (Dickhout et al., 2012). Thus, if the amount of H_2S synthesizing enzymes in the nucleus are reduced, the levels of glutathione would subsequently be reduced, thereby affecting the fate of the cell.

In addition, *CSE* can be regulated by several factors depending on the cell and tissue type. In the liver, the farnesoid X receptor, a bile acid sensor which reduces conversion of cholesterol to bile acids and increase bile acid excretion from hepatocytes, binds to the CSE promoter, resulting in increased transcription of CSE and increased H_2S production. Also, G-protein coupled plasma receptor for secondary bile salts activates cyclic adenosine 3′,5′-monophosphate/protein kinase A (cAMP/PKA) pathway, which results in in the phosphorylation of cAMP-response element binding protein that binds to CSE promoter, thereby increasing *CSE* expression in rats' liver (Renga et al., 2009). Furthermore, the expression of CSE is also regulated by several hormones: insulin treatment reduces expression of CSE and reductions in growth hormone and thyroid stimulating hormone signalling results in elevation in CSE level and H_2S generation (Hine et al., 2017).

MicroRNAs which transcriptionally regulate mRNA levels and translation also influence H_2S production; suppression of CSE mRNA and protein expression by miR-21 directly targeting at transcript factor Sp1 in human aorta SMCs has been demonstrated (Yang et al., 2012). Cindrova-Davies et al. (2013) found that miR-21 is increased in placentas with abnormal Doppler waveforms, and exposure of villus explants to hypoxia-reoxygenation significantly increases miR-21 expression and reduces CSE protein and mRNA expression. It also has been shown that miR-30 family members regulate endogenous H_2S production through interaction with *CSE* mRNA in primary cardiac myocytes, and inhibition of miR-30s increased *CSE* expression (Shen and Zhu, 2012).

This section has discussed multiple ways in which H_2S generating enzymes are regulated at the transcriptional and post-transcriptional level and which result in altered levels of mRNA encoding the key enzymes. Therefore, we sought to examine if the H_2S synthesising enzymes could be differentially regulated in complicated pregnancies by qPCR analysis of these mRNA.

3.2 Results

3.2.1 Patient clinical data analysis

The characteristics of the study participants were described statistically in this section. The aim of this analysis was to find out if there were any significant differences in the patients details between the study groups, how these differences can be interpreted in relation to the study outcomes and how conclusions may be drawn from the data.

3.2.1.1 Normal healthy, PE and FGR groups:

The patient details for normal healthy, PE and FGR groups are shown in Table 2-1 and Table 2-2. In order to identify any confounding factors between groups, the following analysis were carried out. Normal non-labouring group was compared to labouring group. Normal groups then compared to PE groups and FGR group (Table 3-1). The comparison between groups was performed using one-way ANOVA. Where the significant p values were obtained, sub analysis was carried out by t-test (Table 3-2).

Table 3-1: Patient's clinical details for controls, PE and FGR groups. Data are presented as mean ± standard deviation (SD). Analysis between groups were performed using one-way ANOVA, p values < 0.05 were considered statistically significant. Non-labour group controls (NLG-C), labour group controls (LG-C), non-labour PE (NLG-PE), labour PE (LG-PE) and labour FGR (FGR).

Category	NLG-C (n=6)	LG-C (n=6)	NLG-PE (n=4)	LG-PE (n=8)	FGR (n=6)	p-value
Maternal age	30.17±4.11	26±2.28	33.5±3.69	28.50±7.70	27.50±4.50	0.05
Gestational age at delivery (weeks)	39.33±0.51	40±1.54	37.75±1.50	35.75±4.62	36.83±0.98	0.005
Placental weight (g)	721.8±160.6	589.5±74.97	603±111.3	493±179.3	361.0±76.8	0.004
Birth weight (g)	4007±768.4	3719±346.8	3309±401.7	2629±952.5	2174±392.7	0.001
BMI	25.50±2.04	28.32±4.60	36.35±8.74	25.59±3.24	27.72±7.77	0.19

Table 3-2: Sub-analysis of groups that were statistically significant in Table 3-1. The analysis between two groups was performed using *t*-test, p value < 0.05 was statistically significant.

Category	Comparison of groups	*p*-value
Gestational age	NLG-C and LG-C	0.08
	NLG-C and NLG-PE	0.1
	LG-C and LG-PE	0.01
	LG-C and LG-FGR	0.01
Placental weight	NLG-C and LG-C	0.1
	NLG-C and NLG-PE	0.3
	LG-C and LG-PE	0.1
	LG-C and LG-FGR	0.002
Birth weight	NLG-C and LG-C	0.4
	NLG-C and NLG-PE	0.1
	LG-C and LG-PE	0.02
	LG-C and LG-FGR	0.002

Patients' demographics were compared, and the results showed that there were no significant differences in maternal age (years) and BMI of patients between pathological groups and their controls. In contrast, there were significant differences in gestational age, placental weight and birth weight between compared groups (Table 3-1). The mean of gestational age in PE and FGR group, in which women were delivered spontaneously, was significantly less than that of the healthy control of the same mode of delivery ($p = 0.01$ in both comparisons) (Table 3-2). All cases in labour PE group were term at delivery except two cases were preterm at 28 and 29 weeks (Table 2-2). Also, there were significant differences in means $\pm$ SD of placental weight (g) and birthweight (kg) among groups (Table 3-1). The placenta weight (361.0 ± 76.82) and birthweight (2174 ± 392.7) were significantly reduced in the FGR group ($p = 0.002$ and $p = 0.002$, respectively) when compared with the labouring control group. Moreover, the birth weight was significantly reduced in PE group in which women were delivered spontaneously compared with the control group of the same mode of delivery ($p = 0.02$) (Table 3-2).

3.2.1.2 BMI group:

The patient's details for the BMI groups (Table 2-3) were compared using *t*-test, and results are shown in Table 3-3.

Table 3-3: Patient's clinical details for BMI groups. Data are presented as mean ± SD. Analysis between groups were performed *t*-test, *p* values < 0.05 were considered statistically significant

Category	BMI<30 (n=6)	BMI>30 (n=13)	*p*-value
Maternal age	30.17± 4.11	35.00±6.81	0.158
Gestational age at delivery (weeks)	39.33±0.51	38.38±0.76	0.149
Placental weight (g)	721.8±160.6	687.2±151.0	0.765
Birth weight (g)	4007±768.4	3557±568.2	0.179
BMI	25.50±2.045	40.05± 6.508	< 0.0001

Patients' demographics were compared, and the results showed that there were no significant differences in maternal age (years), placental weight and birth weight between the control and BMI group. However, the BMI index was significantly different between the groups.

3.2.2 RNA quality and TaqMan gene assays assessment

Quantification of RNA in the extracted samples is important in order to use approximately the same amounts of RNA when comparing different samples to minimise controllable variables. Also, use of purely and high-quality RNA templates is essential for data accuracy because it promotes uniformity of cDNA synthesis between samples which, again, minimise controllable variables. In this study, all placental tissue cDNA samples used for amplification of the target genes of interest was prepared from RNA with a ratio of absorbance at 260/280 nm between 1.94 and 2.09 and which exhibited a curve similar to the one shown in Figure 3-1. Such a ratio and absence of peaks other than the one at ~260nm indicates the absence of particular contaminants such as guanidine salts or protein that could carry through from the extraction and which could negatively influence cDNA synthesis and PCR amplification.
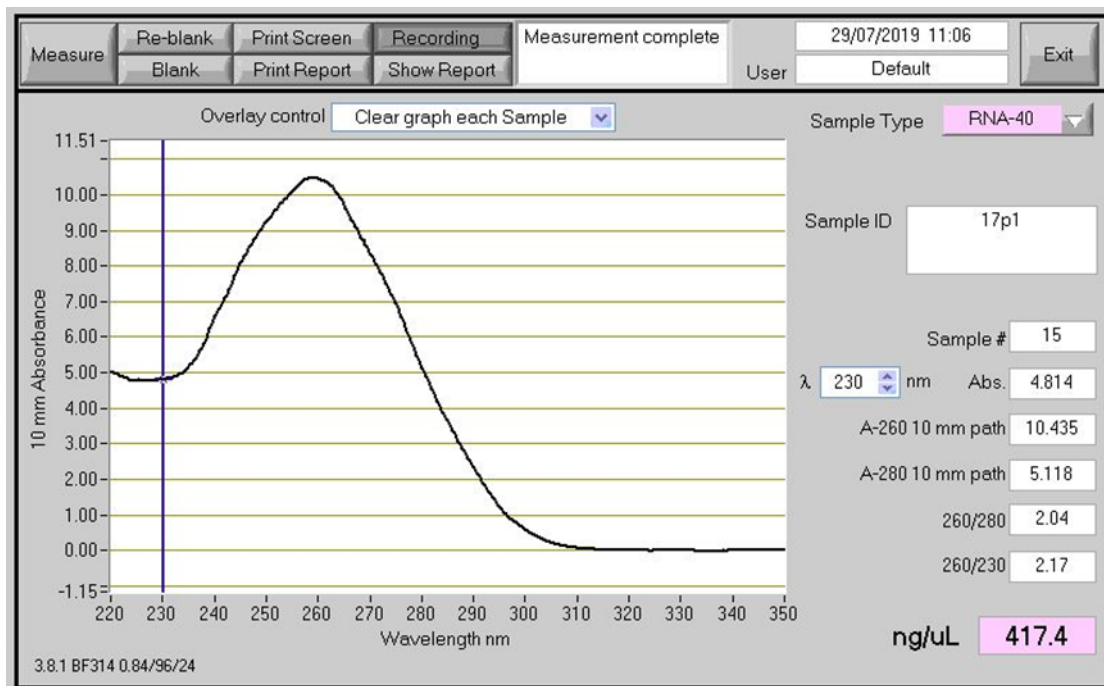
Figure 3-1 RNA concentration of representative placenta sample. The ratio of absorbance at 260 nm and 280 nm (260/280) is given an indication of RNA purity.

qPCR analysis was performed using TaqMan gene assays that designed to detect all transcript variants of *CBS*, *CSE* and *3-MST* as mentioned in section 2.5.3. The experiments were designed to compare the mRNA differential expression between controls and pathological groups, the null hypothesis that the mean of ΔC_T in the groups are the same was tested. The differential expression was done gene by gene by comparing the normalised C_T values (ΔC_T) and the $\log_2$ fold change values. Threshold cycle (C_T) was selected to be in the mid- exponential phase C_T was determined from a log-linear curve where PCR signal plotted against the cycle number, and was obtained from the PCR machine. Fluorescence was generated by extension-polymerisation-dependent hydrolysis of fluorigenic probe hybridised to the target DNA which is better than using a dsDNA-binding fluorophore (e.g, SYBR Green^{TM}) because of the added specificity provided by the fluorogenic probe. Equal efficiency of each type of PCR between samples was assumed; the amplification plots of β-actin (Figure 3-2B) and the genes of interest (Figure 3-3) showed that the PCR amplification curves looked parallel but slopes could not be measured with the software available. Only amplifications where negative controls (no-template control) (Figure 3-2) had fluorescent signals at the background level and where the difference between technical replicates was within 0.5 cycles were considered.

Figure 3-2A displays that the negative control amplification plot shows no expression (Background fluorescent signal can be only seen). The β-actin amplification plot shows a clear expression (accumulation of fluorescent signals above the background level starting

from cycle number 18. The slopes of the β-actin amplification curve are parallel, indicating that the efficiency of PCR reaction is the same for that target DNA from different samples.
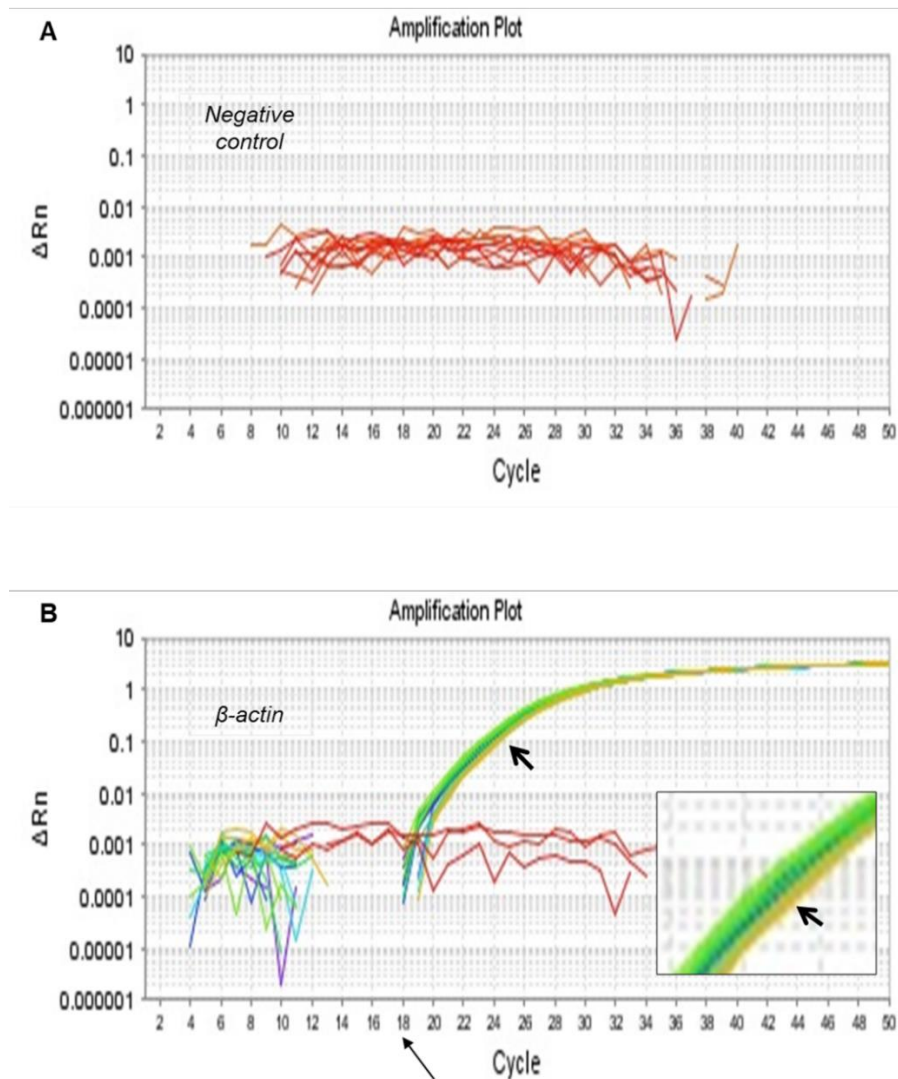
Figure 3-2 PCR amplification plots. (A) An amplification plot of the negative control (Ultrapure H₂O). (B) An amplification plot of β-actin (endogenous control). In PCR data, ΔRn (y-axis) is plotted against PCR cycle number (x-axis). ΔRn is Rn minus the baseline. Rn is the reporter signal normalised to the fluorescence of a passive reference dye (ROX). The thin arrow in B refers to cycle number 18 and the thick arrow refers to slopes of the β-actin amplification curve. The blown-out window in B shows slopes which are parallel.
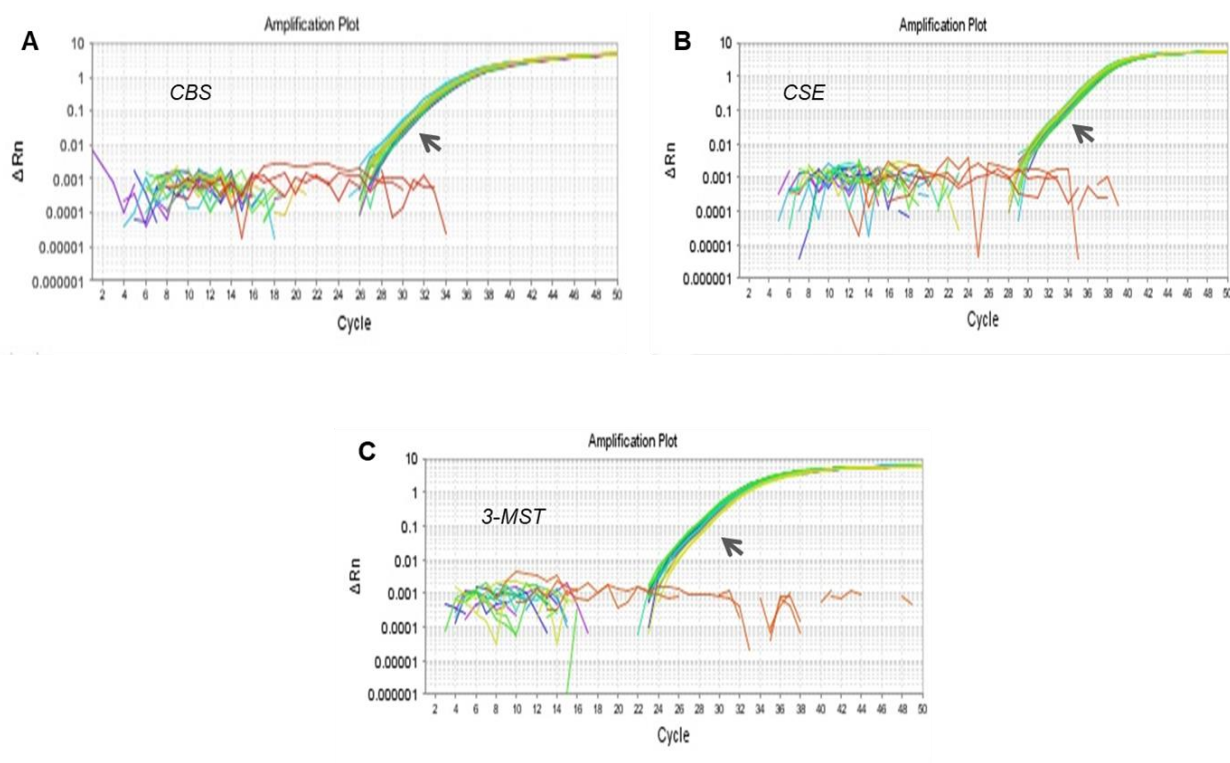
Figure 3-3 PCR amplification plots. (A) *CBS* gene amplification plot, (B) *CSE* gene amplification plot and (C) *3-MST* gene amplification plot. The arrows refer to the log-linear phase of the amplification curve. The slopes of CBS, CSE and 3-MST amplifications plots are parallel.

3.2.3 mRNA expression of H_2S synthesising enzymes (qPCR data analysis) in normal placentas

As previously stated in the hypothesis and aims section, this series of experiments were aiming to examine any variation of CBS, CSE and 3-MST mRNA levels between different zones of normal placental samples from non-labour group (n=6). Placental CBS, CSE and 3-MST mRNA level was determined by qPCR (Figure 3-4). Data are expressed as median and interquartile range. For statistical analysis, Friedman test followed by Dunn's test was used. No significant spatial differences in ΔC_T Mean were found at the mRNA level in non-labour cases. Similarly, a summary of these data was represented in a heat map of $\log_2$ fold change of the CBS, CSE and 3-MSTmRNA level in middle and outer sites from the inner placental site (Figure 3-5). These findings clearly indicate that there is no significant difference in mRNA level of H_2S producing enzymes across different zones of normal healthy placentas.
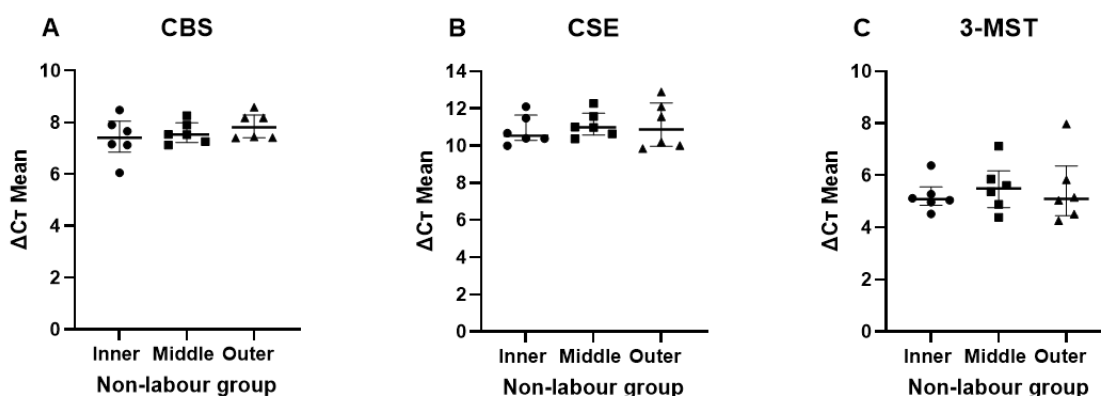
Figure 3-4 mRNA expression profiles in normal placentas. Normalised expression for CBS mRNA (A), CSE mRNA (B) and 3-MST mRNA (C) in inner, middle and outer placental sites within individual placentas from non-labour group (n = 6). The ΔC_T means the normalised C_T value of three technical replicates. Data are presented as median and interquartile range. The thick horizontal bar is the median and the two narrower bars delimit the interquartile range. Comparison between zones was performed using Friedman test.

Log$_2$ fold change in middle and outer sites from the inner site
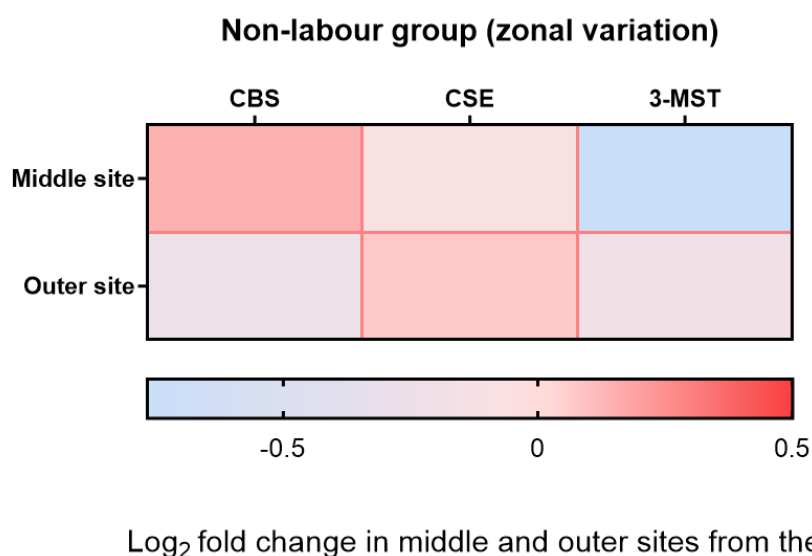
Figure 3-5 Log$_2$ fold change heat map for CBS, CSE and 3-MST genes in individual healthy placentas. Log$_2$ fold change was calculated based on ΔC_T values compared to controls. The red colour implies increased expression while blue colour indicates decreased expression.

3.2.4 mRNA expression of H$_2$S synthesising enzymes between labour and non-labour placentas

This experiment tested whether there were any differences in CBS, CSE and 3-MST mRNA level between labour (n = 6) and non-labour (n = 6) placentas at inner, middle and outer sites (Figure 3-6). Analysis between groups was performed using Mann Whitney test. There were no significant differences in CBS mRNA expression in labour versus non-labour group at all sites. However, there was a significant increase in CSE and 3-MSTmRNA level in labour group ($p = 0.04$) when compared to non-labour group at only middle and inner

placental sites, respectively. In the same way, these data were summarised in a heat map of log$_2$ fold change of the CBS, CSE and 3-MSTmRNA level in labour group from the healthy non-labour controls at three placental sites (Figure 3-7).
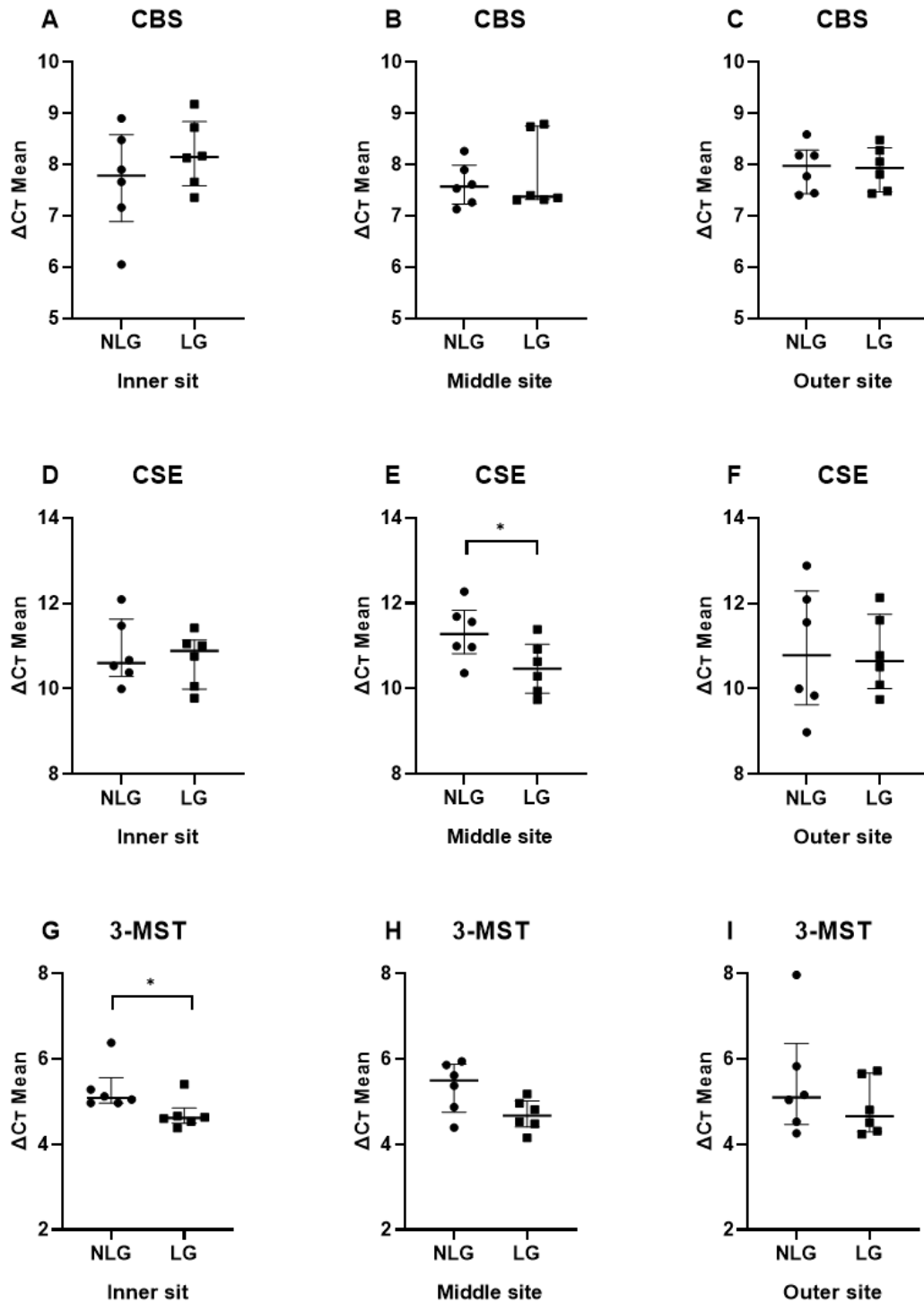
Figure 3-6 mRNA expression profiles in placentas from non-labour (n =6) and labour groups (n = 6). Normalised expression for CBS mRNA (A-C), CSE mRNA (D-F) and 3-MST mRNA (G-H) in labour group compared to non-labour group at inner, middle and outer placental sites. Data are presented as median and interquartile range. Comparison between groups was performed using Mann Whitney test. The asterisk indicates degree of p-value significance, (*) means _p_ < 0.05.

Figure 3-7 Log$_2$ fold change heat map for CBS, CSE and 3-MST genes in labour group. Log$_2$ fold change was calculated based on ΔC_T values compared to controls. The red colour indicates increased expression while blue colour implies decreased expression. The asterisk indicates degree of p-value significance, (*) means $p < 0.05$.

3.2.5 mRNA expression of H$_2$S synthesising enzymes in PE

In this series of experiments the mRNA level of H$_2$S synthesising enzymes was investigated in abnormal placental samples from pregnancies complicated with PE (n = 12) compared with their normotensive controls (n = 12) at different placental sites.

3.2.5.1 CBS mRNA expression in PE

The qPCR data analysis of CBS gene at three placental sites (Figure 3-8) showed that at the inner site there was a significant up-regulation of CBS mRNA in PE group compared with the control ($p = 0.008$), while no significant differences were detected at both middle and outer sites.

Figure 3-8 CBS mRNA expression profiles in placentas from pregnancy complicated with PE. Normalised expression for CBS mRNA in PE group (n =12) in comparison to the healthy control group (n = 12) at (A) inner, (B) middle and (C) outer site. Data are presented as median and interquartile range. Comparison between groups was performed using Mann Whitney test, (**) means $p < 0.01$.

Worth mentioning that labour was a confounder factor in the comparison between PE and control groups. Therefore, when the results were statistically significant, sub-analysis was performed between PE groups and their controls of the same mode of the delivery, in order to investigate effect of labour in gene expression especially, it has been reported that labour factor could affect the gene expression profile in placenta.

The sub-analysis was performed between the PE group in which the women were delivered by CS (NLG-PE, n = 4) and their controls (NLG-C, n = 6), and between the PE, in which the women were delivered spontaneously (LG-PE, n = 8) and their controls (LG-C, n = 6) (Figure 3-9), at the inner site. The CBS mRNA was significantly up-regulated in LG-PE group compared to labouring control ($p = 0.004$).
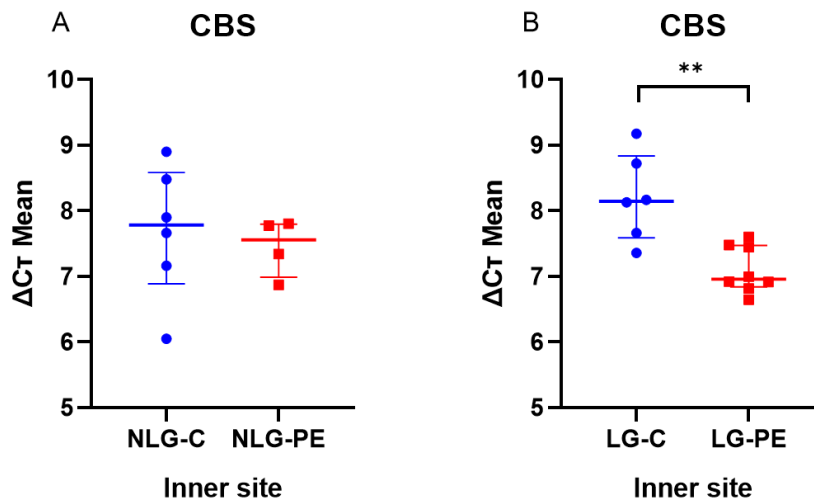
Figure 3-9 Sub-analysis of CBS mRNA expression in placentas from pregnancy complicated with PE. Normalised expression for CBS mRNA in NLG-PE (n = 4) in comparison to the healthy control group (n = 6) (A) and in LG-PE (n = 6) in comparison to healthy controls (n = 6) (B) at the inner site. Data are presented as median and interquartile range. Comparison between groups was performed using Mann Whitney test, (**) means *p* < 0.01.

3.2.5.2 CSE mRNA expression in PE

The qPCR data analysis of CSE gene at three placental sites (Figure 3-10) showed that at the middle site there was a significant increase in CSE mRNA level in PE group compared to the control ($p = 0.04$), while no significant differences were detected at both inner and outer sites.
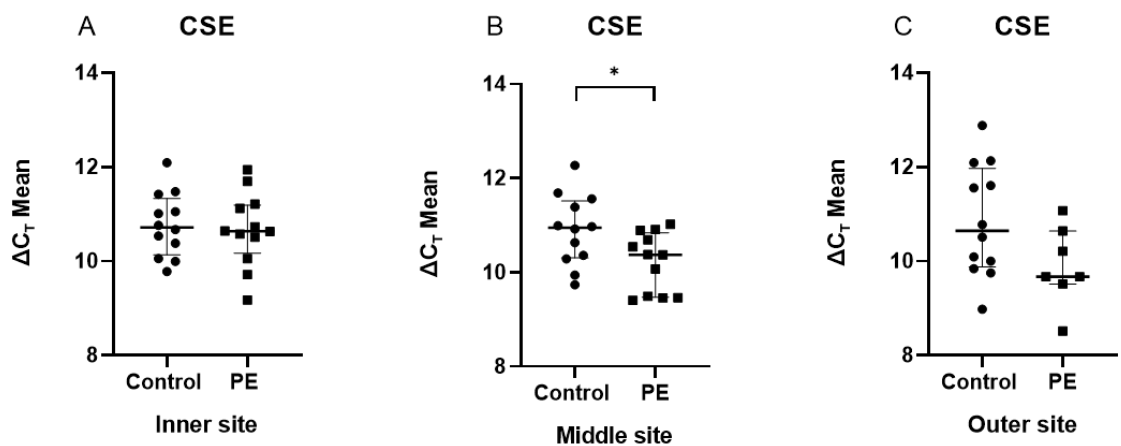
Figure 3-10 CSE mRNA expression profiles in placentas from pregnancy complicated with PE. Normalised expression for CSE mRNA in PE group (n = 12) in comparison to the healthy control group (n = 12) at (A) inner, (B) middle and (C) outer site. Data are presented as median and interquartile range. Comparison between groups was performed using Mann Whitney test, (*) means *p* < 0.05.

Similarly, sub-analysis was performed between the NLG-PE (n = 4), LG-PE (n = 8) and their controls (n = 6) (Figure 3-11) at the middle site. In contrast to CBS where a difference was observed between LG-PE and LG-C, the CSE mRNA was significantly up-regulated in NLG-PE compared to NLG-C ($p = 0.03$).
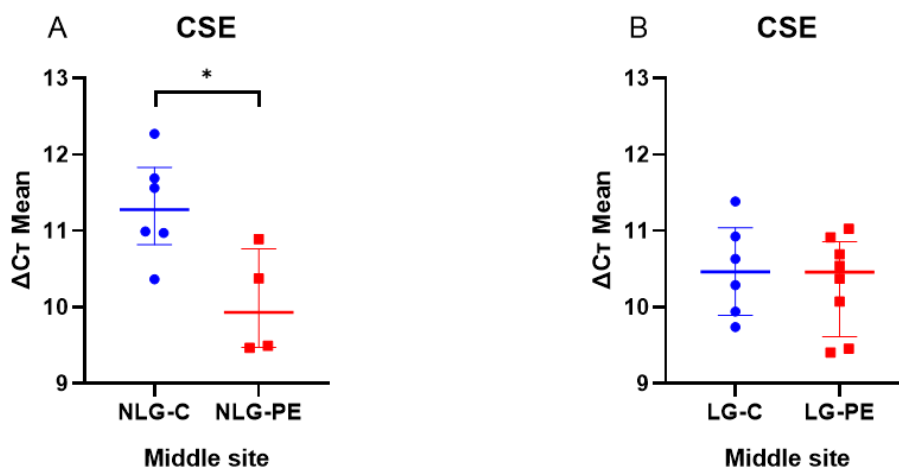
Figure 3-11 Sub-analysis of CSE mRNA expression in placentas from pregnancy complicated with PE. Normalised expression for CSE mRNA in NLG-PE (n = 4) in comparison to the healthy control group (n = 6) (A) and in LG-PE (n = 6) in comparison to healthy controls (n = 6) (B) at the middle site. Data are presented as median and interquartile range. Comparison between groups was performed using Mann Whitney test, (*) means *p < 0.05*.

3.2.5.3 3-MST mRNA expression in PE

The qPCR data analysis of 3-MST gene at three placental sites (Figure 3-12) showed that there were no significant differences in the mRNA level in PE group compared with the control at all sites.
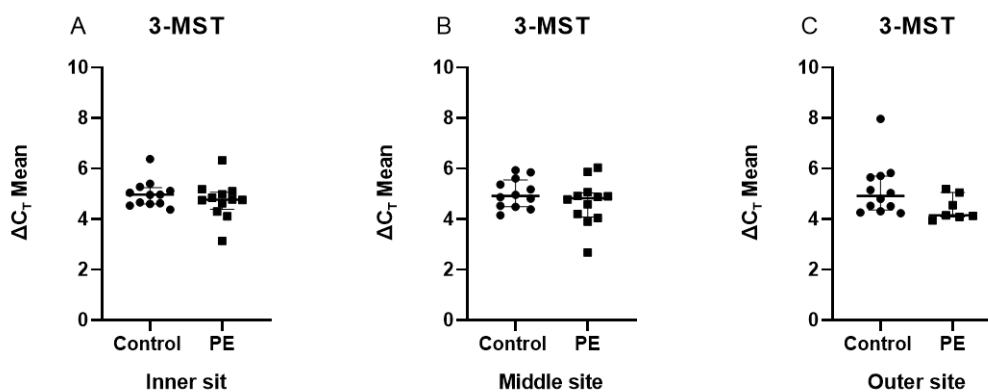
Figure 3-12 3-MST mRNA expression profiles in placentas from pregnancy complicated with PE. Normalised expression for 3-MST mRNA in PE group (n = 12) in comparison to the healthy control group (n = 12) at (A) inner, (B) middle and (C) outer site. Data are presented as median and interquartile range. Comparison between groups was performed using Mann Whitney test.

Similarly, the same generated qPCR data in PE and control groups for the three genes were summarised in a heat map (Figure 3-13) to quickly visualize the differences in mRNA level in three sites. The heat map shows the Log_2 fold change of the CBS, CSE and 3-MST m RNA level in PE group from the control.
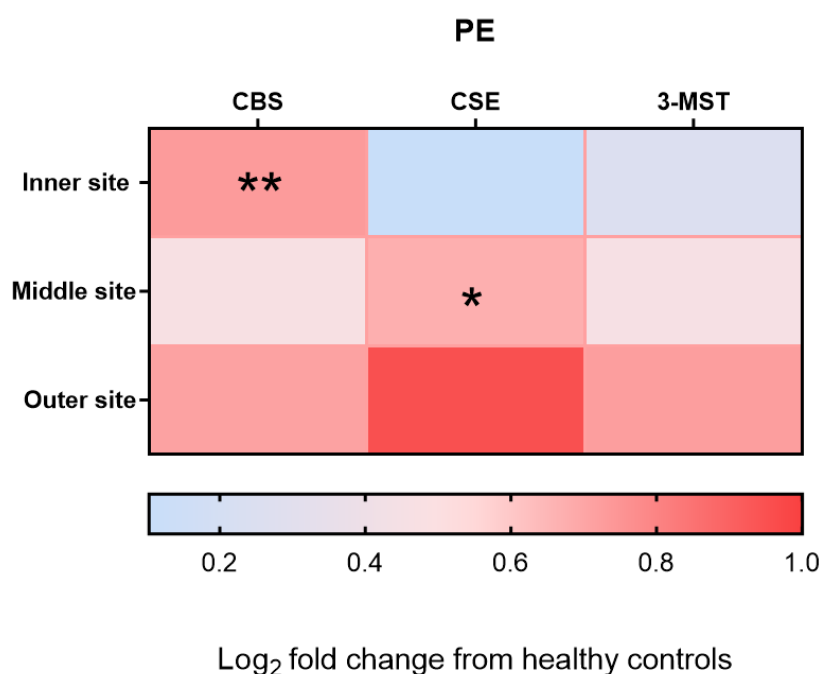
Figure 3-13 Log_2 fold change heat map for CBS, CSE and 3-MST genes in PE group. Log_2 fold change was calculated based on ΔC_T values compared to controls. The red colour implies increased expression while blue colour implies decreased expression. (*) means $p \leq 0.05$, (**) means $p \leq 0.01$.

3.2.6 mRNA expression of H_2S synthesising enzymes in FGR

In this section, the mRNA expression of CBS, CSE and 3-MST was investigated in abnormal placentas from pregnancies complicated with FGR (n = 6) in comparison to healthy placentas from labour group (n = 6) at two sites only, inner and outer. Placentas from pregnancies complicated with FGR were small in size therefore they were divided into only two sites, as previously described in section 2.3.

The qPCR data analysis of CBS gene at two placental sites (Figure 3-14) showed that there was no significant difference in expression of CBS mRNA between the FGR and its control group at all sites.
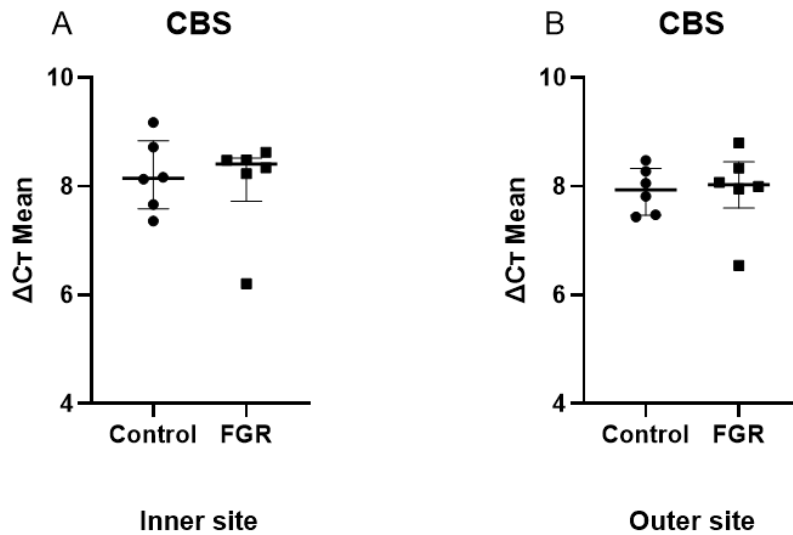
Figure 3-14 CBS mRNA expression profiles in placentas from pregnancy complicated with FGR. Normalised expression for CBS mRNA in FGR group (n = 6) in comparison to the healthy control (n = 6) at inner site (A) and outer site (B). Data are presented as median and interquartile range. Comparison between groups was performed using Mann Whitney test.

Moreover, the qPCR data analysis of CSE gene at two placental sites (Figure 3-15) showed that there was no significant difference in expression of CSE mRNA between the FGR and its control group at both sites.
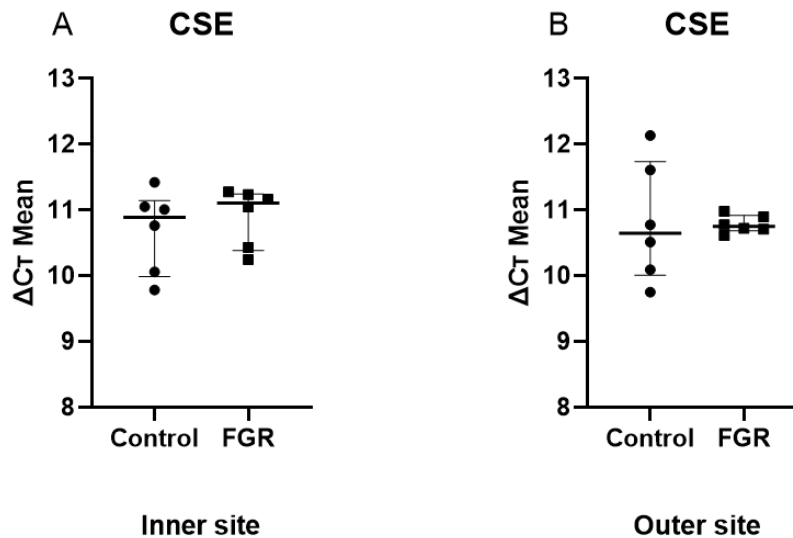
Figure 3-15 CSE mRNA expression profiles in placentas from pregnancy complicated with FGR. Normalised expression for CSE mRNA in FGR group (n = 6) in comparison to the healthy control (n = 6) at inner site (A) and outer site (B). Data are presented as median and interquartile range. Comparison between groups was performed using Mann Whitney test.

Furthermore, the qPCR data analysis of 3-MST gene at inner and outer placental sites (Figure 3-16) showed that there was a significant difference in expression of 3-MST mRNA between the FGR and its control group at the outer site, where the 3-MSTmRNA was up-regulated in FGR group ($p = 0.04$).
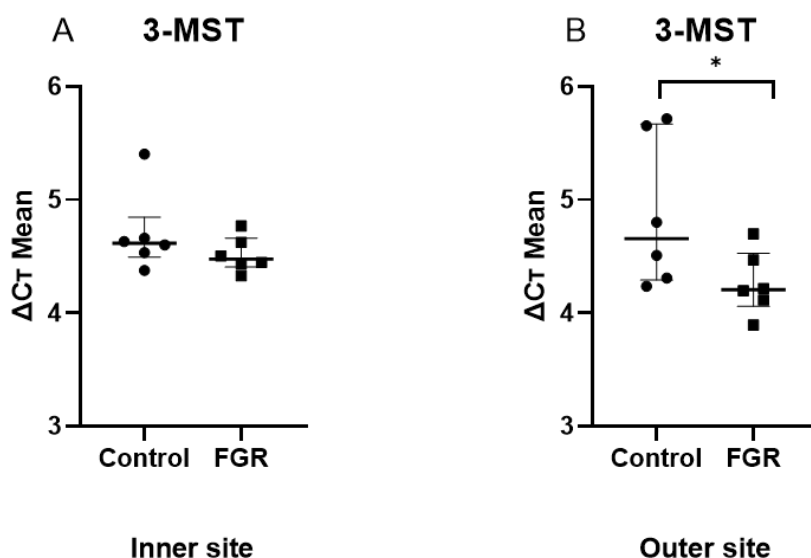
Figure 3-16 3-MST mRNA expression profiles in placentas from pregnancy complicated with FGR. Normalised expression for 3-MST mRNA in FGR group (n = 6) in comparison to the healthy control (n = 6) at inner site (A) and outer site (B). Data are presented as median and interquartile range. Comparison between groups was performed using Mann Whitney test, (*) means $p < 0.05$.

To summarise, the same data in FGR and control group for CBS, CSE and 3-MST genes were presented in a heatmap (Figure 3-17) to visualize the differences in mRNA level in two sites of placenta. The heat map shows the Log_2 fold change of the CBS, CSE and 3-MSTmRNA level in FGR group from the control.
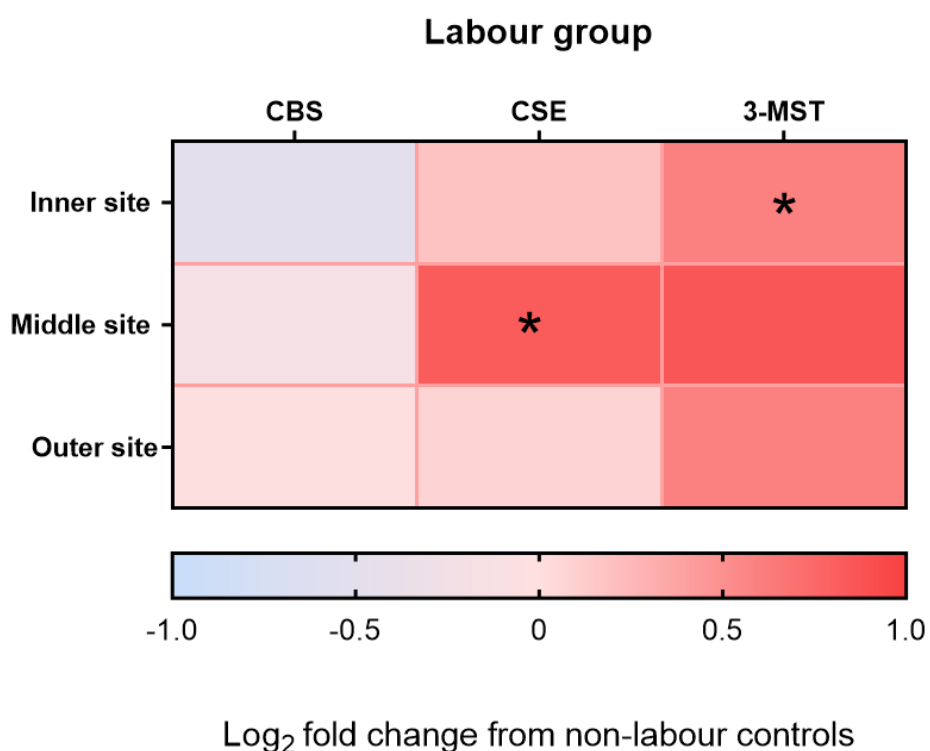
FGR

Log₂ fold change from healthy controls
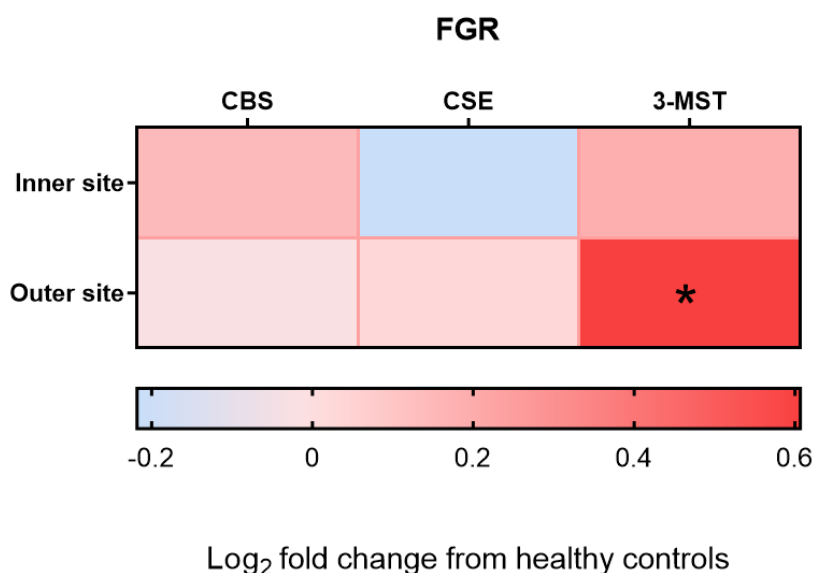
Figure 3-17 Log$_2$ fold change heat map for CBS, CSE and 3-MST genes in FGR group. Log$_2$ fold change was calculated based on ΔC$_T$ values compared to controls. The red colour implies increased expression while blue colour implies decreased expression. (*) means $p \leq 0.05$.

3.2.7 mRNA expression of H$_2$S synthesising enzymes in maternal obesity

In this section, the CBS, CSE and 3-MST expression was investigated in the high BMI group (n = 13) in comparison to the control group (n = 6) at different sites of placentas. The qPCR data analysis of CBS, CSE and 3-MST genes at three placental sites (Figure 3-18) showed that there were no significant differences in normalised expression ratio between control and high BMI groups at three placental sites. Additionally, Figure 3-19 summaries the data analysis in the heatmap of the Log$_2$ fold change of the CBS, CSE and 3-MSTmRNA level in BMI group from the control at three placental sites.

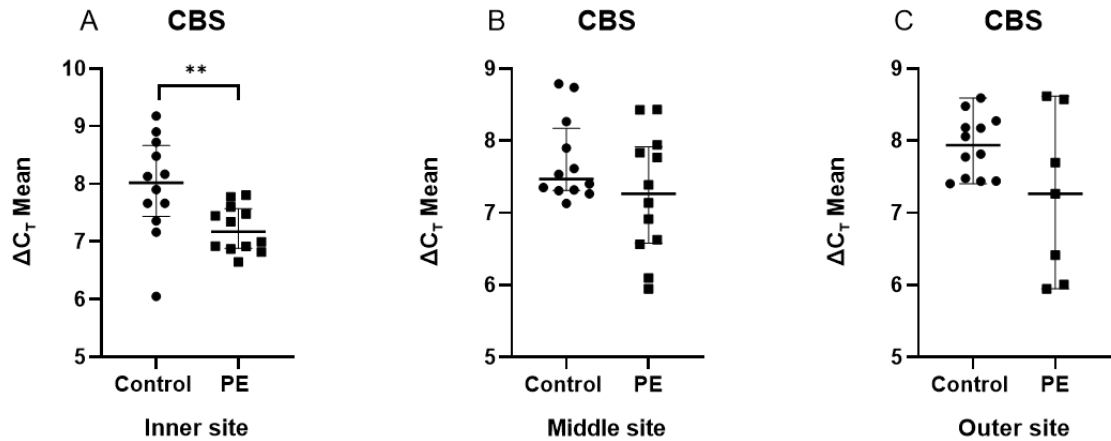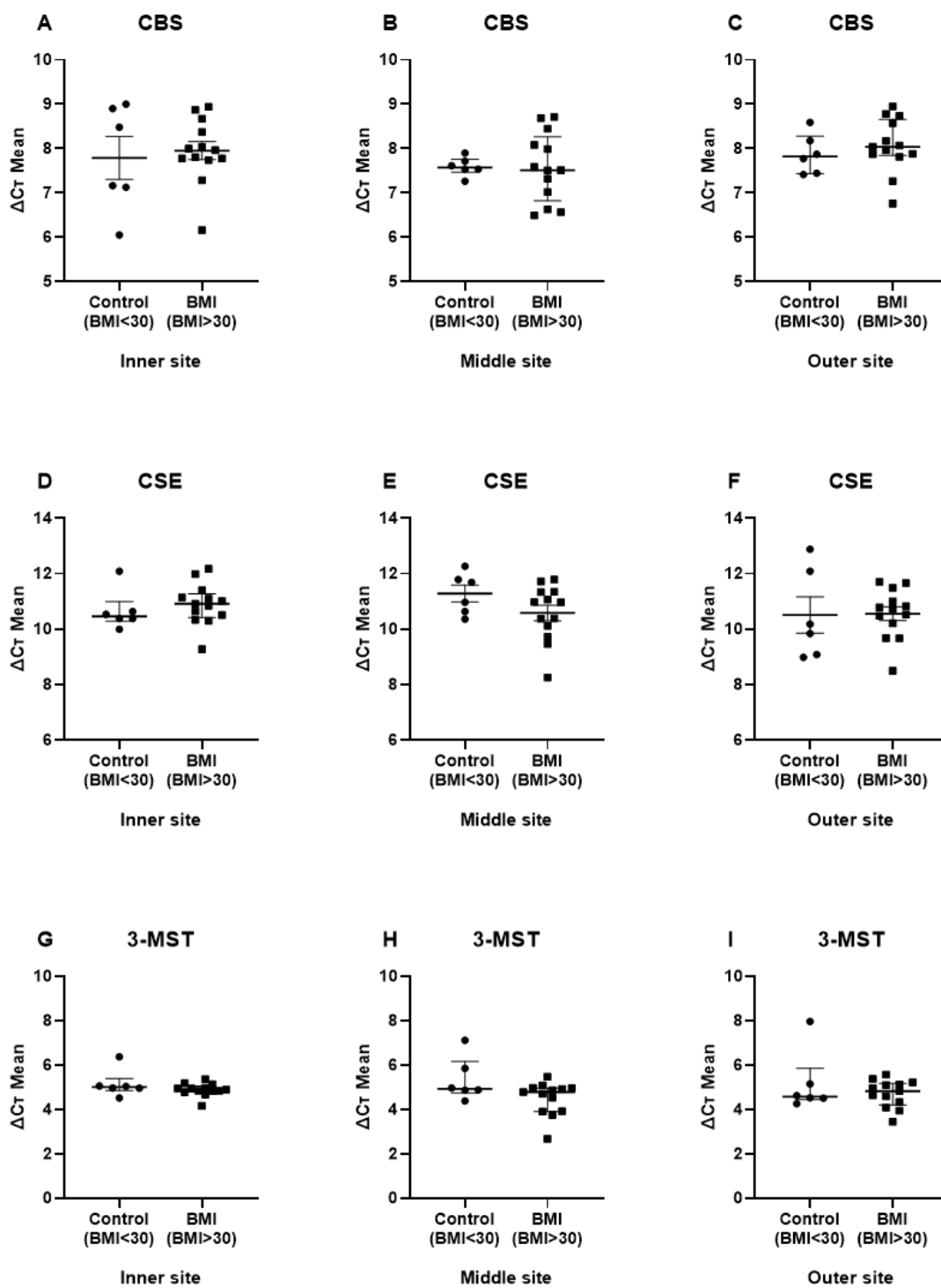**Figure 3-18 mRNA expression profiles in placentas from pregnancy complicated with high BMI. Normalised expression for CBS mRNA (A-C), CSE mRNA (D-F) and 3-MST mRNA (G-H) in high BMI group (n = 13) compared to the controls (n = 6) at inner, middle and outer placental sites. Data are presented as median and interquartile range. Comparison between groups was performed using Mann Whitney test.**

BMI group (BMI>30)
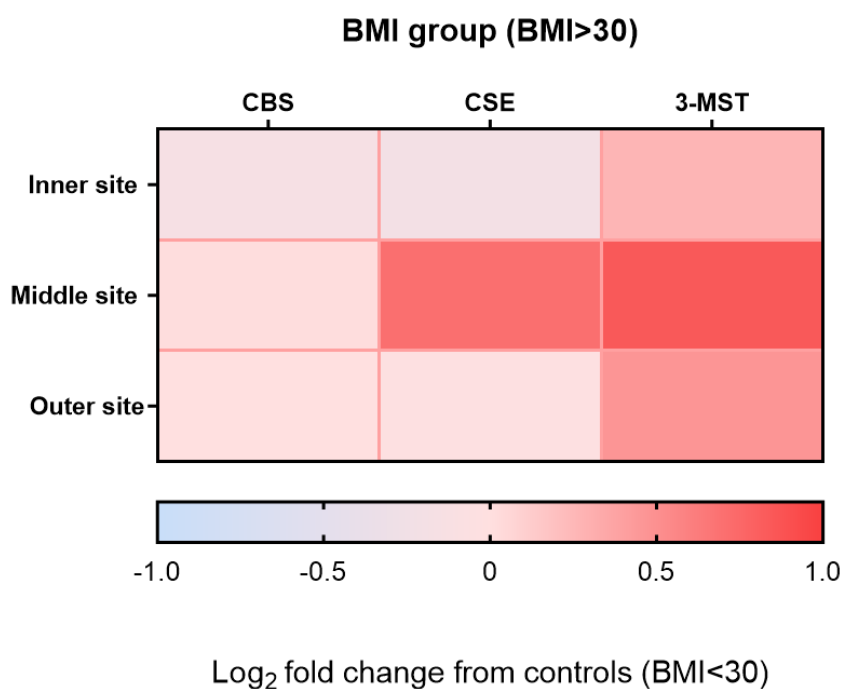
Figure 3-19 Log$_2$ fold change heat map for CBS, CSE and 3-MST genes in high BMI group. Log$_2$ fold change was calculated based on ΔC_T values compared to controls. The red colour implies increased expression while blue colour implies decreased expression.

3.2.8 Summary of the key findings for CBS, CSE and 3-MST qPCR data

A summary of CBS, CSE and 3-MST results in normal and abnormal placentas samples at different placental sites is presented in the Table 3-4. As can be seen from the table, the CBS, CSE and 3-MST mRNA levels were significantly increased in normal and abnormal placental tissues from labour, PE and FGR group at different placental sites, when compared to the control groups.

3.2.8.1 Summary results of mRNA expression of H$_2$S synthesising enzymes in normal pregnancy.

1- Within individual placentas, no spatial differences were found at the mRNA level of CBS, CSE and 3-MST in non-labour group.

2- There was a significant increase in mRNA level of CSE ($p = 0.04$) and 3-MST ($p = 0.04$) at middle and inner sites, respectively.

3.2.8.2 Summary results of mRNA expression of H₂S synthesising enzymes in complicated pregnancy with PE or FGR.

There were significant differences in mRNA expression of CBS and CSE in placentas between the PE and normotensive group. However, no significant findings were detected for 3-MST mRNA expression.

CBS mRNA level was significantly increased in PE when compared to the control at the inner site only ($p = 0.008$). When the sub-analysis of this data set was performed to compare PE group with the control one of the same modes of delivery, the difference was statistically significant in LG- PE ($p = 0.004$).

CSE mRNA level was significantly increased in PE when compared to the normotensive group at the middle site only ($p = 0.04$). When the sub-analysis of this data set was performed to compare PE group with the control one of the same modes of delivery, the difference was statistically significant in NLG- PE ($p = 0.03$).

There was an increase in 3-MST mRNA in FGR group at the outer site ($p = 0.04$). No significant differences in CBS or CSE mRNA expression were found between FGR and the control group.

3.2.8.3 Summary results of H₂S synthesising enzymes encoding genes (mRNA expression) in pregnancy with high BMI.

There were no significant differences in mRNA expression of either CBS, CSE or 3-MST in placentas from women with high BMI group when compared to controls.

Table 3-4: Summary results of qPCR data in normal and abnormal placentas.

Groups	CBS mRNA level			CSE mRNA level			3-MST mRNA level		
	Inner	Middle	Outer	Inner	Middle	Outer	Inner	Middle	Outer
NLG v LG	↔	↔	↔	↔	↑ (red)	↔	↑ (red)	↔	↔
Control v PE	↑ (red)	↔	↔	↔	↑ (red)	↔	↔	↔	
Control v FGR	↔		↔	↔		↔	↔		↑ (red)
Control v BMI G	↔	↔	↔	↔	↔	↔	↔	↔	↔

Transvere arrows indicate no significant differences between groups and red arrows indicate significant upregulation of the gene of interesent in the target groups

3.3 Discussion

Very little was found in the literature on the question of expression of H_2S producing enzymes on normal and abnormal placental tissues. Also, in reviewing the literature, no data were found about sampling of the placenta in those studies. As far as we are aware, this is the first study to investigate expression of H_2S synthesising enzymes in placentas from clearly defined groups of normal pregnancy, PE, FGR and maternal obesity, and relate this to placental zonal variation. Importantly, in this study a systematic sampling method was followed to avoid the arbitrary way of sampling placenta that may mask changes in gene expression.

3.3.1 Results summary and key findings

The current study, in general, found that mRNA expression of H_2S synthesising enzymes was differentially up-regulated during labour and in complicated pregnancies with PE and FGR. The increase in mRNA level of CBS, CSE or 3-MST in labour, PE and FGR at particular sites suggests that there is a controlled spatial change in their expression. The physiological and pathological significance of these remains to be elucidated but oxidative stress is the common link.

The study found that there were no significant differences in mRNA expression of CBS, CSE and 3-MST between the three placental sites within individual healthy placentas, and that the mRNA level of both CSE and 3-MST genes was significantly increased in placentas from women who delivered spontaneously compared with that in placentas from women who delivered by CS at middle and inner sites, respectively.

The most interesting finding is that in pregnancies, which complicated with PE, there was a paradoxical increase in CBS and CSE mRNA expression in PE group compared to the normotensive group at the inner ($p = 0.008$) and middle ($p = 0.04$) placental sites, respectively. Whereas, in FGR only 3-MST mRNA expression was significantly increased in FGR group ($p = 0.04$) compared to the control at the outer placental site only.

Contrary to the expectations, this study did not detect any significant differences in mRNA expression of H_2S producing enzymes coding genes between high BMI group and the control.

3.3.2 The correlation between sampling site and gene expression in placenta

The foremost observed findings in this chapter are that CBS, CSE and 3-MST were differentially expressed in labour and complicated pregnancies across particular placental sites. It is possible that such zonal differences may be related to the structure and vasculature of the placenta. Placental architecture and blood flow are not uniform across the human placental disc (Matijevic et al., 1995). The villous perfusion may be influenced by proximity to the umbilical cord, basal plate or chorionic plate (Benirschke and Kaufmann, 2000). Even at term the central regions of the lobules comprise the zones with least developed villi and the periphery with more mature villi and this affect the patterns of maternal blood flow within the placenta (Schuhmann, 1982). Previously, Wyatt et al. (2005) studied the correlation between sampling site and gene expression in human placenta. They analysed nine different sites from six term placentas obtained following spontaneous vaginal delivery, and the relative gene expression using qPCR was correlated with villous histology. Wyatt et al. (2005) reported that the expression of hypoxia-related genes, including VEGF and connective tissue growth factor in the term human placenta depends on sampling site within the placenta, and likely reflects local differences in villous perfusion. Their study concluded that there was a reduction in expression of hypoxia-related genes near the placental centre at the basal plate and in closeness to the cord insertion, and a higher expression level at the placental periphery at the chorionic plate.

Moreover, Wyatt et al. (2005) suggested that diminished blood flow at the periphery of the placenta predisposes the histological changes characteristic of hypoperfusion as well as up-regulation of some genes in response to hypoxia. Clearly, the mRNA data in this thesis are consistent, in some parts, with their findings. Where the up-regulation in CSE and 3-MST mRNA were correlated to samples from the labour group. This may indicate that placentas underwent stress of labour were affected with the hypoxia-reperfusion insult happing due to uterine contractions. At the present time, it is not clear whether changes in gene expression across placental zones contribute to placental dysfunction, or may represent an adaptive response, designed to attenuate the injury. Although Doppler flow studies of the human placenta consider the gestational dependent perfusion (Konje et al., 2003), detailed mapping of regional perfusion has not been performed. Despite this it seems reasonable that differences in sampling site contribute to variability in gene expression across placental disc.

Furthermore, placental separation is an important part of labour, and the way the placenta separates could explain the variation in gene expression between different placentas. Herman et al. (2002) studied patterns of placental separation by assessing the site from which separation began and by observing its mode of propagation. The study that included 101 singleton pregnant women who underwent sonographic imaging of the second and third stage of labour showed that the process of placental separation from the uterine wall can be divided into three distinct phases; latent, contraction and detachment and expulsion. Herman et al. (2002) found that placental separation is accomplished by multiphasic process with a definite direction and sequence. They noticed that in most cases (90.2%) the placenta separated from the uterine wall in a "down-up" separation, where the separation begun at the lower pole and then progressed sequentially towards the upper pole. However, cases with a previous CS had a higher rate of "up-down" separation. Additionally, they observed that in some case presented with fundal placenta, the separation started at both placental poles, bipolar separation, and the central area of the placenta was the last to separate. A future study investigating the link between the zonal distribution of CBS, CSE and 3-MST and patterns of placental separation would be very interesting.

3.3.3 Expression of H_2S producing enzymes in normal pregnancy and during labour

The present study demonstrated that CBS, CSE and 3-MST genes encoding the enzymes responsible for H_2S synthesis, are present and expressed in a human placenta. Many studies have proved that CBS and CSE, both involved in the transsulfuration pathway, produce H_2S in different cells and tissues. Previously, Patel et al. (2009) showed that CBS and CSE enzymes exist in rat and human placenta, and they are capable to produce H_2S from its precursor L-cysteine *in vitro*. However, little was known about the third enzymatic pathway in production of H_2S. Recently, Kimura and his colleagues have reported that 3-MST in conjunction with CAT contributes significantly in producing H_2S from L-cystine, and that both CAT and 3-MST were localised in brain and vascular endothelium of thoracic aorta (Shibuya et al., 2009a, Shibuya et al., 2009b). In placental tissues, Hu et al. (2017) showed for the first time that 3-MST is expressed in placentas and localised to syncytiotrophoblasts. The current study also has confirmed that 3-MST is expressed in human placentas.

The current study also compared the mRNA abundance of CBS, CSE and 3-MST in normal healthy placentas from both labour and non-labour groups. The qPCR analysis showed that mRNA levels of CSE and 3-MST in placentas from labour group were significantly

increased comparing to those ones from non-labour group. However, the up-regulation was only significant at a particular placental site. Previous publications on expression of H_2S producing enzymes in placenta are few, and none of them investigated the expression of these enzymes in normal placentas exposed to stress of labour in contrast to non-labouring placentas. One study was conducted by (You et al., 2011) to investigate expression of only CBS and CSE in human pregnant myometrium. In the myometrium, the intracellular processes involved in the shift from smooth muscle relaxation to contraction during onset of labour are largely unknown, however, it is suggested that this could be a result of the coordinated expression of contraction associated proteins such as gap junction and the receptors of agonists like oxytocin and prostaglandins (Norwitz et al., 1999). The myometrium undergoes profound structural and functional changes during pregnancy and labour, as it is believed that pregnancy causes changes in the blood flow in myometrium and placenta. Thus, the effect of labour on the uterus might be similar on the placenta. You et al. (2011) reported down-regulation of CBS and CSE mRNA in labouring myometrium. However, the present study has shown an increase in mRNA levels of both CSE and 3-MST genes during labour. A possible explanation for this could be a result of the difference in the studied tissues, or it might be that the level of detection in the RT-PCR was different between the two studies. Peng et al. (2011) previously confirmed that labour and its associated pain cause unique gene regulatory changes in maternal blood, placenta and fetal cord blood.

3.3.3.1 Oxidative stress and inflammatory pathways during labour

As mentioned before both CBS and CSE mRNA are induced by hypoxia, inflammation and oxidative stress such as in rats' liver (Teng et al., 2013) and in rat' kidney (Bos et al., 2013). Oxidative stress due to placental mal-perfusion may lead to production of pro-inflammatory cytokines such as, IL-10 into maternal circulation. Previous research has established that the inflammatory and oxidative stress that occurs during labour and delivery may alter placental gene expression (Lee et al., 2010). The qPCR data generated from placental samples obtained from both labour and non-labour group show differential gene expression. The CSE and 3-MST m RNA levels were found increased with labour and this may be a response to the oxidative stress resulting due to myometrium contractions. Possibly, CSE expression was up-regulated in response to inflammation, when stimulation of macrophage with lipopolysaccharide, a potent activator, leads to increased association of Sp1 with the CSE promoter. Moreover, cAMP-response element binding protein have binding site on the CSE promoter, thereby increasing CSE expression (Renga et al., 2009). 3-MST up-

regulation could be a response to the oxidative stress and to increase H_2S production in placental tissues particularly, syncytiotrophoblasts, to produce its cytoprotective effect. Significant amounts of ROS are produced in mitochondria, to which 3-MST is localised. Cells expressing 3-MST are resistant to oxidative stress caused by glutamate and hydrogen peroxide, suggesting H_2S produced by this enzyme may scavenge ROS in mitochondria of cells (Kimura et al., 2010). H_2S also plays as cytoprotective against oxidative stress by enhancing the cellular production of glutathione and preserving mitochondrial function (Elrod et al., 2007, Kimura et al., 2010).

3.3.4 Expression of H_2S producing enzymes in PE and FGR

The present study showed an increase in CBS and CSE mRNA abundances in PE group compared to the normotensive group. This increase could plausibly be explained by oxidative stress and inflammation which are implicated in pathophysiology of PE. The hypoxia occurring in PE due to incomplete remodelling of spiral arteries up-regulated *CBS* expression at transcriptional level via hypoxia induced factor (HIF-1) (Teng et al., 2013). In contrast to this study, Wang et al. (2013), who studied only CSE mRNA level and immunostaining in PE, suggested a reduction in mRNA level and immunoreactivity in pre-eclamptic placentas when compared to healthy placentas. Hu et al. (2017)'s study was the first study to report expression of 3-MST in normal and pre-eclamptic human placentas but it did not investigate 3-MST expression in placentas from pregnancy complicated with FGR. In this study, 3-MST mRNA expression was significantly higher in the outer site of placentas from FGR group than the controls. Also, since the FGR pregnancies are complicated with increased vascular resistance in placentas, leading to hypoxia and then oxidative stress, increased expression of 3-MST would be expected to increase generation of H_2S which acts as a vascular vasodilator and also to increase H_2S production in mitochondria to respond to the attack of oxidative stress.

3.3.5 The correlation between mRNA level and protein abundance

While qPCR is an excellent method for sensitively measuring level of mRNA abundance, it is not sufficient alone to generate strong conclusions about altered gene expression because changes in mRNA are not necessarily associated with proportional changes of the corresponding protein (Gygi et al., 1999, MacKay et al., 2004). Although for differentially expressed genes transcript abundances are the main determinant of protein abundances (Koussounadis et al., 2015), other factors can affect protein amount. For example, an

increased level of target mRNA may coexist with no changes or a change in the opposite direction at the protein levels due to increased protein degradation (post-translational factors will be discussed in chapter 6). MicroRNAs (miRNAs) which are short non-coding RNA could also be a reason of discrepancies seen between mRNA and protein abundance (Barrett et al., 2012). Considerable evidence now indicates that miRNAs can play a role in post-transcriptionally regulating gene expression by targeting the 3'-untanslated regions of mRNAs for degradation and/or inhibition of translation (Bartel, 2004, Zeng et al., 2003). Yang et al. (2012) reported that miR-21 was found to significantly decrease the Sp1 protein level but not the mRNA level in human aorta smooth muscle cells.

Alternative splicing and RNA stability are post-transcriptional factors that may affect the protein abundance. The potentially large number of transcript isoforms that can be generated from the same gene via alternative splicing could change the protein and mRNA correlation (Brar et al., 2012). Moreover, the mRNA and protein correlation might be influenced by the physical transcript properties that modify translation efficiency at different levels. Some transcripts may have a specific binding site for the ribosome upstream of the start codon which may control the translation efficiency (Maier et al., 2009). Generally, any factor affecting the translation efficiency could result in diverse relation between mRNA and protein levels.

3.4 Conclusion

Analysis of the qPCR has revealed that CBS, CSE and 3-MST were differentially regulated at the level of mRNA abundance in complicated pregnancies and during labour, validating screening by qPCR provided interesting data. Nevertheless, given the small degree of change it was important to test these findings with another approach and also to test if changes in the corresponding proteins could be quantified.

Chapter 4   Western blot optimisation

4.1 Introduction

The CBS, CSE and 3-MST qPCR data showed significant differences in mRNA expression of these genes in some comparison groups but as discussed, there are several reasons why this might not result in changes in protein/enzyme amount. Therefore, it was crucial to investigate their expression at protein level by western blotting to properly explore any role in labour and complicated pregnancies. Multiple problems were encountered during this part of the investigation and this chapter describes the approaches to accurately identify and quantify CBS, CSE, 3-MST protein levels.

Western blotting is the most common technique used to identify specific proteins from the complex mixture of proteins extracted from cells or tissues and for comparing expression of those protein from various tissues and cells. It is superior to other key antibody-based detection techniques such as IHC and enzyme-linked immunosorbent assay (ELISA) in that confidence of the specificity of the signal is enhanced by the relative molecular mass estimation provided by comparative electrophoretic mobility with protein standards of known molecular mass. Nevertheless, its dependence on antibodies, which have unpredictable non-specific binding behaviours, makes careful investigation of the specificity of any signal important for the determination of real amounts of protein. Moreover, relatively modest changes in specific protein expression are impossible to confidently identify without consistency of protein extraction from source, consistency of sample storage and knowledge of relative of protein loading therefore the steps taken to ensure these are described first.

4.2 Consideration for protein specific quantification by western blotting

Cell lysates are the most common form of sample used for western blotting. However, tissue lysates can be also obtained from tissues but require mechanical invention, such as homogenisation or sonication to extract proteins. Protein extraction also should be carried out in a cold temperature with protease inhibitors to prevent proteolysis which can occur once the cells are disrupted (Grabski, 2009). Following protein extraction, quantification of protein (e.g. by Bradford or BCA methods) is usually carried out to ensure that samples are being compared on an equivalent basis however actual quantitation of proteins of interest is

carried out relative to an actual measurement of protein transferred to the membrane such as total protein staining or specific detection of a "housekeeping" protein.

Another consideration to be undertaken is that primary and secondary antibodies need to validated in order to investigate the antibody specificity and selectivity. Although the secondary antibodies are raised towards specific epitopes on the primary antibodies, cross reactivity may occur with other separated proteins or those used for blocking, due to similar peptide sequences (Ramlau, 1987). Therefore, no-primary antibody controls should be undertaken to ensure that the observed bands are not the result of non-specific binding of secondary antibodies.

As the principle of western blotting is detection of proteins through binding and recognition of antibodies, this binding and interaction should be highly specific between a portion of antigen or epitope and the recognition sites found on fragment antigen binding region of the antibody. The primary antibodies should be thoroughly assessed and validated to be specific and more sensitive to detect the intended target proteins. One of the most accepted and trusted validation processes for antibody specificity is genetic knockout (KO) validation (Zhong et al., 2018). In this, if a band on a western blot is the true protein of interest, that band should be absent from a protein sample from cells in which the gene has been specifically knocked out.

4.3 Evaluation of extracted protein quality

This work used a method previously and widely used for investigating these enzymes, which extracts mainly cytoplasmic proteins without detergent extraction, but in the presence of proteinase inhibitors (Lyall et al., 2000, Lyall et al., 2001). The samples used in this study had been stored either as protein extracts or a frozen tissue for months or years therefore, as accuracy of western blot results depends heavily on the quality of the extracted protein, quality comparison of samples was important to conduct. Coomassie blue gel staining was performed in order to determine whether the stored sample proteins showed sign of degradation and if so, to what extent. Stored frozen protein samples were compared with some freshly extracted from frozen placental tissues and also freshly extracted from BeWo and MCF-7 cell lines. The latter two should represent protein samples that were as undegraded as possible to get as they were from actively growing cells. The samples preparation method was standardised by using a consistent protein extraction protocol throughout the duration of the study. The previously extracted protein from placental tissues

and the newly extracted ones, either from placental tissues or cell lines, were run in an SDS-PAGE gel and stained with Coomassie Brilliant Blue (section 2.7.1.3). Figure 4-1A shows that the overall pattern of bands was highly similar in all samples and Figure 4-1B shows that there was no shift to lower MW bands in either the stored protein samples or from the frozen tissue compared to the cell lines indicating there was no significant protein degradation and so the storage conditions had been adequate and that samples could be used with confidence.
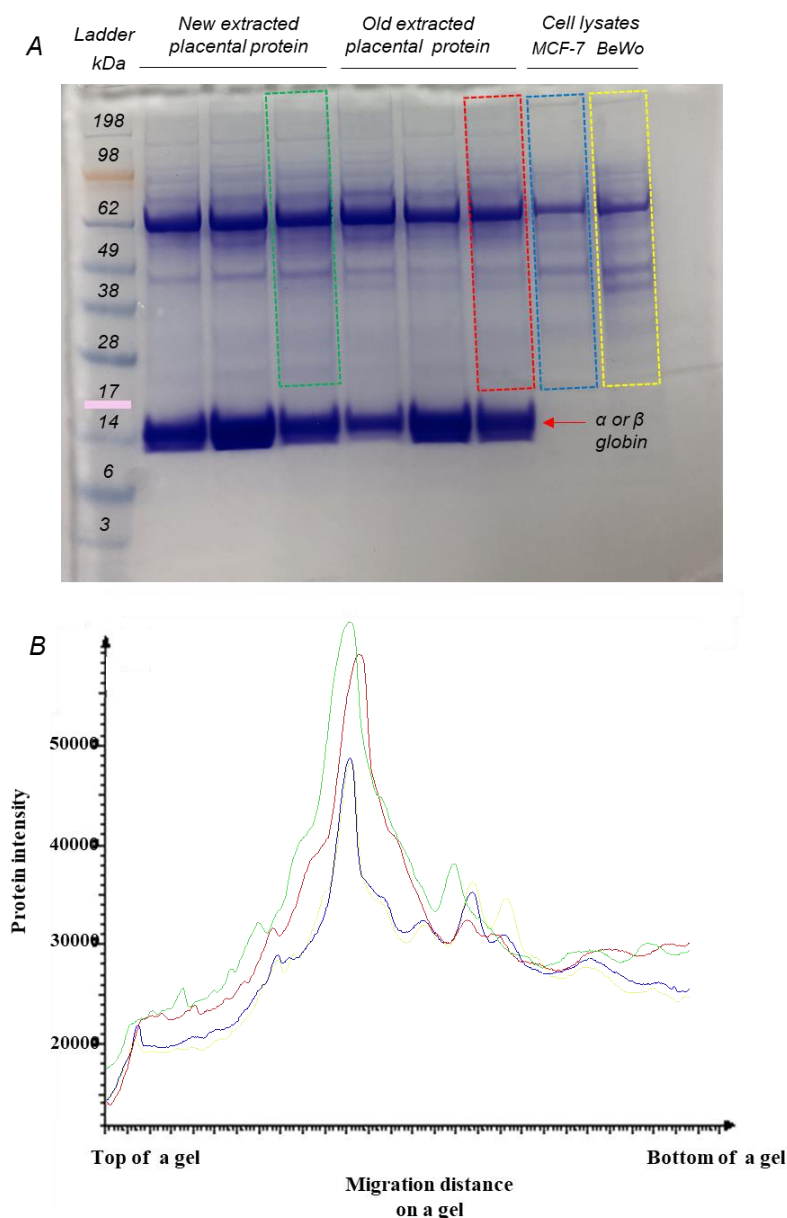
Figure 4-1 Coomassie blue stained SDS-PAGE of 20 µg protein from placental and cellular lysates. (A) The first lane represents the protein molecular ladder, lanes 2-4 represent new extracted placental lysates, lanes 5-7 represent old extracted placental lysates, and lanes 8&9 represent new protein lysates from MCF-7 and BeWo cells, respectively. The green, red, blue and yellow dashed rectangles show the regions subjected to intensity quantification in B. The strong band only seen in the placental samples is probably haemoglobin monomer (α or β globin, ~ 16 kDa) from blood in placental tissue lysates (red arrow). (B) A plot shows the intensity distribution of proteins against the relative electrophoretic mobility (inversely correlated to MW).

4.4 Western blot normalisation

In order to compare target protein expression levels between several different samples, the specific proteins must be measured from the same amount of protein applied to the membrane. This has been traditionally done by comparing the relative abundance of a protein of interest to that of a housekeeping control. However, several recent reports suggest that the use of the most common loading controls including GAPDH, β-actin and tubulin for normalisation of western blot should be carefully evaluated as they can show significant variations at the mRNA and protein levels in various tissues (Pérez-Pérez et al., 2012) and under different physiological and pathological conditions (Ferguson et al., 2005, Lanoix et al., 2012).

Total protein staining of the blotted membrane is an alternative method for normalisation of sample loading in quantitative analysis of western blot data (Fosang and Colbran, 2015, Gilda and Gomes, 2013). For this, Stain-free™ (Bio-Rad), Ponceau S and Amido Black staining have been shown to be suitable alternative to housekeeping proteins as loading controls. Ponceau S stain is fast, inexpensive, non-toxic, does not require protein fixation, is completely reversible and does not interfere with subsequent detection of specific proteins by antibody binding. Of specific relevance to this study, Lanoix et al. (2012) studied the expression of five reference proteins, β-actin, GAPDH, α-tubulin, hypoxanthine phosphoriosyltransferase 1 (HPRT1) and peptidylprolyl isomerase (PPIA), and two general protein stains, Ponceau S and amido black in normal pregnancies and complicated pregnancies with PE or gestational diabetes mellitus. The placental samples were excised from randomly selected regions in the placentas. Lanoix et al. (2012) found that in PE pregnancies placentas, the expression of GAPDH and PPIA was significantly increased compared to normotensive pregnancies, and that GAPDH, PPIA and β-actin expression were significantly increased in gestational diabetes mellitus placentas compared to non-gestational diabetes placentas. It seems that the oxidative stress happening in complicated pregnancies could be the cause for that, especially, it has previously, been reported that oxidative stress is a known inducer of GAPDH and PPIA expression (Baek et al., 2008, Jin et al., 2000). Furthermore, they found that α-tubulin, PPIA and GAPDH were below the inter-group stability acceptable limit for comparison between placentas from normotensive and pre-eclamptic pregnancies. However, β-actin, Ponceau S stain, and amido black were stably expressed between these two groups. Thus, it seemed that the most stable loading controls for comparison between placental samples from pregnancies complicated with PE and their controls were Ponceau S stain, amido black and possibly β-actin. Because the

significant fold difference detected by qPCR between groups in this study were small an investigation of loading controls was carried out.

4.4.1 Housekeeping protein validation

Two proteins (β-actin and α-tubulin) were chosen as candidate internal references for quantification in this study. The apparent molecular weights of these antibodies are ~ 42 and ~ 50 kDa, respectively, as reported by the antibody manufacturer. The first experiment (Figure 4-2) was to test if the antibodies used for β-actin and α-tubulin were specific to their intended target when bound to the membrane as judged by detection of a major single band of the expected MW. Different loading amounts of protein, different dilutions of both primary and secondary antibodies, and different blocking conditions were tried to detect the intended band for each antibody (Appendix 2). Figure 4-2 shows the most successful of these where single bands at the predicted MW were observed.
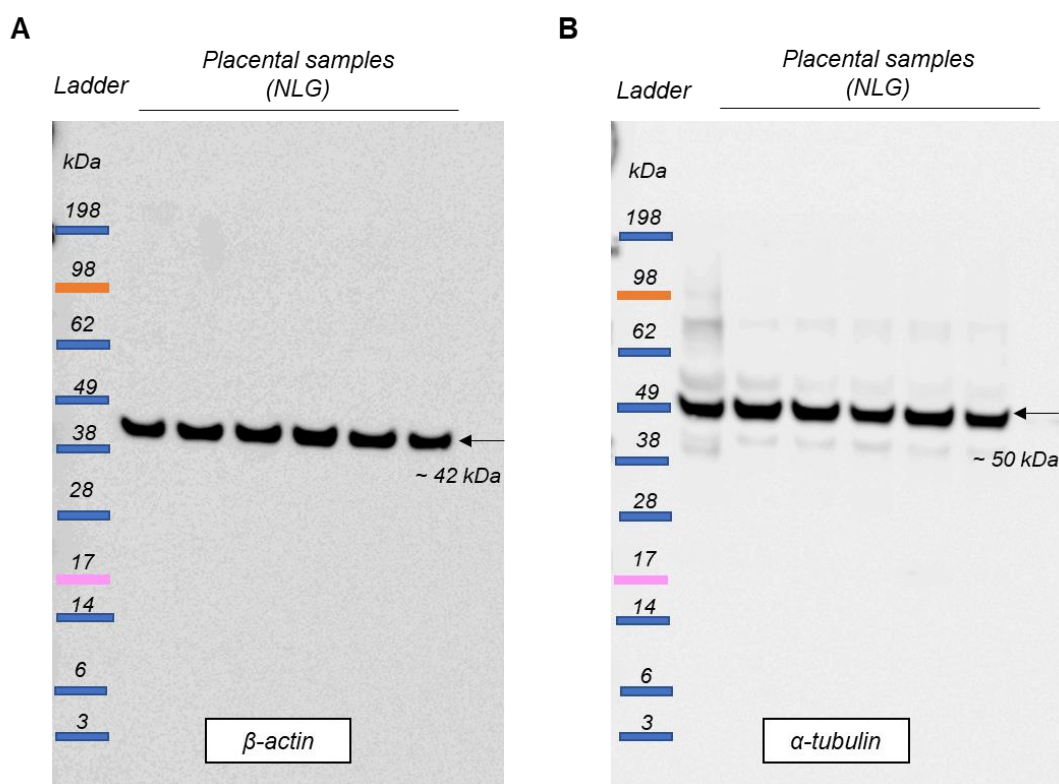
Figure 4-2 Western blotting of placental samples from healthy women (NLG) with housekeeping proteins, β-actin and α-tubulin. 20 μg of protein lysates were loaded into a 4-12% Tri-Bis gel. The first lane represents the protein molecular ladder. MW or proteins determined as described in section 2.7.4. The lanes 2-7 represent the placental lysates. (A) Immunoblotting with β-actin antibody, and an apparent band at ~ 42 kDa was observed. (B) Immunoblotting with α-tubulin antibody, and an apparent band at ~ 50 kDa was observed. The MW of proteins were estimated by referring to the protein marker.

4.4.2 Total protein staining with Ponceau S solution

Recent guidelines from Fosang and Colbran (2015) are that normalisation with respect to total protein is preferrable in quantitative analysis of western blot data. Therefore, the quality of Ponceau S detection of placental proteins transferred to membranes was first assessed to test the correlation of Ponceau S staining intensity with amount of placental protein loaded as measured by Bradford assay. For this experiment, 20 µg (as measured by Bradford assay) of placental lysates were loaded into 4-12% Tri-Bis gel. After gel electrophoresis and transfer, the nitrocellulose membranes were rinsed briefly in distilled water and incubated in Ponceau S solution (0.1% w/v in 5% acetic acid) for 5 minutes followed by destaining in water twice for 10 seconds each, to remove non-specific Ponceau staining so that the lanes and bands were visible on a clear background. The membranes were then inserted between transparency sheets and scanned at 300dpi to TIFF file using a standard scanner, CanoScan 9900F (Figure 4-3). After that, intensities of the bands in each lane were quantified using AIDA software.
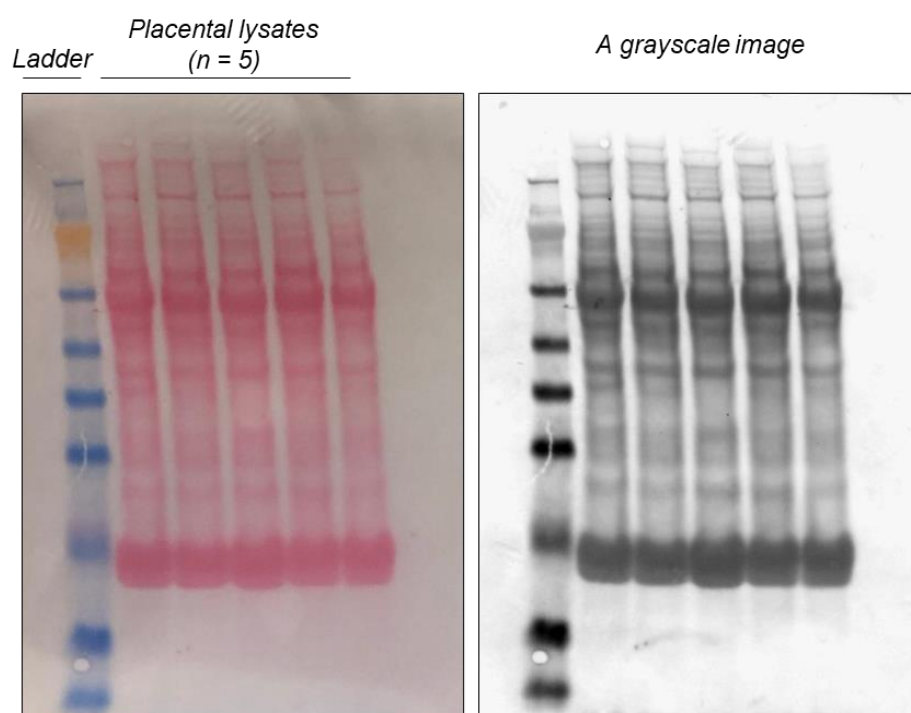
Figure 4-3 Total protein staining of nitrocellulose membrane with Ponceau S stain. 20 µg of placental lysates (NLG) were loaded into a gel run in MES buffer. The first lane refers to the protein molecular ladder and lanes 2-6 represent the placental lysates. Right panel shows the membrane stained with Ponceau S stain. Left panel shows a scanned image of the membrane.

The Figure 4-3 shows that the sample loading among lanes seems to be equal, and this is indicated by similar Ponceau S stain intensities in all lanes. The coefficient of variation (CV) of Ponceau S staining intensity versus Bradford-estimated protein amount lanes was

calculated and found to be low (Figure 4-4) indicating uniform transfer in this gel system and reliability of Ponceau S staining as a reference.
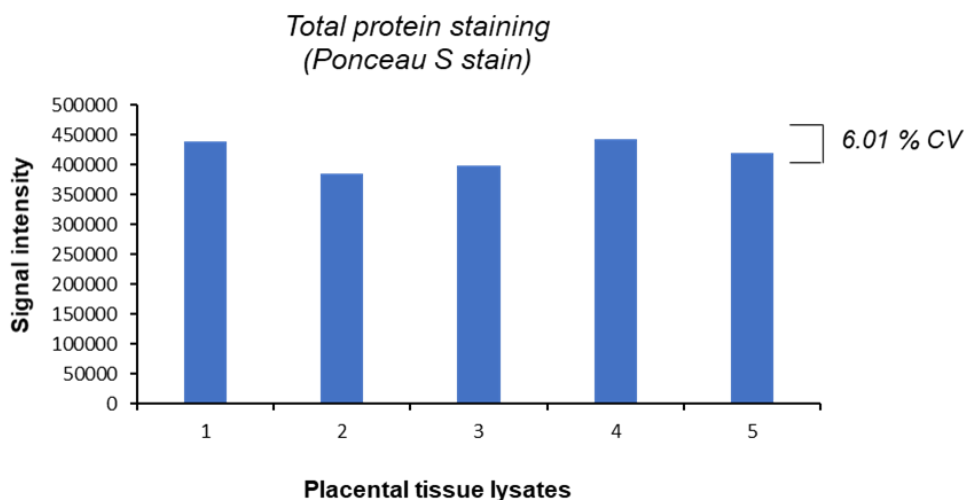
Figure 4-4 Estimation of transfer efficiency. The graph shows the variation among signal intensities of the protein samples used in Figure 4-3. The X-axis represents different placental lysates and the Y-axis represents signal intensities generated from total protein staining with Ponceau S stain in each lane. The CV of transfer efficiency is 6.01 %, which indicates good and uniform transfer.

4.4.3 Dynamic range of detection for loading controls

Another requirement for reference signals is that they display a linear relationship between signal intensity and the mass or volume of sample loaded, and this must be confirmed (Fosang and Colbran, 2015). Normalisation and analysis of the generated data must be performed in the linear range of detection, where a linear response is observed between sample loading and band intensity. Some of the most popular housekeeping proteins are abundantly expressed, which may limit their use as normalisation controls when the protein of interest is much less abundant because under such conditions, loading enough protein to detect the protein of interest could result in an under-saturated signal for a highly expressed loading control. Therefore, signal intensities for two common loading controls and total protein staining have been tested for their liner relationship with the sample loading. Placental tissue lysate was loaded at 10, 20, 30, 40, 50 and 60 µg per lane on a gel to determine if the signal intensity is proportional with the sample concentration and abundance of the protein. After gel electrophoresis and protein transfer, the membrane was stained with Ponceau S stain for 5 minutes and quickly distained in water. The membrane was then imaged and after that the membrane was distained in TBST buffer and β-actin and α-tubulin immunoblotting was performed subsequently (Figure 4-5).
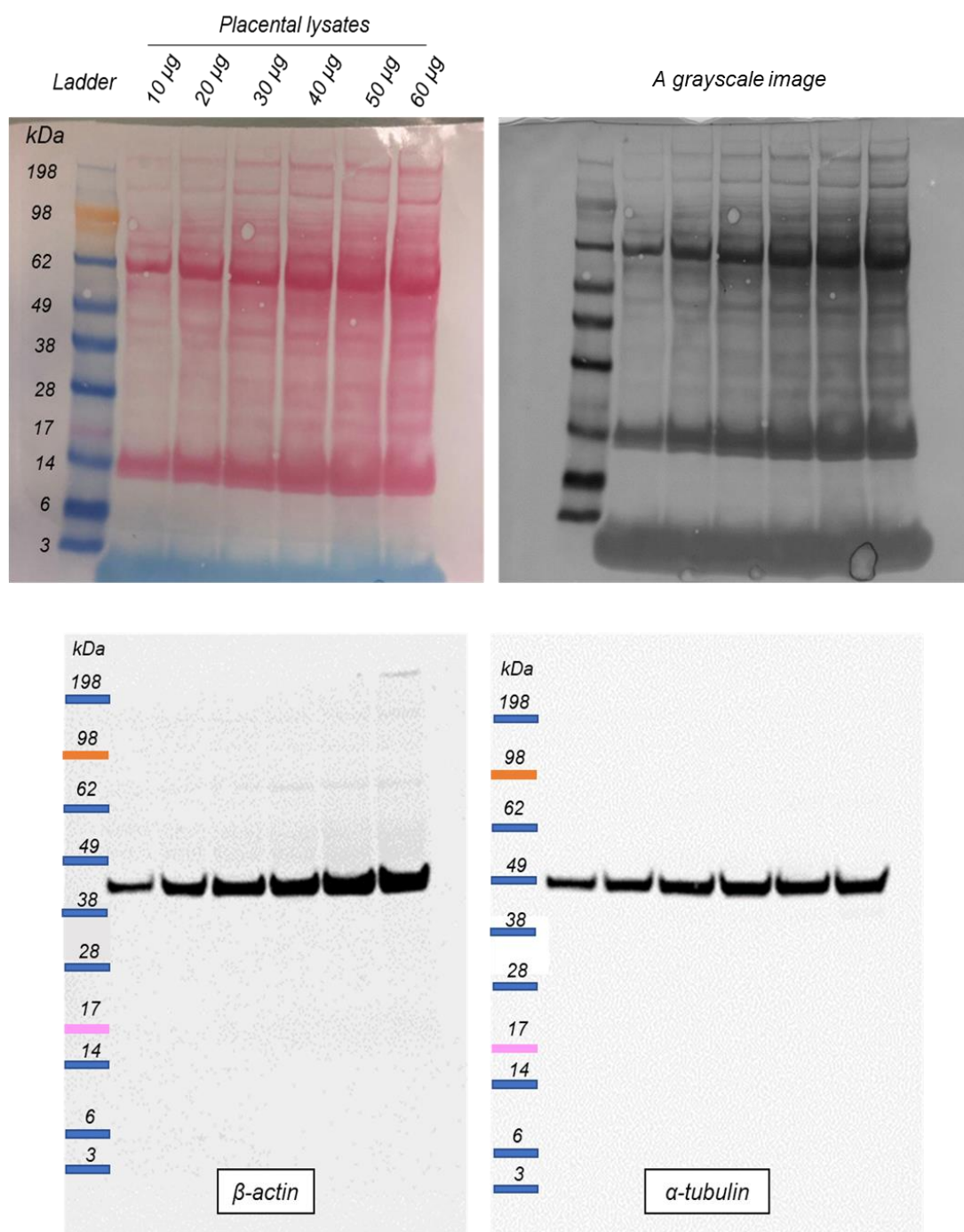
Figure 4-5 Identification of dynamic range of detection. Placental tissue lysate was loaded at 10, 20, 30, 40, 50 and 60 µg per lane into a 4-12% Tri-Bis gel. The upper panel shows the Ponceau S staining and a grayscale image of the scanned membrane. The lower panel shows the immunodetection with β-actin and α-tubulin antibodies. The first lane represents the protein molecular ladder and lanes 2-7 represent a placental lysate loaded at different protein concentration per lane.

The total protein staining, β-actin and α-tubulin band intensities were quantified using an AIDA software. The signal intensity of the bands was plotted versus the concentration of protein loaded on the gel (Figure 4-6).
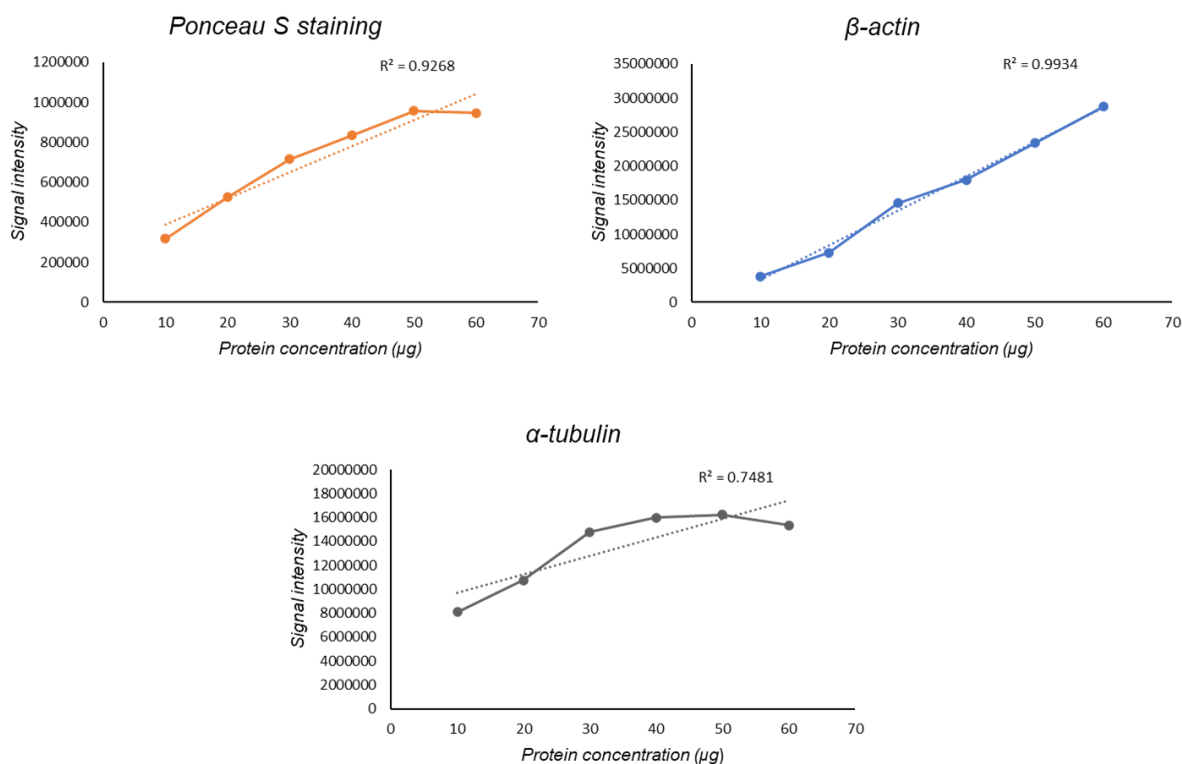
Figure 4-6 Determination of the linear range of detection for total protein staining, β-actin and α-tubulin. Graphs show the relative signal intensity of total protein, β-actin and α-tubulin on the membrane versus the amount of protein loaded on the gel.

From the data in the Figure above, it is apparent that the linearity of total protein staining and β-actin are superior to α-tubulin as a loading control for placental lysate. The squared correlation coefficient (R^2) for linear regression lines of total protein and β-actin were 0.92 and 0.99, respectively compared to 0.74 of α-tubulin. The relationships were reasonably linear up to 50-60 µg of total protein loaded, indicating that there is no limitation of dynamic range imposed by the use of β-actin or Ponceau S stain within this range of applied protein.

4.4.4 Correlation between signal intensities of Ponceau S stain and β-actin

As both Ponceau S stain and β-actin showed a linear relationship with the sample concentration, they should also show a linear relationship when plotted against each other. Therefore, a western blot was performed with 20 µg (as measured by Bradford assay) of protein samples from healthy placentas. The nitrocellulose membrane was stained with Ponceau S stain, and after scanning the membrane, the membrane underwent a process of immunodetection with anti-β-actin antibody. Intensities of bands, either generated from total protein staining or β-actin bands, were quantified. Pearson's correlation was used to examine the correlation between total protein stain and β-actin bands intensities (Figure 4-7).
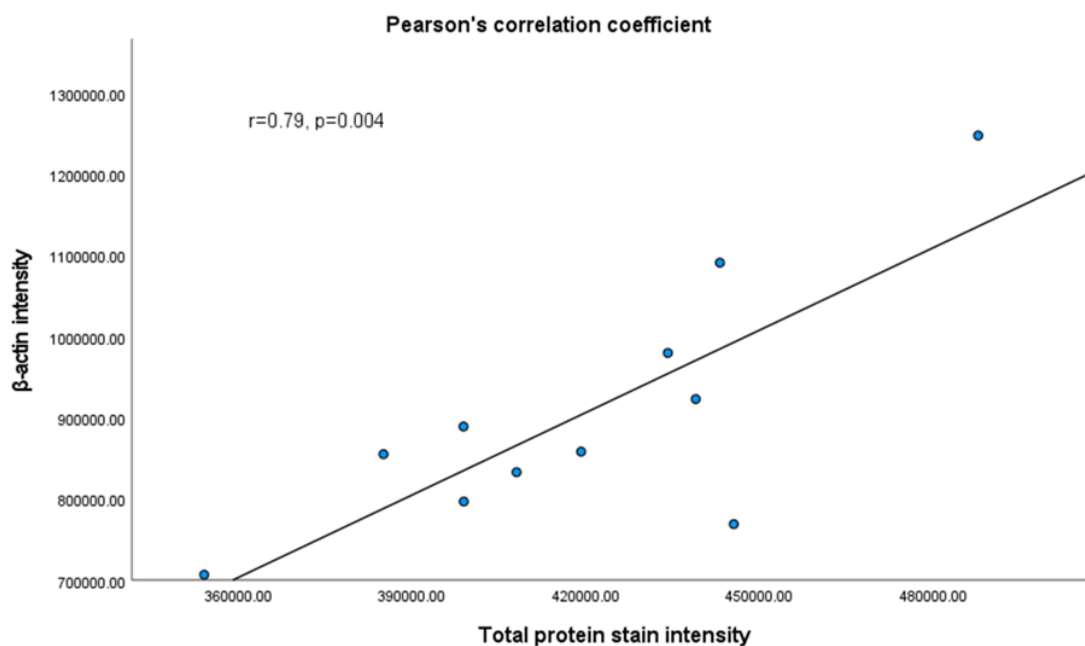
Figure 4-7 Correlation between total protein staining and β-actin densitometric signal intensities. 11 placental samples were loaded into a 4-12% Tri-Bis gel, the membrane was stained with Ponceau S stain and then immunoblotting with anti-β-actin antibody. Intensities of total protein bands and intensities of β-actin bands were quantified using AIDA software. The X axis represent the signal intensity of total protein and Y axis represent the signal intensity of β-actin. The correlation between the signal intensities was measured by Pearson's correlation test. "r" means correlation coefficient that measures both strength and direction of the linear relationship between two variables. "*p*" indicates significance of the correlation.

The correlation between intensities of the bands generated from total protein staining with Ponceau S stain and β-actin is typically around 0.79 (r), which indicates that there is a strong positive linear relationship between variables. The p-value for this correlation (p = 0.004) is less than the significance level of 0.05, which indicates that the correlation coefficient is significant.

Overall, the data obtained from the Dynamic range of detection for total protein staining and β-actin, and the correlation between them provide validation for the use of both β-actin and Ponceau S stain to assess equal loading and normalisation in western blots.

4.4.5 Stripping and re-probing of nitrocellulose membranes

Stripping and re-probing is commonly undertaken to investigate multiple protein targets within a single gel run, and it allows a number of different analyses on a single membrane for example a protein of interest and then a loading control as was the case in this study. Care must be taken to test whether the stripping buffer has removed enough of the first primary + secondary antibodies from the membrane, otherwise these may interfere with the subsequent detection and quantification of the second target protein especially two proteins

of interest are of similar MW. Probing for the loading control is usually done second because this is normally a highly expressed protein (e.g. β-actin) and even if there is residual signal from the first protein, this is too weak to significantly interfere with quantification of the loading control. Although β-actin was considered as a suitable loading control in this project, it was very difficult to cut the membrane to probe with anti-β-actin antibody separately because the MW of β-actin is close to those of proteins of interest. Therefore, stripping of the membrane and re-probing was the only choice to do. To check efficiency of our stripping protocol (section 2.7.5), membranes probed with the 3-MST antibody (Figure 4-8A) were stripped and ECL detection was repeated for the same maximum exposure time as for the detection of 3-MST. This showed no residual signal (Figure 4-8B), indicating removal of the secondary antibody with or without the primary antibody. After that, the membranes were then re-blocked and re-probed with anti-β-actin antibody. This shows that the β-actin signal was easily distinguishable from residual 3-MST which was probably due to incomplete removal of the primary antibody and using the same secondary antibody.
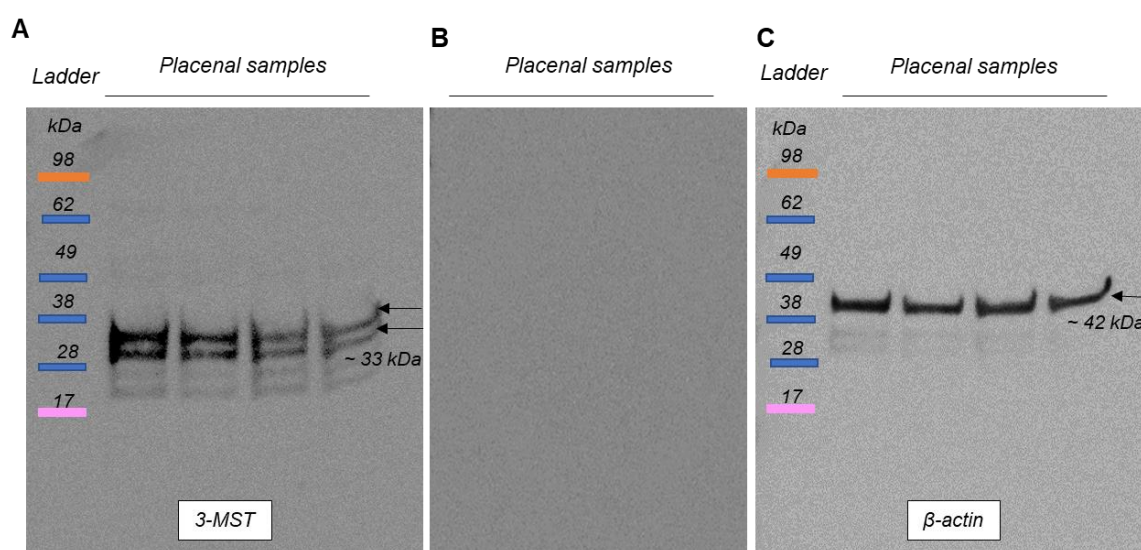
Figure 4-8 Western blots of placental samples showing stripping and re-probing of the membrane. (A) Probing of the membrane with anti-3-MST antibody, (B) ECL exposure after stripping of the same membrane and (C) Re-probing of the same membrane with anti- β-actin antibody. The exposure time was 1 minute in all blots.

4.5 Secondary antibodies validation

Different secondary antibodies (donkey anti-rabbit, goat anti-rabbit, donkey anti-mouse and two goat anti-mouse) were used and tested for cross reactivity and specificity of these secondary antibodies to placental proteins extracted, separated and blotted by the standard method used in this study. 20 µg of placental tissue (NLG) and BeWo cell lysates were loaded into 4-12% Tri-Bis gel, with no-primary antibody incubation. The western blot result

in Figure 4-9A revealed that the donkey anti-rabbit antibody did not show non-specific binding while the goat anti-rabbit was non-specifically bound to other proteins. The donkey anti-mouse showed non-specific binding and also both goat anti-mouse IgGs (Novusbio and Dako) showed non-specific binding (Figure 4-9B) but the Dako goat-anti-mouse had less non-specific binding and was chosen for further use.
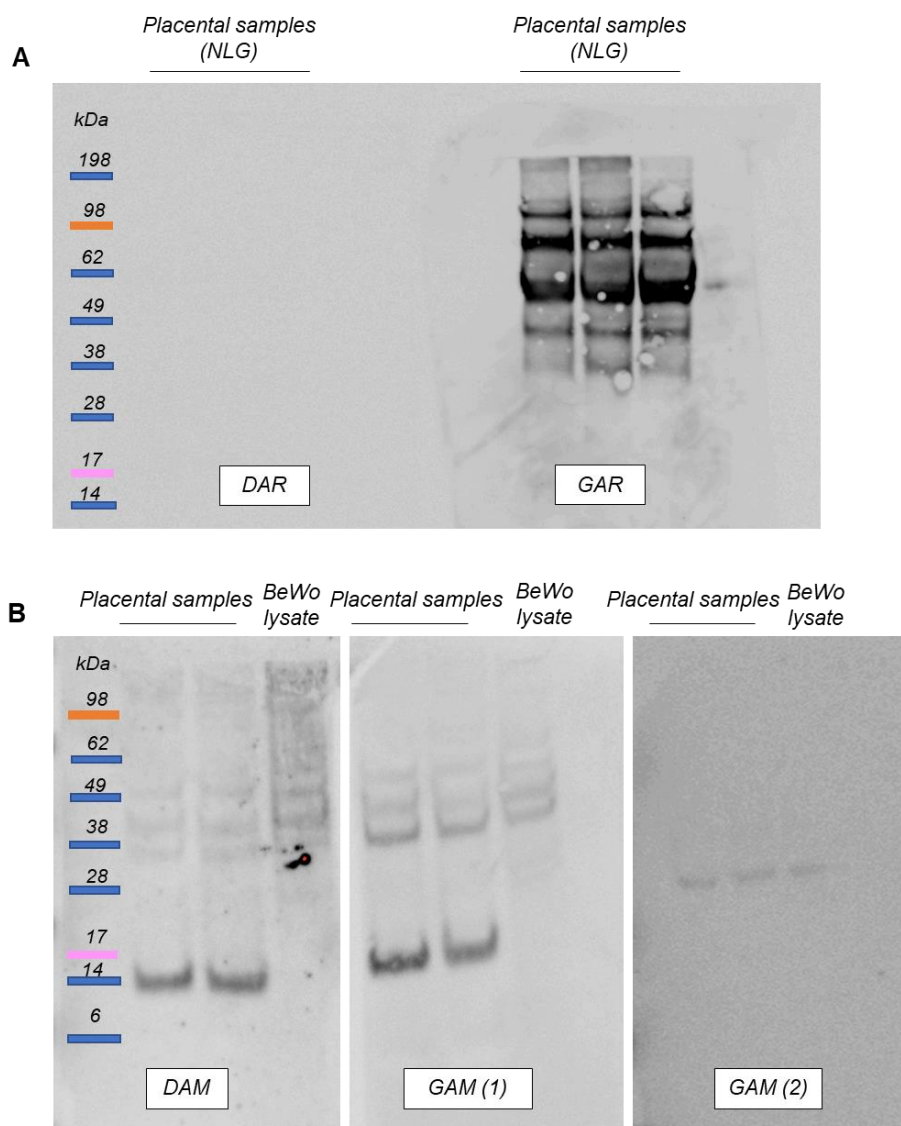
Figure 4-9 Western blotting of placental and BeWo cell lysates for secondary antibodies negative controls. (A) Immunoblotting with HRP donkey anti-rabbit IgG (DAR) versus goat anti-rabbit IgG (GAR) secondary antibody (B) Immunoblotting with donkey anti-mouse IgG (DAM) versus two goat anti-mouse (GAM) secondary antibodies. GAM 1 (Novusbio) and GAM 2 (Dako).

4.6 Primary antibodies Validation

The isoforms of CBS, CSE and 3-MST protein and their expected MW were summarised in Table 4-1. The antibody manufacturers report the sizes of proteins detected by their antibodies for CBS, CSE and 3-MST as ~ 61, 45 and 33 kDa, respectively.

Table 4-1: CBS, CSE and 3-MST protein isoforms. The data about transcript variants and their predicated protein were obtained from human genome browser and NCBI databases. (MW) refers to protein relative molecular mass in kilo Dalton (kDa) and (aa) refers to amino acids.

Gene	Transcript variant	Protein isoform	Length (aa)	MW (kDa)
CBS	Variant 1,2,3 and 4	1	551	60.587
			565	61.863
	Variant 5	2	466	49.219
CSE	Variant 1	1	405	44.508
	Variant 2	2	361	39.505
	Variant 3	3	373	41.26
3-MST	Variant 1	1	317	35.25
	Variant 2, 3 and 4	2	297	33.179
	Variant 5	3	237	26.419

Testing of multiple antibodies against CBS, CSE and 3-MST was carried out as recommended in the accompanied data sheets and as described in the literature. Different loading amounts of protein (20, 30, 40, 50 µg), different dilutions of both primary and secondary antibodies, and different blocking conditions were tried to detect only bands of expected sizes for each antibody (Appendix 2).

4.6.1 Anti-3-MST antibody validation

For the anti-3-MST antibody, the two major bands observed (Figure 4-10) were the size of the two major isoforms generated by alternative splicing (universal protein knowledgebase (UniProtKB) database; Table 4-1). At least one of the smaller bands was the correct size of the only other isoform recorded on the NCBI genome browser database. The same pattern was seen in a western blot of immunodetection of 3-MST in different cell lines (see later section 4.7, Figure 4-14C). Faint bands with smaller and larger sizes than the major 3-MST bands were observed in the blot, and these were non-specific binding.
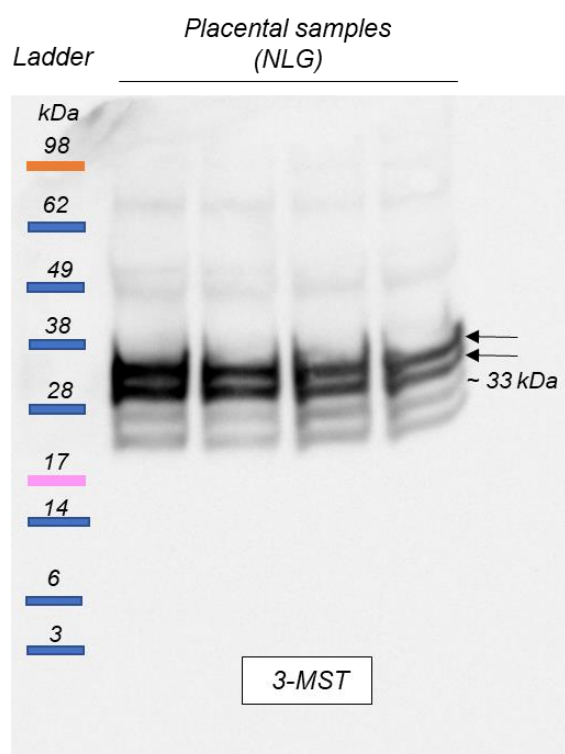
Figure 4-10 Western blotting of four placental samples (NLG) with anti-3-MST antibody. 40 µg of protein was loaded into 4-12% Tri-Bis gel with MES running buffer. Lane 1 represents the molecular ladder. The apparent MW of 3-MST band is at 33 kDa. The black arrows refer to the major 3-MST bands. The faint bands below and above the major bands were non-specific binding.

4.6.2 Anti-CBS antibody validation

Three different anti-CBS antibodies were tried; one recommended by the Sigma research assistant (SAB1405568), one from Abnova (H00000875-M01) and one from Abcam company (ab131155). All three have been used in published studies (Chen et al., 2017, Holwerda et al., 2012, Hu et al., 2016, Mislanova et al., 2011, You et al., 2017) to investigate CBS protein expression by western blotting in cultured trophoblast cells and placental and myometrial tissues. In all cases of antibody testing in this study, although a band with the correct, apparent MW of ~ 61 kDa were seen, multiple other bands of sometimes greater intensity were observed in Figure 4-11 that shows western blotting of placental samples with anti-CBS antibodies. It is not clear that whether those bands were due to non-specific bindings or specific to CBS protein which had migrated at a MW different to the expected size because of, for example, post-translational modifications. Despite prolonged experimentation with alternative blocking solutions, they could not be eliminated. It is not clear whether the published studies that used these antibodies encountered similar problems because in these papers, only a narrow snapshot window of the blot is shown.
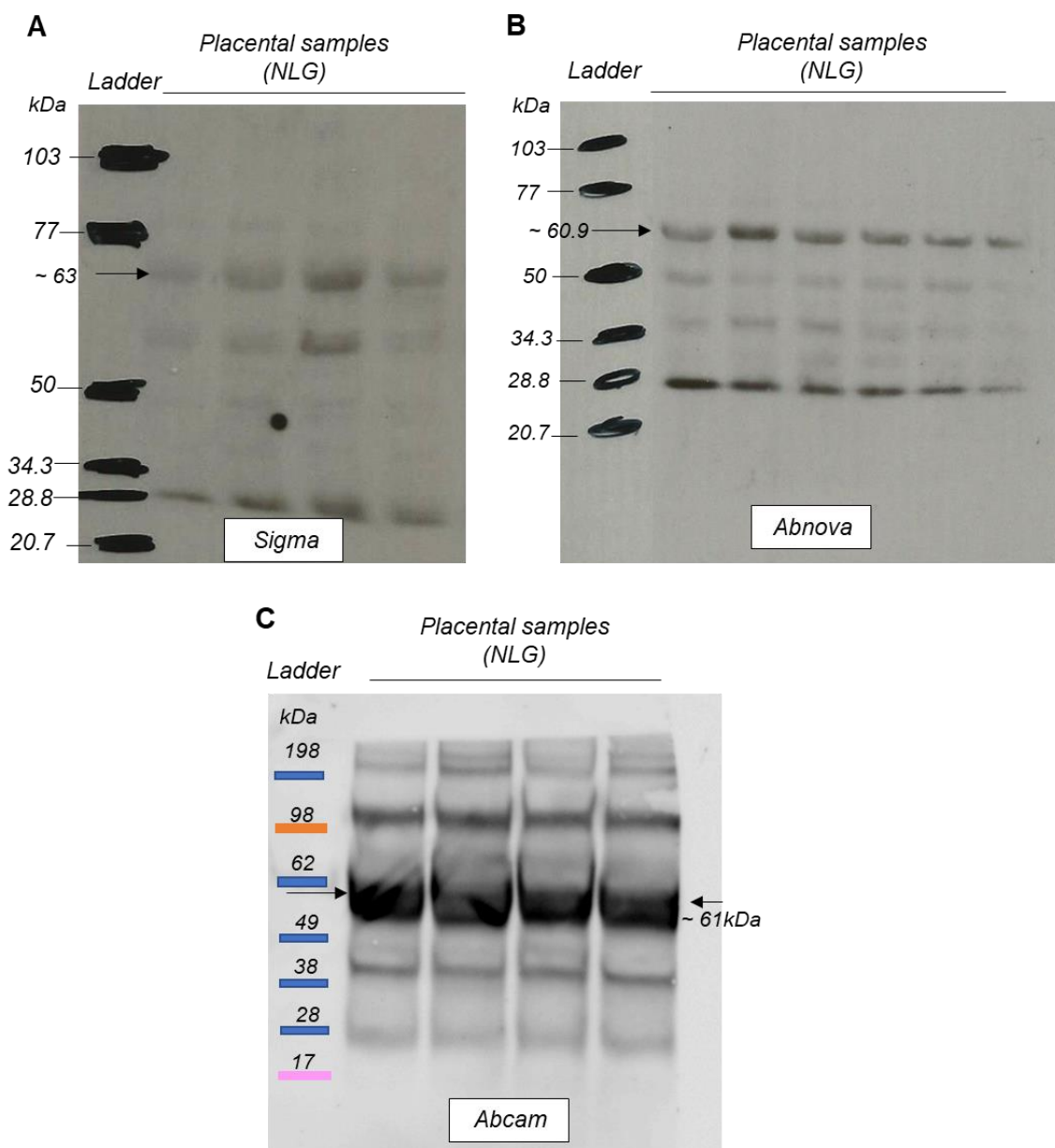
Figure 4-11 Western blotting of placental samples with different anti-CBS antibodies. (A) Immunoblotting with anti-CBS antibody (sigma). (B) Immunoblotting with anti-CBS antibody (Abnova). 50 µg of protein was loaded into 4-10% gel with running buffer. The black marker corresponds to the bands in pre-sained SDS-PAGE protein MW standard (Bio-Rad, cat. no. 161-0305), and the black arrows refer to the estimated MW. (C) Immunoblotting with anti-CBS antibody (Abcam). 40 µg of protein was loaded into 4-12% Tri-Bis gel with MES running buffer. The black arrow refers to the expected CBS band size (~ 61 kDa).

4.6.3 Anti-CSE antibody validation

Four different anti-CSE antibodies were tried; one recommended by Sigma-Aldrich (SAB14035673), one from Abnova (H00001491-M02), one from Abcam (ab54573) which was used in a previous study in human astrocytes and microglia brain cells (Lee et al., 2009) and one from Novusbio (H00001491-M01) which was used by Holwerda et al. (2012) and Cindrova-Davies et al. (2013) to investigate CSE expression by western blotting in human placental tissues. The Anti-CSE antibody (Abcam) was also tested in this study in a human

myometrial lysate which previously extracted from human myometrium (by another PhD student), and human uterus tissue lysate (Abcam, cat. no. ab29509) which was recommended by the Abcam scientific research assistant to use it as a positive control for CSE. Most of the time, although a band with the correct, apparent MW of ~ 39-45 kDa were seen, multiple other bands were observed each time despite several attempts had been made to eliminate them (Appendix 2). As shown in Figure 4-12, multiple bands were observed in all samples including myometrial and uterus tissue lysates, despite prolonged experimentation with alternative blocking solutions and different antibodies concentrations. Here again it is not clear whether the published studies that used these antibodies encountered similar problems because in these papers, western blot images were overcropped showing the target bands only.
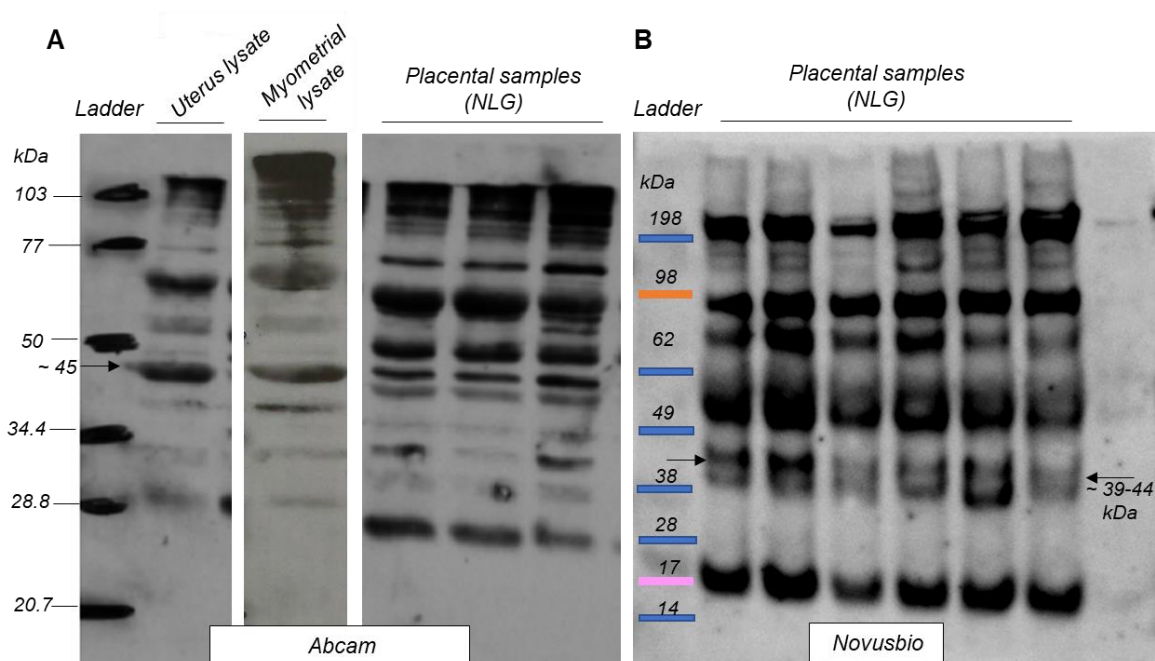
Figure 4-12 Western blotting of placental, myometrial and uterus tissue lysates with anti-CSE antibodies. (A) Western blotting with anti-CSE antibody (Abcam). 50 μg of uterus, myometrial and placental protein were loaded into 4-10% gel with running buffer. (B) Western blotting of placental tissue lysates (NLG) with anti-CSE antibody (Novusbio). 40 μg of placental protein was loaded into 4-12% Tri-Bis gel with MES running buffer. The apparent MW of CSE band is at ~ 39- 44 or 45 kDa (black arrows).

Although Figure 4-1 had shown that overall (Coomassie stained) proteins looked similar suggesting no degradation of proteins from placental tissues after storage, it was possible CBS and/or CSE were hypersensitive to degradation and so patterns were compared between the previously extracted and the newly extracted ones. This showed there were no differences in pattern of bands in CBS and CSE immunodetection (Figure 4-13) and that protein degradation was not the cause of the multiple banding.
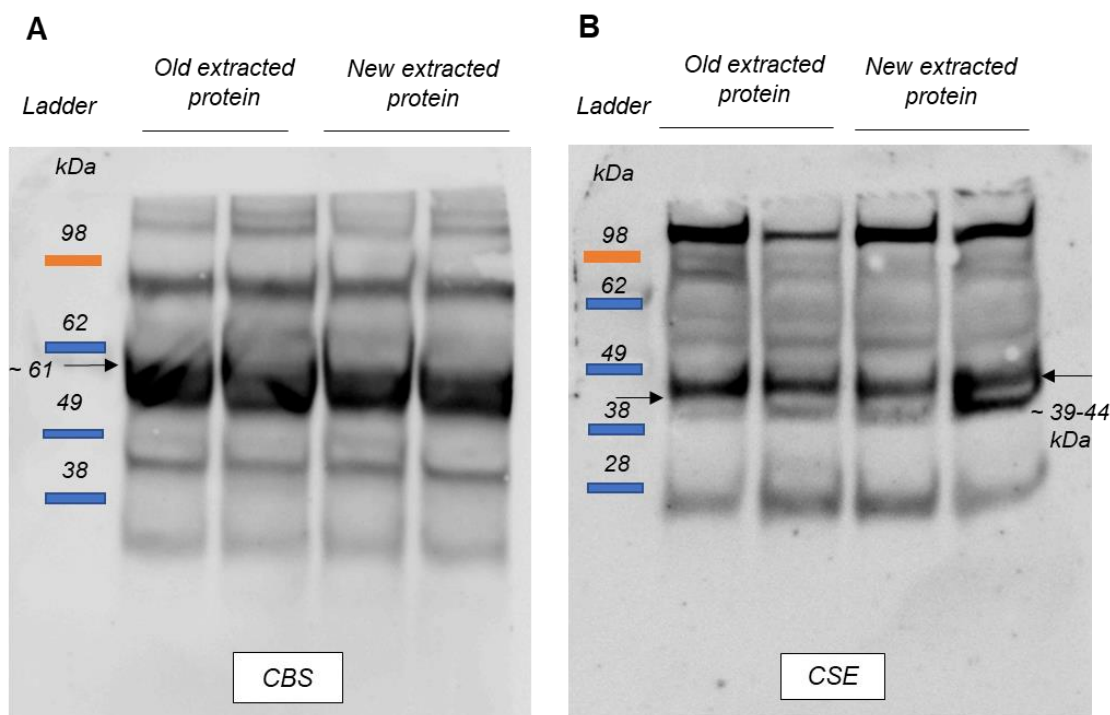
Figure 4-13 Western blotting of old and recently extracted proteins from frozen placental tissues (NLG). 40 µg of protein was loaded into 4-12% Tri-Bis gel with MES running buffer. (A) Immunoblotting with anti-CBS antibody, and the black arrows refer to the predicted MW (~ 61 kDa). (B) Immunoblotting with anti-CSE antibody, and the black arrows refer to the predicted MW (~ 39-44 kDa).

4.7 Side-by-side comparison of CBS and CSE expression pattern in placental tissue and other cells

It was then investigated whether the non-specific binding of primary antibodies was problematic only with the placental samples by comparing with proteins extracted from cell lines. The cell line BeWo has been widely used as a placental model therefore, it was chosen as a comparison that might have similar protein expression patterns as the placental samples. Two other human, non-placental cell lines were also compared to provide further points of comparison: MCF-7 and HEK293. Protein samples were extracted from cultured cells in the same way as for placental samples and CBS and CSE immunoblotting was performed as in section 2.7. The western blots comparing the protein expression of CBS, CSE and 3-MST in placental tissues, MCF-7 (two different extracts), BeWo and HEK293 cells are shown in Figure 4-14.
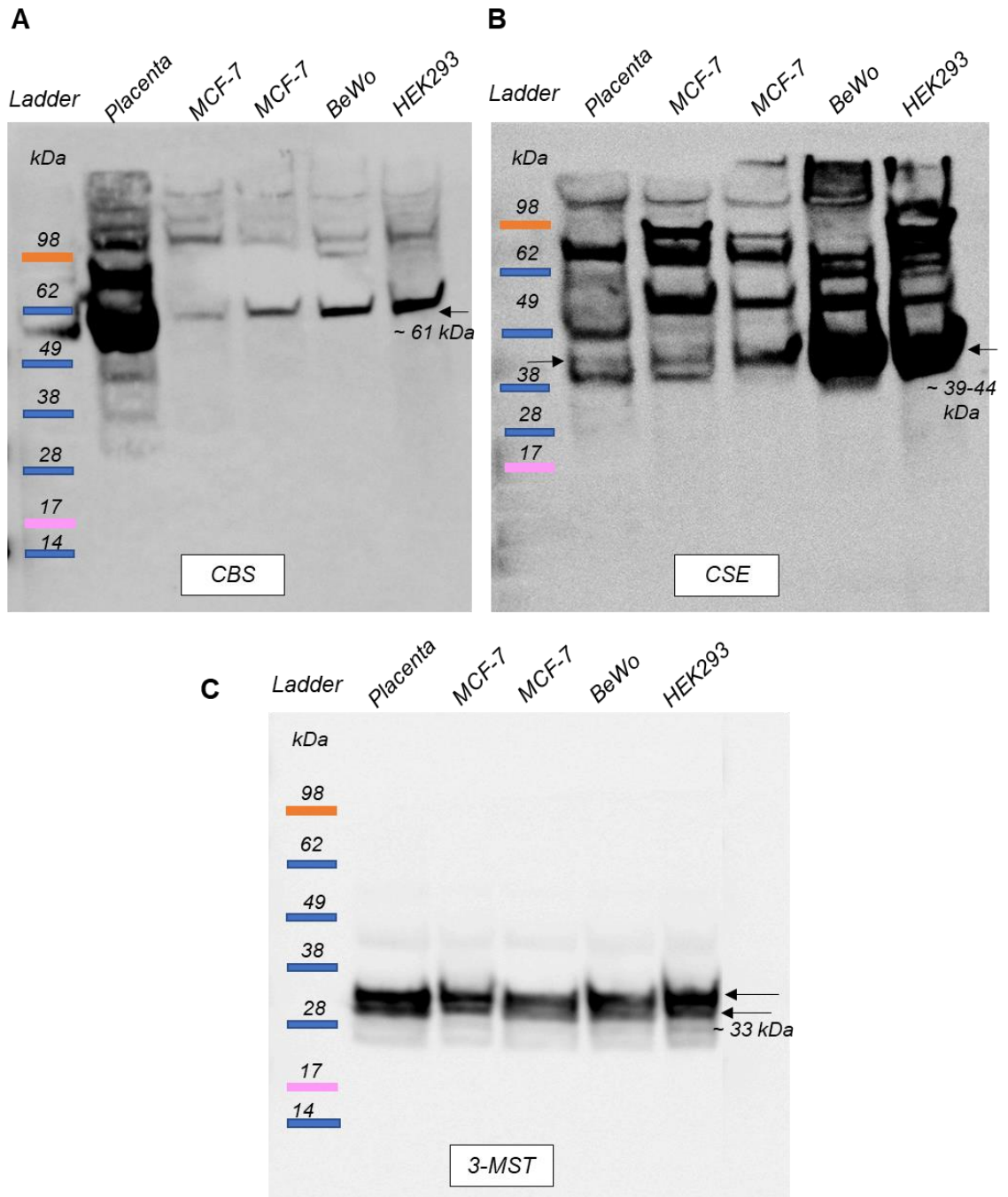
Figure 4-14 Western blotting of placental tissue, MCF-7, BeWo and HEK293 cells with anti-CBS, CSE and 3-MSTantibodies. 40 µg of protein lysates were loaded into 4-12% Tri-Bis gel with MES running buffer. Lane 1: Molecular ladder, lane2: placental lysate, lane 3-4: MCF-7 cell lysate, lane 5: BeWo cell lysate and lane 6: HEK293 cell lysate. (A) Immunodetection with anti-CBS, (B) Immunodetection with anti-CSE antibody and (C) Immunodetection with anti-3-MST antibody. Black arrows refer to the predicted MW.

The pattern of 3-MST bands in cell lines was the same as seen with placental tissues with little non-specific binding, indicating that that anti-3-MST antibody bound the target protein specifically and selectively. This also supports the claim that the placental protein samples were still of high enough quality for analysis. Regarding the CBS immunoblotting, multiple bands were detected with both tissue and cell lysates. However, the pattern of the CBS bands in placental lysate was slightly different comparing to that in cell lines. This may reflect to

the differences in cells and tissues behaviour and type or it may be as a result of post-translational modifications. Similarly, the CSE immunoblotting showed multiple bands with both tissue and cell lysates, with slightly different pattern of the CSE bands. Although these antibodies have been used in other published studies for expression analysis of CBS and CSE in cultured trophoblast cells and placental tissues (Chen et al., 2017, Cindrova-Davies et al., 2013, Holwerda et al., 2012, Hu et al., 2016, Mislanova et al., 2011), and in our hands do indeed detect proteins of approximately the correct MW, the presence of so many other presumably non-specific bands undermined our confidence in using these antibodies without further tests of specificity. For example, it was possible that ***none*** of the bands detected were CBS or CSE i.e. even those of the correct approximate MW could be non-specific proteins that co-incidentally were the same MW as CBS or CSE. Therefore, to properly test the specificity of anti-CBS and CSE antibodies it was decided to generate genetic knockout in MCF-7 and BeWo cell lines that should lack the proteins of interest using Clustered Regularly Interspaced Short Palindromic Repeat (CRISPR) system (discussed in chapter 5) to identify the genuine CBS and CSE bands among the multiple bands background.

4.8 Conclusion

The western blotting technique provides valuable information about a protein including abundance, the apparent molecular mass, post-translational modifications and splice variants. However, analysis of the protein can be difficult if multiple bands appear on the blot, and it is important to determine whether they are due to technical artifacts or they represent true variants of the protein of interest. Good antibodies should exhibit target specificity and sensitivity, allowing them to identify the protein of interest even at low expression levels. However, this is not always the case and they may show cross-reactivities with off-target proteins. Although the extensive validation of multiple primary and secondary antibodies had been undertaken in this study in order to allow the highly specific antibody to be selected, further optimisation was required to test specificity of anti-CBS and CSE antibodies. This chapter also demonstrated the importance of using an accurate loading control in order to obtain correct results in quantitative western blot experiments. The results of optimisation of different loading controls showed that both Ponceau S stain and β-actin can be used for loading controls.

Chapter 5   Testing antibodies specificity by CRISPR/Cas9- mediated knockout

5.1 Introduction

Knockout validation (Zhong et al., 2018) is the one of the best processes for testing antibody specificity as it should result in the loss of only the protein of interest and thus loss only of specific signal from the antibody-detection technique being used allowing the user to determine which and how much signal is specific. This has been made possible by technologies such as RNA interference and CRISPR/Cas9 genome editing. Genome editing is a group of technologies in which scientists change an organism's DNA sequences, adding, removing or altering the genetic material at particular locations in the genome. One very useful version of this is using CRISPR/Cas9 to induce double-stranded breaks (DSBs) at a target genomic locus which then repaired by the major pathway for DNA damage repair, non-homologous end joining (NHEJ). This is an error prone mechanism and tend to introduce short insertions or deletions (INDELs) which, when positioned within early open reading frames (ORFs), generates genetically knocked out cells by permanently disrupting the function of genes of interest by frameshift mutations. In this study, this was carried out on the CBS, CSE or 3-MST in both MCF-7 or BeWo cell lines in order to then help in validation of anti-CBS and CSE antibodies. Although the anti-3-MST antibodies had shown good enough specificity (Figure 4-10), knockout of this gene was also carried out as positive control for the approach, and gave intriguing, preliminary results that could be the basis for further investigations (see sections 7.2 and 7.3).

5.1.1 CRISPR/Cas9 system

This technology is derived from a bacterial immune adaptive system which protects the host bacterial cells from invading viruses and plasmids. The CRISPR loci in microbes include non-coding RNA elements and enzymes that collectively have the ability to recognise and cleave foreign nucleic acids based on their sequence. These systems rely on small RNAs for sequence-specific detection of foreign nucleic acids through Watson-Crick base paring with target DNA (Garneau et al., 2010, Jinek et al., 2012).

There are three known types of CRISPR/Cas system; type I, II and III (Makarova et al., 2011). In type I and III CRISPR systems, specialised Cas endonucleases process the precursor CRISPR RNA (crRNA), and once mature, each crRNA assembles in a large multi-

Cas protein complex which is capable of recognising and cleaving nucleic acids complementary to crRNA (Jinek et al., 2012). In contrast, type II CRISPR system processes the precursor crRNA by a different mechanism. Type II CRISPR system requires only a single protein e.g. Cas9 from Streptococcus pyogenes (spCas9), to perform the target cleavage so are more useful for technologies.

Naturally, Cas9 uses two RNA components: a target-specific crRNA that encodes the guiding RNA, and a trans-activating crRNA (tracrRNA or scaffold sequence) that facilitates crRNA maturation, binds the cRNA and also binds Cas9 (Garneau et al., 2010, Jinek et al., 2012). To simplify use of this in foreign systems such as mammalian cells, the crRNA and tracrRNA, can be fused to form a single guiding RNA (sgRNA), which can have even superior efficiency compared with the split design (Hsu et al., 2013). The Cas9 enzyme contains two nuclease domains; the RuvC-like domain and the HNH domain each responsible for cleavage of one strand of the double strand DNA target molecule. Jinek et al. (2012) have reported that the Cas9 HNH domain cleaves the complementary DNA strand, while the RuvC-like domain cleaves the non-complementary DNA strand. The basic principle for CRISPR/Cas9 knockout strategy as seen in Figure 5-1 is first, the introduction of targeted DNA cleavage in the form of DSBs by expression of Cas9 and an sgRNA complementary to the locus of interest followed by DNA repair process via NHEJ which results in small random INDELs (insertion/deletion) at the repair site causing frameshift mutation (Bibikova et al., 2002).
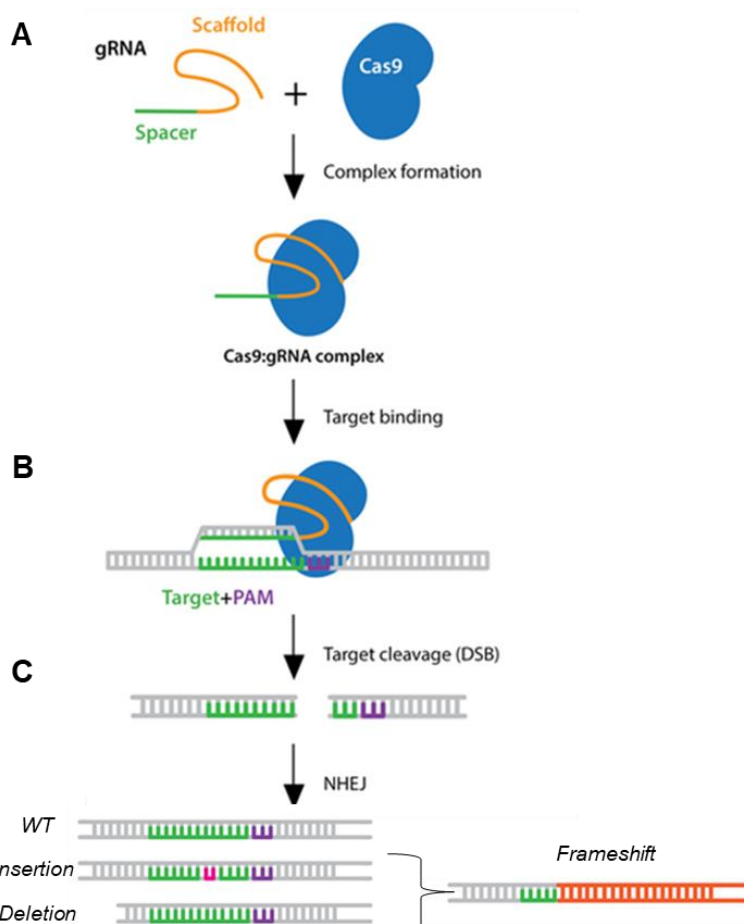
Figure 5-1 CRISPR expression system. (A) A sgRNA binds the Cas9 protein. (B) The sgRNA recognises the genomic target sequence. (C) The Cas9 nuclease causes target-specific DSBs, and the cleavage site is repaired by NHEJ repair pathway, resulting in INDELs. The image adapted from www.addgene.org/guides/crispr.

5.1.2 Designing the sgRNA

The CHOPCHOP online tool (https://chopchop.cbu.uib.no/) was used to identify optimal sgRNA sequences for CBS, CSE and 3-MST for a knockout strategy in human cells. This selects sequences based on their high predicted efficiency, minimal predicted off-target sites to minimise undesirable mutagenesis and minimal internal secondary structure. It also takes into account the requirement of a "NGG" protospacer adjacent motif (PAM) immediately downstream of the sgRNA-targeting region which serves as a binding signal for Cas9, and it is required for cleavage but it is not part of the sgRNA sequence. Forward and reverse oligos based on the sequences identified by CHOPCHOP were designed with additional nucleotides added for cloning into the BbsI site in px330 (see section 2.9.1 for oligo sequences). If the sequence identified by CHOPCHOP did not begin with a guanine 'G' nucleotide, this was added to the 5'end of the sgRNA because U6 RNA polymerase III promoter used to express sgRNA prefers G as the first base at the transcription start site (Guschin et al., 2010). sgRNAs were also selected such that that they targeted an exon

common to all splice variants of each target gene because variant expression patterns were unknown in the cells used.
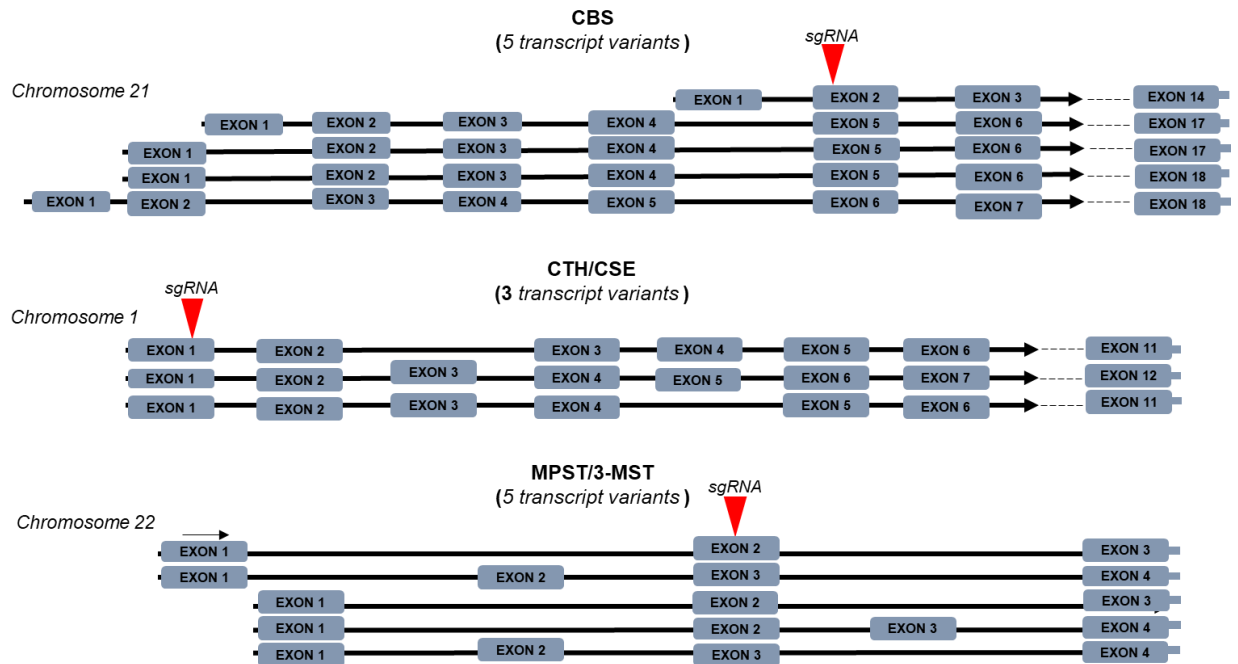
Figure 5-2 Schematic drawing showing the designed sgRNA sites to target CBS, CTH/CSE and MPST/3-MST genes located on chromosomes 21, 1 and 22, respectively. For CBS, the designed sgRNA targeted the shared exons (2,5,6) among all CBS splice variants. For CTH, the designed sgRNA targeted the first exon in all variants. For MPST, the designed sgRNA targeted the shared exons (2, 3) among all MPST splice variants. The red triangle refers to where the chosen sgRNA should cut. The black arrows and black dashed lines refer to the continuation of exons until the last shown exon. The exons and introns are not in a scale.

5.1.3 CRISPR expression system: px330-mcherry plasmid

A tool to deliver the guide RNA and Cas9 protein into target cells is required in order to introduce cleavage and generate knockouts. Transfection of plasmid vectors that express both a target-specific sgRNA and Cas9 protein in target cells is the simplest method. The px330-mcherry plasmid (Addgene, cat, no. 98750) is one such vector plasmid for which a pair of annealed oligos can be ligated immediately downstream the (U6) promoter (Figure 5-3) to create a new transcription unit which will produce the desired sgRNA in a target cell.

5.1.4 Delivery method for mammalian cell lines and puromycin selection

The transfection method used in this project was lipofection which is simple to apply and can be used for transient or stable expression (Holmen et al., 1995). For successful stable transfection, there needs to be some way of selecting from the transfected cell population cells that are likely to have the constructed plasmid. The method chosen in this study was

co-transfection of the cells with a separate plasmid encoding puromycin resistance (PSCB-puro) for positive selection. In the strategy used here, this plasmid integrates either in the site cut by Cas9 guided by the sgRNA or at a random double-stranded break elsewhere in the genome. In the former scenario, function of the target gene (i.e. CBS, CSE or 3-MST) is disrupted by the plasmid integration. In the latter scenario, any puromycin resistant clones are very likely to have the target genes are mutated by error-prone NHEJ because the CRISPR plasmid and the puro plasmid were co-transfected. The plasmid pSCB-puro, with the pac gene expressed from the CMV promoter, and linearised by digestion with Nco1 was obtained from Dr Andrew Hamilton and used in this project. For the two different cell lines, MCF-7 and BeWo used here, 1 µg/ml Puromycin was enough to kill the cells within 2-3 days (section 2.9.8). The whole workflow of CRISPR experiment is shown in Figure 5-3.
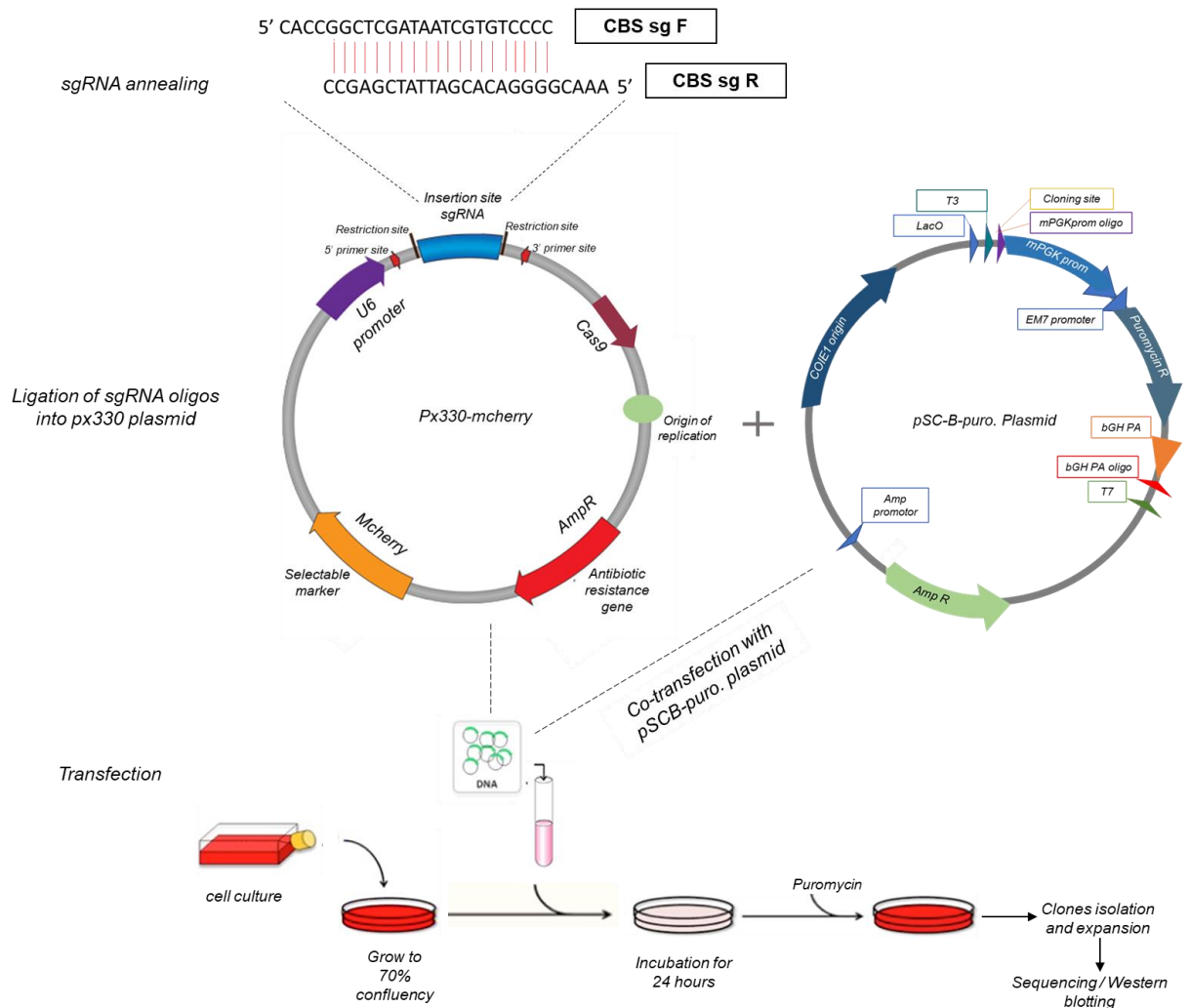
Figure 5-3 Workflow of the CRISPR experiment illustrating a summary of vector plasmid construction and cells transfection. The workflow shows annealing of sgRNAs, ligation into px330 plasmid to form the constructed plasmid, and transfection of the target cells with the constructed vector and puromycin resistance plasmid.

5.2 Results

5.2.1 Cloning of targeting constructs

The forward and reverse oligos were phosphorylated and annealed to form duplexes. The design means these have overhangs compatible with *BbsI* sites in px330 downstream of the U6 promoter and upstream of the tracr region. These duplexes were ligated with *Bbs 1*-digested-plasmid which was then transformed into competent *Ecoli* (section 2.9), plated on LB agar plates with ampicillin. Colonies were miniprepped and initially screened by diagnostic restriction enzyme digestion and positive clones (pCBSsg1, pCSEsg1 and p3-MSTsg1 plasmids) were verified by sequencing from U6 promotor through the sgRNA insertion site. The sequencing data showing the successful cloning are shown in Figure 5-4.
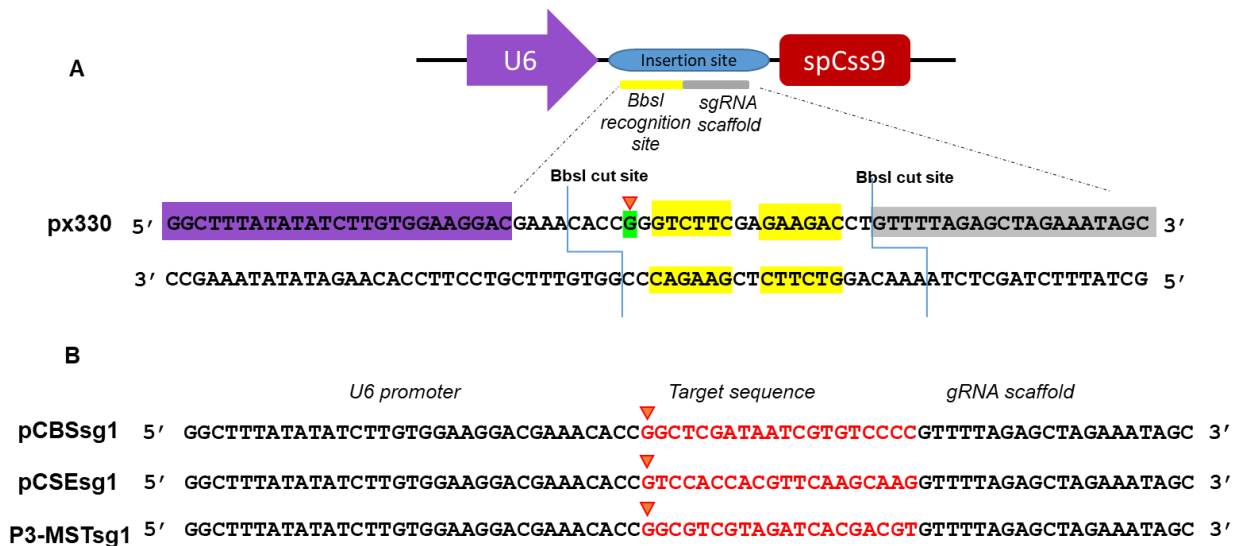
Figure 5-4 Confirmation of recombination as shown by sequencing results of the extracted plasmid. (A) px330 sequence as obtained from Addgene with the insertion site. The U6 sequence shown highlighted in purple, the sgRNA scaffold shown highlighted in grey, the BbsI recognition sites shown highlighted in yellow and the transcription start site shown highlighted in green. The blue solid connectors refer to the BbsI cut site. (B) Sequencing results from GATC company showed successful ligation where the insertion site in px330 was replaced by the target oligos (red colour). The red triangles refer to (G), the transcription start site.

5.2.2 Generation of puro-resistant clones in MCF-7 cells

pCBSsg1 or pCSEsg1 were transfected, along with digested puromycin resistance plasmid pSCB-puro into MCF-7 cells and puromycin selection begun 24 hours later. Colonies started to appear as early as day 6-7 post transfection. No colonies were observed from control non-transfected cells treated with puromycin the same way indicating that the colonies were the result of plasmid integration and expression rather than spontaneous puromycin resistance.

Some colonies disappeared at early time or following isolation and expansion. These may represent the result of transient expression of the puromycin resistance gene or silencing of an integrated one. The growth number of clones obtained for each plasmid is summarised in Figure 5-5.
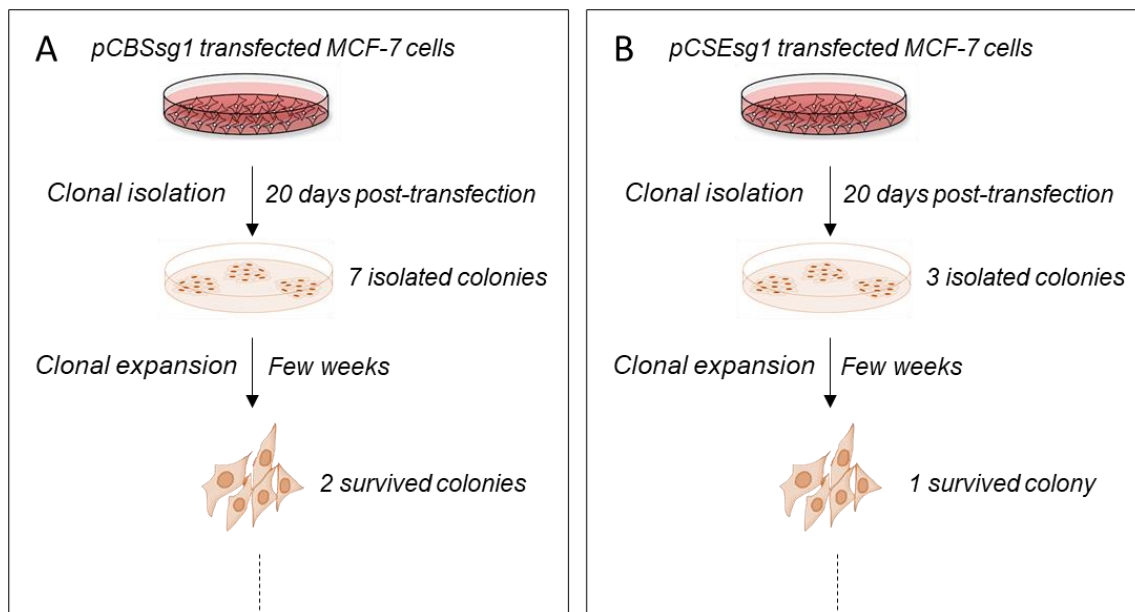
Figure 5-5 Outcomes of puro-resistant clones in MCF-7 transfected cells. (A and B) show the growth number of pCBSsg1 and pCSEsg1 colonies, respectively.

5.2.3 Generation of puro-resistant clones in BeWo cells

pCBSsg1, pCSEsg1 or p3-MSTsg1 plasmid were transfected, along with digested puromycin resistance plasmid pSCB-puro into BeWo cells and puromycin selection begun 24 hours later. Colonies started to appear as early as day 6-7 post transfection. None were observed from control non-transfected cells treated with puromycin the same way. Some colonies disappeared at early time or following isolation and expansion. These may represent the result of transient expression of the puromycin resistance gene or silencing of an integrated one. The growth number of clones obtained for each plasmid is summarised in Figure 5-6.
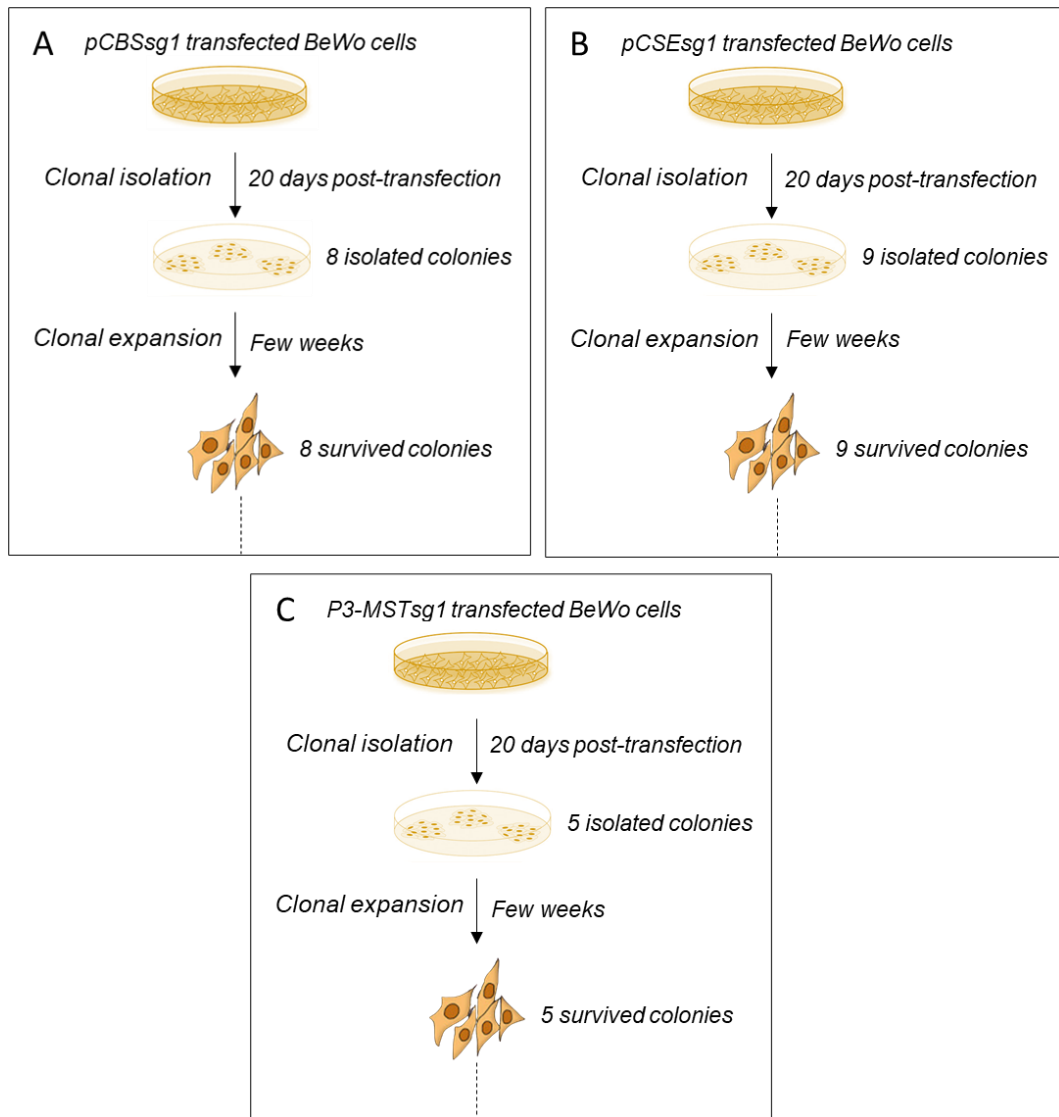
Figure 5-6 Outcome of puro-resistant clones in BeWo cells. (A, B and C) show the growth number of pCBSsg1, pCSEsg1and p3-MSTsg1 colonies, respectively.

5.2.4 Screening of clones and Validation of knockouts

From each clone, between 225-773 bp of the DNA flanking the sgRNA target side was amplified by PCR, gel purified and sent for standard Sanger sequencing. The .abi files provided by the sequencing company were then analysed by Inference of CRISPR Editing (ICE) analysis, an online tool that analyse Sanger sequencing data to determine editing efficiency. This software was developed to determine editing efficiency from, for example a Cas9 + sgRNA-transfected cell population with many possible INDELs but also can be used to assess the simpler distribution of knockout/non-mutated allelic frequency in clones. It is important to note that because MCF-7 and BeWo are both aneuploid cell lines, the copy number of any of the target genes is unknown and might be more than two. Given an sgRNA sequence and a reference wild-type .abi file, the software predicts the possible mutations and matches the sequencing data to these possibilities to see what degree and type of mutations

best fits the actual sequencing data from DNA from the mutant clones. It shows the model fit by an R^2 value: the closer the R^2 value is to 1 the higher confidence that the estimated mutant distribution is correct. It has been shown to be equal in accuracy to Next-Generation Sequencing (NGS) approaches. ICE predictions were strongly correlated with mutations detected by NGS with an overall $r^2 = 0.93$ (Hsiau et al., 2018).

5.2.4.1 Validation of CBS knockout clones in transfected MCF-7 cells

Two survived pCBSsg1 MCF-7 clones were screened for CBS knockout. Genomic DNA was extracted from both WT (unedited control) and edited clones (MCF7-C1 and C2). The PCR products were run on a 1% agarose gel to verify that amplification generates a single band of the correct size for the WT sample. The gel result of PCR products (Figure 5-7A) shows only a single band in WT, C1 and C2 lanes, and that the amplicon size from PCR products was almost the same in both WT and transfected clones at ~ 773 bp. The INDELs caused by CRISPR/Cas9 editing are often small and would not be easily detected by gel electrophoresis. Then, the purified PCR products were sequenced and the resulting .abi files analysed by ICE. The knockout scores of both pCBSsg1 clones and the indel percentage are 100% as seen in Figure 5-7B, indicating no contamination by wild-type MCF7. The Indel type in both MCF-7 clones were an insertion of one nucleotide at the sgRNA target site. Such frameshift should result in a truncated or non-functional protein. ICE does not distinguish polymorphic INDELS of the same number (Figure 5-7B) but inspection of the electropherograms (Figure 5-8) shows both clones to have an insertion of either an A or a G at exactly the predicted cut site of Cas9 with this sgRNA (between nucleotide 3 and 4 upstream of PAM sequence). The similar peak height suggests there are only two CBS genes in MCF7 and that clone 1 and 2 may have arisen from the same edited cell. Later on, both clones were further confirmed mutant for CBS by western blot analysis, in order to test specificity of anti-CBS antibody. The western blot data are presented in section 5.2.5.2.
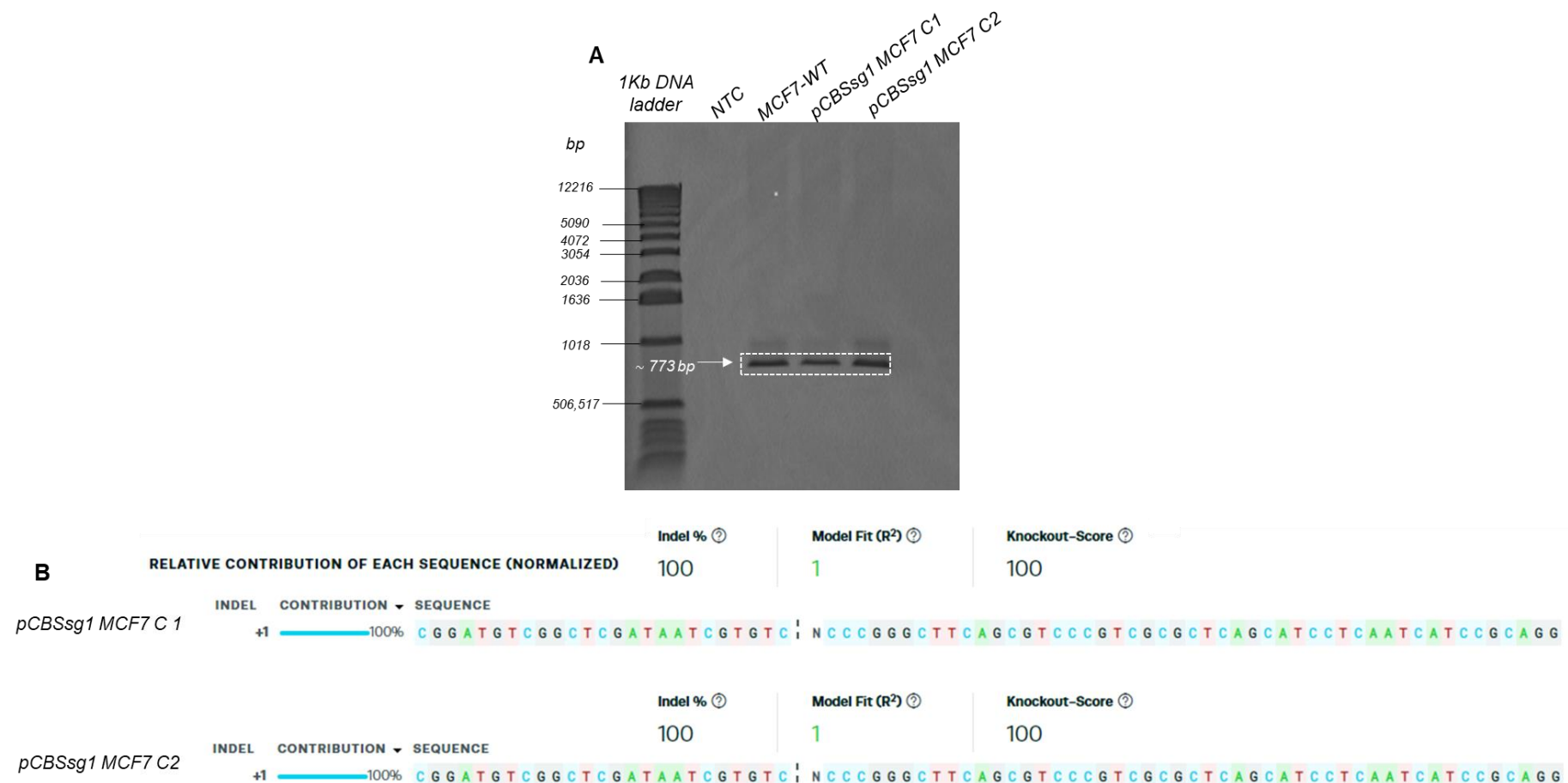
Figure 5-7 Screening of CBS knockout clones in transfected MCF-7 cells. (A) A 1% agarose gel of PCR products illustrating the desired amplicon size in WT control sample. Lane 1 represents the 1kb DNA molecular ladder, lane 2 represents the no-template control (NTC), lane 3 represents the MCF-7 WT and lanes 4 and 5 represent the pCBSsg1 MCF-7 C1 and C2, respectively. The white arrow refers to the amplicon size of the PCR product at ~ 773bp, and the white dashed box refers to the excised bands for purification and sequencing. (B) ICE analysis results of pCBSsg1 MCF-7 clones displaying the indel type, percentage, relative contribution of each sequence and the knockout score. The indel sizes in both clones are +1. The black dashed line refers to the sgRNA cut site.
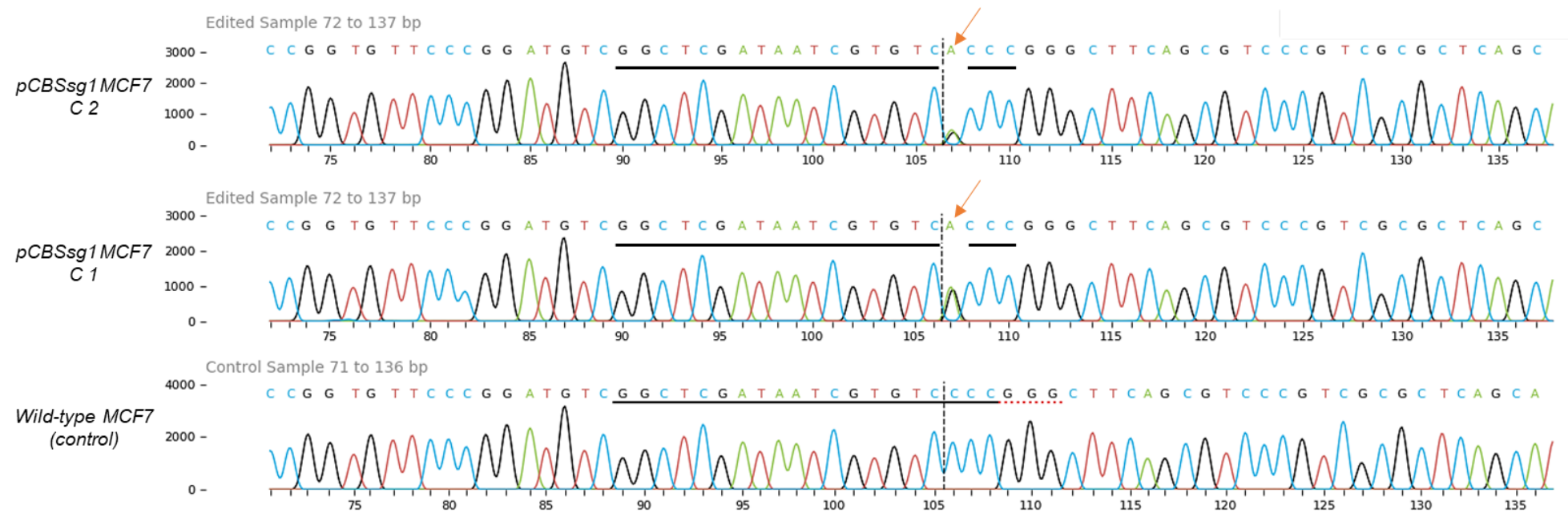
Figure 5-8 Chromatogram from Sanger sequence of WT (control) and pCBSsg1 MCF-7 edited sequences in the region around the guide sequence.
The output shows the edited (top and middle) and control (bottom)Sanger traces in the region around the sgRNA binding site. The horizontal black underlined regions represent the sgRNA sequence, the dashed red underlined region represents the PAM site, the vertical black dotted lines represent the cut site which is 3bp upstream of the PAM site, and the red arrows refers to the insertion site of one nucleotide (A) in both edited samples.

5.2.4.2 Validation of CBS knockout clones in transfected BeWo cells

Among eight survived pCBSsg1 BeWo clones, only three clones (C1, C2 and C5) were chosen for screening because of time constraints and financial resources limits. Genomic DNA was extracted from these clones and PCR was performed to amplify the target region of interest. The gel result of PCR products (Figure 5-9A) shows that the size of DNA bands from PCR products was almost the same in both WT and BeWo clones at ~ 773 bp. Similarly, the purified PCR products were sent along with the primers for sequencing. The chromatogram trace in the control sample showed well-formed peaks with absence of the background signals indicating pure and high-quality DNA.

The results of Sanger sequencing of WT control and these three pCBSsg1 BeWo clones were analysed by ICE analysis. As seen in Figure 5-9B, the knockout scores and the indel percentage for pCBSsg1 BeWo C1 and C2 are 64 and 94, respectively. The edited and unedited control sequences in the region around the sgRNA binding site are shown in Figure 5-10. Distribution of indel sizes in the entire edited populations as seen in Figure 5-9B revealed mixed INDELs and sequences in pCBSsg1 BeWo C1; a deletion of one pb (-1) contributes of 52% of the edited population, a deletion of 8 pb (-8) contributes of 12% of the edited population. The WT sequence contributes of 32% of the edited population, (R^2 value = 0.96). The indel distribution plot of pCBSsg1 BeWo C2 shows only edited sequences (-2 (52%) and -8 (42%) with no WT alleles present, (R^2 value = 0.94). In contrast, the indel percentage in pCBSsg1 BeWo C5 was 100% but with 0% knockout score because all genes had a 9 bp deletion (R^2 value = 1). The Synthego software scores this as no knockout because it is an in-frame deletion. Later on, these clones were further confirmed mutant for CBS by western blot analysis, in order to test anti-CBS antibody specificity. The western blot data are presented in section 5.2.5.2.

.
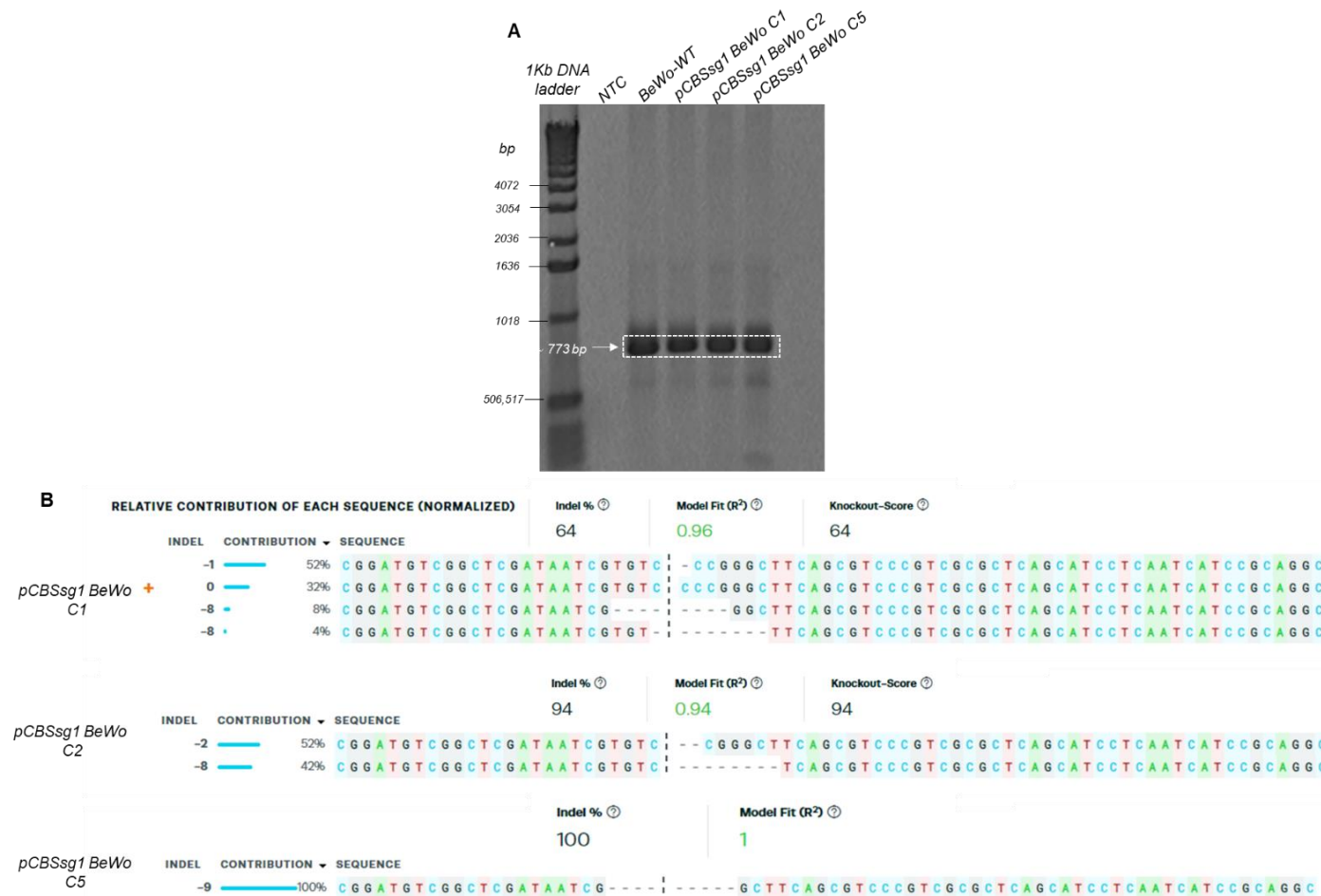
Figure 5-9 Screening of CBS knockout clones in transfected BeWo cells. (A) A 1% agarose gel of PCR products showing the desired amplicon size in WT control sample. Lane 1 represents the 1kb DNA molecular ladder, lane 2 represents the no-template control, lane 3 represents the BeWo WT and lanes4-6 represent the pCBSsg1 BeWo C1, C2 and C5, respectively. The white arrow refers to the amplicon size of the PCR products at ~ 773 bp, and the white dashed box refers to the excised bands for purification and sequencing. (B) ICE analysis of pCBSsg1 BeWo clones displaying the indel type, percentage, relative contribution of each sequence and knockout scores.
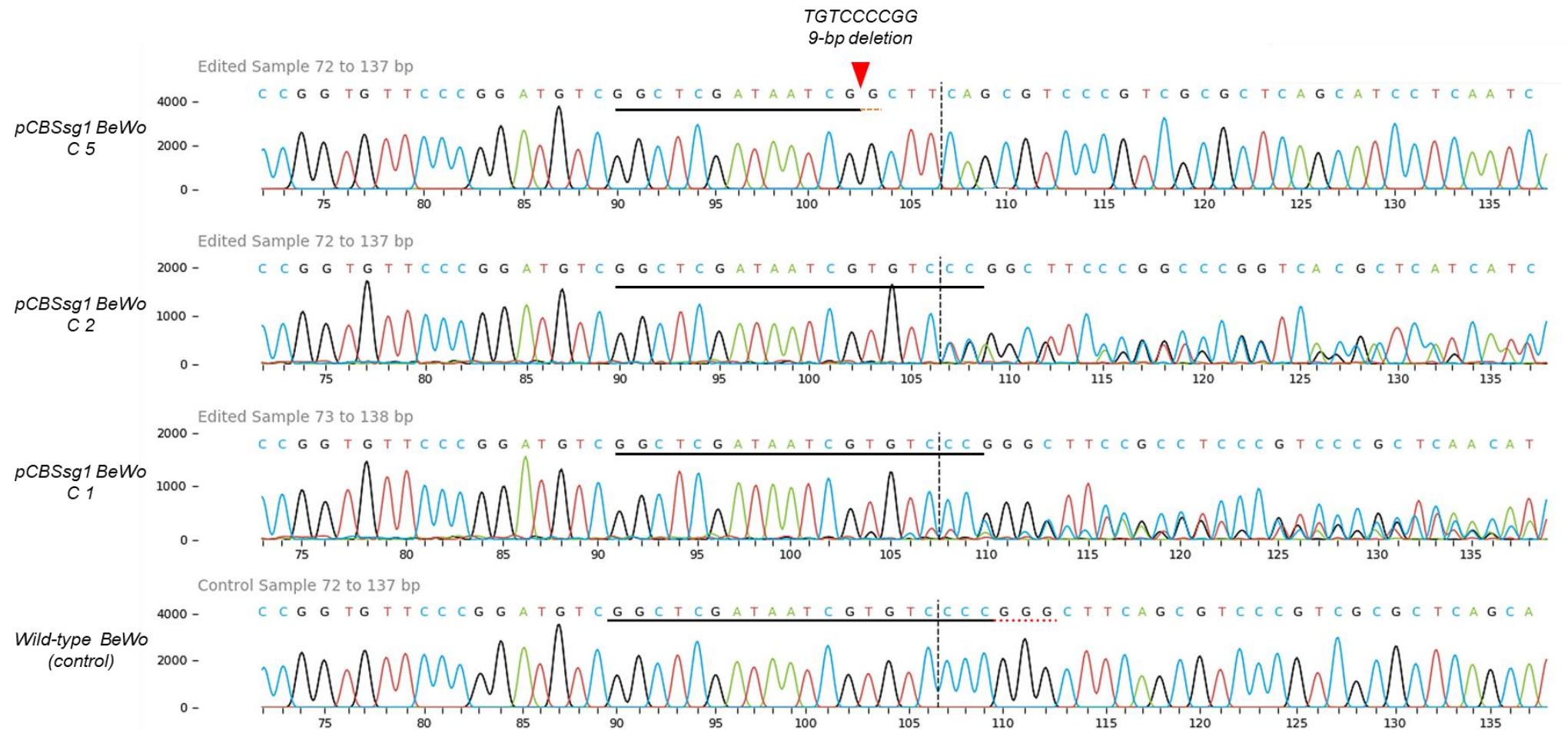
Figure 5-10 Chromatogram from Sanger sequence of WT (control) and pCBSsg1 BeWo edited sequences in the region around the guide sequence. The output shows the edited (top and two middles) and control (bottom)Sanger traces in the region around the sgRNA binding site. The horizontal black underlined regions represent the sgRNA sequence, the dashed red underlined region represents the PAM site, the vertical black dotted lines represent the cut site which is 3 bp upstream of the PAM site. The trace in C1 and 2 show mixed sequences around the cut site indicated by overlapping peaks, and the trace in C5 shows a deletion of 9 bp around the cut site (red triangle).

5.2.4.3 Validation of CSE knockout clones in transfected BeWo cells

The only obtained pCSEsg1 MCF7 clone was initially screened by western blotting (see section 5.2.5.3), and found to look similar to WT so was not analysed by sequencing. Among nine survived pCSEsg1 BeWo colonies, only four clones (C7, C10, C11 and C12) were chosen for screening. PCR was performed for these clones (Figure 5-11A) and shows a single major ~ 500 bp band in WT, C7 and C12 and two major DNA bands in C10 and C11 (~ 500 bp and one slightly at higher size). Purified PCR products of C7 and C12 were sent for sequencing and the resulting .abi files was analysed by ICE. Visual inspection of the chromatograms in Figure 5-12 showed clear sequence throughout for wild type and C12 but overlapping peaks after the cut site indicating mixed sequences with different INDELs in the PCR product of C7. ICE analysis gave knockout scores and the indel percentage for pCSEsg1 BeWo C7 of 95%, as seen in Figure 5-11B, while in pCSEsg1 BeWo C12, the indel percentage was 0 % with no knockout score. The indel size of pCSEsg1 BeWo C7 shows a sequence with a deletion of 10pb (-10) that contributes of 47% of the edited population and a sequence with a deletion of 11 pb (-11) that contributes of 48% of the edited population (R^2 value = 0.95). The indel distribution of pCSEsg1 BeWo C12 shows only a WT sequence (100%) (R^2 = 1.0).

Although pCSEsg1 BeWo C10 and C11 were not sequenced, the gel result of PCR showed two bands with slightly different size from that seen in the WT sample, suggesting they may also be mutants so these were also screened by western blotting alongside C7 and C12 (section 5.2.5.3).
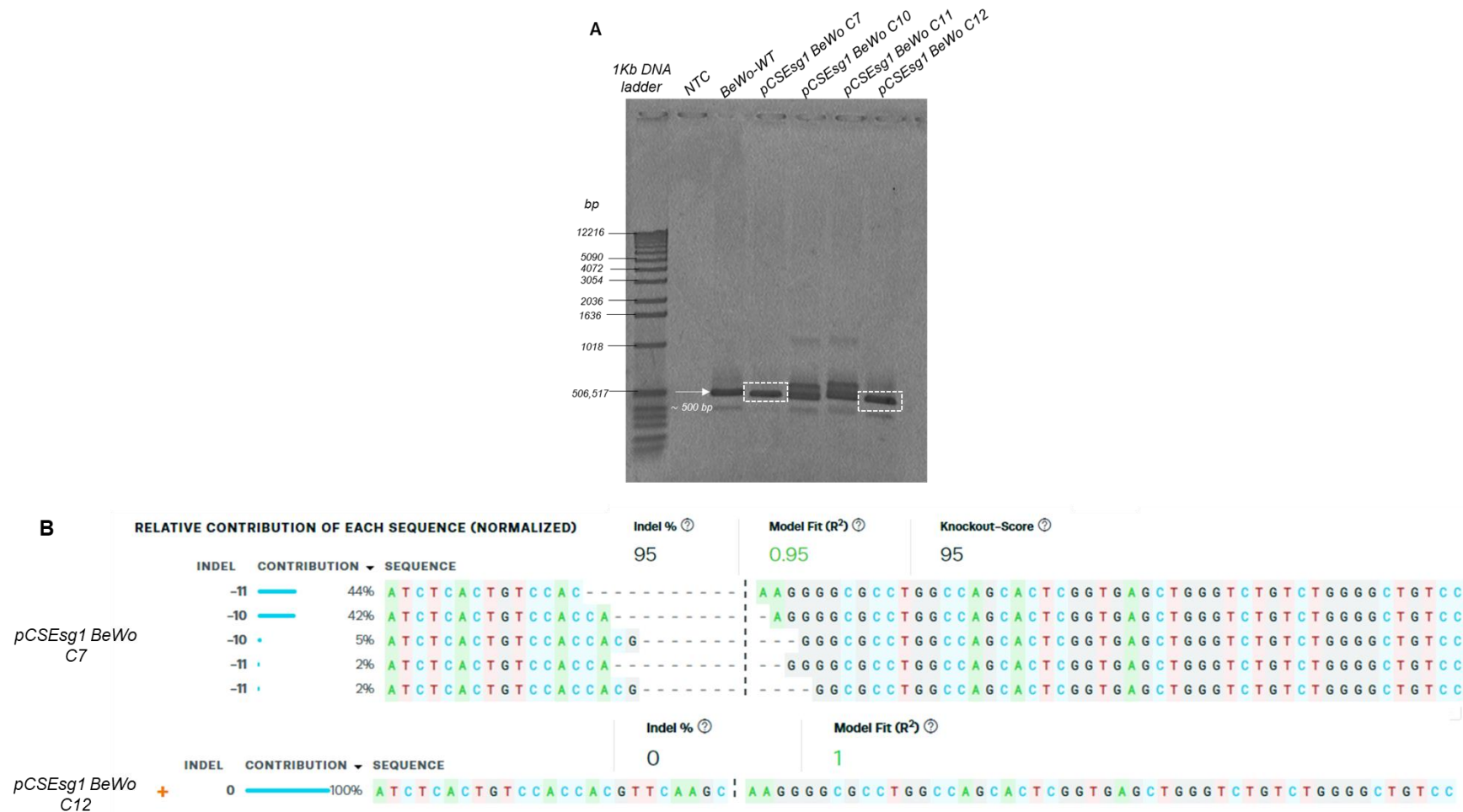
Figure 5-11 Screening of CSE knockout clones in transfected BeWo cells. (A) A 1% agarose gel of PCR products displaying the desired amplicon size in WT control sample. Lane 1 represents the 1kb DNA molecular ladder, lane 2 represents the no-template control, lane 3 represents the BeWo WT and lanes 4-7 represent the pCSEsg1 BeWo C7, C10, C11 and C12, respectively. The white arrow refers to the amplicon size of the PCR products at ~ 500 bp, and the white dashed box refers to the excised bands for purification and sequencing (B) ICE analysis of pCSEsg1 BeWo C7 and C12 showing the indel type, percentage, relative contribution of each sequence and knockout scores.
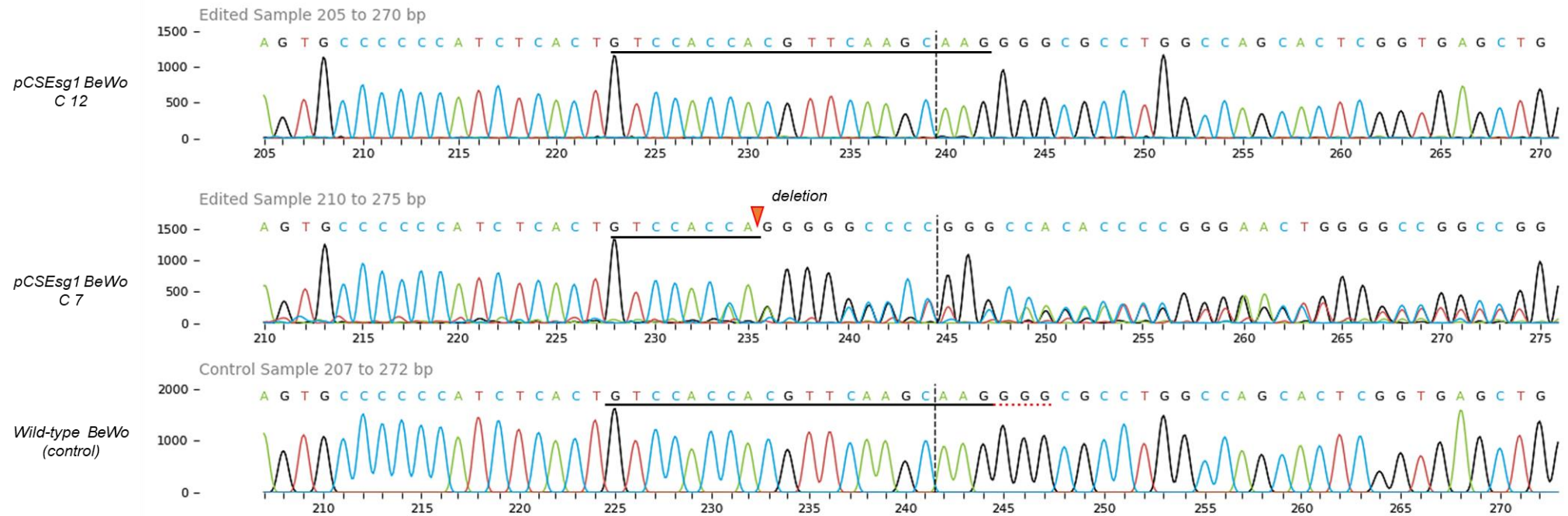
Figure 5-12 Chromatogram from Sanger sequence of WT (control) and pCSEsg1 BeWo edited sequences in the region around the guide sequence. The output shows the edited (top and middle) and control (bottom)Sanger traces in the region around the sgRNA binding site. The horizontal black underlined regions represent the sgRNA sequence, the dashed red underlined region represents the PAM site, the vertical black dotted lines represent the cut site which is 3 bp upstream of the PAM site.

5.2.4.4 Validation of 3-MST knockout clones in transfected BeWo cells

Among 5 survived p3-MSTsg1 BeWo colonies, four clones (C2, C5, C6 and C10) were screened by PCR and gel electrophoresis.   The gel result of the PCR products (Figure 5-13A) shows a single major band in WT and all clones at size of ∼ 225 bp. Additionally, there are other significantly larger DNA bands in C6 lane at higher sizes which might be from fragments of pSCB-puro integrated into the Cas9 cut site. The purified PCR products of C5, C6 and C10 only were sent for sequencing and results were analysed by ICE analysis. Distribution of indel sizes in Figure 5-13B displayed that the indel type in C6 is an insertion of two nucleotides at the sgRNA target site, which should shift the reading frame resulting in a truncated, non-functional protein. The percentage of this indel type is 96% and the knockout scores and editing efficiency are 96 % (R^2 = 0.96), indicating the same mutation presents in all 3-MST alleles in this clone. The indel size in the other two clones C5 and C10 was 0, indicating that they were puromycin-resistant WT clones and were not screened further.   Figure 5-14 shows the Sanger traces for p3-MSTsg1 C6 only because the chromatogram of the C5 and C10 are similar to the control one. Figure 5-13B shows only one mutant sequence in C6, in which two nucleotides (C, G) were inserted at the cut site indicating the same mutation present in all 3-MST alleles in this clone. p3-MSTsg1 C6 and unsequenced clones (p3-MSTsg1 C2 and C8) were analysed by western blotting confirming 3-MST knockout in C6 (section 5.2.5.1).
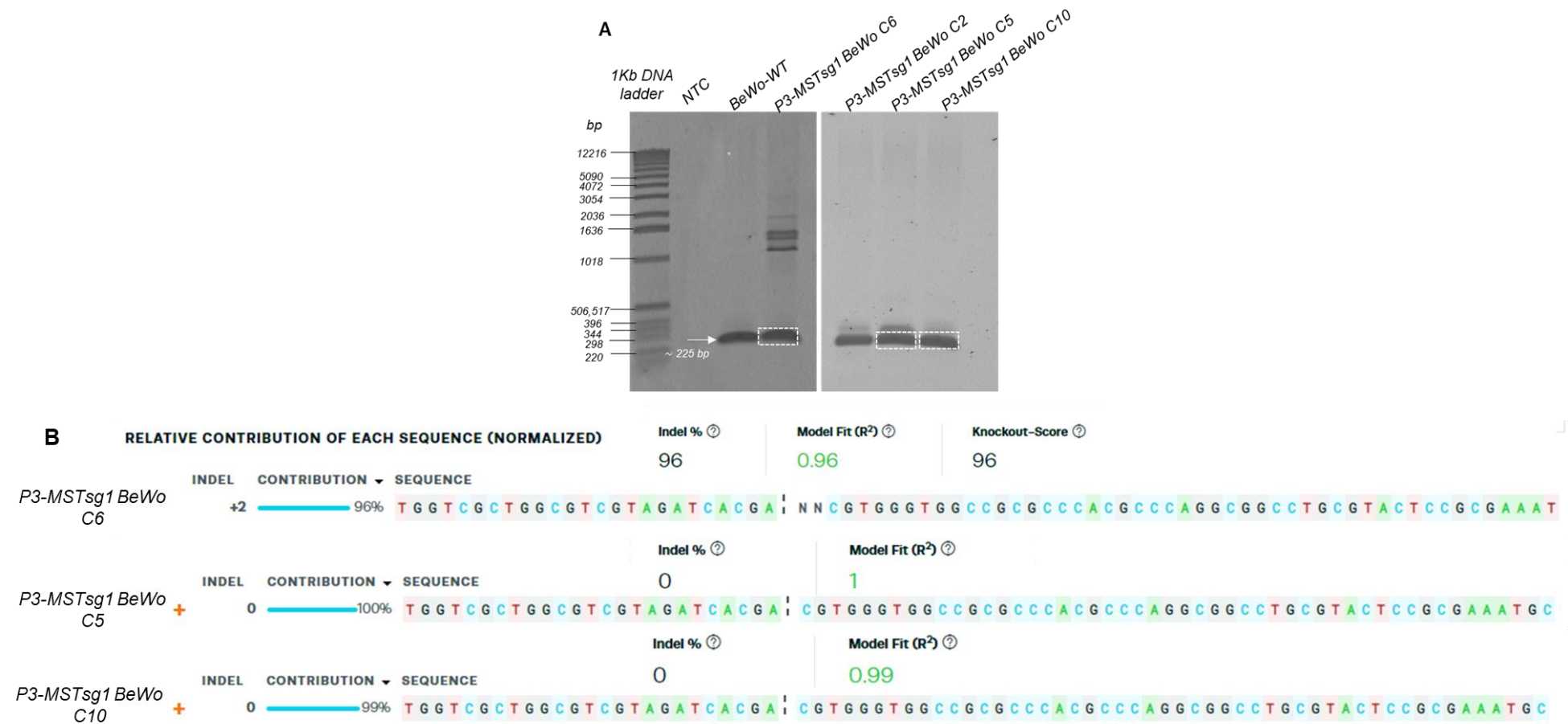
Figure 5-13 Screening of 3-MST knockout clones in transfected BeWo cells. (A) A 1% agarose gel of PCR products showing the desired amplicon size in WT control sample. Lane 1 represents the 1kb DNA molecular ladder, lane 2 represents the no-template control, lane 3 represents the BeWo WT, lane 4 represents the p3-MSTsg1 BeWo C6 and lane 5-7 represent the p3-MSTsg1 BeWo C2, C5 and C10, respectively. The white arrow refers to the amplicon size of the PCR product, at ~ 225 bp, and the white dashed box refers to the excised bands for purification and sequencing (B) ICE analysis of p3-MSTsg1 BeWo C5, C6 and C10. displaying the indel type, percentage, relative contribution of each sequence and knockout scores.
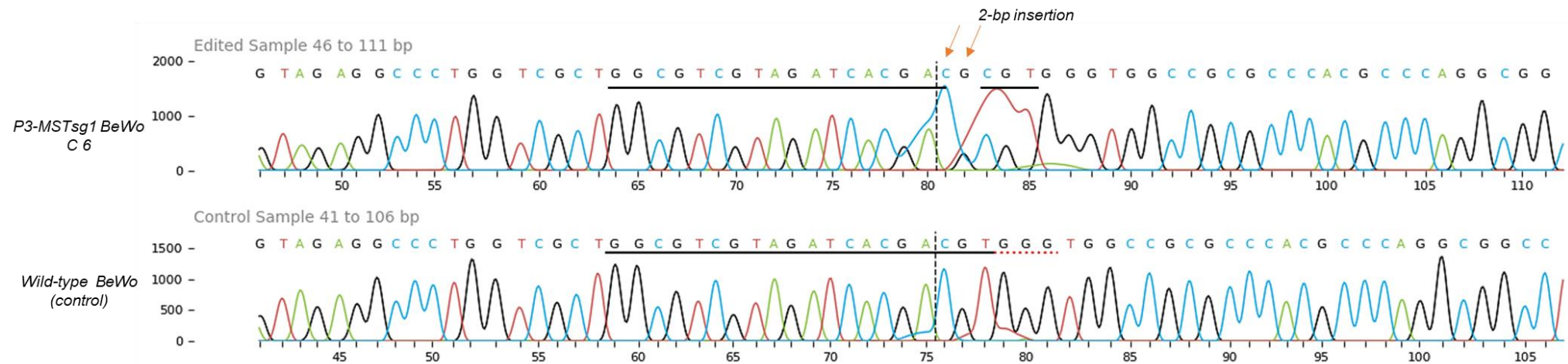
Figure 5-14 Chromatogram from Sanger sequence of WT (control) and p3-MSTsg1 BeWo C6 edited sequences in the region around the guide sequence. The output shows the edited (top) and control (bottom)Sanger traces in the region around the sgRNA binding site. The horizontal black underlined regions represent the sgRNA sequence, the dashed red underlined region represents the PAM site, the vertical black dotted lines represent the cut site which is 3bp upstream of the PAM site, and the red arrows refers to the insertion site of two nucleotides (C, G) in the edited sample.

5.2.5 Testing antibodies specificity in knockout clones

5.2.5.1 Testing of anti-3-MST antibody specificity in 3-MST knockout BeWo cells

20 µg of protein from WT and 3-MST knockout BeWo C6 (KO score: 96%) was loaded into 4-12% Tri-Bis gel run in MES buffer, blotted then immunodetection with anti-3-MST antibody was performed (Figure 5-15A). The absence of bands in the sequenced-confirmed knockout clone C6 at the expected ~ 33 kDa confirms the antibody is detecting 3-MST. 3-MST BeWo clones C2 and C8 had not been purified and sequenced due to limited resources but proteins were also loaded in this gel as to extend 3-MST-knockout clone screening but neither showed any reduction in 3-MST protein. The effects of 3-MST elimination in clone C6 on aspects of mitochondrial biology were explored further in chapter 7. Immunodetection with a loading control (β-actin) was carried out on the same membrane to ensure samples equal loading (Figure 5-15B).
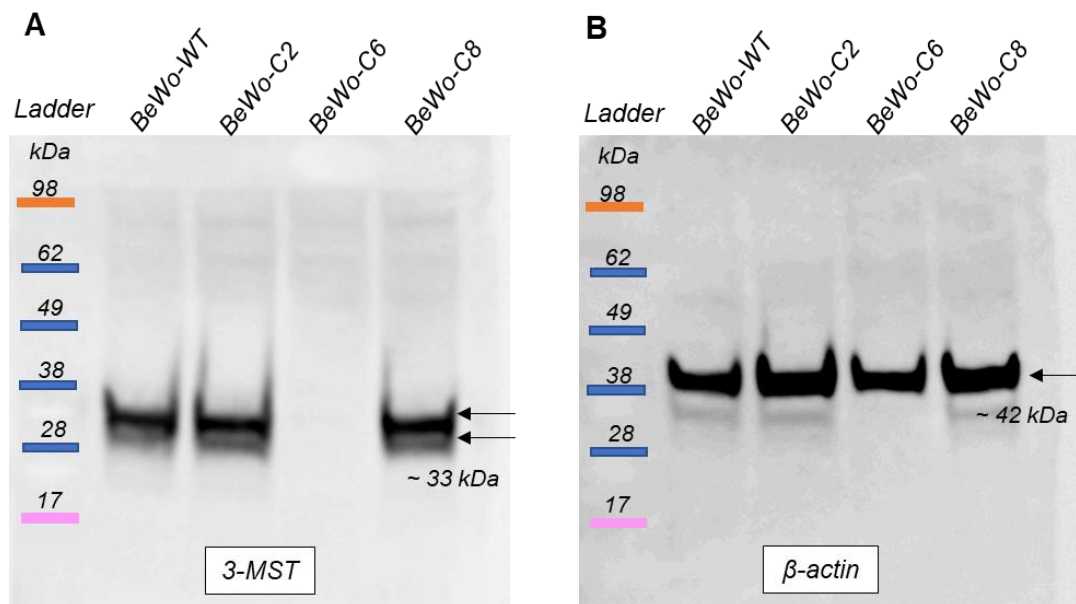
Figure 5-15 Western blotting of p3-MSTsg1 BeWo clones with anti-3-MST and anti-β-actin antibodies. 20 µg of protein was loaded into 4-12% Tri-Bis gel. Lane 1: Molecular ladder, lane2: BeWo-WT cell lysate and lane 3-5: BeWo (C2,6 &C8) lysates. (A) Immunoblotting with anti-3-MST antibody. The black arrow refers to the predicted MW (~ 33kDa). (B) Immunoblotting with a loading control (anti-β-actin antibody). The black arrow refers to the predicted β-actin MW (~ 42 kDa).

5.2.5.2 Testing of anti-CBS antibody specificity in CBS knockout MCF-7 and BeWo cells

20 μg of protein from a normal placental sample, WT MCF-7 cells (four different protein extracts using protease cocktail inhibitors with and without EDTA) and sequenced-confirmed CBS knockout MCF-7 clones C1 and C2 (replicates) (KO score: 100%, section 5.2.4.1) was loaded into 4-12% Tri-Bis gel run in MES buffer, blotted then immunodetection with anti-CBS antibody was performed (Figure 5-16A). The absence of bands in both knockout clones at the expected ~ 61 kDa confirms the antibody is detecting CBS but also that it binds to multiple non-CBS proteins as background bands and that this non-specific binding varies even between samples from the same cell line (as seen in MCF7-WT (2) compared with other three MCF-7 WT) again showing the difficulty using anti-CBS antibodies. The second band clearly absent from the knockout clones (~ 98 kDa) is likely to be related to CBS although does not correspond to any known splice variant. The placental sample lane showed multiple major bands including one at ~ 61 kDa, the same size as the major absent band in the MCF7 knockout clones which is likely to be placental CBS. Immunoblotting of the same membrane with the loading control (β-actin) was carried out (Figure 5-16B).
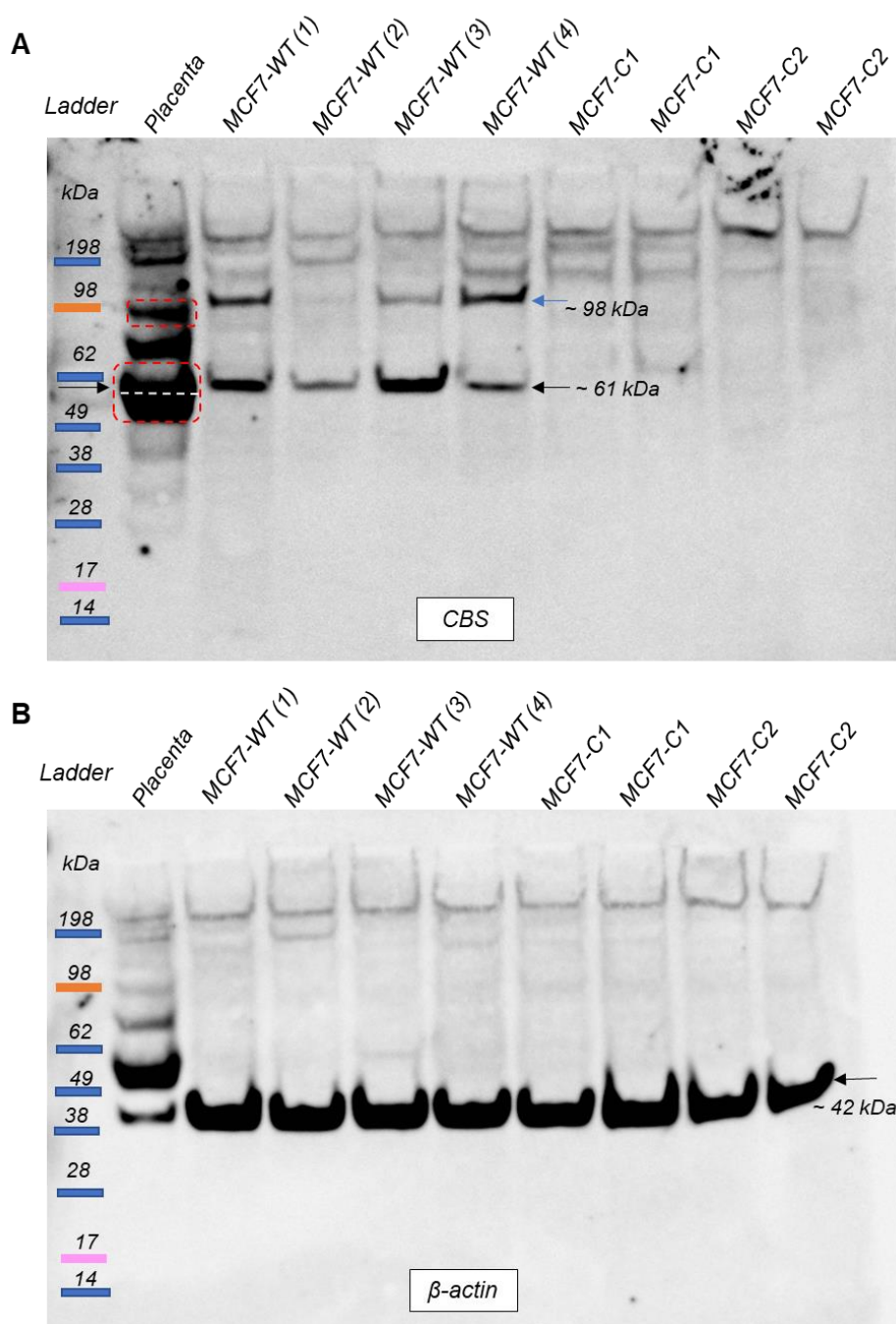
Figure 5-16 Western blotting of placental sample and pCBSsg1 MCF-7 knockout clones with anti-CBS and anti- β-actin antibodies. 20 μg of protein was loaded into 4-12% Tri-Bis gel. Lane 1: Molecular ladder, lane2: placental lysate, lane 3-6: different MCF7-WT cell lysates and lane 7-10: MCF-7(C1 &C2) cell lysates. (A) Immunoblotting with anti-CBS antibody. The black arrow refers to the predicted MW (~ 61kDa) of CBS and the blue arrow refers to another CBS related band seen in MCF7-WT lanes. The red dashed boxes refer to the placental CBS bands which would be quantified in placental samples in chapter 6. The white dashed line splits the major CBS band so the top half would be also quantified (B) Immunoblotting with a loading control (anti-β-actin antibody). The black arrow refers to the predicted β-actin MW (~ 42 kDa).

The same anti-CBS antibody was also tested for specificity in CBS knockout BeWo clones. 20 μg of protein from a normal placental sample, WT BeWo cells, CBS knockout BeWo clones C1, C2 (KO score: 64% and 94%, respectively) and also non-knockout sequenced C5 was loaded into 4-12% Tri-Bis gel run in MES buffer, blotted then immunodetection with anti-CBS antibody was performed (Figure 5-17A). The absence of bands in C2 at the

expected ~ 61 kDa again confirms the antibody is detecting CBS but also that it binds to multiple non-CBS proteins as background bands. The unexpected CBS band at ~ 98 kDa was again evident in BeWo cells. Although C1 had a KO score of only 64%, the western blot showed complete elimination of CBS protein. It is possible the non-mutant allele(s) in this clone are naturally silent and do not contribute to CBS protein expression. The 9bp deletion in C5 seems to have been sufficient to eliminate detection by the antibody. It is important to note that in this gel the major CBS band (~ 61 kDa) in BeWo-WT looks slightly larger to the relative major placental bands whereas the major CBS band in MCF-7 looked similar in size to the upper major band(s) in placenta in Figure 5-16. However, the CBS bands in placenta, MCF-7 and BeWo cells had looked similar in size in earlier analyses e.g Figure 4-14A, suggesting the CBS protein might exhibit some natural variation in electrophoretic mobility. Likewise, to confirm samples equal loading, the membrane was stripped and re-probed with β-actin (Figure5-17B).
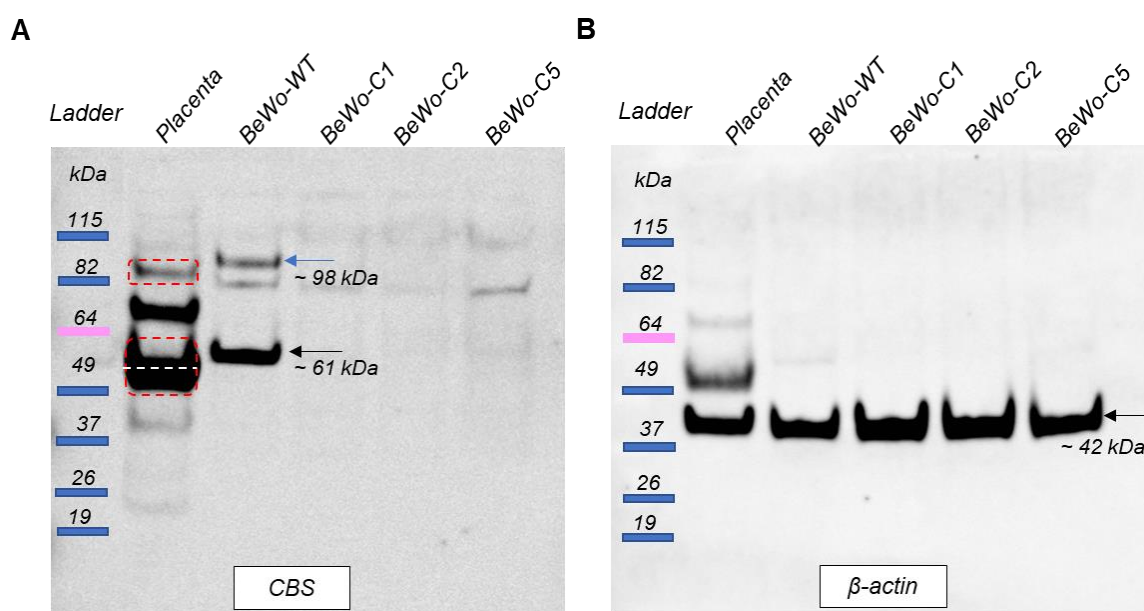
Figure 5-17 Western blotting of placental tissue and pCBSsg1 BeWo clones with anti-CBS and anti-β-actin antibodies. 20 μg of protein was loaded into 4-12% Tri-Bis gel. Lane 1: Molecular ladder (BenchMark™ pre-stained protein standard, Novex, cat. no. 10748-010), lane2: placental lysate, lane 3: BeWo-WT lysate and lane 4-6: BeWo-C1, C2 and C5 lysates. (A) Immunoblotting with anti-CBS antibody. The black arrow refers to the predicted MW (~ 61kDa) of CBS and the blue arrow refers to another CBS related band seen in BeWo-WT lane. The red dashed boxes refer to placental CBS bands which would be quantified in chapter 6. The white dashed line splits the major CBS band so the top half would be also quantified. (B) Immunoblotting with anti-β-actin antibody. The black arrow refers to the predicted β-actin MW (~ 42 kDa).

5.2.5.3 Testing of anti-CSE antibody specificity in CSE knockout MCF-7 and BeWo cells

pCSEsg1 MCF-7 C1, the only survived clone, was screened only by western blotting and the pattern of bands was identical to what seen in the WT (Figure 5-18).
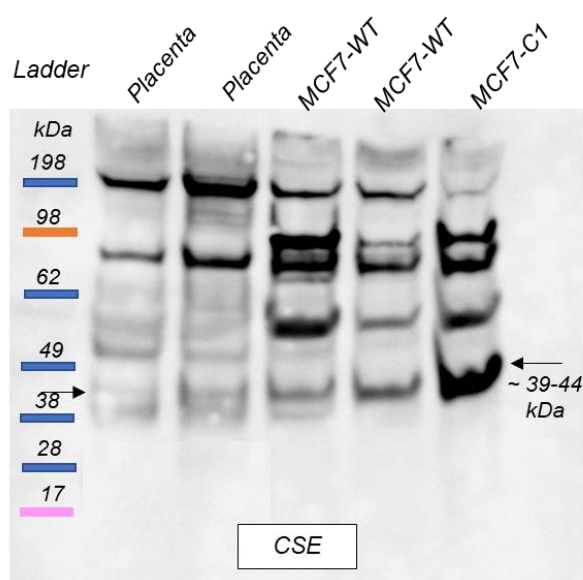
Figure 5-18 Western blotting of placental tissue and pCSEsg1 MCF7-C1 lysates with anti-CSE antibody. 20 µg of protein were loaded into 4-12% Tri-Bis gel. Lane 1: Molecular ladder, lane 2: placental lysate, lane 3-4: MCF7-WT lysates, lane 5: CSE MCF7-C1 lysate. The black arrows refer to the predicted CSE MW (~ 39-44 kDa).

Anti-CSE antibody specificity was tested in CSE knockout BeWo clones. 20 µg of protein from a normal placental sample, WT BeWo cells, CSE knockout BeWo clone C7 (KO score: 95%), unsequenced clones pCSEsg1 BeWo C10 and C11 and non-knockout sequenced C12 was loaded into 4-12% Tri-Bis gel run in MES buffer, blotted then immunodetection with anti-CSE antibody was performed (Figure 5-19A). The absence of bands in knockout clone C7 at the expected ~ 39-44 kDa confirms the antibody is detecting CSE but also that it binds to multiple non-CSE proteins as background bands. Both unsequenced clones C10 and C11 also look to be knockout clones and as expected the sequenced non-knockout clone C12 had a protein pattern similar to WT. A second band clearly absent from the knockout clones (~70 kDa) therefore, it is also likely to be from CSE gene but it does not correspond to any known splice variant of CSE. The placental sample lane showed one band the same size as the upper part of the thick CSE band in BeWo-WT lane which probably encompasses 2 or 3 of the three known splice variants (39, 41 and 44 kDa), and also showed another smaller size band which could be corresponding to the splice variant 2 (~ 39kDa). These two placental CSE bands would be used for quantification of placental CSE in later analyses (chapter 6). Again, to confirm equal sample loading, the same membrane was stripped and re-probed with β-actin (Figure5-19B).
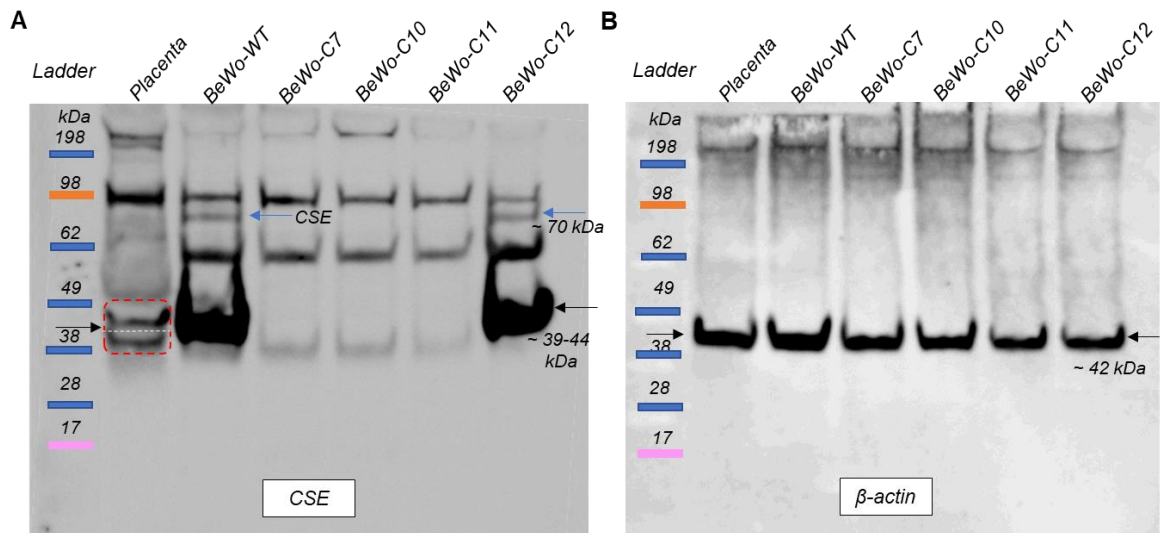
Figure 5-19 Western blotting of placental tissue and pCSEsg1 BeWo clones with anti-CSE and anti-β-actin antibodies. 20 µg of protein were loaded into 4-12% Tri-Bis gel. Lane 1: Molecular ladder, lane 2: placental sample lysate, lane 3: BeWo-WT cell lysate, lane 4-7: BeWo C7, C10, C11&C12 cell lysates. (A) Immunoblotting with anti-CSE antibody. The black arrows refer to the predicted CSE MW (~ 39-44 kDa), and the blue arrows refer to another higher band related to CSE. The red dashed box refers to placental CSE bands for quantification. The white dashed line splits the two CSE bands so the top band would be quantified separately. (B) Immunoblotting with anti-β-actin antibody. The black arrows refer to the predicted β-actin MW (~ 42 kDa).

5.3 Discussion

In general, Sanger sequencing and ICE analysis confirmed that a high proportion of puromycin resistance clones obtained after co-transfection with plasmid containing an sgRNA and Cas9 have frameshift mutations expected to knocked out CBS, CSE and 3-MST genes in both human MCF-7 and BeWo cell lines. These clones allowed confirmation that the antibodies used for these proteins did indeed detect the CBS, CSE and 3-MST as the western blots showed that protein bands of the predicted size disappeared in knockout clones. However, they also showed that, as suspected, the anti-CBS and CSE antibodies in particular have high levels of background bands as these bands remained present in samples from the knockout clones. As discussed in the previous chapter, this background could not be eliminated by a range of experimental conditions.

Two inconsistencies were found between the Sanger sequencing/ICE analysis of knockout clones and the western blot results of those clones: CBS BeWo C1 and C5. In CBS BeWo C1, ICE analysis of the .abi file gave indel percentage and knockout score of 64% with wild type sequence contributing 32% of the remainder. Therefore, CBS protein was expected to be still expressed in that clone albeit at a reduced level. However, the western blot result showed complete elimination of CBS protein in this clone. There are several possible explanations for this. First is that sometimes ICE analysis might underestimate the knockout frequency. This software has shown high concordance with data obtained by NGS (Hsiau et al., 2018) but one cannot exclude occasional exceptions occur. Another possibility is that the clone from which DNA was extracted became accidentally contaminated by wild type BeWo cells. Analysis of clones established from single cells of this clones could be done to see if that was true. Another possibility is that this clone is genuinely a mixture of WT and mutant alleles but the WT alleles are naturally silent and do not contribute to CBS protein expression.

Western blot of CBS detection in BeWo C5 clone was also surprising. ICE scored this as 0% knockout because all alleles had a deletion of 9bp which is not a frameshift. However, in the CBS BeWo C5 no CBS protein was detected by western blotting. This could be because the deletion eliminated the epitope recognised by the used antibody. It was also surprising to see only that precise 9b deletion in the population as it is expected to see at least two alleles in each cell. This may be because all alleles underwent the same edit and so have the same indel (-9pb). But it could also be explained if some of the alleles have been inactivated by insertion of puromycin plasmid causing inactivating mutation but also which

would stop them being amplified by Taq polymerase as the fragments would be too large. To test that, other PCR reactions using primers for pSCB-puro plasmid sequences may be required.

The knockout approach for testing anti-CBS and CSE antibodies was also informative in showing how using knockout and western blot of knockouts can reveal unexpected forms of a protein that might be missed especially if they are not abundant and in the middle of no-specific background. The western blot data in Figure 5-16 and 5-17 showed a higher CBS band at 98 kDa beside the major CBS band (~ 61kDa). Similarly, the western blot data in Figure 5-19 revealed another CSE band at nearly ~70kDa alongside the major CSE bands (between 39-44 kDa). These higher bands could not be explained by known CBS or CSE splice isoforms because the molecular masses of these isoforms are close to ~ 61 and ~ 39-44, respectively (see Table 4-1). These higher MW forms of CBS and CSE proteins may be explained by post-translational modifications which may increase the size of protein for example SUMOylation or S-glutathionylation which affect the migration of protein in SDS-PAGE, so the size observed differs from that predicted. Previous studies, *in vivo* and *in vitro*, have shown SUMOylation of CBS presenting higher bands at ~ 80 and 110 kDa alongside the 63 kDa band of the native unmodified CBS protein (Kabil et al., 2006). CSE is also subjected to *in vitro* SUMOylation and two major bands with molecular mass of ~ 65 and 85 kDa were observed combined with the unmodified CSE protein at 45kDa (Agrawal and Banerjee, 2008). Moreover, two CBS bands with molecular masses of ~ 63 and ~130 kDa were detected due to S-glutathionylation of CBS protein (Niu et al., 2015). The suggestion for post-translationally modified CBS and CSE opens the doors for further experiments to investigate if these higher bands could be related to post-translational modifications (will be discussed in chapter 8).

5.4 Conclusion

It was concluded that all antibodies used to detect the proteins of interest and the patterns on western blots were now able to be interpreted with sufficient confidence to go on to analyse expression in placenta samples. Furthermore, the knockouts clones also would be useful to assess the accuracy of *in situ* methods (IHC and IF) and to study the effect of proteins per se (chapter 7).

Chapter 6 Protein expression analysis by western blotting of hydrogen sulfide producing enzymes in placentas from healthy and complicated pregnancies

6.1 Introduction

In chapter 3, regulation of H_2S synthesising enzymes at level of mRNA abundance was discussed, and that CBS, CSE and 3-MST levels were investigated among the study groups. Some significant differences were found and, having verified that the chosen antibodies detected these proteins and optimised as much as possible by western blots, the level of these proteins was investigated in the same groups where significant differences in mRNA levels had been found.

6.1.1 Regulation of CBS, CSE and 3-MST protein abundance

Expression of CBS and CSE is regulated primarily at transcriptional as well as at post-transcriptional level, and this was discussed in chapter 3. These proteins can also be regulated at the translational/post-translational level. These modifications may alter the structure or function of protein or they affect the abundance of the protein by stabilising it or can target it for destruction (Wu et al., 2008). The synthesis and degradation rates of a protein and its encoding mRNA are sometimes markedly different, resulting in poor correlation (Maier et al., 2009), and therefore mRNA measurements provide only partial understanding of differential gene expression regulation.

Additionally, proteins could be regulated post-translationally by covalent modifications or association with other molecules, leading to a change in their abundances. For example; CBS protein is activated allosterically by AdoMet which is an intermediate product of methionine metabolism and a universal methyl group donor. AdoMet binds to the C-terminal regulatory domain of the CBS protein, and it increases its stability against proteolysis (Roper and Kraus, 1992). The full length of the enzyme binds to 1 mol AdoMet per mole of monomeric subunit, which increases the catalytic activity of the enzyme about 2-fold (Taoka et al., 1999). Methionine restriction leads to a significant reduction (> 10-fold) in CBS protein levels due to decrease in AdoMet concentration and destabilisation of CBS (Prudova et al., 2006). CBS activity is also activated by a cleavage at its C-terminal at arginine (R^{413}) to generate a 45 kDa isoform with higher basal catalytic activity than the full

length form (Kery et al., 1998). Calcium-calmodulin binds CSE protein resulting in an increase in its activity (Yang et al., 2008), but no regulation of CSE at the level of protein stability was found in the literature. The 3-MST enzyme is primarily regulated intrinsically by its redox state rather than post-translational modifications or transcriptional regulation. The 3-MST contains surface and catalytic site cysteines (Cys^{247}, Cys^{154} and Cys^{263}) each of which is redox active (Nagahara and Nishino, 1996). Oxidants inhibits 3-MST activity via both intermolecular and intramolecular redox-sensing switches. The intermolecular switch occurs by the formation of disulfide bond between two surface cysteine (Cys^{154} and Cys^{263}) of two 3-MST molecules and the intramolecular switch occurs by oxidation of the catalytic site cysteine (Cys^{247}) to cysteine sulfenate. The 3-MST enzymatic activity is restored upon reduction by thioredoxin of either 3-MST with oxidised cysteine or the disulfide-linked homodimer (Nagahara and Katayama, 2005). These switches regulate the functions of 3-MST as an antioxidant and/or to produce H_2S.

In general, there are many types of post-translational modifications that can cause changes in amounts of protein detected the most common of which is phosphorylation (Khoury et al., 2011) which occurs mainly in the serine, threonine and tyrosine residues of target substrate proteins (Olsen et al., 2006) and affects protein stability, protein interactions, and cellular localisation of proteins. Ubiquitination is another common post-translational protein modification involved in many biological processes, including immune responses (Tsuchida et al., 2010), apoptosis (Schile et al., 2008) and cancer (Vandenberg et al., 2003). Ubiquitin molecules bind to target proteins to form poly-ubiquitin chains, which can be identified by the 26S proteasome, which is a large protease, causing protein degradation (Deveraux et al., 1994). Carbonylation is another type of post-translational modifications that is a consequence of oxidative stress. It targets the modified protein for degradation and can result in formation of protein aggregates (Stadtman and Berlett, 1991). SUMOylation is a reversible post-translational modification which also affect the protein activity and localisation (Ayaydin and Dasso, 2004). SUMOylation of CBS, in which the CBS modified at its C-terminal regulatory domain by the ~11 kDa small ubiquitin-like modifier-1 protein (SUMO-1) protein was reported (Agrawal and Banerjee, 2008). This modification reduces CBS activity by approximately 70% and changes its subcellular localisation into the nucleus (Kabil et al., 2006). *In vitro* SUMOylation of CSE was also reported (Agrawal and Banerjee, 2008). However, whether the SUMOylation of CSE occurs within the cell and has a physiological effect in consequence is not clear.

The qPCR data in chapter 3 showed an increase in CBS, CSE and 3-MST mRNA abundance in labour and complicated pregnancies at particular placental sites. However, how these transcripts reflect the protein abundance in placental tissues is unknown. Some proteins might be subjected to regulatory mechanism that could affect their abundances. Therefore, measuring CBS, CSE and 3-MST protein levels was important.

6.2 Western blot normalisation and quantification

In order to confidently assess any variation in observed levels of CBS, CSE or 3-MST between groups, the data obtained from the western blots were separately normalised to two loading controls: β-actin and Ponceau S stain which does not affect the sensitivity detection of the protein of interest by western blot (Sander et al., 2019). The concentration of the Ponceau S stain and the staining time seems to be effective in protein detection in this study within the range of protein amount standardly loaded for western blotting (Figure 4-6). The Ponceau S concentration used for staining in this study was 0.1% (w/v) in 5% acetic acid, and Sander et al. (2019) reported that irrespective of the Ponceau S stain concentration (between 0.001-2%), acid concentration and type (acetic acid, trichloroacetic acid or sulfosalicylic acid), the sensitivity of protein detection remained constant. Moreover, Sander et al. (2019) observed that the Ponceau S staining did not affect the sensitivity detection of protein of interest when they compared western blots which were stained with Ponceau S stain to blots that were not stained with Ponceau S stain.

For Ponceau S stain quantification of signal intensities, AIDA digital quantification software was used: boxes of identical dimension were drawn around each whole lane but excluding the haemoglobin band, which varies from sample to sample depending on blood content of the original placental sample. An example is shown in Figure 6-1A. For quantification of the housekeeping protein, β-actin, or the protein of interest, a box of the same size for each lane was made around the band identified as the specific signal (Figure 6-1B). A box the same size was positioned in an area of the image where there should be no protein and the signal within that used as background signal intensity and subtracted from the signal intensity of each individual lane or band to give the corrected values for each. The protein signal intensities for each of the proteins of interest was calculated as the corrected value divided by the corrected value for the loading control, either total protein stain or β-actin. The statistical analysis was performed by comparing the normalised signal intensities of proteins of interest between control and pathological groups using Mann Whitney test (justification for this test is in 2.14).

Both CBS bands of approximately ~ 61 kDa and ~ 98 kDa, which were confirmed CBS-related in CBS knockout clones (section 5.2.5.2), were quantified. The major band at ~ 61 kDa appears thick in placental samples with the upper part the same size as the band missing in the knockout clones (Figure 4-14A, 5-16A and 5-17A). The lower bands maybe other CBS isoforms but this can be said with less confidence therefore quantification was applied separately to the whole or to the upper half of the band. Although CSE bands of approximately ~ 39-44 kDa and ~ 70 kDa, were confirmed CSE-related in CSE knockout clones (section 5.2.5.3), only the major band at ~ 39-44 kDa was quantified in placental samples because the other band which was at ~ 70 kDa was not found in placental samples. There was also a smaller size band which close to the band at ~ 39-44 kDa. This band could be an isoform corresponding to the CSE variant 2 (~39kDa) (see Table 4-1). Therefore, it was worth to quantify both bands separately in addition to the upper band quantification.
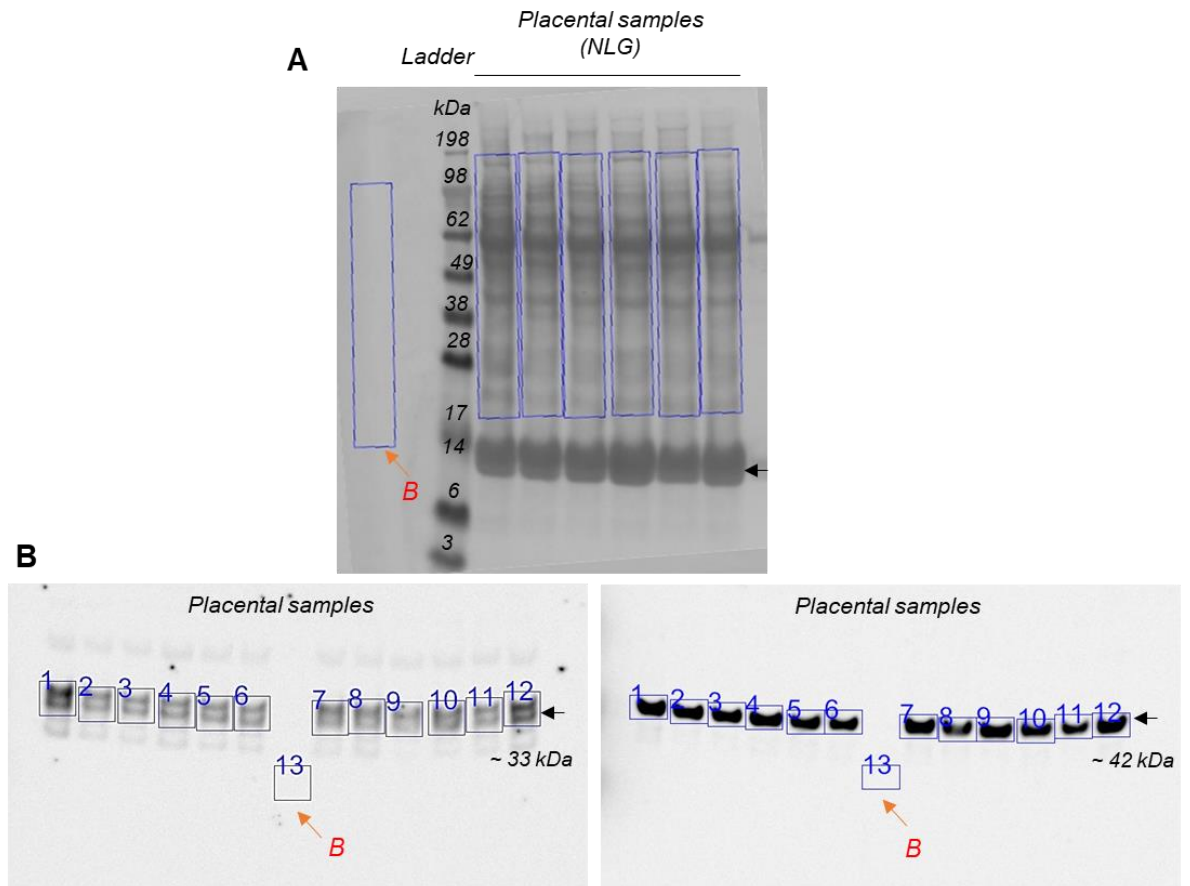
Figure 6-1 Typical images exemplifying process for quantification of band intensity. (A) Densitometric quantification from total protein staining with Ponceau S stain. The back arrow refers to the probable globin bands which were excluded from quantification. (B) Densitometric quantification from protein of interest in this case 3-MST (left panel) and housekeeping protein β-actin (right panel). The red B indicates the boxed area background for subtraction.

6.3 Results

6.3.1 3-MST protein expression during labour

The qPCR data showed an increase in mRNA level of 3-MST in labour group compared to non-labour group at the inner placental site (Figure 3-6G). Therefore, the difference in 3-MST protein abundance between non-labour group (n = 6) and labour group (n = 6) at the inner placental site was investigated. The 3-MST western blot revealed a set of two bands of approximately 33 kDa corresponding to 3-MST (Figure 6-3A). In this comparison, the signal intensity of the 3-MST was normalised to total protein staining with Ponceau S stain (Figure 6-2), and was also normalised to housekeeping protein, β-actin (Figure 6-3B).
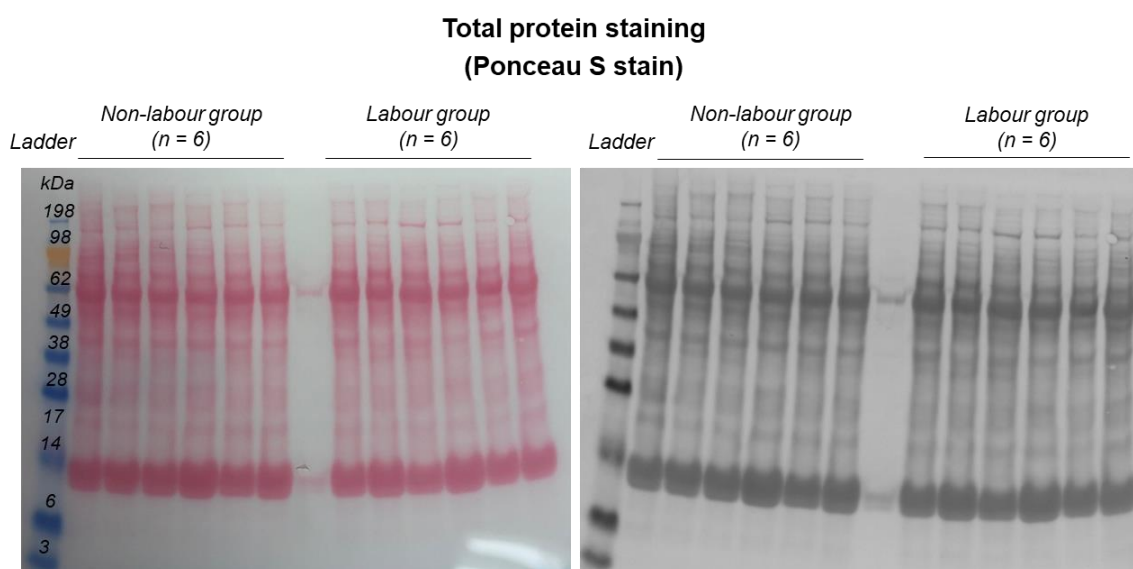
Figure 6-2 Ponceau S stain of transferred proteins of placental samples from healthy non-labour and labour groups (inner site). The left panel represents a scanned image of stained membrane and the right panel represents the grayscale image of the same stained membrane.

A   **3-MST (Inner site)**

B   **β-actin (Inner site)**

Figure 6-3 Western blots of placental (inner site) expression of 3-MST and β-actin protein in healthy non-labour (n = 6) and labour groups (n = 6). 20 μg of protein was loaded into 4-12% Tri-Bis gel. (A) Immunoblotting with anti-3-MST antibody. The targeted band was detected at ~ 33 kDa (black arrows). (B) β-actin immunodetection after stripping the same membrane. The β-actin bands were detected at ~ 42 kDa (black arrow). The bands indicated by the black arrows were quantified. The red dashed box is an example of the quantification boxes around the indicated bands.

The two sets of normalised signal intensities of 3-MST protein were compared between labour and non-labour groups at the inner placental site (0-2cm from the cord insertion) using Mann-Whitney test (Figure 6-4). Although the level of 3-MST appears somewhat higher in the labour group when compared to the non-labour as indicated by qPCR, this increase was not statistically significant with either normalisation approaches.

A

3-MST
(Normalised to Ponceau S stain)

B

3-MST
(Normalised to β-actin)
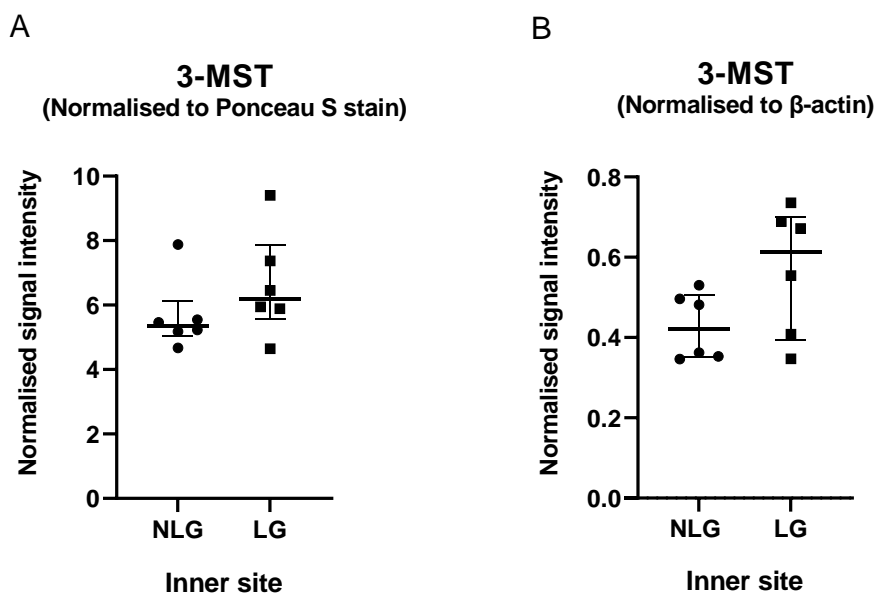
Figure 6-4 Quantitative western blot analysis of 3-MST protein in placentas from non-labour and labour groups. (A) Normalised 3-MST signal intensity to signal intensity of total protein staining with Ponceau S stain. (B) Normalised 3-MST signal intensity to β-actin signal intensity. Data are presented as median and interquartile range. The thick horizontal bar represents the median and the two narrower bars delimit the interquartile range. Comparison between groups was performed using Mann Whitney test.

6.3.2 3-MST protein expression in pregnancies complicated with FGR

Similarly, the qPCR data showed an increase in mRNA level of 3-MST in FGR group compared to the control group at the outer placental site (Figure 3-16). Therefore, 3-MST protein abundance was compared between FGR group (n = 6) and the control group (n = 6) at the outer placental site. The membrane stained with Ponceau S stain is shown in Figure 6-5, while the western blots of 3-MST and β-actin are shown in Figure 6-6.

**Total protein staining
(Ponceau S stain)**
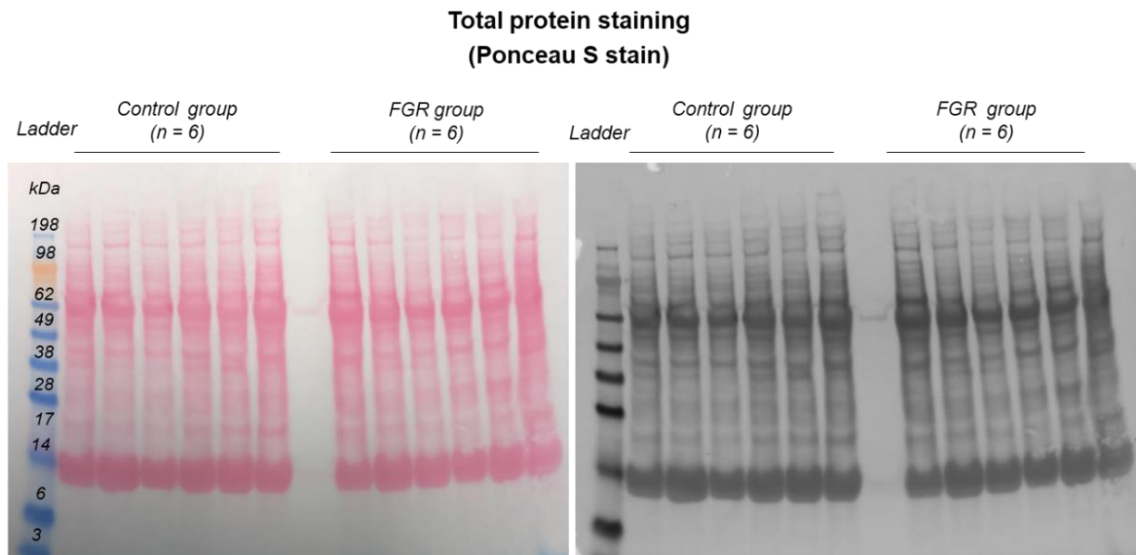
Figure 6-5 Ponceau S stain of transferred proteins of placental samples from healthy pregnancies and pregnancies complicated with FGR (outer site). The left panel represents a scanned image of the stained membrane and the right panel represents the grayscale image of the same stained membrane.

A   **3-MST (Outer site)**

B   **β-actin (Outer site)**

Figure 6-6 Western blots of placental (outer site) expression of 3-MST and β-actin protein in healthy placentas (n = 6) and FGR placentas (n = 6). 20 μg of protein was loaded into 4-12% Tri-Bis gel. (A) Immunoblotting with 3-MST. The targeted band was detected at ~ 33 kDa (black arrows). (B) The β-actin immunodetection after stripping the same membrane. The β-actin bands were detected at ~ 42 kDa (black arrow). The bands indicated by the black arrows were quantified. The red dashed box is an example of the quantification boxes around the indicated bands.

Figure 6-7 shows the statistical analysis of two sets of normalised signal intensities of 3-MST protein. The data were compared using Mann Whitney test. 3-MST protein level was significantly increased in the FGR group compared to the control group at the outer site (p = 0.002) when the 3-MST signal intensities were normalised to β-actin consistent with the change in 3-MST mRNA measured by qPCR (Figure 3-16). However, when the signal intensities were normalised to Ponceau S stain, the difference in 3-MST protein abundance between the FGR and control group was not significant (p = 0.06) (Figure 6-7). The inconsistency in the results obtained from the two normalisation approaches assumed likely due to a single data point in graph (A) which deviated from the other data points and it was thought possible that the Ponceau S stain might have understained this lane. To investigate that the Ponceau S stain: β-actin ratio of the sample was calculated and compared to ratio of other data points in a box plot graph. That single data point clearly deviated from the other data points being well outside the interquartile range and was away from the lower limit of the data range (Figure 6-8A). This justified removing that sample from this analysis and when the data were re-analysed without it, the Ponceau S stain normalised data showed a significant difference (p = 0.004) similar to the β-actin normalised data (Figure 6-8B).

Figure 6-7 Quantitative western blot analysis of 3-MST protein in placentas from pregnancies complicated with FGR. (A) Normalised 3-MST signal intensity to signal intensity generated from total protein staining with Ponceau S stain. (B) Normalised 3-MST signal intensity to β-actin signal intensity. Data are presented as median and interquartile range. Comparison between groups was performed using Mann Whitney test. The asterisk indicates degree of p-value significance, ** means *p* < 0.01.

A

Box plot showing an outlier data point

B

3-MST
(Normalised to Ponceau S stain)
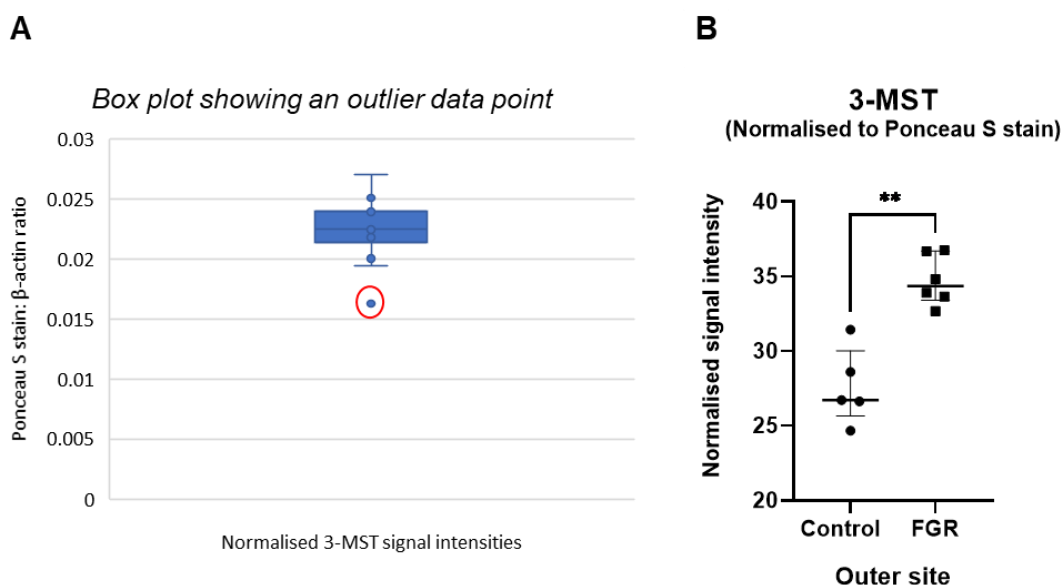
Figure 6-8 Identification of outliers in a data set and re-analysis of the data. (A)Shows a box plot of Ponceau S stain: β-actin ratio. The red circle indicates the outlier data point. (B) Re-analysis of the normalised 3-MST signal intensity to signal intensity generated from Ponceau S stain after exclusion the outlier sample. Data are presented as median and interquartile range. Comparison between groups was performed using Mann Whitney test. The asterisk indicates degree of p-value significance, ** means *p* < 0.01.

6.3.3 CBS protein expression in pregnancies complicated with PE

The qPCR data also showed an increase in mRNA level of CBS in pre-eclamptic placentas compared to healthy placentas at the inner placental site (Figure 3-8). Therefore, the difference in CBS protein level between control healthy (n = 12) and PE group (n =11) at the inner placental site was investigated. The CBS western blots are shown in Figure 6-10A, and they revealed multiple bands, but the bands of approximately ~ 61 kDa and ~ 98 kDa were corresponding to CBS. Normalisation of the data was performed to total protein staining with Ponceau S stain (Figure 6-9) and β-actin (Figure 6-10B).
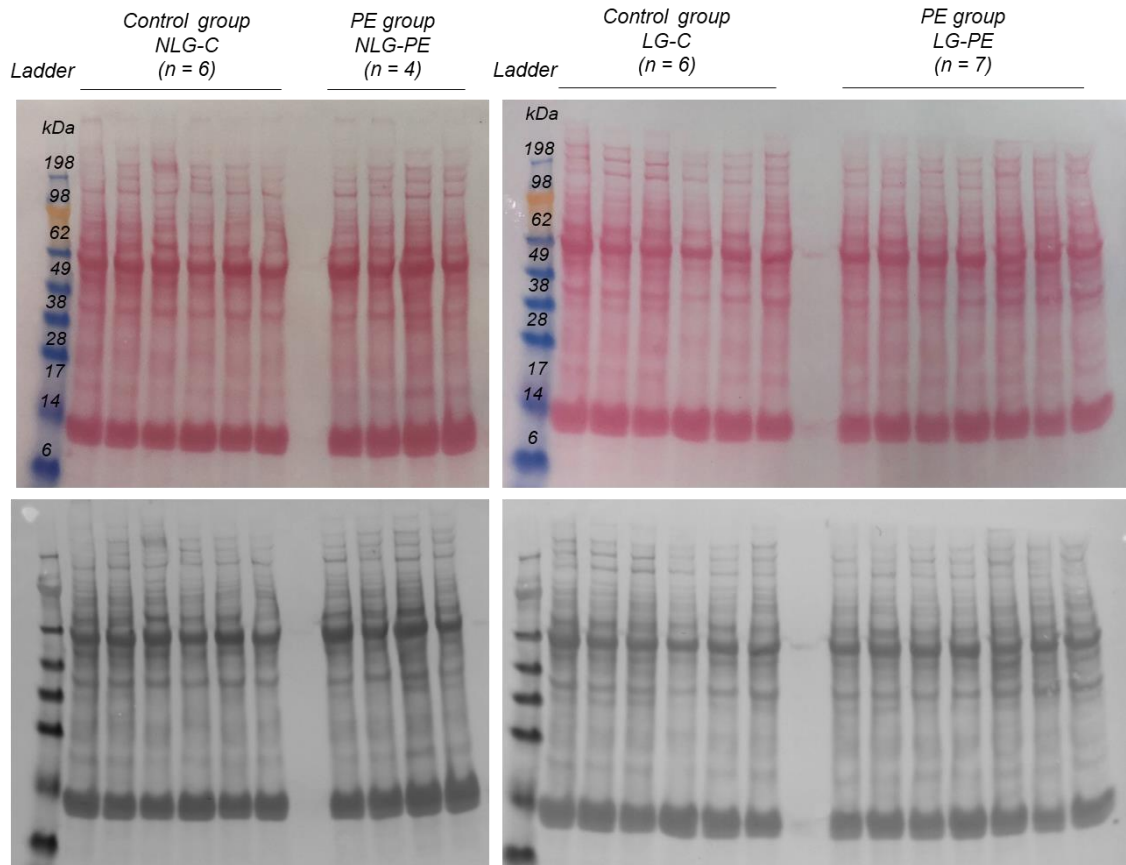
Figure 6-9 Ponceau S stain of transferred proteins of placental samples from healthy control (NLG and LG) and PE (NLG and LG) groups (inner site). The upper panel represents scanned images of the stained membranes, and the lower panel represents the grayscale images of the same stained membranes.
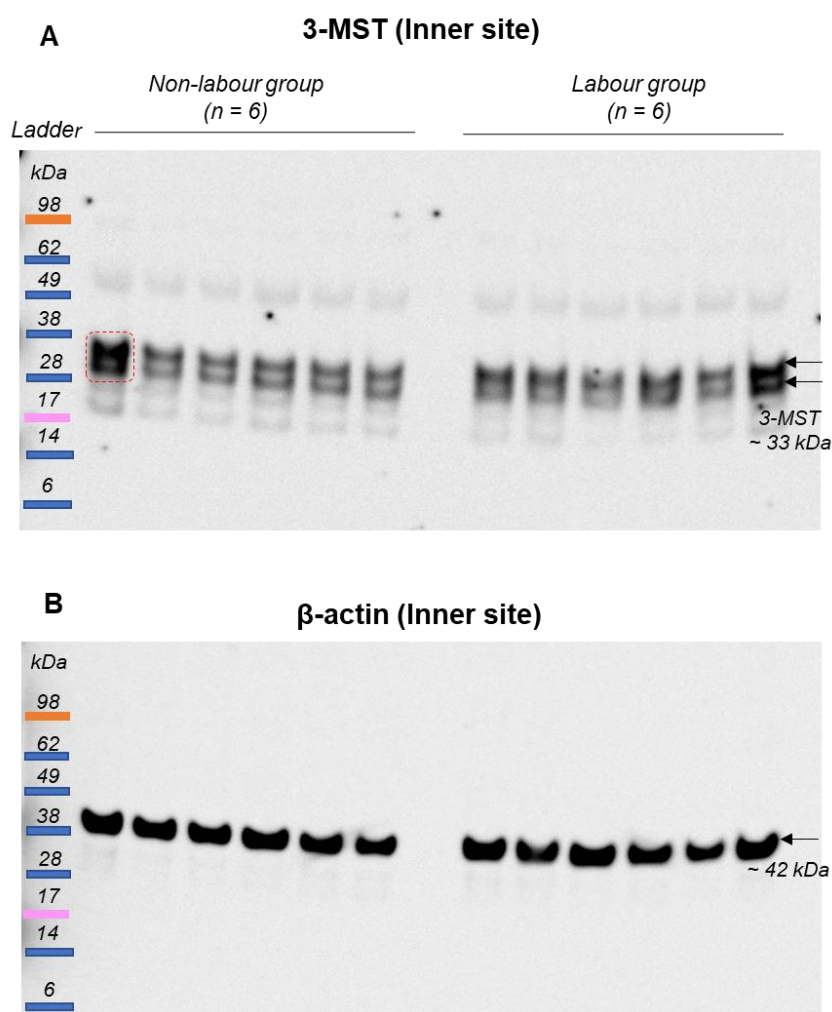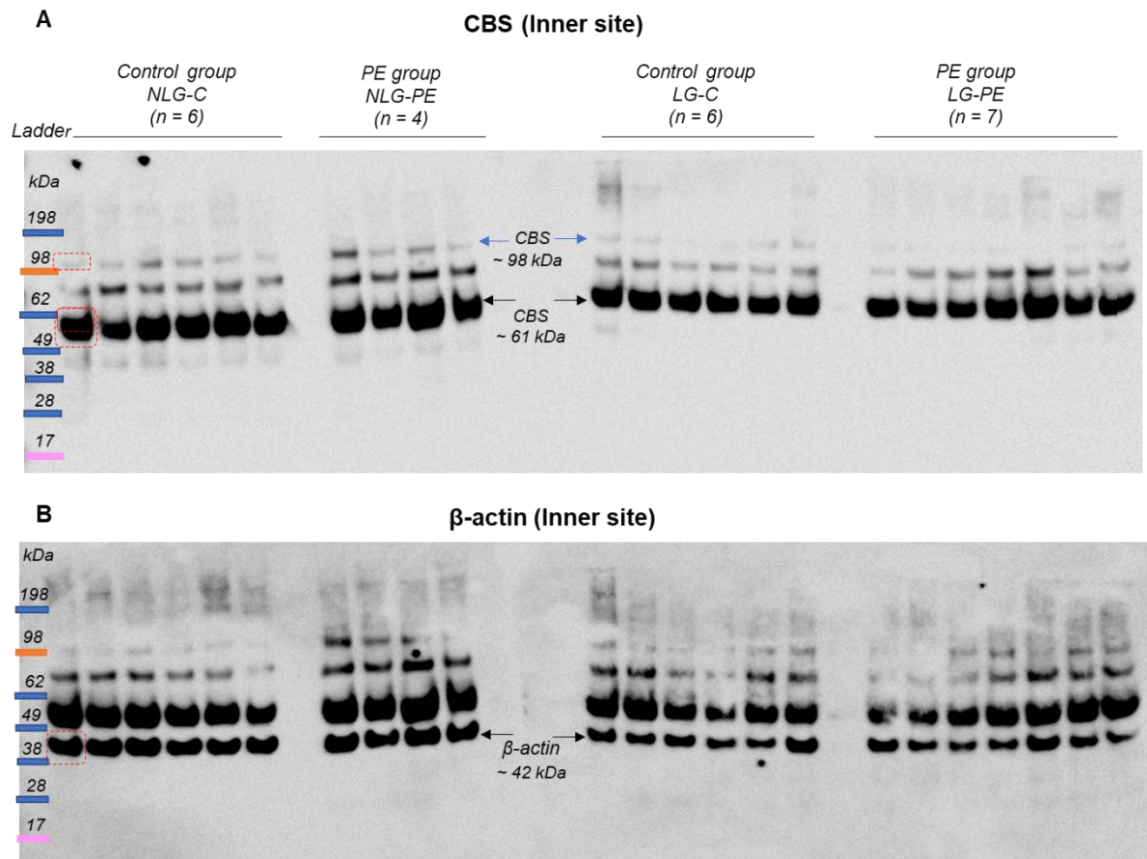
Figure 6-10 Western blots of placental (inner site) expression of CBS and β-actin protein in healthy placentas (n = 12) and pre-eclamptic placentas (n = 11). 20 µg of protein was loaded into 4-12% Tri-Bis gel. (A) Immunoblotting with CBS. The CBS bands were detected at ~ 61(black arrows) and ~ 98 kDa (blue arrows). (B) The β-actin immunodetection after stripping the membrane. The β-actin bands were detected at ~ 42 kDa (black arrows). The bands indicated by the black and blue arrows were quantified. The red dashed box is an example of the quantification boxes around the indicated bands.

The graphs in Figure 6-11 display the analysis of two CBS bands. Graphs in (A-B), (C-D) and (E-F) represent the protein analysis of the whole CBS band at ~ 61 kDa, the upper half of the CBS band at ~ 61 kDa and the CBS band at ~ 98 kDa, respectively. Both Ponceau S stain and β-actin were used as loading controls. There was not any statistically significant ($p > 0.05$) decrease in CBS protein level in PE group when compared to the control group in contrast to the qPCR results.
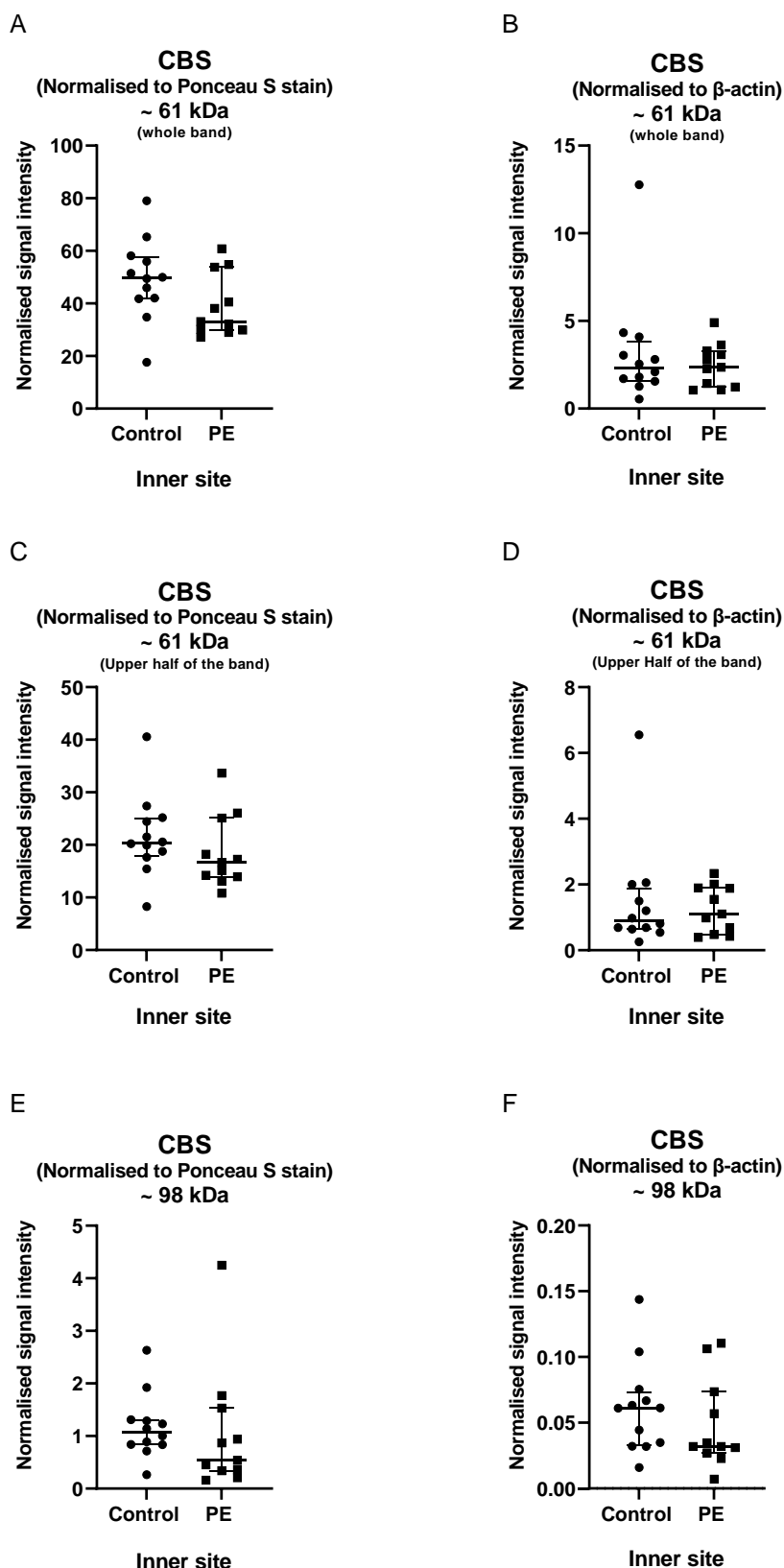
Figure 6-11 Quantitative western blot analysis of CBS protein in placentas from pregnancies complicated with PE. (A, C & E) Normalised CBS signal intensity to signal intensity generated from Ponceau S stain. (B, D & F) Normalised CBS signal intensity to β-actin signal intensity. Graphs (A & B) show quantification of the whole major CBS band (~ 61 kDa), graphs (C & D) show quantification of the upper half the major CBS band and graphs (E & F) show quantification of CBS band (~ 98 kDa). Data are presented as median and interquartile range. Comparison between groups was performed using Mann Whitney test.

6.3.4 CSE protein expression during labour

An increase in mRNA level of CSE was found in labour group when compared to non-labour group at middle placental site (Figure 3-6E) therefore, the CSE protein abundance in non-labour group (n = 6) and labour group (n = 6) at the middle placental site was compared. The CSE western blot result is shown in Figure 6-13A, and it revealed multiple bands but a major band of approximately ~ 39-44 kDa was corresponding to CSE protein and another smaller band could be also related to CSE (~ 39 kDa). Normalisation of the data was performed to total protein staining (Figure 6-12) and β-actin (Figure 6-13B).

**Total protein staining
(Ponceau S stain)**
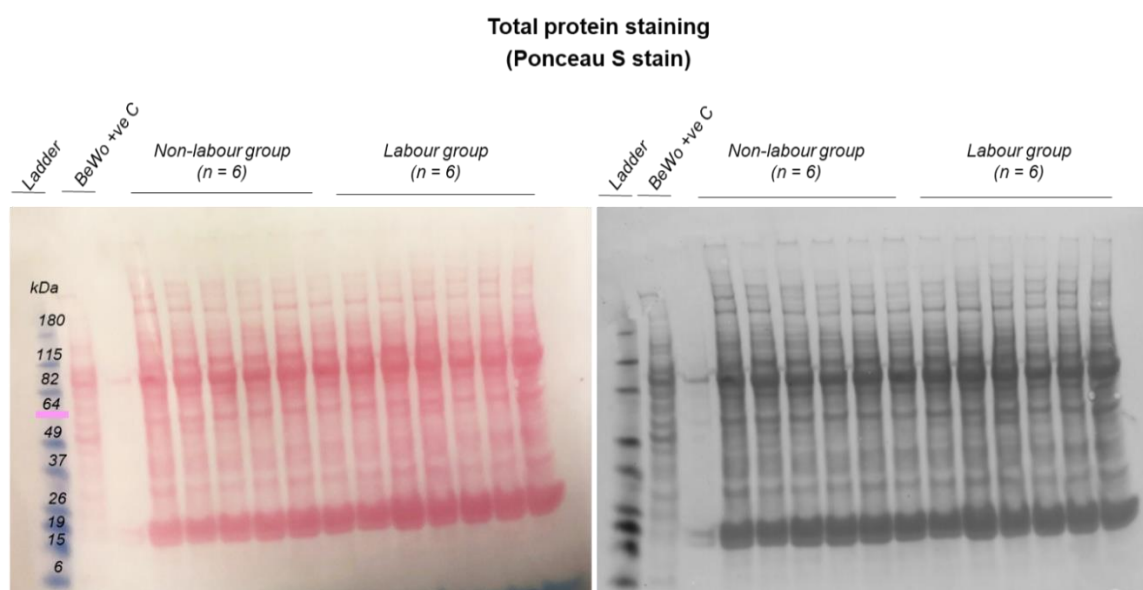
Figure 6-12 Ponceau S stain of transferred proteins of placental samples from healthy non-labour and labour groups (middle site). The left panel represents a scanned image of the stained membrane, and the right panel represents the grayscale image of the same stained membrane.
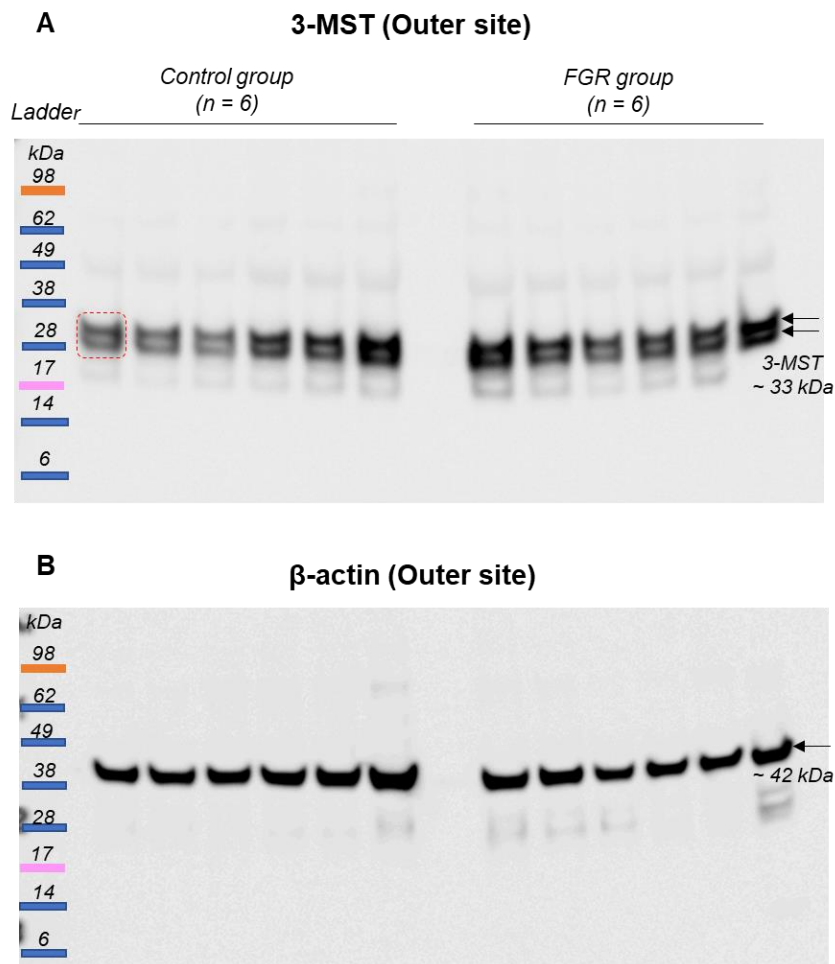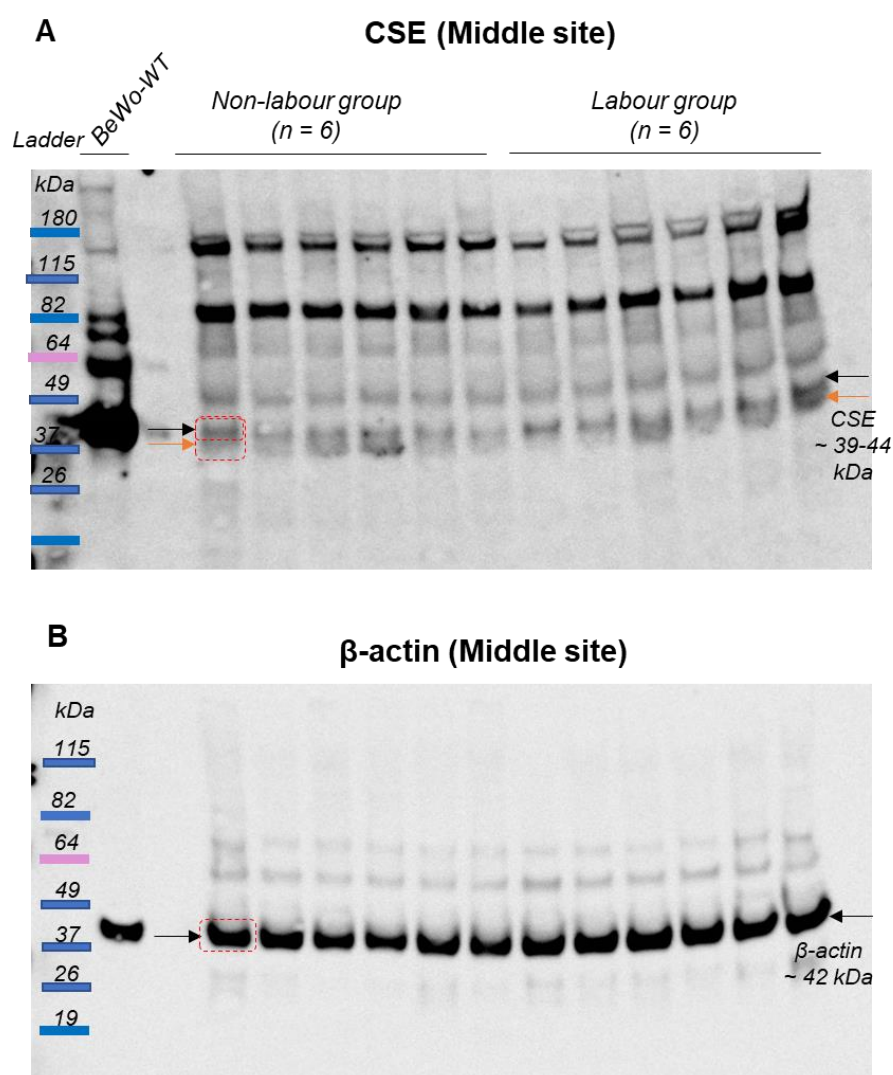
Figure 6-13 Western blots of placental (middle site) expression of CSE and β-actin protein in healthy non-labour (n = 6) and labour groups (n = 6). A WT BeWo cell lysate was also loaded beside the placental samples. 20 μg of protein was loaded into 4-12% Tri-Bis. (A) Immunoblotting with anti-CSE antibody. The targeted band was detected at ~ 39-44 kDa (black arrows). (B) The β-actin immunodetection after stripping the membrane. The β-actin band bands were detected at ~ 42 kDa (black arrow). The bands indicated by the black and red arrows were quantified. The red dashed box is an example of the quantification boxes around the indicated bands.

The normalised signal intensities of CSE protein bands were compared between groups using Mann Whitney test, and graphs are presented in Figure 6-14. The single most striking observation to emerge from the data comparison was that the there was a significant increase in CSE protein abundance in labour group when compared to non-labour group with both normalisation approaches; Ponceau S stain ($p = 0.04$ (upper band) and $p = 0.04$ (both bands)) and β-actin ($p = 0.02$ (upper band) and $p = 0.04$ (both bands)).
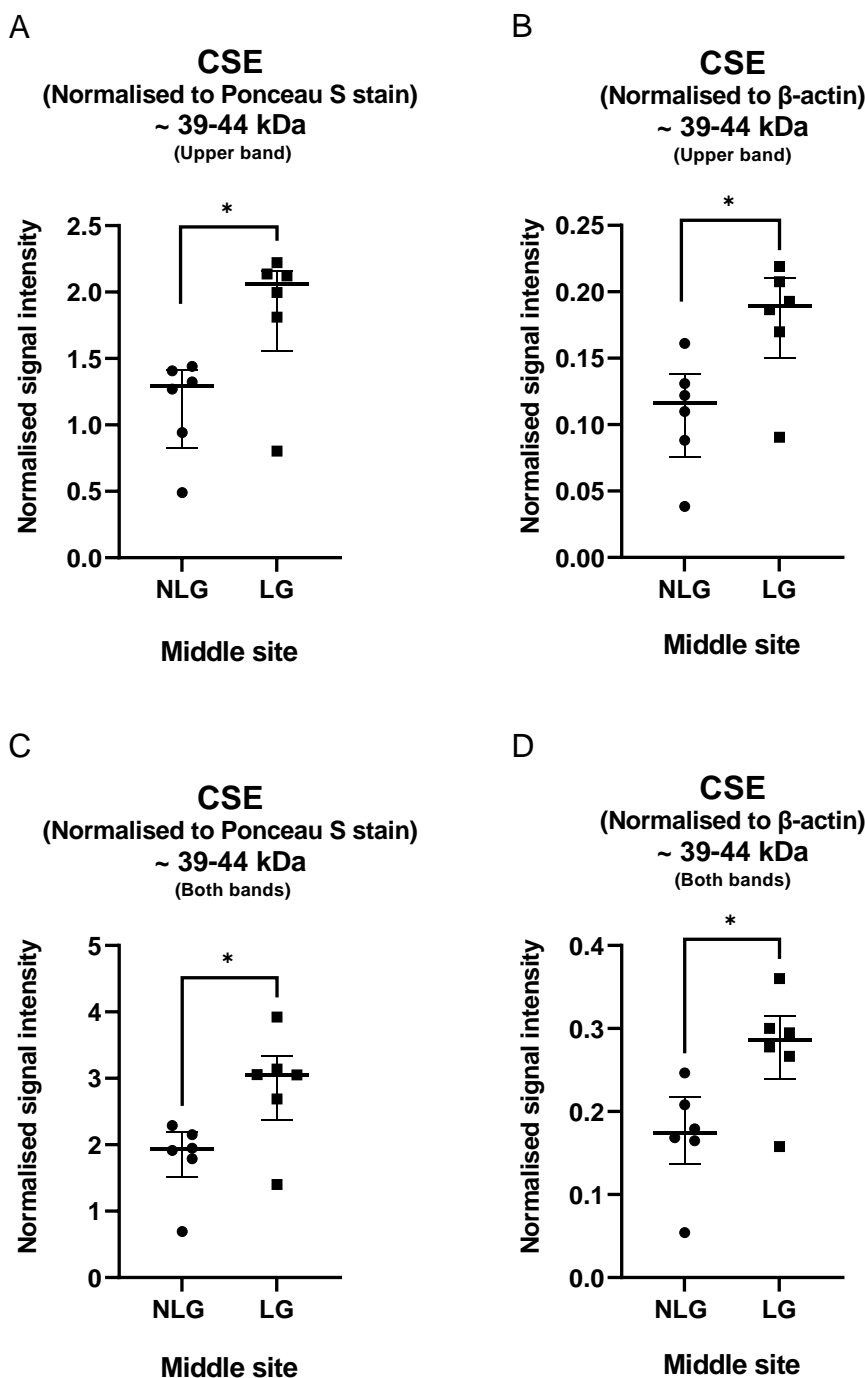
Figure 6-14 Quantitative western blot analysis of CSE protein in placentas from labour group. (A & C) Normalised CSE (~ 39-44kDa band) signal intensity to signal intensity generated from Ponceau S stain. (B & D) Normalised CSE (~ 39-44kDa band) signal intensity to β-actin signal intensity. Graphs (A & B) show quantification of the upper CSE band and graphs (C & D) show quantification of both CSE bands. Data are presented as median and interquartile range. Comparison between groups was performed using Mann Whitney test. The asterisk indicates degree of p-value significance, * means $p < 0.05$.

6.3.5 CSE protein expression in pregnancies complicated with PE

AS an increase in mRNA level of CSE in pre-eclamptic placentas at middle placental site was observed (Figure 3-10), the CSE protein abundance was also investigated between

control healthy (n = 12) and PE group (n = 11) at the middle placental site. The representative CSE western blot is shown in Figure 6-16A. It showed multiple bands, but the band of approximately ~ 39-44 kDa was corresponding to CSE. Normalisation of the data was performed to total protein staining (Figure 6-15) and β-actin (Figure 6-16B).
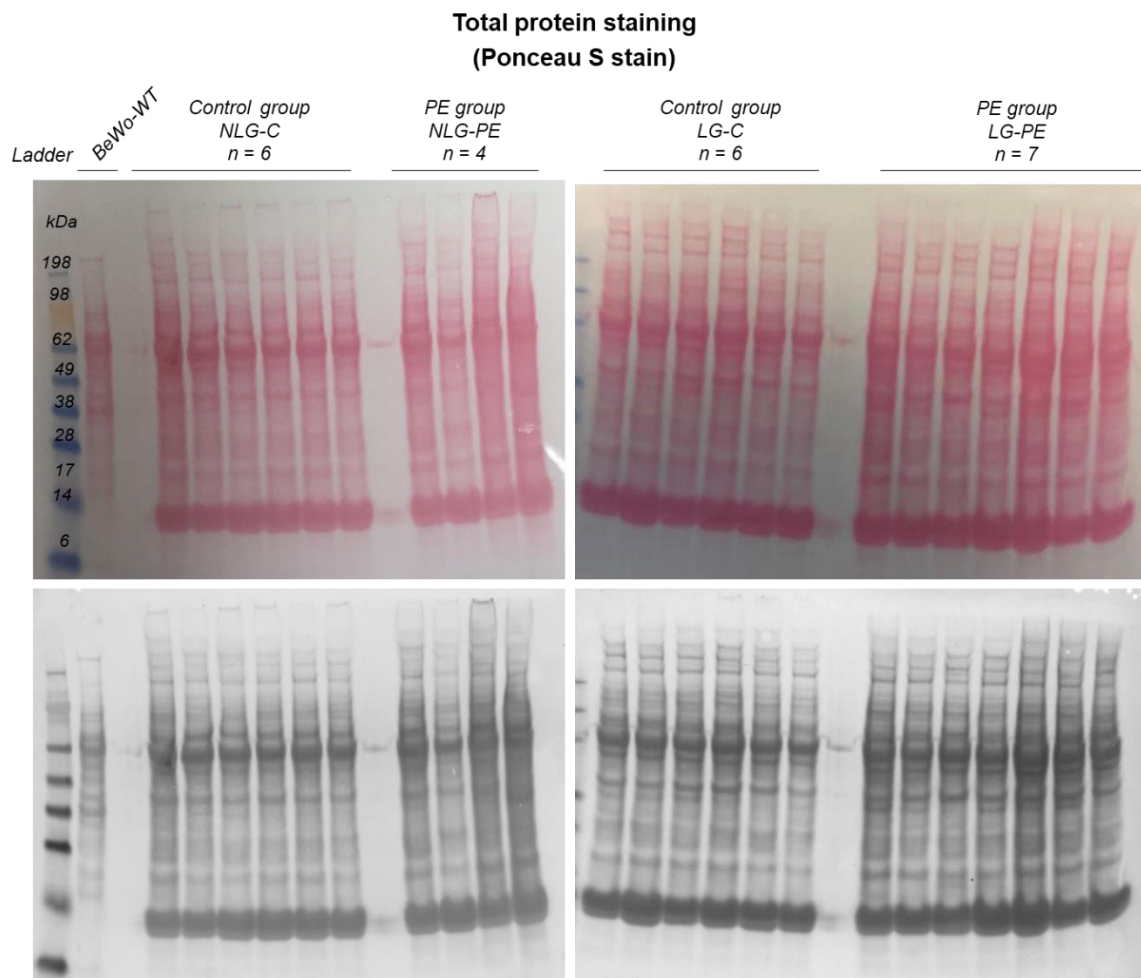
Figure 6-15 Ponceau S stain of transferred proteins of placental samples from healthy control and PE groups (middle site). The upper panel represents scanned images of the stained membranes, and the lower panel represents the grayscale images of the same stained membranes.
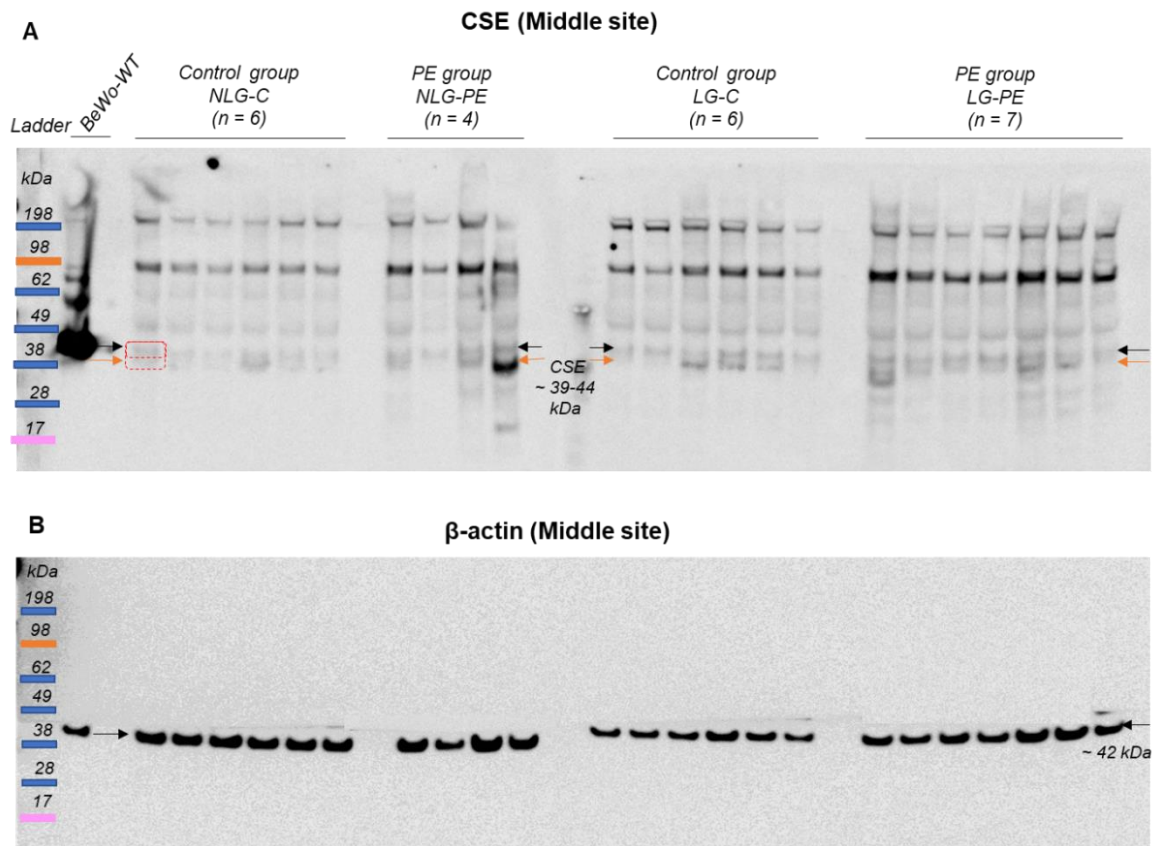
Figure 6-16 Western blots of placental (middle site) expression of CSE and β-actin protein in healthy placentas (n = 12) and pre-eclamptic placentas (n = 11). A WT BeWo cell lysate was loaded beside the placental samples. 20 μg of protein was loaded into 4-12% Tri-Bis gel. (A) Immunoblotting with anti-CSE antibody. The CSE bands were detected at ~ 39-44 kDa (black arrows). (B) The β-actin immunodetection after stripping the membrane. The β-actin bands were detected at ~ 42 kDa (black arrows). The bands indicated by the black and red arrows were quantified. The red dashed box is an example of the quantification boxes around the indicated bands.

The statistical analysis of CSE normalised signal intensities is displayed in Figure 6-17. From this data, it can be seen that there was no significant difference in CSE protein abundance between PE and control groups in contrast to the qPCR measurements.

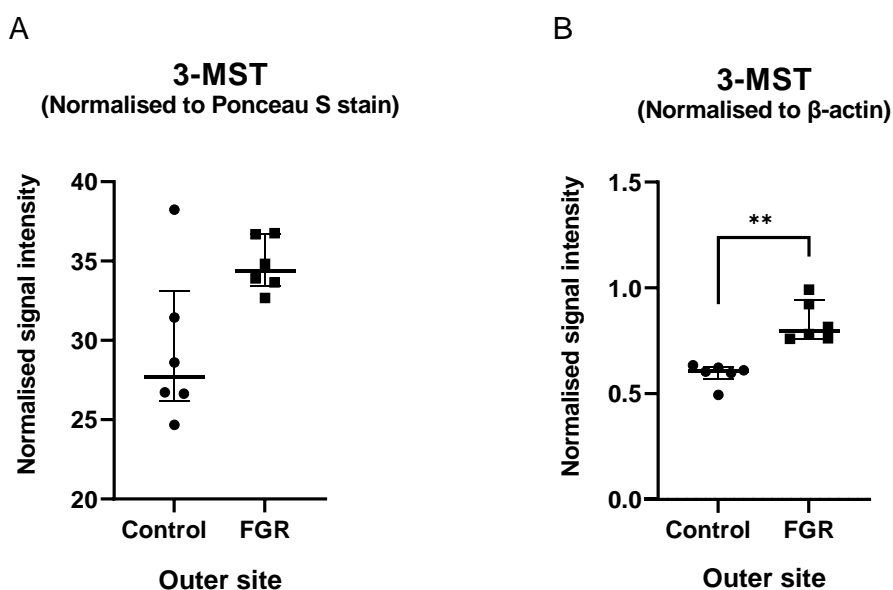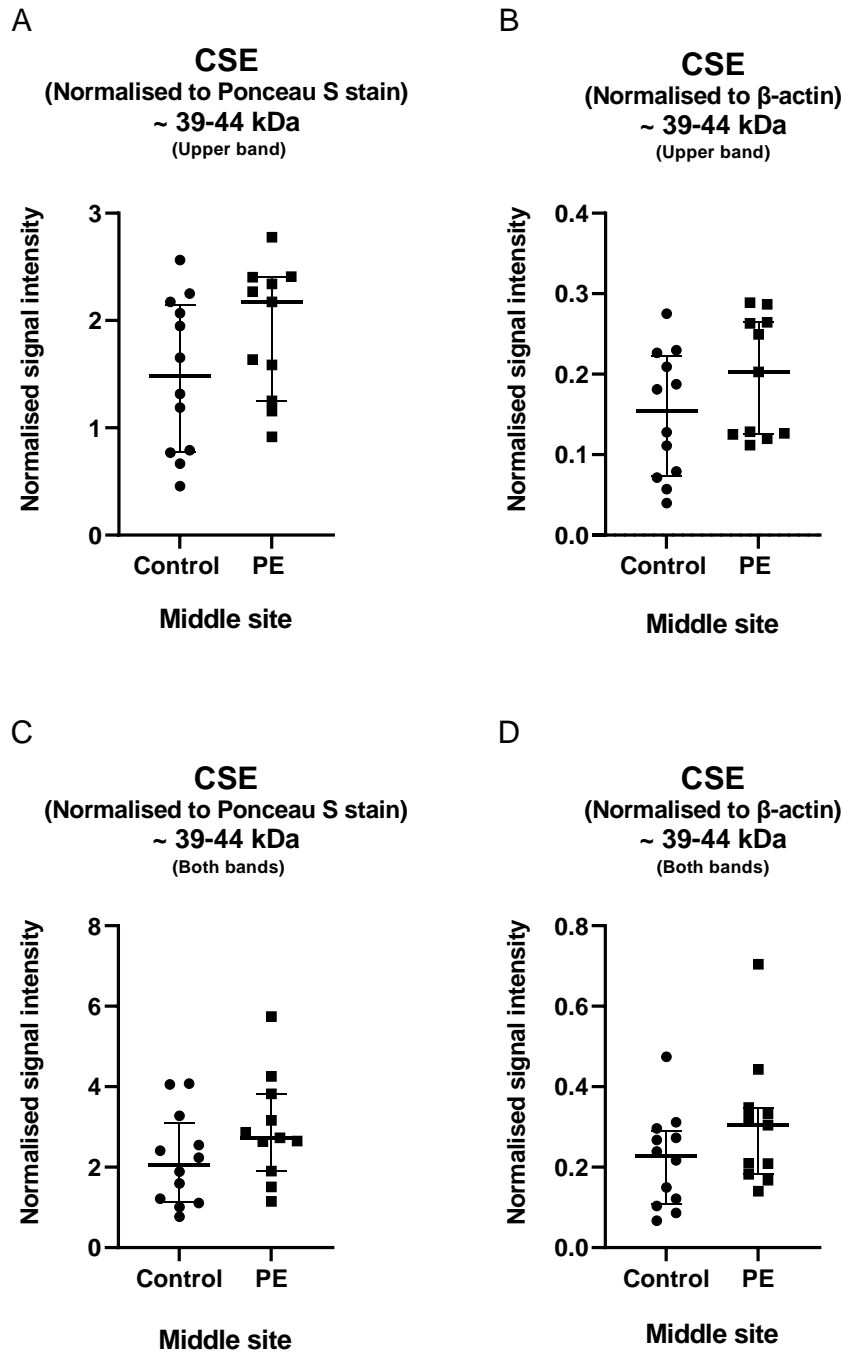**Figure 6-17 Quantitative western blot analysis of CSE protein in placentas from pregnancies complicated with PE. (A & C) Normalised CSE (~ 39-44kDa upper band/ both bands) signal intensity to signal intensity generated from Ponceau S stain. (B & D) Normalised CSE (~ 39-44 kDa bands) signal intensity to β-actin signal intensity. Data are presented as median and interquartile range. Comparison between groups was performed using Mann Whitney test.**

6.4 Discussion

In all comparison groups except one, both normalisation approaches were consistent with each other increasing confidence in the findings. The reason for the one inconsistency (Figure 6-7) was a single data point which showed deviation in the Ponceau S stain: β-actin ratio in comparison to the other data points and may have been the result of saturation of the Ponceau S stain signal giving an artefactually lower reading and thereby increasing the 3-MST normalised value. Demonstrable measurement errors justify exclusion of such outliers and when removed, the two methods of normalisation gave consistent results for this analysis (Figure 6-8). Overall, the western blots of 3-MST in FGR and CSE in labour group gave results consistent with changes in mRNA found by qPCR and the results of western blots of 3-MST in labour and CBS and CSE in PE showed no change in protein abundance.

The current study showed that CSE protein abundance was significantly increased in placentas from women who delivered spontaneously compared to those who were not in labour ($p = 0.04$ when signal intensities normalised to Ponceau stain, and $p = 0.02$ when signal intensities normalised to β-actin). This result supports the qPCR analysis in chapter 3 (Figure 3-6E). The present study also displayed that in pregnancies complicated with FGR, the protein level of 3-MST was significantly increased at the outer placental site when compared to healthy pregnancies. This comes in the same direction with the qPCR data of the same group. These significant increases in proteins are most simply explained by the up-regulation in mRNA level which may be due to oxidative stress occurring during labour and also in pathological pregnancies. Labour is a complex process involving different inflammatory and apoptotic pathways that are linked to oxidative stress which would be expected to cause alteration of placental gene expression of many genes such as genes involved in stress response and development of blood vessels (Lee et al., 2010). It is known that oxidative stress increases nuclear factor kappa B which is a protein transcription factor that targets inflammation by increasing the production of inflammatory cytokines. It also activates nitric oxide synthase, nitric oxide release and subsequently increases CSE activity and H_2S production in a cGMP-dependent manner (Zhao et al., 2003). The higher expression of 3-MST in FGR placentas ($p = 0.002$) may be to increase H_2S production in placental villi exposed to hypoxia resulting in oxidative stress. Then, the H_2S could act as a vasodilator by relaxing of vascular smooth muscles and could act in attempt to inhibit the oxidant attack. Also, H_2S is a cytoprotectant rescuing placental cells from oxidative stress mainly by enhancing the cellular production of glutathione, a major endogenous antioxidant, and also redistributing of glutathione to mitochondria, preserving mitochondrial function (Kimura et

al., 2010). To explore the up-regulations in CSE and 3-MST expression found here, a high-powered study with larger sample size could be used and measurements of enzyme activity also taken to compare with the levels of mRNA and protein. Also, in situ methods such as IHC on placental section could be useful in detecting and quantifying the protein abundances in intact placental tissues. This is because in western blotting proteins are extracted from homogenised tissue which could mask spatial variation in protein abundances between cells/different placental tissues that does not amount to a change in total protein abundance.

Furthermore, the current study showed that 3-MST protein abundance in labour group (Figure6-4) and CBS and CSE protein abundances in PE groups (Figure 6-11 and 6-17) in comparison to the controls did not show significant differences despite differences having been recorded in mRNA levels. Such discrepancy in mRNA and protein abundances was previously reported for CSE: You et al. (2011) reported a reduction in CSE mRNA abundance in labouring myometrium and no change in protein abundance (see Table 1-1). Also, Holwerda et al. (2012), who investigated expression of CBS and CSE, in normal pregnancy and pregnancies presented with PE, did not detect any significant differences in CBS and CSE protein expression between PE groups and their controls even though CBS mRNA was significantly decreased (see Table 1-1). In contrast to the data shown here, Hu et al. (2015), who performed only western blotting to investigate expression of CBS and CSE in PE, reported that both CBS and CSE protein levels were significantly down-regulated in pre-eclamptic placentas compared with those in healthy placentas. This discrepancy might be explained by the difference in the severity of PE cases included in the two studies. Most of the subjects included in this study were diagnosed with late-onset PE.

In this study, the inconsistency between mRNA and protein levels may be explained regulatory mechanisms already discussed in chapter 3 and in section 6.1.1. A further complication with CBS protein analysis might arise from a combination of the method of protein extraction used in this study (which is widely used in placental research (Lyall et al., 2000, Lyall et al., 2001)) that extracts mainly cytoplasmic proteins. This gives cleaner protein preparations without DNA contamination but omits nuclear proteins. Since CBS protein shuttles between nuclear and cytoplasmic compartment due to post-translational modifications its possible nuclear CBS could be lost in the pellet after extraction of the lysate, affecting the protein abundance.

6.5 Conclusion

The obtained western blot data were precisely normalised using two loading controls and the data analysis showed consistency in results between both normalisation approaches most of the time. However, this work also showed how even small errors in internal control measurements can affect results and conclusions. Overall, the western blot analyses have revealed that CSE and 3-MST proteins were differentially expressed, at particular placental sites in labour and complicated pregnancies. The data also showed that in some groups the protein abundance was not positively correlated to transcript abundance, suggesting possibility of post-transcriptional or post-translation regulations of proteins. However, further exploration of protein expression using other techniques such as in situ hybridization (IHC) was worth consideration. It is obvious that the signalling and regulatory pathways for expression and/or regulation of CBS, CSE and 3-MST/H_2S system in labour and pathological conditions are dynamic and complicated. Therefore, further exploration into the regulation and feedback of CBS, CSE and 3-MST is critical to fully understand their functions in the placenta.

Chapter 7   Use of the CRISPR knockout clones to test feasibility of *in situ* methods and to further explore molecular biology of CBS, CSE and 3-MST genes.

This chapter details further use of the CRISPR knockout clones to evaluate the usefulness of *in situ* with the currently available antibodies for CBS and CSE and also to explore interactions between the three H_2S generating enzymes and effects on mitochondrial biology.

7.1 Validating accuracy of *in situ* IHC on placental sections.

Even healthy placentas can show extensive variation in structure and cells composition, localised areas of pathology and the syncytia structure. Each cell type has a unique epigenetic and gene expression profile (Hogg et al., 2014). Even though western blotting is the most accepted and commonly used approach for detecting protein abundance in different extracts and can also provide quantitative data about the target protein it can miss spatial variation in gene expression that does not result in an overall change in gene expression. Immunocytochemistry, IF and IHC are three closely related methods that also use antibodies raised to the proteins of interest to examine levels of proteins in fixed cells or tissues. At the very beginning of this PhD project, on instruction from the supervising academic at that time, an extensive series of IHC to examine the expression of CBS and CSE proteins was carried out using placentas sections from normal heathy pregnancies and pregnancies complicated with PE, FGR and high BMI. These were the same placental samples that would be used for the qPCR and western blot analysis already described in chapters 3 and 6.   A large number of placental tissues slides were stained and scanned using SlidePath digital image for histoscore and analysis (Appendix 3).   However, subsequent use of different anti-CBS and CSE antibodies in western blots that revealed multiple bands and non-specific binding (chapter 4) raised concerns about validity of the IHC data. Although different anti-CBS and CSE antibodies were used in IHC, it was a concern that these might also have non-specific binding activity. In fact, non-specific binding should be an even greater concern for *in situ* methods compared to western blots because *in situ* methods do not have the additional measurement of MW that westerns have to aid checking of specificity.

As already discussed, the generation of knockout clones by CRISPR is a valuable tool for testing antibody specificity therefore 20 µg of protein from a normal placental sample, WT BeWo cells, CBS knockout BeWo clones (C1, C2 and C5) or CSE knockout BeWo clones (C7, C10 and C11) was loaded into a 4-12% Tri-Bis gel run in MES buffer, blotted then immunodetection with the anti-CBS (Abcam, cat.no. ab54883) or anti-CSE (Abcam, cat. no. ab54573) antibodies already used in IHC was performed. This (Figure 7-1) showed that these antibodies bound to CBS and CSE proteins specifically, but, as with the other antibodies, they also non-specifically bound to some unknown proteins in the samples confirming suspicions that these antibodies may have problems of non-specificity.
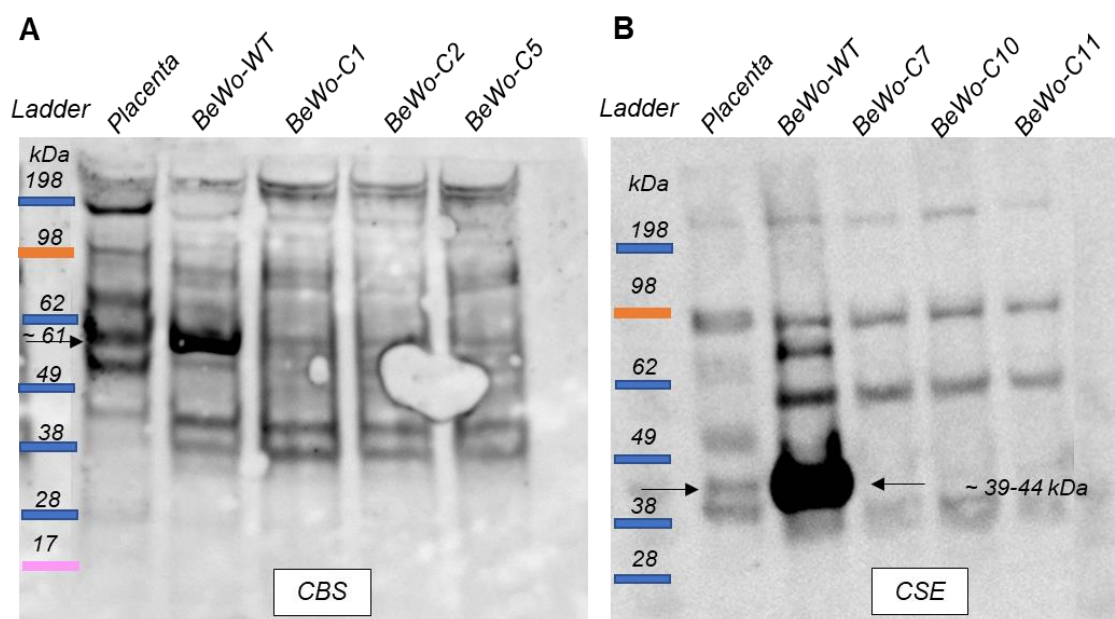
Figure 7-1 Western blotting of placental tissue, WT BeWo cells, CBS and CSE knockout BeWo clones with anti-CBS and CSE antibodies. 20 µg of protein lysates were loaded into a 4-12% Tri-Bis gel with MES running buffer. (A) Immunoblotting of placental tissue, WT BeWo cells and CBS knockout clones with anti-CBS antibody. Lane 1: Molecular ladder, lane2: Placental lysate, lane 3: BeWo-WT lysate and lane 4-6: CBS knockout BeWo-C1, C2 and C5 lysates. (B) Immunoblotting of placental tissue, WT BeWo cells and CSE knockout clones with anti-CSE antibody. Lane 1: Molecular ladder, lane2: placental lysate, lane 3: BeWo-WT lysate and lane 4-6: CSE knockout BeWo-C7, C10 and C11 lysates. The black arrows refer to the predicted MW (~ 61kDa) of CBS and (~ 39-44 kDa) of CSE.

However, it is not necessarily the case that these antibodies would also have the non-specific binding when used with *in situ* methods because the way the proteins are presented in western blotting and *in situ* methods is different although the principle of detection is more or less the same. The denaturation of proteins samples prior to SDS-PAGE and binding to a nitrocellulose membrane in western blotting could present a very different array of non-specific binding sites to the antibody compared to proteins fixed within cells in *in situ* methods where proteins are most likely in near native conformation. Thus, the non-specific

binding of an antibody in western blot does not mean this antibody will behave the same way in a *in situ* method, although it certainly raises the possibility.

Again, the CBS knockout clone (C2) and CSE knockout clone (C7) were used to test non-specificity on antibodies but this time in BeWo cells fixed in the same way as the placental sections had been (Appendix 3) to present the antigen in as much as the same way as possible. As for western blots, a no-primary control to test for non-specific binding of secondary antibody was also carried out. Also, for all comparative fluorescence images, only images taken with identical exposure times were compared and displayed with identical brightness and contrast settings (Figure 7-2).
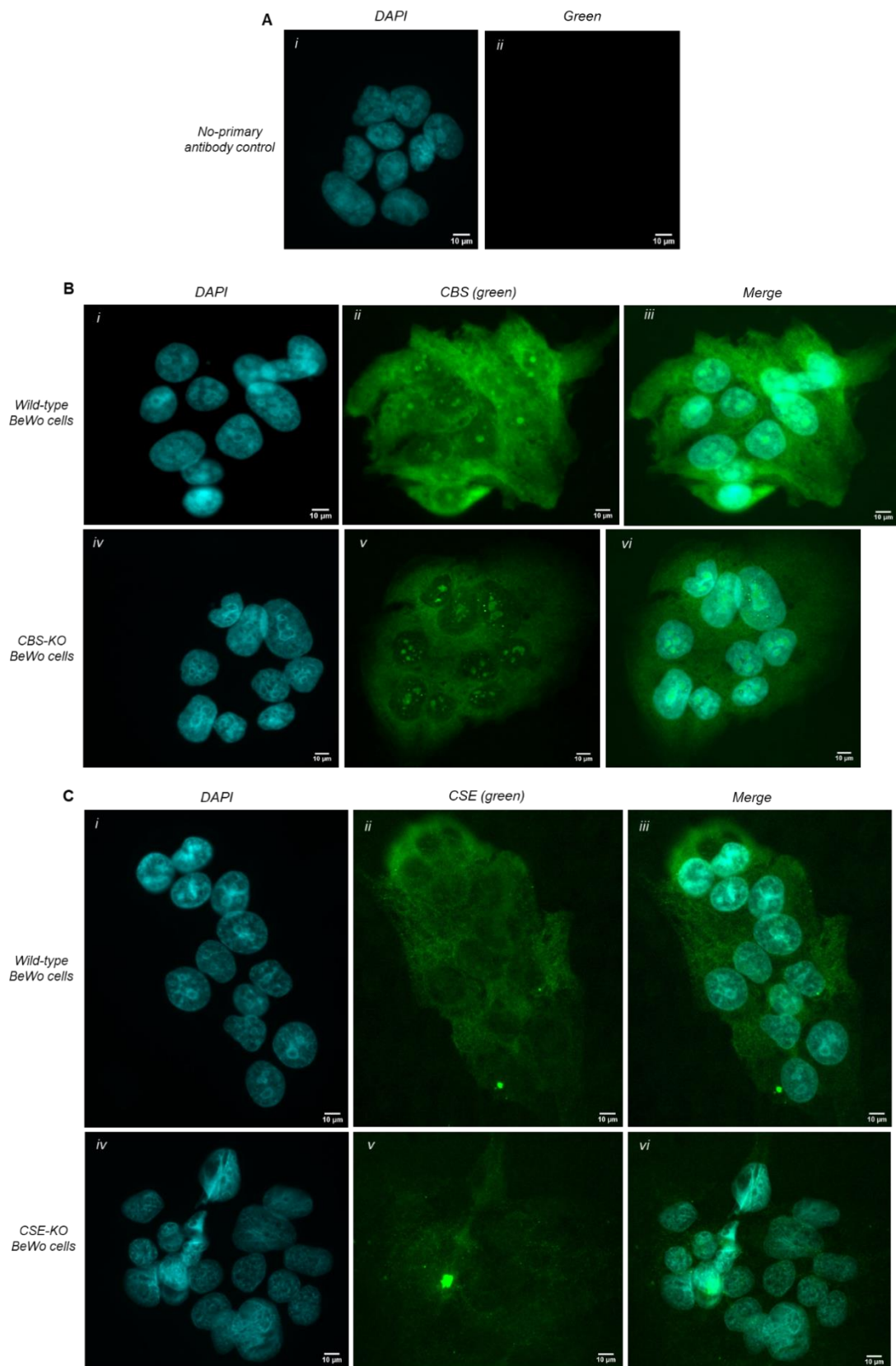
Figure 7-2 Immunofluorescence images showing CBS and CSE staining in WT BeWo cells, CBS and CSE knockout BeWo cells. (A) A negative control with no primary antibody and only a secondary antibody. DAPI staining (cyan) (i) and green fluorescence (ii). (B) CBS immunostaining in WT and CBS knockout BeWo cells. (C) CSE immunostaining in WT and CSE knockout BeWo cells. DAPI staining (i & iv in B & C), green fluorescence (ii &v in B & C) and merged images showing a combination of both DAPI and green fluorescence (iii &vi in B&C). Images were captured using a 400x epifluorescence microscope using same exposure time and are shown with the same brightness and contrast. Scale bars are 10 μm in all shown images.

The no-primary antibody control showed no detectable signal on the same channel as the other images, indicating no background signal from the secondary antibody. Both CBS and CSE immunofluorescences of the WT and knockout clones showed fluorescence signals in both WT and knockout BeWo controls. The signal in knockout clones was not quite as much as in the WT, suggesting there was both specific and non-specific binding to proteins. Because IHC has also lower signal: noise properties compared to fluorescence methods the large data set of already completed IHCs was deemed unreliable and has only been included in an appendix. The technology for generating the knockouts was not available at the beginning of this project.

Although the anti-3MST antibody showed much greater specificity for binding the target protein in the western blot (Figure 4-10), its specificity was not tested with the 3-MST knockout BeWo cultured cells in the same way because during the lockdown the placental tissue slides that would be needed for subsequent IHC were accidently discarded by laboratory staff after a freezer breakdown. This would have been a good thing to explore since the comparative western blot data in chapter 6 showed some significant changes in abundance of 3-MST protein and mRNA in the same direction in pregnancies complicated with FGR.

7.2 Crosstalk or feedback regulation of H_2S synthesising enzymes

The existence of all three H_2S synthesizing enzymes in cells makes understanding their relative contribution to H_2S production a challenge but also raises the question of how each affects the other. All three share intermediates to some extent (Figure1-5). CBS and CSE produce H_2S via transsulfuration pathway which is the only route for cysteine biosynthesis, while 3-MST synthesises H_2S by via cysteine oxidation. Although CBS and CSE are cytoplasmic enzymes and 3-MST synthesises H_2S inside the mitochondria, CBS and CSE proteins can be subjected to re-localisation to mitochondria increasing the likelihood of cross-talk. CBS protein was shown recently to be present in mitochondria of ovarian cancer (Bhattacharyya et al., 2013) and colon cancer cells (Szabo et al., 2013). Teng et al. (2013) found that under normoxia conditions CBS protein was present in rats' liver mitochondria at low level, however, its level increased after liver ischemia. Also, the accumulated CBS proteins were rapidly return to basal levels after reperfusion of the liver for 10 minutes. In addition to this, Teng et al. (2013) reported that the ischemia-reperfusion injury did not affect level of CBS proteins in cytosolic fractions or the whole tissue homogenate of rat liver.

Degradation and accumulation of CBS proteins in mitochondria were explained by presence of Lon protease which is a major proteolytic enzyme in mitochondria matrix. The Lon protease recognised and degraded CBS by specifically targeting at the oxygenated heme group of CBS proteins, and hypoxia leads to deoxygenation related conformational changes of the heme so that CBS cannot be recognised and degraded by Lon protease. CSE proteins have also been reported to present in mitochondria. Fu et al. (2012), demonstrated that in mice's smooth muscle cells, CSE can translocate from cytosol to the mitochondria under conditions of cellular stress, such as increases in intracellular Ca^{2+} level. CSE is considered as the major H_2S synthesising enzyme in cardiovascular system and its translocation to mitochondria is to promote H_2S production which subsequently sustains mitochondrial ATP production under hypoxic conditions. Then, CBS and CSE protein are co-localised into mitochondria under oxidative stress to maintain cellular health by regulating the redox balance and mitochondrial energy production. Similarly, 3-MST enzyme in mitochondria is regulated by its redox-sensitive status. Since CBS and CSE employ various combinations of the same substrates in their H_2S-generating reactions, regulation of one enzyme may affect the other, due to increased or decreased substrate availability.

Some feedback mechanisms between CBS, CSE and substrates of transslufuration pathway have recently been found. Nandi and Mishra (2017), showed that increasing levels of H_2S can decrease expression of CSE protein in mouse cardiomyocytes by inhibiting SP1 activation and CSE transcription. However, they showed that increasing homocysteine level increases the expression of CSE. Moreover, an opposite effect on CBS expression has been reported, where increasing H_2S and homocysteine levels result in increasing and decreasing CBS expression, respectively. Clearly, homocysteine down-regulates CBS but up-regulates CSE whereas H_2S donor up-regulates CBS but down-regulates CSE. This indicted that when CBS is up-regulated CSE is down-regulated. Therefore, Nandi and Mishra (2017) used CBS deficient mice and controls to investigate effect of CBS deficiency on CSE expression. They measured both CBS and CSE mRNA and protein levels and found that in CBS deficient mice CBS expression was decreased in heart but CSE expression was increased as compared to the control mice. They also found that the SP1 activity was increased in CBS deficient mice, thereby up-regulating CSE. Their results revealed a negative feedback regulation of CBS and CSE in cardiomyocytes. Additionally, Wang et al. (2009) suggested an inverse correlation between CSE mRNA expression and H_2S level in mice's aorta which may be a consequence of a positive feedback mechanism in which decreased H_2S production is compensated for by increased CSE gene expression.

Overall, it is emerging that expression of H_2S synthesising enzymes and their activity and H_2S synthesis are controlled by a complex integration of multiple mechanisms and further exploration into regulation and feedback of CBS, CSE and 3-MST is required. The generation of knockout clones of each in BeWo cells provided an opportunity to explore the effects of the absence of each H_2S synthesising enzyme on protein abundance of the others. Furthermore, this could be done with relevance to the placenta because BeWo cells are accepted as a valid model to study trophoblasts physiology and function.

7.2.1 Results and discussion

7.2.1.1 Expression of CSE and 3-MST in absence of CBS

Three CBS knockout BeWo clones (C1, C2 and C5) were used in this model alongside a WT control sample (BeWo-WT cells). 20 µg of protein was loaded into a 4-12% Tri-Bis gel. Firstly, immunodetection with anti-CBS antibody was performed to re-confirm the absence of CBS then immunodetection with anti-CSE, 3-MST and β-actin antibodies were carried out. The β-actin was used as a sample loading control and for normalisation. This was carried out three separate times; a single representative western blot (probed four times) is shown in Figure 7-3. The signal intensities of CBS, CSE and 3-MST were normalised to the intensity of β-actin after subtracting the background. Then, the abundance of CBS, CSE and 3-MST in clones was calculated relative to the WT control.
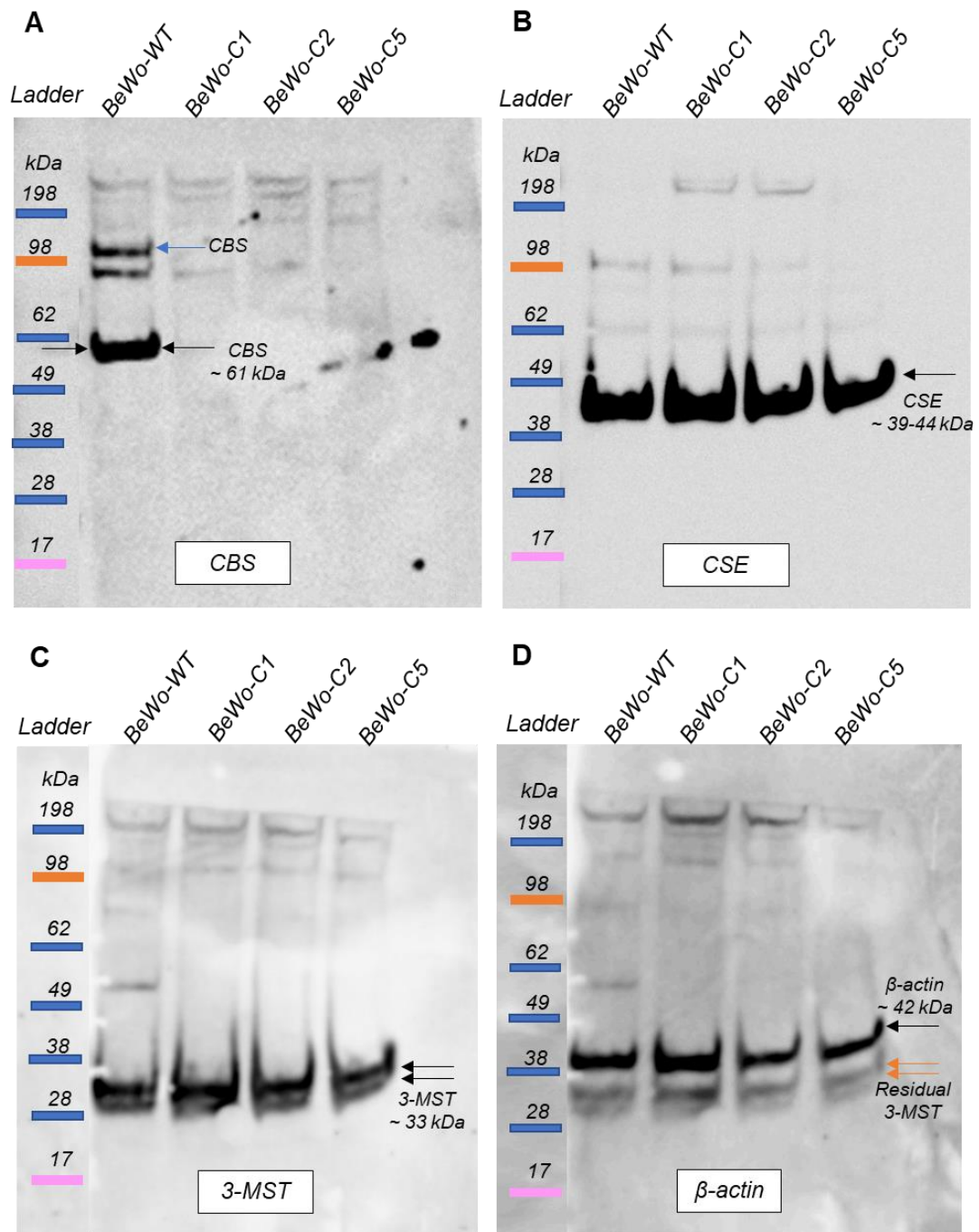
Figure 7-3 Representative western blots of CBS, CSE, 3-MST and β-actin antibodies in WT and CBS knockout BeWo cells. (A, B, C and D) show immunoblotting with anti-CBS, CSE, 3-MST and β-actin antibodies, respectively. Lane 1: the molecular ladder, lane 2: BeWo-WT lysate and lanes 3-5: BeWo-C1, C2 and C5 lysates, respectively. The black arrows refer to the apparent MW of each protein. The blue arrow in (A) refers to the other expected CBS band and the red arrows in (D) refer to the residual 3-MST from the previous probing with anti-3-MST antibody.

Mean (of three independent blots) normalised (relative to β-actin) expression of each protein relative to wild type (set as 1) is displayed in Figure 7-4. CBS knockout BeWo clones (C1, C2 and C5) were not expressing CBS protein: the reduction in protein abundance relative to the WT control was by 99% ($p < 0.05$). However, there were not any significant differences in CSE and 3-MST protein abundances in these clones relative to the WT BeWo control.
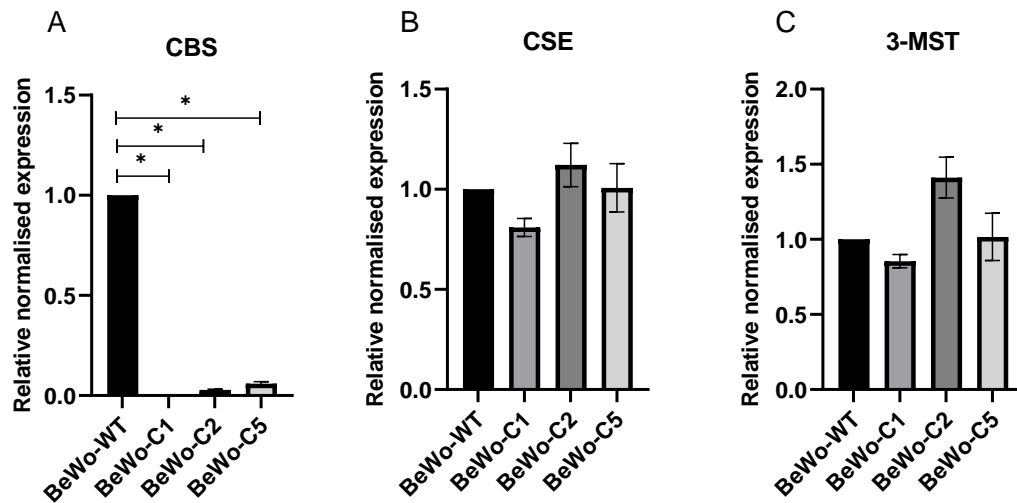
Figure 7-4 CBS, CSE and 3-MST protein abundances in CBS knockout clones. Graphs A, B and C represent the CBS, CSE and 3-MST protein abundance in CBS knockout clones relative to the WT control, respectively. The mean of the normalised intensities proportional to WT was plotted for each sample on a bar graph. Error bars indicates the standard deviation for the three measurements. The statistical significance was determined by using _t_-test, with significance level < 0.05. The control sample is indicated by a black bar. (*) means _p_ < 0.05.

7.2.1.2 Expression of CBS and 3-MST in absence of CSE

Three CSE knockout BeWo clones (C7, C10 and C11) were used alongside a WT control (BeWo-WT cells) and WT-puromycin-resistant clone (BeWo-C12). 20 μg of protein was loaded into a 4-12% Tri-Bis gel. Firstly, immunodetection with anti-CSE antibody was performed to re-confirm absence of CSE then subsequently immunodetection with anti-CBS, 3-MST and β-actin antibodies were carried out. This was carried out three separate times; a single representative western blot (probed four times) is shown in Figure 7-5.
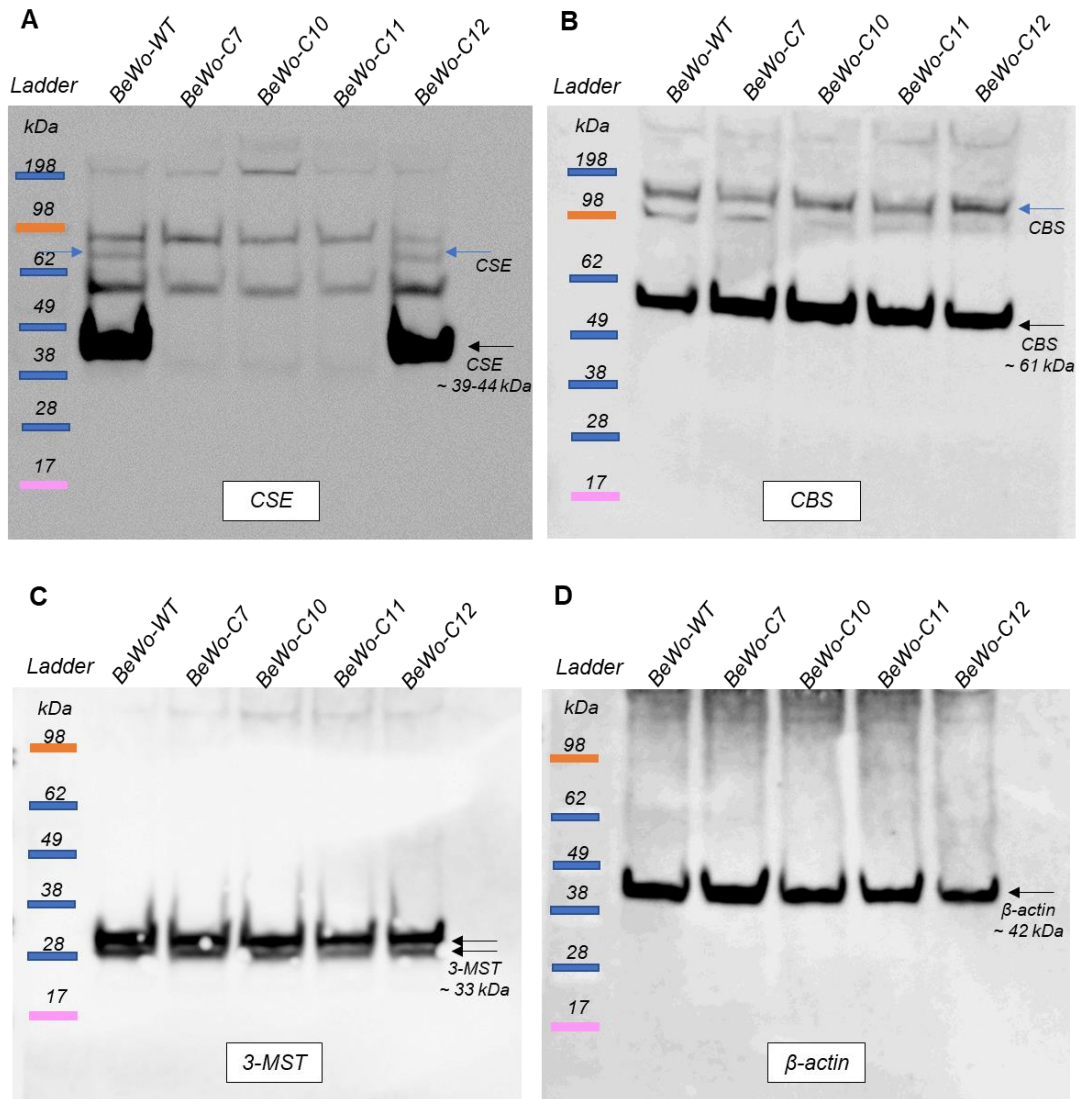
Figure 7-5 Representative western blots of CBS, CSE, 3-MST and β-actin in WT and CSE knockout BeWo cells. (A, B, C and D) show immunoblotting with anti-CSE, CBS, 3-MST and β-actin antibodies, respectively. Lane 1: the molecular ladder, lane 2: BeWo-WT lysate and lanes 3-6: BeWo-C7, C10, C11 and C12 lysates, respectively. The black arrows refer to the apparent MW of each protein. The blue arrows refer to the other expected CSE and CBS bands.

Mean (of three independent blots) normalised (relative to β-actin) expression of each protein relative to wild type (set as 1) is in Figure 7-6. There was a reduction in CSE protein abundance by 99% in CSE knockout BeWo clones (C7, C10 and C11) ($p = 0.01$). The CSE protein abundance in CSE puromycin-resistant clone (BeWo-C12) was not significantly different relative to WT control. There was no statistically significant difference in the abundance of CBS and 3-MST proteins in the absence of CSE protein.
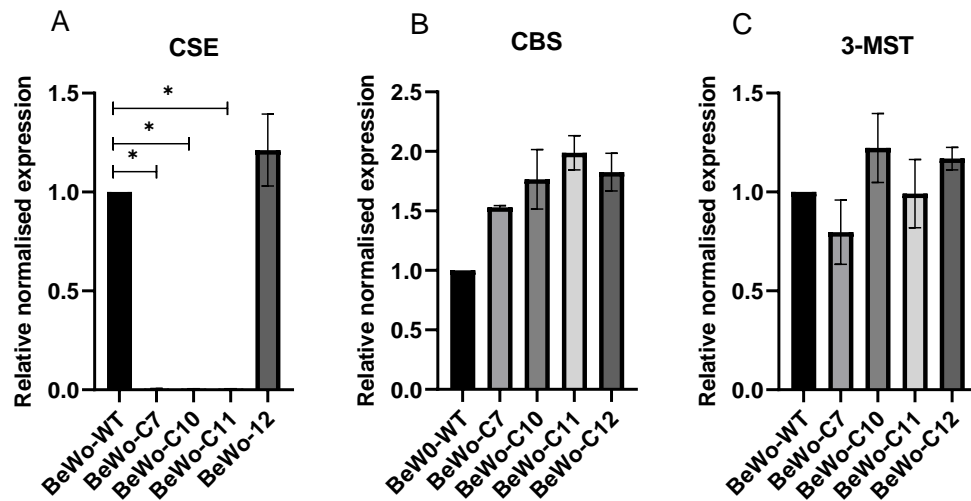
Figure 7-6 CBS, CSE and 3-MST protein abundances in CSE knockout clones. Graphs A, B and C represent the CSE, CBS and 3-MST protein abundance in CSE knockout clones relative to the WT control, respectively. The mean of the normalised intensities proportional to WT was plotted for each sample on a bar graph. Error bars indicates the standard deviation for the three measurements. The statistical significance was determined by using *t*-test, with significance level < 0.05. The control sample is indicated by a black bar. (*) means p < 0.05.

7.2.1.3 Expression of CBS and CSE in absence of 3-MST

The only 3-MST-knockout BeWo clone (C6) was used alongside a WT control (BeWo-WT) cells and WT-puromycin resistant clones (BeWo-C2 and C8). 20 µg of protein was loaded into a 4-12% Tri-Bis gel. Initially, immunodetection with anti-3-MST antibody was performed to re-confirm absence of 3-MST in C6. Then, subsequently immunodetection with anti-CBS, CSE and β-actin antibodies were carried out. This was carried out three separate times; a single representative western blot (probed four times) is shown in Figure 7-7.
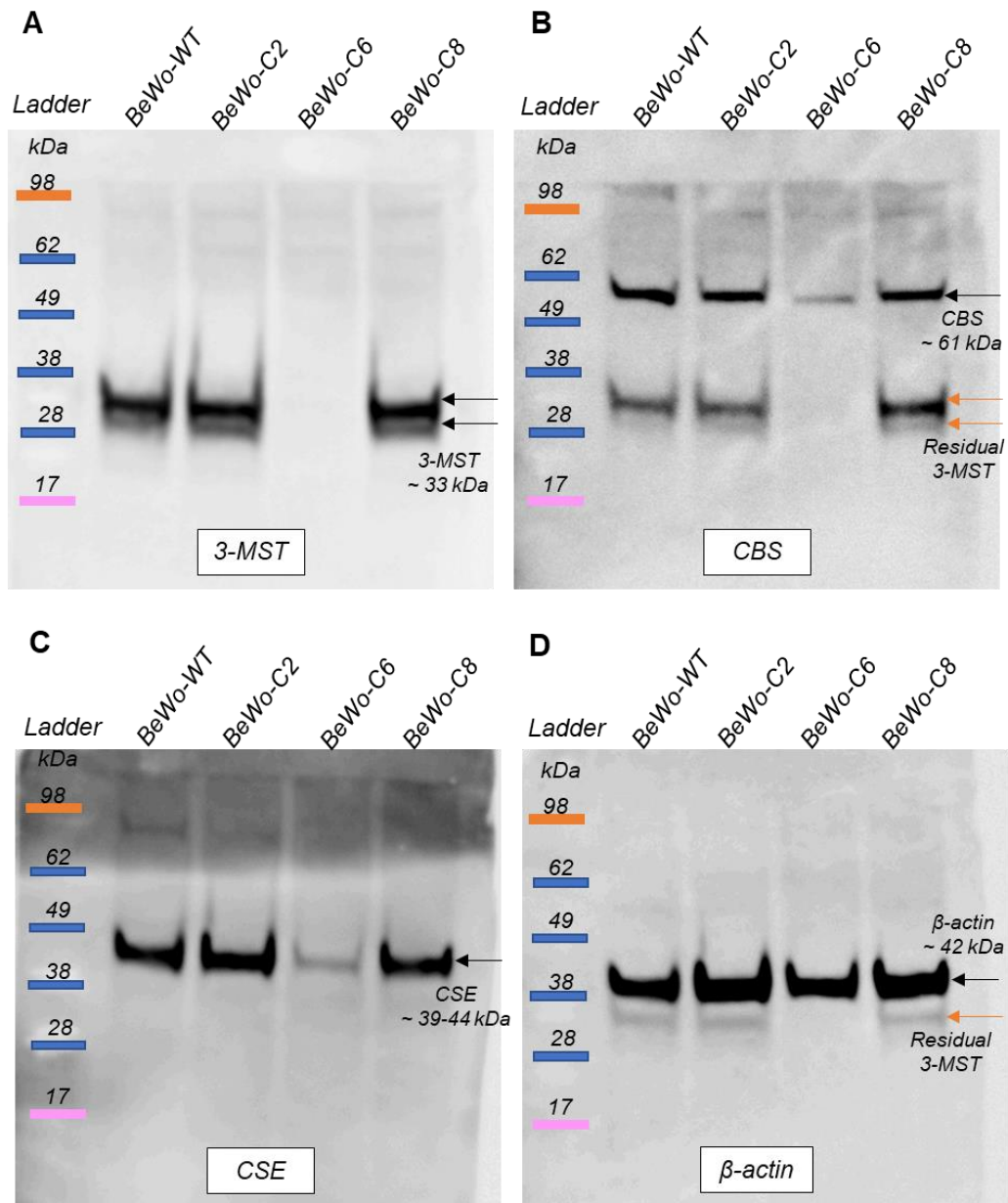
Figure 7-7 Representative western blots of CBS, CSE, 3-MST and β-actin in WT and 3-MST knockout BeWo cells. (A, B, C and D) show immunoblotting with anti-3-MST, CBS, CSE and β-actin antibodies, respectively. Lane 1: the molecular ladder, lane 2: BeWo-WT lysate and lanes 3-5 represent BeWo-C2, C6 and C8 lysates, respectively. The black arrows refer to the apparent MW of each protein. The red arrows in (B and D) refer to the residual 3-MST from the previous probing with anti-3-MST antibody.

Mean (of three independent blots) normalised (relative to β-actin) expression of each protein relative to wild type (set as 1) is in Figure 7-8. The 3-MST protein abundance was reduced by 96% in 3-MST knockout BeWo clone C6 ($p = 0.001$). There was a significant decrease in both CBS ($p = 0.04$) and CSE ($p = 0.001$) protein abundances in C6 3-MST Knockout clone relative to WT control. The variability between the replicates in these analyses was low (CV = 7% and 11%, respectively).
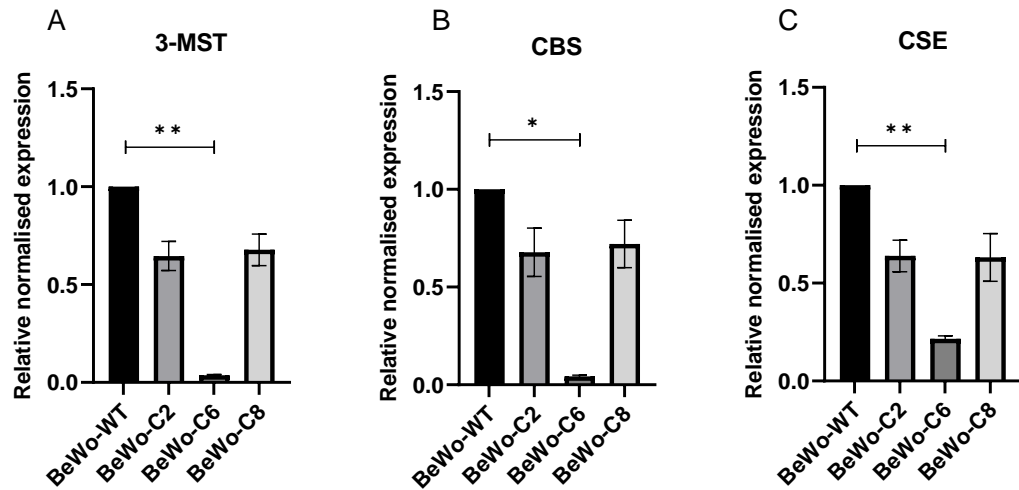
Figure 7-8 CBS, CSE and 3-MST protein abundances in 3-MST knockout clone. Graphs A, B and C represent the 3-MST, CBS and CSE proteins abundance in 3-MST clones relative to the WT control, respectively. The mean of the normalised intensities proportional to WT was plotted for each sample on a bar graph. Error bars indicates the standard deviation for the three measurements. The statistical significance was determined by using _t_-test, with significance level < 0.05. The control sample is indicated by a black bar. (*) means p < 0.05 and (**) means p < 0.01.

The data generated from the knockout BeWo models showed that the abundance of the target proteins in knockout clones of the same protein type was near zero relative to the control sample. This was consistent with the ICE analysis of PCR amplified 3-MST DNA from this clone (chapter 5). The WT-puromycin resistant clones such as CSE BeWo-C12 and 3-MST BeWo-C2 and C8 were also included as (positive controls). Although both C2 and C8 had slightly reduced 3-MST compared to WT, the CBS and CSE protein abundances were not-significantly different in these relative to WT control.

Because only one 3-MST knockout clone was obtained it is possible that the reduction in CBS and CSE abundances in 3-MST knockout clone is due to particular off-target effects of the CRISPR mutagenesis in this clone. This however seems unlikely to explain the reduction in both CBS and CSE abundances because it would be highly unlikely to have simultaneous off-target effects in two biochemically related, but genetically unrelated sequences (i.e. CBS and CSE) at the same time. More likely the possibility is that there might be a crosstalk between CBS, CSE and 3-MST, in which deficiency of the latter may control the expression of the first two. 3-MST generates H_2S and pyruvate through the breakdown of cysteine in a two steps manner. Therefore, absence of 3-MST enzyme could result in accumulation of cysteine which in turn could negatively affect CBS and CSE enzymes. It has reported that reducing 3-MST activity under mild oxidative conditions results in an increase in cysteine concentrations _in vitro_ (Yadav et al., 2013). An important experiment to test this would be

re-expression of WT 3-MST protein in the knockout C6 (i.e. a rescue experiment using e.g. plasmid containing the WT 3-MST gene) and subsequently investigating the CBS and CSE protein abundances. Additionally, more CRISPR knockout experiments to obtain more, independent 3-MST knockout clones should be carried out and then tested to see if CBS and CSE abundances are reduced in them as independent knockout clones would likely have different off-target mutations. 3-MST is the main H_2S producer in mitochondria which enhances mitochondrial electron transport and cellular biogenesis (Módis et al., 2013) and also acts as cytoprotective from oxidative stress by enhancing glutathione production and preserving mitochondrial function (Elrod et al., 2007). The fact that the C6 clone also had reduced CSE and CBS expression suggested it could be severely compromised in H_2S production, especially in mitochondria. Therefore, it was thought worth investigating general aspects of mitochondrial biology in clone C6 (the following section).

7.3 Phenotype Characterisation of 3-MST knockout clone/ assessing mitochondrial biology

Mitochondria are considered one of primary targets of H_2S signalling. H_2S plays an antiapoptotic role by inhibiting the proapoptotic mitogen activated protein kinase (MAPK) pathway, which is mediated by activation of mitochondrial K_{ATP} channels as shown *in vitro* in neuroblastoma cell line (Hu et al., 2009). H_2S has been found to inhibit ROS generation, supress the phosphorylation of MAPKs and decrease apoptosis (Zhang et al., 2018). Also, persulfidation of mitochondrial ATP5A1 at Cys^{244} induce resistance to mitochondrion-mediated apoptosis induced by lipopolysaccharides (LPS) in adrenal glands of mice (Wang et al., 2018). Vitvitsky et al. (2018) suggest that oxidation of H_2S by cytochrome c when released into the cytoplasm can propagate the persulfidation of nearby target proteins, such as procaspase 9 resulting in its inhibition and consequential inhibition of the caspase cascade and mitochondrion-dependent apoptosis.

The generation of new mitochondria is also regulated by H_2S through increasing transcription of nuclear-encoded mitochondrial proteins (Johri et al., 2013). Furthermore, H_2S has been reported to impact mitochondria morphogenesis. It decreases mitochondrial fragmentation in endothelial cells in a high-glucose environment by reducing levels of phosphorylated dynamin-related protein, and this in turn prevented ROS accumulation and apoptosis (Liu et al., 2017). Moreover, H_2S donor, NaHS, has been shown inhibiting mitochondrial fission in a dose-and time-dependent manner *in vitro* in mouse neuroblastoma cells (Qiao et al., 2017). Chakraborty et al. (2018) has also reported that CBS regulates

mitochondrial morphogenesis in ovarian cancer, and that CBS-dependent H_2S promotes mitochondrial fusion by selectively regulating the stability of mitofusin 2 in a redox-sensitive manner in ovarian cancer cells. So, absence of 3-MST in C6 ought to decrease H_2S production in mitochondria thereby affecting the mitochondrial biology and function. This suggestion requires further assessing for the mitochondrial biology. As the first part of such an investigation, the number of mitochondria and the level of mitochondrial translation were measured in normally growing BeWo cells (WT vs C6). For the former, IF detection of the mitochondrion-specific marker, mitochondrion-encoded cytochrome oxidase 1 protein (MTCO1) and quantification of fluorescence was used. This protein is encoded by mitochondrial DNA and is an essential component of the oxidative phosphorylation pathway. For measuring mitochondrial translation, labelling with an alkyne-modified amino acid analogue of Met, HPG (Zhang et al., 2014) in the presence of CHI was used. Subsequent click chemistry in which the alkyne group is specifically coupled to a fluorescently labelled azide allows HPG-labelled proteins to be visualised and to comparatively quantify mitochondrial translation between WT and C6 BeWo cells.

7.3.1 Results and discussion

7.3.1.1 Expression of MTCO1 in 3-MST knockout BeWo cells (C6)

WT and 3-MST knockout BeWo cells were used to assess expression of the specific mitochondrial marker using immunofluorescence staining with anti-MTCO1 antibody. Representative images of the mitochondrial immunofluorescence staining with anti-MTCO1 in both WT and C6 3-MST knockout BeWo cells along with no-primary negative control are shown in Figure 7-9. The no-primary antibody control showed no detectable signal on the same channel as the other images, indicating no background binding of the secondary antibody. The green fluorescence intensities of MTCO1 in both WT and 3-MST knockout BeWo cells were quantified using Image J software and normalised to DAPI staining. The normalised fluorescence intensities in both groups were compared and the data analysis was presented in Figure 7-9D which showed that the mean fluorescence signal of MTCO1 was not significantly different between WT and 3-MST-knockout BeWo cells ($p = 0.7$) and indicating there was not change in mitochondrial number in absence of 3-MST in normally cultured cells.
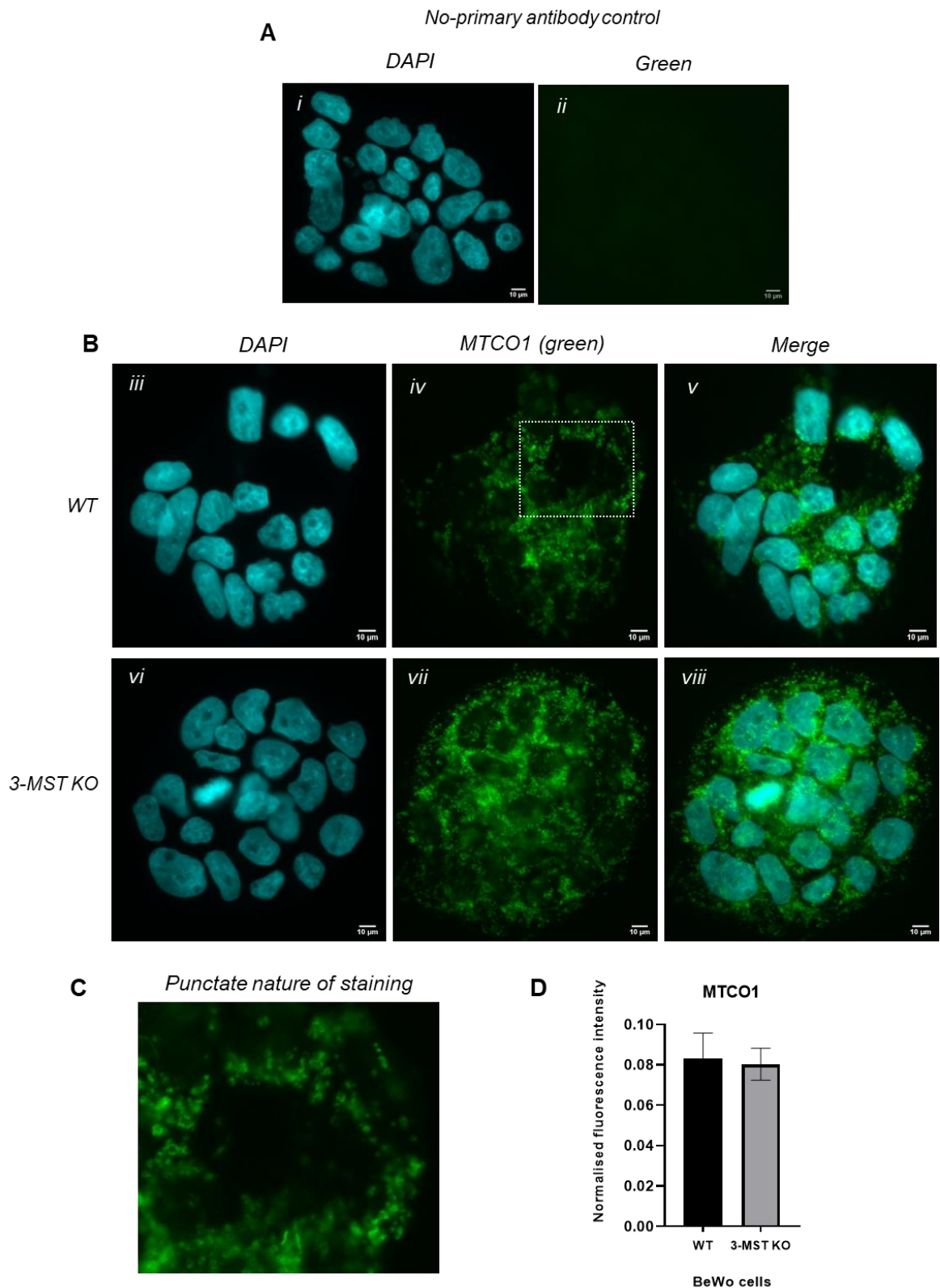
Figure 7-9 Representative immunofluorescence images showing MTCO1 staining in WT and 3-MST knockout BeWo cells. (A) A negative (no-primary antibody) control. (B) MTCO1 IF detection. DNA was detected by DAPI staining (i, iii and vi) and MTCO1 protein was detected by green fluorescence (ii, iv and vii). Merged images of both DAPI and green fluorescence are shown in (v, viii). DAPI exposure time was for 20 ms and green fluorescence exposure time was for 1000 ms. Scale bars are10 μm in all shown images. (C) A zoomed-in image of the squared area in (iv) showing the punctate nature of mitochondrial staining. (D) A graph of MTCO1 fluorescence intensity in WT and 3-MST knockout BeWo cells. The mean fluorescence intensity was plotted for each sample on a bar graph. Error bars indicates the standard deviation for each measurement. The _p_ value was calculated using _t_-test, with significance level < 0.05.

7.3.1.2 Mitochondrial translation

Mitochondrial translation was assessed and compared between WT and 3-MST knockout BeWo cells. Representative images showing mitochondrial translation labelling in WT and 3-MST knockout cells are displayed in Figure 7-10. The negative controls represented the cells exposed to the same click reaction with no prior labelling with HPG. The positive controls represented the cells incubated with HPG only without CHI and exposed to the same click reaction. The mitochondrial translation represents the cells incubated with HPG and CHI.

The negative control (no-HPG + click reaction) showed some very low background signal indicating low non-specific reaction and/or binding of the azide fluorophore. The control labelling without CHI is largely composed of cytoplasmic translation products and one shorter exposure is shown to reveal the pattern of this. CHI completely blocks cytoplasmic translation revealing the underlying mitochondrial translation and this was quantified and compared between WT and C6. Figure 7-10D showed that there was no significant difference in fluorescence intensities of mitochondrial translation between the WT and 3-MST knockout cells. Both MTCO1 expression and mitochondrial translation used as a measure for mitochondrial function showed no significant differences between the WT and C6.
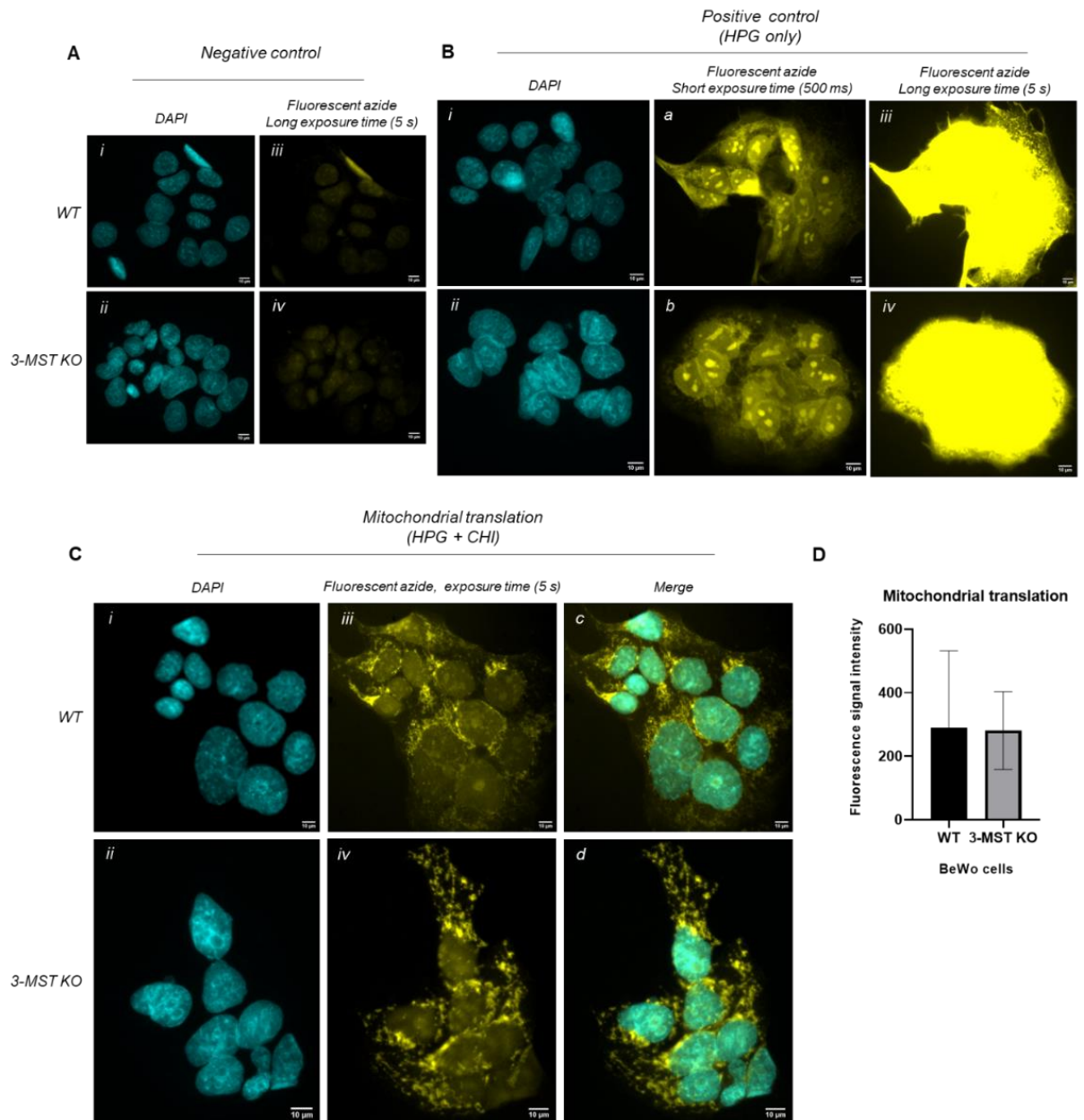
Figure 7-10 Visualisation and quantification of mitochondrial translation in WT and 3-MST knockout BeWo cells. (A) The cells were labelled without HPG (negative controls). (B) The cells were labelled with HPG only (positive control). (C) The cells were labelled with HPG in presence of CHI (mitochondrial translation). DNA was detected by DAPI staining (i and ii) in A, B and C. Translation was detected by click reaction with fluorescent azide (iii, iv, a and b). DAPI exposure was for 10 ms. The fluorescence azide exposure was for 500ms (a &b) in B and for 5 seconds (iii & iv) in B and C. Merged images show a combination of DAPI and fluorescent azide in C are shown in (c &d). Images with same exposure time displayed with the same brightness and contrast setting. Scale bars: 10 μm. D) A graph of mitochondrial translation fluorescence intensity in WT and 3-MST knockout BeWo cells. The mean mitochondrial fluorescence intensity was plotted for each sample on a bar graph. Error bars indicates the standard deviation for each measurement. The *p* value was calculated using *t*-test, with significance level < 0.05.

Although neither measurement revealed any difference between mitochondria in C6 vs WT BeWo cells, many other analyses should now be carried out to explore this further. Confocal microscopy might reveal whether mitochondria are more or less fused in absence of 3-MST. Mitochondrial metabolic function and efficiency of the oxidative phosphorylation could be assessed by measuring the amount of oxygen consumed for a given amount of ATP synthesised in mitochondria or by measuring NADH turnover (Grey et al., 2019) Furthermore, growing the cells under conditions of oxidative stress might be required to reveal any dependence on H_2S production but because of the time constraints, it was only possible to carried out the mentioned experiments.

7.4 Conclusion

Once again, the shortcomings of the antibodies available for studying CBS and CSE have been highlighted and also the value of CRISPR knockout technology to assess the specificity of antibodies was shown. A plausible hypothesis of proposed crosstalk/ negative feedback regulation between 3-MST, CBS and CSE was proposed although support for that needs to be sought by obtaining further 3-MST knockouts and carrying out gene rescue experiments. One would predict that inhibiting of 3-MST activity in WT BeWo cells by using 3-MST inhibitors such as H_2O_2 might reduce CBS and CSE levels. Measuring level of H_2S production in CBS, CSE and 3-MST knockout clone and comparing it with that in WT BeWo cells could help understand which pathway is the key H_2S producer in BeWo cells and, by extension, possibly placenta. Additionally, measuring level and activity of CAT enzyme, which works in a combination with 3-MST to produce H_2S from cysteine, in both WT and 3-MST knockout cells may be informative.

Chapter 8   General discussion, conclusions and future directions

8.1 General discussion

The primary aim of this study was investigating the expression of H_2S synthesising enzymes in healthy and complicated pregnancies at both mRNA and protein abundances, using a systematic method of sampling. However, attempted optimisation of anti-CBS and CSE antibodies for protein analysis by western blotting never eliminated multiple band-background despite extensive experimentation testing of multiple primary and secondary antibodies. Our CRISPR knockout approach showed that these antibodies did identify specific bands (being absent in knockouts) but persistently also bound non-specifically to other proteins in MCF-7 and BeWo cell lines in western blotting (sections 5.2.5.2 and 5.2.5.3) and in BeWo cells *in situ* method IF (section 7.1). The specific bands were always surrounded by other very closely sized bands especially in placental samples and these bands did not disappear in knockout samples (Figure5-16, Figure5-17 and Figure5-19) making it difficult to determine which one is of the correct size unless run side by side with knockout samples. Since both these proteins have several different possible MWs and since protein standards do not absolutely accurately size comparatively run sample proteins, this makes determining which is the specific CBS or CSE proteins on western by size alone problematic. This in turn raised concerns over many previous publications on these enzymes because the same antibodies have been widely used for western blots and/or IHC by other groups and conclusions drawn based on the supposed expression variability.

Focusing just on literature specifically with trophoblast cells and placental tissues (Chen et al., 2017, Cindrova-Davies et al., 2013, Holwerda et al., 2012, Hu et al., 2016, Mislanova et al., 2011): all used anti-CBS and CSE antibodies were tested and found wanting in this study. Moreover, in each case, all western blot figures in these publications showed only a narrow window of the gel blot raising a major question of how one could be sure that the shown CBS or CSE bands were of the correct MW. Since a close range of MWs are possible for each protein and some artefactual bands are in the same range, confidence in published data with regard to these enzymes' differential regulations is further undermined. None of these papers showed experimental details or supplementary data about testing specificity of the antibodies, for example by knockout controls or blocking peptides nor were any whole blots shown in supplementary figures. These problems have been identified as a major general issue in biomedical research and a source of growing concern relating to the performance

and reproducibility of research findings (Baker, 2016, Fosang and Colbran, 2015, Lithgow et al., 2017, Pillai-Kastoori et al., 2020). It is likely that issues with antibody specificity are partly to blame for the fact that around 50% of the major findings in cancer research have not been able to be reproduced (Errington et al., 2021). In the following sections, western blot and IHC data on CBS and CSE from other studies will be taken at face value for the purpose of discussion however, it remains the case that these data must be regarded with caution for the reasons described above.

Detection of a single, distinct protein band of the expected MW on a blot may not always indicate antibody specificity. Moreover, if a Western blotting shows multiple bands, this might not necessarily indicate non-specific binding, as additional bands may represent protein degradation, post-translational modification cleavage, splice variants of the target protein, or other proteins that also contain the target epitope. This study shows how the efficient, rapid and inexpensive generation of knockout clones using CRISPR can be used to investigate antibody performance and specificity and identified unexpected isoforms of proteins even when antibody specificity is poor (Figures 5-16, 5-17 and 5-19). Although similar approaches have been available for longer using siRNA to specifically knock down gene expression, the CRISPR approach is better in that it generates stronger elimination of the protein of interest and, crucially, knockouts can be independently verified by simple sequencing and data analysis such as ICE.

The study employed sample collection by a systemic sampling method to avoid missing spatial differences in gene expression. This approach was justified in light of one of the main findings i.e. that CBS, CSE and 3-MST were differentially expressed across different placental zones although these differences were only significant at particular placental sites and in some groups. It could be a result of the vascular biology in implantation and placentation as discussed in chapter 3. It also could be related to the abnormal biology of vascular changes that occur in placenta in pathological pregnancies. The overwhelming majority of the published papers for similar studies did not follow controlled sampling method which may influence study results (Mayhew, 2008). This may explain such discrepancy seen in the literature in measurement of CBS and CSE mRNA and protein because in those studies they used random sampling. For example, Cindrova-Davies et al. (2013) reported a reduction in CSE mRNA and protein levels in PE whereas, Holwerda et al. (2012) did not find significant differences in CSE mRNA and protein levels in PE compared to the control group but it is possible they sampled from different areas of the placenta. Therefore, one aim of this thesis was to understand if this could, at least in part, be

explained by sampling approaches. However, none of the changes measured in this study reconciled previously conflicting results. Once again, it is more likely that the previous discrepancies noted (Table 1-1) were at least part due to the poor quality of antibodies available for these enzymes, because, for example, the large amount of non-specific binding to proteins of similar MW to the target proteins could result in investigators quantifying the wrong bands.

The study investigated expression of the three H_2S synthesising enzymes in placentas from healthy and complicated pregnancies because most of the previous studies focused only on CBS and CSE enzymes as the main H_2S producers. This well justified in the light of another of this study's finding i.e. that 3-MST protein levels affect both CBS and CSE but not the reverse, possibly implicating 3-MST levels as more important. This will be important to follow up by the experiments already suggested in section 7.2.

CSE mRNA (Figure 3-6E) and protein abundance (Figure 6-14) were positively correlated and significantly increased during labour. Also, the 3-MST mRNA increased in labour albeit in a different placental zone. The up-regulation of CSE and 3-MST expression during labour could be explained as a response to increase the H_2S production to attenuate the inflammation and oxidative stress happening during labour, and also to cause vasorelaxation in the placenta to maintain uterine quiescence (Wang, 2002). It is known that inflammatory mediators such as interleukin 1 beta (IL-1β), IL-6 and TNF-α stimulate the expression of contraction-associated proteins, such as oxytocin receptor, connexin 43, prostaglandin H synthase-2 and prostaglandin receptors, in myometrium, leading to onset of labour (Chow and Lye, 1994). Expression of pro-inflammatory cytokines and infiltration of myometrium, cervix, and fetal membranes by neutrophils and macrophages are increased prior to onset of term and preterm labour (Bokstrom et al., 1997, Osmers et al., 1995). Liu et al. (2016) investigated whether H_2S affects the timing of birth in LPS-induced preterm labour mouse model and examined inflammatory profile in gestational tissues of the mice: H_2S significantly delayed LPS-induced preterm labour and suppressed LPS-induced inflammation in myometrium. If increased H_2S production during labour is a response to the natural inflammatory processes that occur, it follows that H_2S could be a useful therapeutic agent for example in preterm labour which occurs in 8-10% of all pregnancy and is the major cause of perinatal morbidity and mortality (Goldenberg, 2002). H_2S donors such as sulfide salts, H_2S-releasing derivatives of other drugs and plant-derived products are all possible ways for delivering H_2S therapeutically and a promising area for experimental studies of therapeutic use. Such donors would have therapeutic potential for other diseases

such as arterial hypertension (Rossoni et al., 2010), atherosclerosis (Zhang et al., 2012), ischemic-reperfusion injury (Wang et al., 2009) and chronic inflammatory diseases (Gong et al., 2011).

Another significant finding in the current study was that 3-MST mRNA (Figure 3-16B) and protein (Figure 6-7 and 6-8) levels were consistently increased in complicated pregnancies with FGR comparing to normal pregnancies but only at the periphery of placenta. The increase in 3-MST could be a response to increase H_2S production in placenta in order to decrease the vascular resistance in fetoplacental circulation. The present study is the first to study 3-MST expression during labour and in pregnancies complicated with FGR. The vasodilator effect of H_2S in cardiovascular system by hyperpolarising and relaxing the SMCs through opening K_{ATP} channels has been confirmed by Zhao et al. (2001). Cindrova-Davies et al. (2013) also, reported a K_{ATP} channel dependent reduction in vascular resistance by administration of exogenous H_2S donor. Lu et al. (2017) investigated the hypothesis of remodelling of stem villous arteries contributes to FGR via oxidative stress and reducing H_2S signalling. They claimed there was a reduction in CSE mRNA and protein expression, as well as CSE immunostaining in stem villous artery explants in FGR group compared with age matched preterm controls. However, these authors did not disclose information about testing specificity of antibodies they had used nor did they employ zonal sampling therefore, it is not possible to directly compare these results with those in this study in which no difference was found in either CSE mRNA or CSE protein between any zones comparing placentas form the FGR group with controls. Also, the inconsistency in findings between the two studies could be due to the difference in severity of FGR cases included. In Lu et al's (2017) study, the FGR cases were severe and preterm deliveries (the mean gestational age was 29 weeks) whereas, in this study they were late onset and delivered at term (the mean gestational age was 36 weeks). So, it could be in more severe FGR, the oxidative insult was more because the H_2S is reduced/fails to rise.

The current study also showed that CBS mRNA (Figure 3-8A) and CSE mRNA abundances (Figure 3-10B) were significantly higher in PE group than the normotensive group at the inner ($p = 0.008$) and middle ($p = 0.04$) placental sites, respectively. However, no significant changes in protein levels were detected. The discrepancy between the mRNA and protein levels of CBS and CSE could be explained by post-transcriptional and post-translational regulations as previously discussed in sections 3.3.5 and 6.1.1. Hu et al. (2017) examined the expression and localisation of 3-MST in normal and pre-eclamptic placentas. Hu et al. (2017) found that there was no significant difference in 3-MST mRNA and protein

expression between healthy and pre-eclamptic placenta. The present study also did not find any differences in 3-MST expression between PE groups and their controls. However, Hu et al. (2017) found that the rate of H_2S production was significantly decreased in pre-eclamptic placenta, and therefore they suggested a reduction in CBS and/or CSE was responsible but in that study, they did not measure these proteins. It can be hypothesised that the rise in CBS and CSE mRNA in PE without corresponding rise in CBS or CSE proteins recorded in this might reflect some translational regulation of these proteins that might also result in reduced enzyme activity. It was not possible to study H_2S production in this study because of the time constraints and need for rapid access to placentas after delivery.

The comparison between this study and the other studies is difficult because of severity of PE cases included in the studies. The placentas used in PE group in this study were all from women who diagnosed with late-onset PE apart from two cases. However, in the previous studies they were from women who presented with both early and late-onset severe PE. Holwerda et al. (2012) did not find differences in CBS and CSE protein levels between PE groups and their controls, however, they found significant differences in CBS and CSE proteins between early and late-onset PE groups. Cindrova-Davies et al. (2013) also reported inconsistency in expression of CSE in PE. They found a significant reduction in CSE mRNA and protein levels in PE group with abnormal doppler results and a significant increase in the PE group with normal doppler results. This could reflect the differences in pathophysiology of early and late-onset PE. In early pregnancy, the pathophysiology of PE is established when a variety of deficiencies in placentation affect the key process of spiral artery remodelling. Whereas, as pregnancy progresses to the third trimester, other placental and maternal factors, converging to activate the maternal immune and cardiovascular system may cause the underlying pathology (Egbor et al., 2006, Myatt et al., 2014). Even the long-term health consequences for women who have had early-onset PE are different. Two epidemiological studies have shown the risk of cardiovascular disease in later life with earlier onset PE is 8 to 10 fold (Irgens et al., 2001, Mongraw-Chaffin et al., 2010) compared to 2 fold when PE presents close to term.

Furthermore, the comparisons between the studies are difficult because they are further complicated by the gestational age of the PE groups. In the current study, most of women in PE group and control group were term at time of delivery except 2 cases in LG-PE (Table 2-2) but this was also one reason for the relatively small sample size. In the study carried out by Holwerda et al. (2012), the average gestational age in the early-onset PE group was

about 28 weeks and around 38 weeks in the control group. Also, in Cindrova-Davies et al's study, the mean gestational age was between 28.5 and 29.5 weeks in PE groups and 39 weeks in the healthy control group. Gestational age is a known variable in studies of other placental and fetal genes: the CRH transcript was up-regulated over gestation, whereas the expression of fibroblast activation protein and β-tubulin were decreased over gestation (Lian et al., 2013). However, it may not be an issue for H_2S synthesis because no differences were reported in CBS mRNA expression measured in the first trimester and term human placenta (Solanky et al., 2010).

It is well known that maternal obesity promotes a state of inflammation, oxidative stress and lipotoxicity in the placenta (Malti et al., 2014) which may in turn lead to alteration in maternal vascular endothelial function and alteration in trophoblast invasion and differentiation (Jarvie et al., 2010). Also, it causes dysregulation of genes related to lipid metabolism, angiogenesis and inflammation (Saben et al., 2014). It was therefore, expected that some H_2S synthesising enzymes would increase in maternal obesity because of its protective role against oxidative stress and inflammation. However, the current study did not show any significant differences in expression of CBS, CSE and 3-MST between high BMI and control groups. Why H_2S might protect against deleterious effects of inflammation in some circumstances but not others would be an avenue for further research.

In the present study labour was a confounder factor in FGR group. It was difficult to obtain placentas from women who presented with FGR and delivered by CS. Therefore, the FGR group was compared to the control group of the same mode of delivery to maintain consistency between the groups. Thus, the oxidative stress occurring due FGR pathology could be superimposed by stress of labour, resulting in the increase in 3-MST expression. It could be argued that the meaningful results in this comparative group were due to effect of labour on placenta which superimpose on the effect of FGR. There is no doubt that the uterine contractions associated with labour provide the basis for ischemia-reperfusion type injury to the placenta. Doppler ultrasound studies have demonstrated a linear inverse relationship between uterine artery resistance and the intensity of the uterine contractions during labour (Brar et al., 1988).

8.2 Difficulties and limitations

The difficulties encountered using the only commercially available antibodies have already been described. Another limitation of the current study was that the sample size was small

in some groups because of the difficulties faced when collecting clinical samples from patients, and also because the sample size was also determined by Prof. Lyall and I was not able to collect more samples. However, these results could be preliminary results for a further study with a larger sample size in order to detect even small size effect between the comparative groups. Finally, lack of lab access during lockdown, loss of samples after a freezer failure and financial resource limitations all had significant impact on this study.

8.3 Conclusions and further direction

Overall, this study contributes important data to the area of placenta research and could potentially lead to an improvement in placenta research field by following systematic sampling methods that could enable studies to be compared. Since western blots and immunocytochemistry are mainstay techniques in this filed, it also highlights the importance of thorough investigation of antibody specificity and shows how CRISPR knockout approaches can be used to clarify data analysis. The incomplete reporting of the experimental details of primary antibodies, lack of antibodies validation and differences in the analytic techniques has been well documented and this study further highlights how this could affect the research reproducibility.

Importantly, the study provided insights into the expression of H_2S producing enzymes during labour and in complicated pregnancies, and showed up-regulation of CSE and 3-MST in labour and FGR. However, it will be crucial to test whether increased levels of H_2S producing enzymes is matched by actual increases in H_2S production as activity of these enzymes and availability of substrates for these enzymes may also be regulated. A number of methods are available such as colorimetric assays, fluorescence probes, chromatography and mass spectrometry but are limited by stability of H_2S presenting a problem for organs such as placenta where rapid access to tissue is hard to guarantee. It could be measured in the urine of pregnant women with healthy and complicated pregnancies but this would not directly measure placental H_2S. The end metabolites of H_2S, sulfate and thiosulfate (measured using ion chromatography with mass spectrometry) are more stable and are thought to be a reliable estimate for H_2S bioavailability (Kangas and Savolainen, 1987). These could be used instead on placental tissue accessible at varaible times after delivery.

Although the present study confirmed the presence of three H_2S synthesising enzymes in placental tissues, the quantitative contribution that each of the three H_2S synthesising enzymes makes to the levels of H_2S found naturally in placentas in health and disease

remains unclear. This is important since the presence and/or activity of such enzymes may be useful biomarkers of disease progression in some cases and it is critical to understand which H_2S synthesizing enzyme is important in which cell at which time point and how this is affected by disease. For this goal, BeWo cell line could be used as a model for placental cells. H_2S production from the CRISPR BeWo CBS, CSE knockout clones could be compared with WT cells to measure contributions by these enzymes with the residual attributed to 3-MST. 3-MST knockout clones could not be used due to the additional effects on CSE and CBS. H_2S measurement from cell lines could be achieved for example by using free H_2S gas assay kit. This technique used for measurement of free H_2S gas emission where cells would be seeded in a 96 well microplate. Then the released H_2S gas into the air will be captured in a gel spot containing silver ions on the underside of the microplate lid just above the target well. The resulting silver sulfide produced inside the spot creates a brownish colour that can be measured using a spectrophotometer at 405nm. Further investigation of why, and which mechanism(s) CBS and CSE proteins were reduced in absence of 3-MST were described in chapter 7.

Because cell lines only provide an approximation of *in vivo* situations it would be worth considering the use of placental tissue *ex vivo*. In particular, investigating the effect of hypoxia and subsequent normoxia (model of ischemic-reperfusion injury) on expression of H_2S synthesising enzymes in a placental tissue culture would be another possible area of future research. The current study showed that CBS, CSE and 3-MST levels were significantly increased in labour and PE. One explanation for this increase was the ischemia-reperfusion insult resulting in oxidative stress in placenta. So, it would be worth to investigate the expression of H_2S synthesising enzymes in placental tissues exposed to 2% (hypoxia) O_2 and then followed by an exposure to 8% (normoxia) O_2 for different time points in order to mimic the ischemia-reoxygenation happening in placenta during labour and PE.

The suggestion for post-translationally modified CBS and CSE in this thesis (section 5.3) opens the doors for further studies to confirm the hypothesis that CBS or CSE could be regulated post-translationally in placentas for example by SUMOylation or S-glutathionylation. The physiological relevance of these modifications are important questions that need to be addressed in the future. Immunodepletion with anti-SUMO antibody or anti-glutathione (anti-SSG) antibodies prior to detection of CBS and CSE would address whether these modifications were responsible for the much higher than expected MW of these bands. This could also be done with placental lysates from healthy and complicated pregnancies.

Finally, since the specificity of antibodies is identified as the major challenge in validity and reproducibility of the western blotting findings in the published literature, further work is urgently required to allow the field to progress. Generally, simple practical recommendations such as complete reporting of the experimental details of the antibodies validation in the assay context could help researchers best choose, validate and use research antibodies. Raising antibodies against different epitopes of CBS or CSE by using short recombinant proteins or synthetic peptide sequences would be a first approach. As outlined in this study, the gold standard of specificity is the absence of detection in genetic knockouts and these should be used as a matter of course in antibody development.

Appendices

Appendix 1

Maternity Department
Southern General Hospital
1345 Govan Road
G51 4TF

Patient information sheets for collecting placentas and blood samples

Dr Akrem Abdulsid (Researcher)
Dr Kevin Hanretty (Consultant Obstetrician)
Prof Fiona Lyall (Professor)

Title: Understanding the cause of small birth weight babies and high blood pressure in pregnancy.

(Title of the project: An investigation of the regulation and functions of the stress pathways in pregnant women and in the human placenta.
Full title: An investigation of the regulation and functions of the inflammation, stress and apoptotic path-ways in pregnant women and in the human placenta focused on the impact of pre-eclampsia and fetal growth restriction on these pathways.)

Invitation: you are being invited to take part in a research study. Before you decide it is important for you to understand why the research is being done and what it will involve. Please take time to read the following information carefully and discuss it with others if you wish. Ask us if there is anything that is not clear or if you would like more information. Take time to decide whether or not you wish to take part.

What is the purpose of the study? Some mums have high blood pressure when pregnant. In some cases, the mums can be quite sick and the babies can be small for dates. The reasons for that are not known. We are studying the blood and afterbirth (placenta) as it may give us important clues to understanding the above conditions. We are interested in inflammatory and oxidative stress proteins which involved in immunity response against microorganism at maternal-fetal interface. We are trying to understand why this protein does not always work properly in pregnancies where the baby was small for dates or when the mum had very high blood pressure. Our study will last for 5 years to give us enough time to perform all the experiments and collect sufficient numbers of samples.

Why have I been chosen? To perform our research, we therefore need to collect blood and placentas after the baby has been born. We will collect placentas from mums with high blood pressure, mums whose babies were small for dates and mums who had uncomplicated pregnancies.

Do I have to take part? It is up to you to decide whether or not to take part. If you do decide to take part you will be given this information sheet to keep and be asked to sign a consent form. If you decide to take part you are still free to withdraw at any time and without giving a reason. A decision to withdraw at any time, or a decision not to take part, will not affect the standard of care you receive.

What will happen if I take part? If you do take part, we will collect the blood samples <1 teaspoon before and after delivery from a line that is already in place. Few placenta samples will be taken and transport to the laboratory. Then we will study different proteins to try and find out how they differ between the different pregnancies.

What are the possible benefits of taking part? This study will not be of any use to you if you had a small baby or high blood pressure. However, by studying the placenta and blood markers we may understand these conditions better with a hope of one day finding a treatment.
If you wish to complain or have any concerns about any aspect of the way you have been approached or treated during the course of this study, the normal National Health Service complaints mechanism may be available to you.
Normally placentas are incinerated. We will take few samples from placenta for the research and these samples will be stored until end of the study and then will be discard
Incidental finding: as the implications of these results are as yet clinically uncertain, no action can be justified in direct response.

Will taking part in this study be kept confidential? All information which is collected about you (blood pressure, baby's weight, and your age, etc) will be kept strictly confidential. Any information about you which leaves the hospital will have your name and address removed so that you cannot be recognised from it i.e. it is will be strictly anonymous.

What will happen to the results of the study?
When our studies are complete, we will publish them in scientific journals. If you are interested, then a copy of the results can be obtained from us and our contact details are given.

Who is funding the research? Fund for this project covers by a PhD scholarship from Libyan Ministry of Higher Education and Scientific Research
The patient will be given a copy of the information sheet and a signed consent form to keep.

Thank you again for your time.

1. Dr Akrem Abdulsid (Researcher)
PhD student
University of Glasgow
Medical Genetics Department
Dalnair Street
Glasgow
G3 8SJ
2. Dr Kevin Hanretty (Consultant Obstetrician)
Maternity Department
1345 Goven Road
Glasgow
G51 4TF
3. Prof Fiona Lyall (Professor)
Professor of Maternal and Fetal Health

University of Glasgow
Medical Genetics Department
Dalnair Street
Glasgow
G3 8SJ

NHS
Greater Glasgow
and Clyde

Maternity Department
Southern General Hospital
1345 Govan Road
G51 4TF

CONSENT FORM

Title of the project: Understanding the cause of small birth weight babies and high blood pressure in pregnancy.

(Full title: An investigation of the regulation and functions of the inflammation, stress and apoptotic pathways in pregnant women and in the human placenta focused on the impact of pre-eclampsia and fetal growth restriction on these pathways)

Researcher's names: Dr. K. Hanretty (CI), Dr. A. Abdulsid (PI) and Prof. F. Lyall (AS)

Please initial Box

1. *I confirm that I have read and understand the information sheet dated 08/07/2013 of the above study. I have had the opportunity to consider the information, ask questions and have had these answered satisfactorily.*

2. *I understand that my participation is voluntary and that I am free to withdraw at any time without giving any reason, without my medical care or legal rights being affected.*

3. *I understand that sections of any of my medical notes may be looked at by responsible individuals from regulatory authorities where it is relevant to my taking part in research. I give permission for these individuals to have access to my records.*

4. *I agree to blood samples being taken and to placental examination to be undertaken.*

5. *I agree to these samples being stored for the study time duration.*

6. *I agree to take part in the above study.*

------------------------------------ ----------------------- --------------------------- -
Name of patient   *Date*   *Signature*

------------------------------------ ----------------------- ---------------------------
Name of person taking consent   *Date*   *Signature*
(If different from researcher)

------------------------------------ ------------------------- -----------------------------
.
Doctor   *Date*   *Signature*

1 copy for the patient; 1 for researcher site file; 1 (original) to be kept in medical notes

WoSRES
West of Scotland Research Ethics Service

NHS
Greater Glasgow
and Clyde

Dr Kevin Hanretty
Senior University Clinical Teacher/ Honorary
Consultant Obstetrician & Gynaecologist
GGC NHS Board
Reproductive & Maternal Medicine
Level 2, McGregor Building
Western Infirmary, Glasgow
G11 6NT

West of Scotland REC 4
Ground Floor - Tennent Building
Western Infirmary
38 Church Street
Glasgow
G11 6NT

Date	22 July 2013
Direct line	0141 211 2482
Fax	0141 211 1847
E-mail	rose.gallacher@ggc.scot.nhs.uk

Dear Dr Hanretty

Study title:	**An investigation of the regulation and functions of the inflammation, stress and apoptotic pathways in pregnant women and in the human placenta. In particular, the impact of pre-eclampsia and fetal growth restriction on these pathways will be investigated.**
REC reference:	**13/WS/0149**
Protocol number:	**VERSION 2**
IRAS project ID:	**130896**

Thank you for your letter received 17 July 2013 responding to the Committee's request for further information on the above research and submitting revised documentation.

The further information has been considered on behalf of the Committee by the Chair.

We plan to publish your research summary wording for the above study on the NRES website, together with your contact details, unless you expressly withhold permission to do so. Publication will be no earlier than three months from the date of this favourable opinion letter. Should you wish to provide a substitute contact point, require further information, or wish to withhold permission to publish, please contact the Co-ordinator Ms Evelyn Jackson, evelyn.jackson@ggc.scot.nhs.uk.

Confirmation of ethical opinion

On behalf of the Committee, I am pleased to confirm a favourable ethical opinion for the above research on the basis described in the application form, protocol and supporting documentation as revised, subject to the conditions specified below.

Ethical review of research sites

NHS sites

The favourable opinion applies to all NHS sites taking part in the study, subject to management permission being obtained from the NHS/HSC R&D office prior to the start of the study (see "Conditions of the favourable opinion" below).

Conditions of the favourable opinion

The favourable opinion is subject to the following conditions being met prior to the start of the study.

Management permission or approval must be obtained from each host organisation prior to the start of the study at the site concerned.

Management permission ("R&D approval") should be sought from all NHS organisations involved in the study in accordance with NHS research governance arrangements.

Guidance on applying for NHS permission for research is available in the Integrated Research Application System or at http://www.rdforum.nhs.uk.

Where a NHS organisation's role in the study is limited to identifying and referring potential participants to research sites ("participant identification centre"), guidance should be sought from the R&D office on the information it requires to give permission for this activity.

For non-NHS sites, site management permission should be obtained in accordance with the procedures of the relevant host organisation.

Sponsors are not required to notify the Committee of approvals from host organisations

It is the responsibility of the sponsor to ensure that all the conditions are complied with before the start of the study or its initiation at a particular site (as applicable).

Approved documents

The final list of documents reviewed and approved by the Committee is as follows:

Document	Version	Date
Covering Letter		23 May 2013
Investigator CV		22 May 2013
Other: Academic Supervisor CV: Lyall		22 May 2013
Other: Student CV: Abdulsid		22 May 2013
Participant Consent Form	3	08 July 2013
Participant Information Sheet	3	08 July 2013
Protocol	2	16 May 2013
REC application		23 May 2013
Response to Request for Further Information		

Appendix 2

Table1: Optimisation of anti-CBS, CSE and 3-MST antibodies

Antibody	Blocker solution	Primary antibody solution	Secondary antibody solution	Results
Anti-CBS (Sigma)	5% normal dokeny serum (NDS) in TBST for 1 hour	1:1000 in 5 % normal human serum in TBST for 1 hour	Donkey anti-mouse 1:1000 in 5% BSA in TBST for 1 hour	Multiple bands
Anti-CBS (Sigma)	5% NDS in TBST for 1 hour	1:2000 in 5 % normal human serum in TBST for 1 hour	Donkey anti-mouse 1:1000 in 5% BSA in TBST for 1 hour	Multiple bands
Anti-CBS (Sigma)	5% NDS in TBST for 1 hour	1:2000 in 5 % normal human serum in TBST for 1 hour	Donkey anti-mouse 1:3000 in 5% BSA in TBST for 1 hour	Multiple bands
Anti-CBS (Sigma)	5% NDS in TBST for 1 hour	1:1000 in 5 % normal human serum in TBST for 1 hour	Donkey anti-mouse 1:5000 in 5% BSA in TBST for 1 hour	Multiple bands
Anti-CBS (Abnova)	5% NDS in TBST for 1 hour	1:1000 in 5 % normal human serum in TBST for 1 hour	Donkey anti-mouse 1:1000 in 5% BSA in TBST for 1 hour	Multiple bands
Anti-CBS (Abnova)	5% NDS in TBST for 1 hour	1:2000 in 5 % normal human serum in TBST for 1 hour	Donkey anti-mouse 1:1000 in 5% BSA in TBST for 1 hour	Multiple bands
Anti-CBS (Abnova)	5% milk in TBST for 1 hour	1:2000 in 5 % milk in TBST for 1 hour	Donkey anti-mouse 1:3000 in 5% milk in TBST for 1 hour	Multiple bands (Weak signal)

Anti-CBS (Abnova)	5% NDS in TBST for 1 hour	1:1000 in 5 % normal human serum in TBST for 1 hour	Donkey anti-mouse 1:5000 in 5% BSA in TBST for 1 hour	Multiple bands
Anti-CBS (Abcam)	5% NDS in TBST for 1 hour	1:1000 in 5 % normal human serum in TBST for 1 hour	Donkey anti-rabbit 1:1000 in 5% BSA in TBST for 1 hour	Multiple bands
Anti-CBS (Abcam)	5% NDS in TBST for 1 hour	1:2000 in 5 % normal human serum in TBST for 1 hour	Donkey anti-rabbit 1:1000 in 5% BSA in TBST for 1 hour	Multiple bands
Anti-CBS (Abcam)	5% NDS in TBST for 1 hour	1:2000 in 5 % normal human serum in TBST for 1 hour	Donkey anti-rabbit 1:3000 in 5% BSAin TBST for 1 hour	Multiple bands
Anti-CBS (Abcam)	5% NDS in TBST for 1 hour	1:1000 in 5 % normal human serum in TBST for 1 hour	Donkey anti-rabbit 1:5000 in 5% BSAin TBST for 1 hour	Multiple bands
Anti-CBS (Abcam)	5% milk in DPBS for 1 hour	1:1000 in 5% milk in DPBS for overnight at 4 ℃	Donkey anti-rabbit 1:3000 in 5% milk in TBST for 45 minutes	Multiple faint bands (Weak signals)
Anti-CBS (Abcam)	5% BSA in DPBS for 1 hour	1:1000 in 5% BSA in DPBS for overnight 4 ℃	Goat anti-rabbit 1:3000 in 5% BSA in DPBS for 1 hour	Multiple faint bands
Anti-CBS (Abcam)	5% BSA in DPBS for 1 hour	1:1000 in 5% BSA in DPBS for overnight at 4 ℃	Goat anti- rabbit 1:3000 in 5% BSA in DPBS for 1 hour	Multiple faint bands (Weak signals)
Anti-CBS (Abcam)	5% BSA in DPBS for 1 hour	1:1000 in 5% BSA in DPBS for overnight at 4 ℃	Goat anti- rabbit 1:3000 in 5% BSA in DPBS for 1 hour	Multiple faint bands (Weak signals)
Anti-CBS (Abcam)	5% milk in TBST for 1 hour	1:1000 in 5% BSA in TBST for 1 hour	Donkey anti-rabbit 1:3000 in 5% milk in TBST for 1 hour	Multiple bands

Anti-CBS (Abcam)	5% milk in TBST for 1 hour	1:2000 in 5% BSA in TBST for 1 hour	Donkey anti-rabbit 1:3000 in 5% milk in TBST for 1 hour	Multiple bands
Anti-CSE (Sigma)	5% NDS in TBST for 1 hour	1:1000 in 5 % normal human serum in TBST for 1 hour	Donkey anti-mouse 1:1000 in 5% BSA in TBST for 1 hour	Multiple bands
Anti-CSE (Sigma)	5% NDS in TBST for 1 hour	1:2000 in 5 % normal human serum in TBST for 1 hour	Donkey anti-mouse 1:1000 in 5% BSA in TBST for 1 hour	Multiple bands
Anti-CSE (Sigma)	5% milk in TBST for 1 hour	1:2000 in 5 % BSA TBST for 1 hour	Donkey anti-mouse 1:2000 in 5% BSA in TBST for 1 hour	Multiple bands
Anti-CSE (Abnova)	5% NDS in TBST for 1 hour	1:1000 in 5 % normal human serum in TBST for 1 hour	Donkey anti-mouse 1:5000 in 5% BSA in TBST for 1 hour	Multiple bands
Anti-CSE (Abnova)	5% NDS in TBST for 1 hour	1:1000 in 5 % normal human serum in TBST for 1 hour	Donkey anti-mouse 1:10000 in 5% BSA in TBST for 1 hour	Multiple bands
Anti-CSE (Abnova)	5% Milk in TBST for 1 hour	1:1000 in 5 % BSA in TBST for 1 hour	Donkey anti-mouse 1:10000 in 5% BSA in TBST for 1 hour	Multiple bands
Anti-CSE (Abnova)	5% BSA in TBST for 1 hour	1:1000 in 5 % BSA in TBST for overnight at 4 °C	Donkey anti-mouse 1:10000 in 5% BSA in TBST for 1 hour	Multiple bands
Anti-CSE (Abcam)	5% NDS in TBST for 1 hour	1:1000 in 5 % normal human serum in TBST for 1 hour	Donkey anti-mouse 1:1000 in 5% BSA in TBST for 1 hour	Multiple bands
Anti-CSE (Abcam)	5% NDS in TBST for 1 hour	1:2000 in 5 % normal human serum in TBST for 1 hour	Donkey anti-mouse 1:1000 in 5% BSA in TBST for 1 hour	Multiple bands

Anti-CSE (Abcam)	5% NDS in TBST for 1 hour	1:2000 in 5 % normal human serum in TBST for 1 hour	Donkey anti-mouse 1:2000 in 5% BSA in TBST for 1 hour	Multiple bands
Anti-CSE (Abcam)	5% NDS in TBST for 1 hour	1:1000 in 5 % normal human serum in TBST for 1 hour	Donkey anti-mouse 1:5000 in 5% BSA in TBST for 1 hour	Multiple bands
Anti-CSE (Abcam)	5% NDS in TBST for 1 hour	1:1000 in 5 % normal human serum in TBST for 1 hour	Donkey anti-mouse 1:10000 in 5% BSA in TBST for 1 hour	Multiple bands
Anti-CSE (Abcam)	5% NDS in TBST for 1 hour	1:2000 in 5 % normal human serum in TBST for 1 hour	Donkey anti-mouse 1:3000 in 5% BSA in TBST for 1 hour	Multiple bands
Anti-CSE (Abcam)	5% NDS in TBST for 1 hour	1:5000 in 5 % normal human serum in TBST for 1 hour	Donkey anti-mouse 1:3000 in 5% BSA in TBST for 1 hour	Multiple faint bands (Weak signals)
Anti-CSE (Abcam)	5% NDS in TBST for 1 hour	1:10000 in 5 % normal human serum in TBST for 1 hour	Donkey anti-mouse 1:3000 in 5% BSA in TBST for 1 hour	Multiple faint bands (Weak signals)
Anti-CSE (Abcam)	5% milk in TBST for 1 hour	1:2000 in 5% BSA in TBST for 1 hour	Donkey anti-mouse 1:3000 in 5% milk in TBST for 1 hour	Multiple bands
Anti-CSE (Abcam)	5% milk in TBST for 1 hour	1:2000 in 5% BSA in TBST for 1 hour	Donkey anti-mouse 1:5000 in 5% milk in TBST for 1 hour	Multiple bands
Anti-CSE (Abcam)	5% milk in TBST for 1 hour	1:2000 in 5% BSA in TBST for 1 hour	Donkey anti-mouse 1:10000 in 5% milk in TBST for 1 hour	Multiple faint bands (Weak signals)
Anti-CSE (Novusbio)	5% milk in DPBS for 1 hour	1:2000 in 5% milk in DPBS for 1 hour	Goat anti-mouse (Novusbio) 1:2000 in 5% milk in DPBS for 1 hour	Multiple faint bands (Weak signals)

Anti-CSE (Novusbio)	5% milk in DPBS for 1 hour	1:1000 in 5% milk in DPBS for overnight at 4 ℃	Goat anti-mouse (Novusbio) 1:2000 in 5% milk in DPBS for 1 hour	Multiple faint bands (Weak signals)
Anti-CSE (Novusbio)	5% milk in DPBS for 1 hour	1:2000 in 5% milk in DPBS for overnight at 4 ℃	Goat anti-mouse (Novusbio) 1:2000 in 5% milk in DPBS for 1 hour	Multiple faint bands (Weak signals)
Anti-CSE (Novusbio)	5% BSA in DPBS for 1 hour	1:1000 in 5% BSA in DPBS for overnight 4 at ℃	Goat anti-mouse (Dako) 1:2000 in 5% BSA in DPBS for 1 hour	Multiple faint bands (Weak signals)
Anti-CSE (Novusbio)	5% BSA in DPBS for 1 hour	1:2000 in 5% BSA in DPBS for overnight at 4 ℃	Goat anti-mouse 1:2000 in 5% BSA in DPBS for 1 hour	Multiple faint bands (Weak signals)
Anti-CSE (Novusbio)	3% BSA+1% milk in TBST for 1 hour	1:2000 in 5% BSA in TBST for 1 hour	Goat anti-mouse 1:2000 in 5% BSA in TBST for 1 hour	Multiple bands
Anti-CSE (Novusbio)	3% BSA in TBST for 1 hour	1:2000 in 3% BSA in TBST for 1 hour	Goat anti-mouse (Novusbio) 1:2000 in 3% BSA in TBST for 1 hour	Multiple bands
Anti-CSE (Novusbio)	5% BSA in TBST for 1 hour	1:2000 in 5% BSA in TBST for overnight at 4 ℃	Goat anti-mouse (Novusbio) 1:2000 in 5% BSA in TBST for 1 hour	Multiple bands
Anti-CSE (Novusbio)	5% milk in TBST for 1 hour	1:2000 in 5% BSA in TBST for 1 hour	Donkey anti-mouse 1:3000 in 5% milk in TBST for 1 hour	Multiple bands
Anti-CSE (Novusbio)	5% milk in TBST for 1 hour	1:2000 in 5% BSA in TBST for 1 hour	Donkey anti-mouse	Multiple bands

			1:5000 in 5% milk in TBST for 1 hour	
Anti-CSE (Novusbio)	5% milk in TBST for 1 hour	1:2000 in 5% BSA in TBST for 1 hour	Goat anti-mouse (Novusbio) 1:3000 in 5% milk in TBST for 1 hour	Multiple bands
Anti-CSE (Novusbio)	5% milk in TBST for 1 hour	1:2000 in 5% BSA in TBST for 1 hour	Goat anti-mouse (Novusbio) 1:5000 in 5% milk in TBST for 1 hour	Multiple bands
Anti-CSE (Novusbio)	5% milk in TBST for 1 hour	1:2000 in 5% BSA in TBST for 1 hour	Goat anti-mouse (Dako) 1:1000 in 5% milk in TBST for 1 hour	Multiple bands
Anti-3MST (Novusbio)	5% BSA in TBST for 1 hour	1:250 in 5% BSA in TBST for 1 hour	Goat anti-rabbit (Abcam) 1:2000 in 5% BSA in TBST for 1 hour	Two close bands at 33kDa and non-specific binding
Anti-3MST (Novusbio)	5% BSA in TBST for 1 hour	1:250 in 3% BSA in TBST for 1 hour	Donkey anti-rabbit 1:1000 in 5% BSA in TBST for 1 hour	Two close bands at 33kDa With faint non-specific binding

Table 2: Optimisation of anti-β-actin and α-Tubulin antibodies (loading controls)

Antibody	Blocker solution	Primary antibody solution	Secondary antibody solution	Results
Anti-β-actin	5% BSA in TBST for 1 hour	1:2000 in 5% BSA in TBST for 1 hour	Goat anti-rabbit 1:2000 in 5% BSA in TBST for 1 hour	Multiple bands
Anti-β-actin	5% milk in TBST for 1 hour	1:4000 in 5% BSA in TBST for 1 hour	Goat anti-rabbit 1:3000 in 5% milk in TBST for 1 hour	Multiple bands
Anti-β-actin	5% milk in TBST for 1 hour	1:2000 in 5% BSA in TBST for 1 hour	Donkey anti-rabbit 1:3000 in 5% milk in TBST for 1 hour	Single band
Anti-alpha Tubulin	5% BSA in TBST for 1 hour	1:1000 in 5% BSA in TBST for 1 hour	Goat anti-rabbit 1:2000 in 5% BSA in TBST for 1 hour	Multiple bands
Anti-alpha Tubulin	5% milk in TBST for 1 hour	1:1000 in 5% BSA in TBST for 1 hour	Goat anti-rabbit 1:2000 in 5% milk in TBST for 1 hour	Multiple bands
Anti-alpha Tubulin	5% milk in TBST for 1 hour	1:2000 in 5% BSA in TBST for 1 hour	Donkey anti-rabbit 1:3000 in 5% milk in TBST for 1 hour	Single band

Appendix 3

Immunohistochemistry (IHC)

IHC reagents

PBS buffer, pH 7.5 (phosphate buffered saline tablets, Sigma-Aldrich, cat.no. P4417-50TAB)**,** Acetone, Extra Pure, SLR (Fisher Scientific, Cat. no. 10314930) and 30% H_2O_2 (VWR, cat. no. 23619.297) were used. Moreover, Alcohol, 50%, 70% and 100%, Hematoxylin solution, Harris Modified (Sigma-Aldrich, cat. no. HHS32-1L), Scott's Tap Water Substitute: 40 gm of Magnesium sulphate ($MgSO_4 • 7H_2O$) +and 7 gm of sodium hydrogen carbonate ($NaHCO_3$) were added to 2L of dH_2O, Histo-clear (histological clearing agent) (National Diagnostics, cat. no. HS-200), DPX Mountant for microscopy (BDH, cat. no. 360294H) and Immunoedge pen (ImmEdge Hydrophobic Barrier PAP Pen, Vector Labs, cat. no. H-4000) were used in this experiment.

IHC method

Snap frozen placental tissues were retrieved from - 80°C storage. Sections were cut on a Bright OTF cryostat at 6 um. Slides were immersed in acetone directly after cutting for 10 minutes and then allowed to air dry. This step was carried out by Clare Orange.

Slides were fixed in acetone for 15 minutes and then washed in PBS buffer for 5 minutes. The sections were incubated in 0.3% H_2O_2 in distilled water for 15 minutes on a stirrer. Next, the sections were washed in PBS buffer for 5 minutes. The section edges were marked with immunoedge pen (Dako pen) to create a barrier. Then, the sections were incubated with diluted normal horse serum (50μl of normal blocking serum stock added to 5 ml of PBS buffer) for 20 minutes. The sections were then incubated with primary antibody diluted in buffer for 30 minutes at room temperature for CBS antibody (1:100 dilution) (abcam, Cat.no. ab54883) or for overnight at 4°C for CSE antibody (1:200 dilution) (abcam, Cat. no. ab54573). The slides were then washed in PBS buffer for 5 minutes and then incubated for 30 minutes with diluted biotinylated secondary antibody solution (100μl of normal blocking serum stock added to 5ml PBS buffer. Subsequently, the slides were washed in PBS buffer for 5 minutes and after that were incubated with Vectastain *Elite* ABC Reagent (Vector Labs, cat. no. PK-6200) for 30 minutes: reagent A (Avidin DH solution) and reagent B (biotinylated enzyme) were mixed, and allowed to stand for about 30 minutes before use.

After that, the slides were washed in PBS buffer for 5 minutes. Then, the slides were incubated in peroxidase substrate solution (DAB) (Vector Labs, cat. no. SK-4100) until the desired stain develops for about 5 minutes. The excess DAB was drained off and the sections were rinsed in tap water in sink for 5 minutes. The slides were counterstained with haematoxylin and Scott's Tap Water Substitute (S.T.W.S). The slides were submerged in haematoxylin for 30 seconds until a red colour develop on the tissue. The slides after that immersed in S.T.W.S for 30 seconds to produce blue staining as a contrast to the stained antigen. For Dehydrating and mounting of the slides, the slides were dehydrated by immersing them through a serious of alcohol washes with increasing percentage: 50% for 1 minute, 70% for 1 minute, 100% for 2x1 minute and then 2x 1 minute in histo-clear. The slides were finally mounted with coverslips using DPX mountant and stored at room temperature. In each experiment a negative control with no primary antibody and only secondary antibody was included to ensure no background signal. Finally, the stained slides were scanned using Hamamatsu NanoZoomer Digital Pathology 2.0-HT scanner (Welwyn Garden City, Hertfordshire, UK) at objective magnification x 20. Visualisation and image analysis assessment was carried out using SlidePath Digital Image Hub, version 3.0 and 4.0.1, (SlidePath, Leica Biosystems, Milton Keynes, UK) which is a secure web-enabled digital slide management system.

Some representative images showing CBS and CSE immunostaining in placental tissues

Frozen placental tissues from healthy women (NLG) were stained with anti-CBS or CSE antibody. No primary antibody control was performed. CBS immunostaining was observed in both cytoplasm and nucleus (Figure 1-1C), while CSE immunostaining was observed in cytoplasm (Figure 1-1D). The no-primary control (Figure 1-1A, B) showed no brownish staining, indicating specificity of the secondary antibody. Localisation of CBS and CSE proteins within normal placental tissues (Figure 1-2).
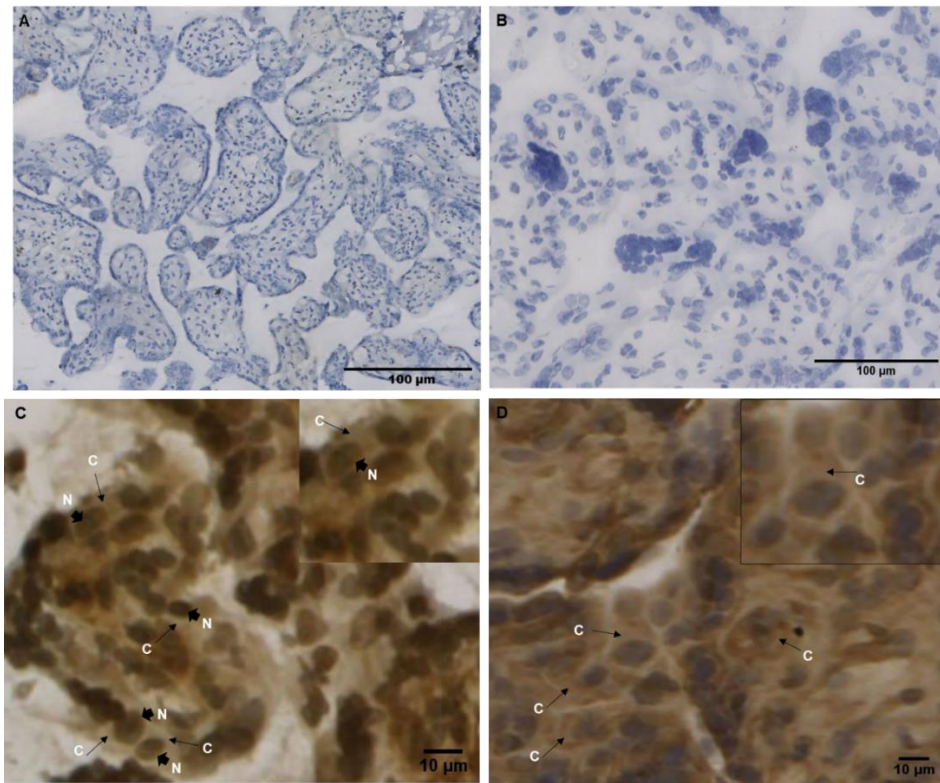
Figure 1-1 immunohistochemistry staining of healthy placental tissues (NLG). (A) shows a negative (no-primary antibody) control, 10X and 100 µm scale bar. (B) shows a negative (no-primary antibody) control, 20X and 100 µm scale bar. (C) CBS immunostaining, 40X and 10µm scale bar. (D) displays CSE immunostaining, 40X and 10µm bar scale. C refers to cytoplasm and N refers to nucleus.
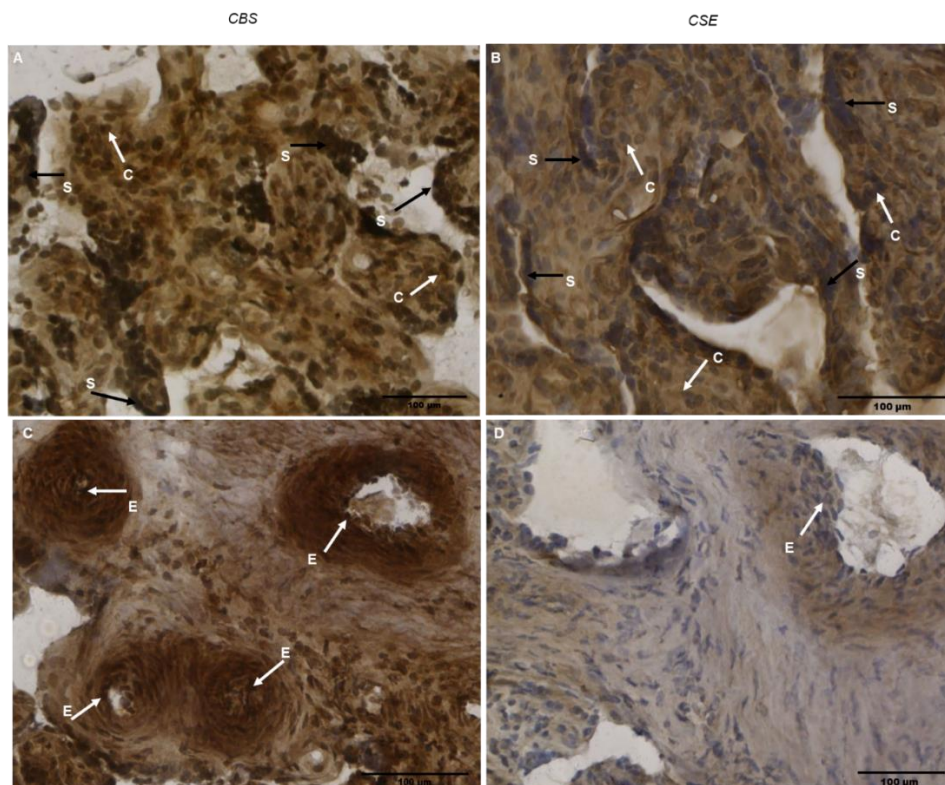
Figure 1-2 immunohistochemistry staining of healthy placental tissues (NLG). (A) and (C) show CBS immunostaining in syncytiotrophoblas(S) and cytotrophoblast (C) cells and endothelium (E) of fetal vasculature, respectively. (B) and (D) show CSE immunostaining in syncytiotrophoblas(S) and cytotrophoblast (C) cells and endothelium (E) of fetal vasculature, respectively, 20X and 100 µm scale bar.

CBS and CSE immunoreactivity in labour

Frozen Placental tissues (inner, middle and outer sites) slides from NLG (n =6) and LG (n=6) were stained with anti-CBS or CSE antibody. Representative images of the stained placentas tissues are illustrated in Figure 1-3.
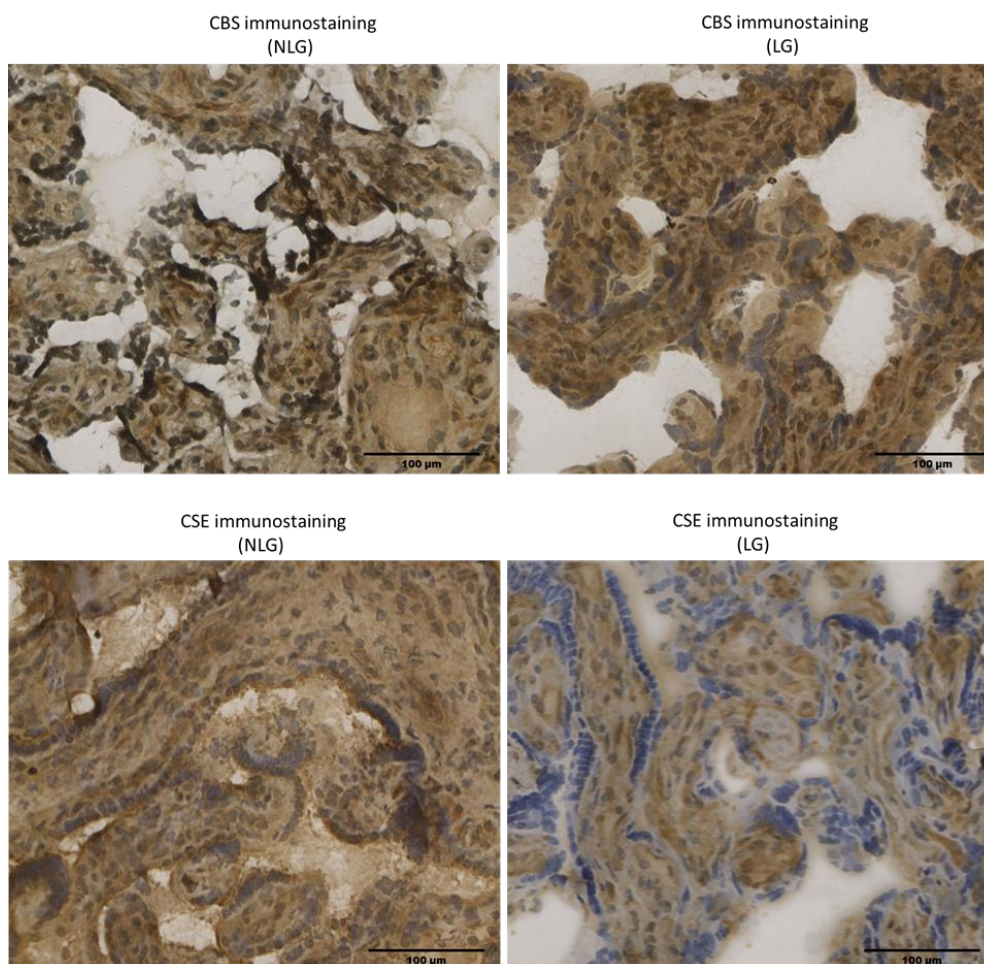
Figure 1-3 Representative images of CBS and CSE immunostaining in placental tissues from non-labour group (NLG) and labour group (LG). the upper panel shows the CBS immunostaining and the lower panel shows the CSE immunostaining. 20X and 100 μm scale bar.

CBS and CSE immunoreactivity in PE

Placental tissues from healthy control (n = 12) and PE group (n = 12) at inner, middle and outer sites were stained with anti-CBS or CSE antibody. Representative images are displayed in Figure 1-4.
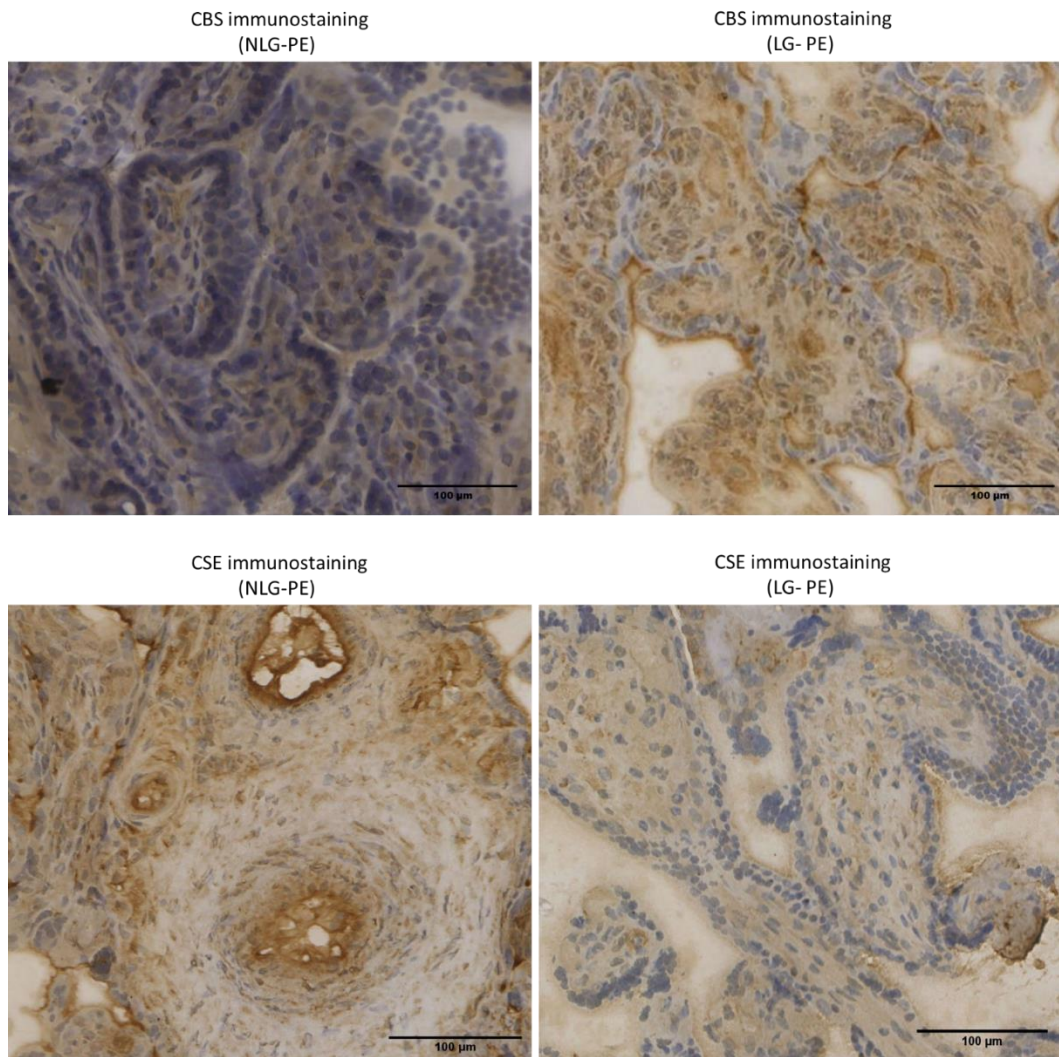
Figure 1-4 Representative CBS and CSE immunostaining in pre-eclamptic placental tissues. Upper panel shows CBS immunostaining in NLG-PE and LG-PE. Lower panel shows CSE immunostaining in NLG-PE and LG-PE. 20X and 100 μm scale bar.

CBS and CSE immunoreactivity in FGR

Placental tissues from healthy control (n = 6) and FGR group (n = 6) were stained with anti-CBS or CSE antibody. Representative images are displayed in Figure 1-5.
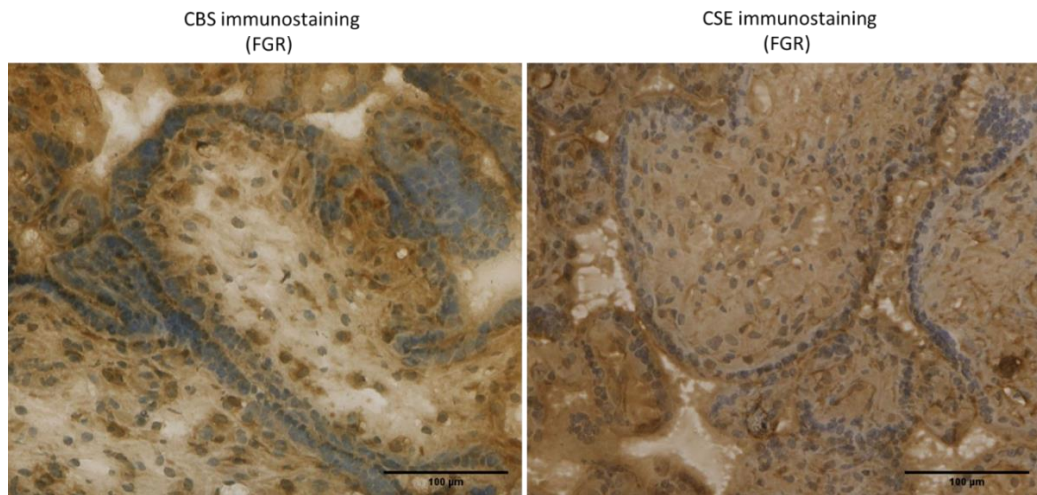
Figure 1-5 Representative CBS and CSE immunostaining in placental tissues from FGR group. The right panel shows CBS immunostaining in FGR group and the lift panel shows CSE immunostaining in FGR group. 20X and 100 μm scale bar.

CBS and CSE immunoreactivity in pregnant women with high BMI

Placental tissues from healthy control and high BMI groups at three placental sites were stained with anti-CBS or CSE antibody (Figure 1-6).
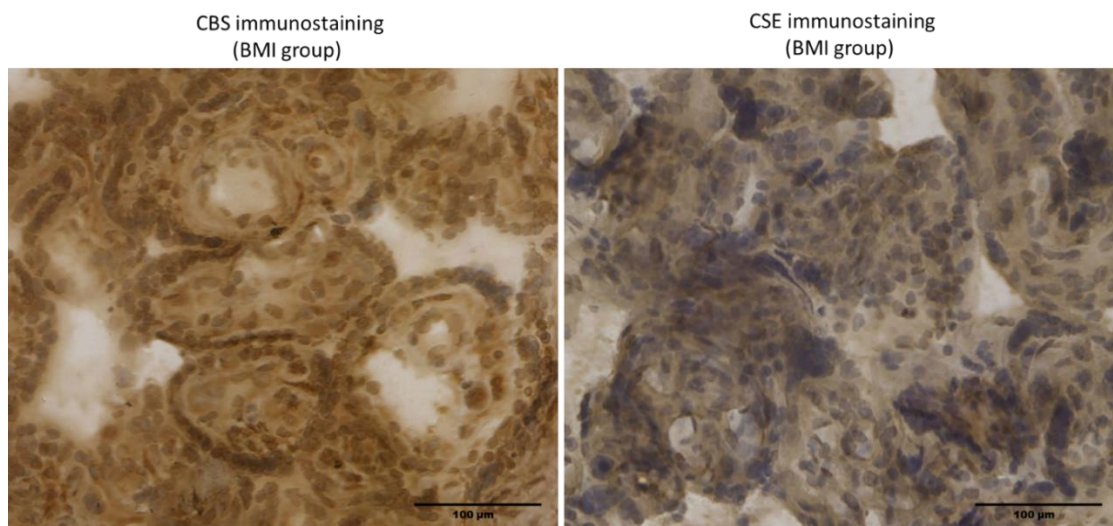
Figure 1-6 Representative CBS and CSE immunostaining in placental tissues from high BMI group. The right panel shows CBS immunostaining and the lift panel shows CSE immunostaining in high BMI group. 20X and 100 μm scale bar.

List of References

Abe, K. and Kimura, H. (1996) 'The possible role of hydrogen sulfide as an endogenous neuromodulator', *The Journal of Neuroscience,* 16(3), pp. 1066-1071.

Acevedo, C. H. and Ahmed, A. (1998) 'Hemeoxygenase-1 inhibits human myometrial contractility via carbon monoxide and is upregulated by progesterone during pregnancy', *Journal of Clinical Investigation,* 101(5), pp. 949-955.

Agrawal, N. and Banerjee, R. (2008) 'Human polycomb 2 protein is a SUMO E3 ligase and alleviates substrate-induced inhibition of cystathionine beta-synthase sumoylation', *PLoS One,* 3(12), pp. e4032.

Ahmad, S. and Ahmed, A. (2004) 'Elevated placental soluble vascular endothelial growth factor receptor-1 inhibits angiogenesis in preeclampsia', *Circulation Research,* 95(9), pp. 884-91.

Ahmed, A., Rahman, M., Zhang, X., Acevedo, C. H., Nijjar, S., Rushton, I., Bussolati, B. and St John, J. (2000) 'Induction of placental heme oxygenase-1 is protective against TNFalpha-induced cytotoxicity and promotes vessel relaxation', *Molecular medicine,* 6(5), pp. 391-409.

Ayaydin, F. and Dasso, M. (2004) 'Distinct in vivo dynamics of vertebrate SUMO paralogues', *Molecular Biology of the Cell,* 15(12), pp. 5208-18.

Baek, D., Jin, Y., Jeong, J. C., Lee, H. J., Moon, H., Lee, J., Shin, D., Kang, C. H., Kim, D. H., Nam, J., Lee, S. Y. and Yun, D. J. (2008) 'Suppression of reactive oxygen species by glyceraldehyde-3-phosphate dehydrogenase', *Phytochemistry,* 69(2), pp. 333-8.

Baeten, J. M., Bukusi, E. A. and Lambe, M. (2001) 'Pregnancy complications and outcomes among overweight and obese nulliparous women', *American Journal of Public Health,* 91(3), pp. 436-440.

Bahado-Singh, R. O., Kovanci, E., Jeffres, A., Oz, U., Deren, O., Copel, J. and Mari, G. (1999) 'The Doppler cerebroplacental ratio and perinatal outcome in intrauterine growth restriction', *American Journal of Obstetrics and Gynecology,* 180(3 Pt 1), pp. 750-6.

Baker, M. (2016) '1,500 scientists lift the lid on reproducibility', *Nature,* 533(7604), pp. 452-454.

Bao, L., Vlček, Č. r., Pačes, V. and Kraus, J. P. (1998) 'Identification and tissue distribution of human cystathionine β-synthase mRNA isoforms', *Archives of biochemistry and biophysics,* 350(1), pp. 95-103.

Barber, A., Robson, S. C. and Lyall, F. (1999) 'Hemoxygenase and nitric oxide synthase do not maintain human uterine quiescence during pregnancy', *The American journal of pathology,* 155(3), pp. 831-40.

Barber, A., Robson, S. C., Myatt, L., Bulmer, J. N. and Lyall, F. (2001) 'Heme oxygenase expression in human placenta and placental bed: reduced expression of placenta endothelial HO-2 in preeclampsia and fetal growth restriction', *FASEB journal : official publication of the Federation of American Societies for Experimental Biology,* 15(7), pp. 1158-68.

Barker, D. J. (1992) 'Fetal growth and adult disease', *British Journal of Obstetrics and Gynaecology,* 99(4), pp. 275-6.

Barrett, L. W., Fletcher, S. and Wilton, S. D. (2012) 'Regulation of eukaryotic gene expression by the untranslated gene regions and other non-coding elements', *Cellular and Molecular Life Sciences,* 69(21), pp. 3613-3634.

Bartel, D. P. (2004) 'MicroRNAs: genomics, biogenesis, mechanism, and function', *Cell,* 116(2), pp. 281-97.

Baschat, A. A., Galan, H. L. and Gabbe, S. G. (2012) 'Intrauterine Growth Restriction', in Gabbe, S.G., Niebyl, J.R., Galan, H.L., Jauniaux, E.R.M., Landon, M.B., Simpson,

J.L. & Driscoll, D.A. (eds.) *Obstetrics: Normal and Problem Pregnancies* six edition ed: Elsevier Health Sciences, pp. 706-741.

Bateman, A. (1997) 'The structure of a domain common to archaebacteria and the homocystinuria disease protein', *Trends in Biochemical Science,* 22(1), pp. 12-3.

Baum, M., Schiff, E., Kreiser, D., Dennery, P. A., Stevenson, D. K., Rosenthal, T. and Seidman, D. S. (2000) 'End-tidal carbon monoxide measurements in women with pregnancy-induced hypertension and preeclampsia', *American Journal of Obstetrics and Gynecology,* 183(4), pp. 900-3.

Benirschke, K., Burton, G. and Baergen, R. (2012a) 'Macroscopic Features of the Delivered Placenta', *Pathology of the Human Placenta*: Springer, pp. 13-15.

Benirschke, K., Burton, G. J. and Baergen, R. N. (2012b) 'Early Development of the Human Placenta', *Pathology of the Human Placenta*. Berlin, Heidelberg: Springer Berlin Heidelberg, pp. 41-53.

Benirschke, K. and Kaufmann, P. (2000) *Pathology of the human placenta.* 4th edn. New York: Springer.

Bernstein, I. M., Horbar, J. D., Badger, G. J., Ohlsson, A. and Golan, A. (2000) 'Morbidity and mortality among very-low-birth-weight neonates with intrauterine growth restriction. The Vermont Oxford Network', *American journal of obstetrics and gynecology,* 182(1 Pt 1), pp. 198-206.

Bhattacharyya, S., Saha, S., Giri, K., Lanza, I. R., Nair, K. S., Jennings, N. B., Rodriguez-Aguayo, C., Lopez-Berestein, G., Basal, E., Weaver, A. L., Visscher, D. W., Cliby, W., Sood, A. K., Bhattacharya, R. and Mukherjee, P. (2013) 'Cystathionine beta-synthase (CBS) contributes to advanced ovarian cancer progression and drug resistance', *PLoS One,* 8(11), pp. e79167.

Bibikova, M., Golic, M., Golic, K. G. and Carroll, D. (2002) 'Targeted chromosomal cleavage and mutagenesis in Drosophila using zinc-finger nucleases', *Genetics,* 161(3), pp. 1169-75.

Bing, C., Bao, Y., Jenkins, J., Sanders, P., Manieri, M., Cinti, S., Tisdale, M. J. and Trayhurn, P. (2004) 'Zinc-alpha2-glycoprotein, a lipid mobilizing factor, is expressed in adipocytes and is up-regulated in mice with cancer cachexia', *Proceedings of the National Academy of Sciences of the U S A,* 101(8), pp. 2500-5.

Bir, S. C. and Kevil, C. G. (2013) 'Sulfane sustains vascular health: insights into cystathionine gamma-lyase function', *Circulation,* 127(25), pp. 2472-4.

Blair, E. and Stanley, F. (1990) 'Intrauterine growth and spastic cerebral palsy. I. Association with birth weight for gestational age', *American Journal of Obstetrics and Gynecology,* 162(1), pp. 229-37.

Bloxam, D. L. and Bobinski, P. M. (1984) 'Energy metabolism and glycolysis in the human placenta during ischaemia and in normal labour', *Placenta,* 5(5), pp. 381-94.

Bodnar, L. M., Catov, J. M., Klebanoff, M. A., Ness, R. B. and Roberts, J. M. (2007) 'Prepregnancy Body Mass Index and the Occurrence of Severe Hypertensive Disorders of Pregnancy', *Epidemiology,* 18(2), pp. 234-239.

Bodnar, L. M., Ness, R. B., Harger, G. F. and Roberts, J. M. (2005a) 'Inflammation and triglycerides partially mediate the effect of prepregnancy body mass index on the risk of preeclampsia', *American journal of epidemiology,* 162(12), pp. 1198-206.

Bodnar, L. M., Ness, R. B., Markovic, N. and Roberts, J. M. (2005b) 'The risk of preeclampsia rises with increasing prepregnancy body mass index', *Annals of epidemiology,* 15(7), pp. 475-82.

Bokstrom, H., Brannstrom, M., Alexandersson, M. and Norstrom, A. (1997) 'Leukocyte subpopulations in the human uterine cervical stroma at early and term pregnancy', *Human reproduction,* 12(3), pp. 586-90.

Boney, C. M., Verma, A., Tucker, R. and Vohr, B. R. (2005) 'Metabolic Syndrome in Childhood: Association With Birth Weight, Maternal Obesity, and Gestational Diabetes Mellitus', *Pediatrics,* 115(3), pp. e290-e296.

Bos, E. M., Wang, R., Snijder, P. M., Boersema, M., Damman, J., Fu, M., Moser, J., Hillebrands, J.-L., Ploeg, R. J., Yang, G., Leuvenink, H. G. D. and van Goor, H. (2013) 'Cystathionine γ-lyase protects against renal ischemia/reperfusion by modulating oxidative stress', *Journal of the American Society of Nephrology : JASN,* 24(5), pp. 759-770.

Bourjeily, G., Paidas, M., Khalil, H., Rosene-Montella, K. and Rodger, M. (2010) 'Pulmonary embolism in pregnancy', *The Lancet,* 375(9713), pp. 500-512.

Bouw, G. M., Stolte, L. A. M., Baak, J. P. A. and Oort, J. (1976) 'Quantitative morphology of the placenta 1. Standardization of sampling', *European Journal of Obstetrics & Gynecology and Reproductive Biology,* 6(6), pp. 325-331.

Boveris, A. (1984) 'Determination of the production of superoxide radicals and hydrogen peroxide in mitochondria', *Methods in Enzymology,* 105, pp. 429-35.

Bowyer, L. 2008. The confidential enquiry into maternal and Child health (CEMACH). Saving mothers' lives: reviewing maternal deaths to make motherhood safer 2003–2005. The seventh report of the confidential enquiries into maternal deaths in the UK. SAGE Publications Sage UK: London, England.

Brar, G. A., Yassour, M., Friedman, N., Regev, A., Ingolia, N. T. and Weissman, J. S. (2012) 'High-resolution view of the yeast meiotic program revealed by ribosome profiling', *Science,* 335(6068), pp. 552-7.

Brar, H. S., Platt, L. D., DeVore, G. R., Horenstein, J. and Medearis, A. L. (1988) 'Qualitative assessment of maternal uterine and fetal umbilical artery blood flow and resistance in laboring patients by Doppler velocimetry', *American journal of obstetrics and gynecology,* 158(4), pp. 952-6.

Brouard, S., Otterbein, L. E., Anrather, J., Tobiasch, E., Bach, F. H., Choi, A. M. and Soares, M. P. (2000) 'Carbon monoxide generated by heme oxygenase 1 suppresses endothelial cell apoptosis', *Journal of Experimental Medicine,* 192(7), pp. 1015-26.

Buhimschi, C. S., Buhimschi, I. A., Malinow, A. M. and Weiner, C. P. (2004) 'Intrauterine pressure during the second stage of labor in obese women', *Obstetrics and gynecology,* 103(2), pp. 225-30.

Burton, G. J. and Jauniaux, E. (2011) 'Oxidative stress', *Best practice & research. Clinical obstetrics & gynaecology,* 25(3), pp. 287-99.

Burton, G. J., Jauniaux, E. and Watson, A. L. (1999) 'Maternal arterial connections to the placental intervillous space during the first trimester of human pregnancy: The Boyd Collection revisited', *American Journal of Obstetrics & Gynecology,* 181(3), pp. 718-724.

Burton, G. J., Sebire, N. J., Myatt, L., Tannetta, D., Wang, Y. L., Sadovsky, Y., Staff, A. C. and Redman, C. W. (2014) 'Optimising sample collection for placental research', *Placenta,* 35(1), pp. 9-22.

Burton, G. J., Sibley, C. P. and Jauniaux, E. R. M. (2012) 'Placental Anatomy and Physiology', in GABBE, S.G., NIEBYL, J.R., SIMPSON, J.L., LANDON, M.B., GALAN, H.L., JAUNIAUX, E.R.M. & DRISCOLL, D.A. (eds.) *Obstetrics : normal and problem pregnancies.* sixth ed. Philadelphia: Elsevier/Saunders, pp. 5-22.

Caliendo, G., Cirino, G., Santagada, V. and Wallace, J. L. (2010) 'Synthesis and Biological Effects of Hydrogen Sulfide (H2S): Development of H2S-Releasing Drugs as Pharmaceuticals', *Journal of Medicinal Chemistry,* 53(17), pp. 6275-6286.

Campbell, S. and Dewhurst, C. (1971) 'Diagnosis of the small-for-dates fetus by serial ultrasonic cephalometry', *The Lancet,* 298(7732), pp. 1002-1006.

Chaiworapongsa, T., Romero, R., Korzeniewski, S. J., Kusanovic, J. P., Soto, E., Lam, J., Dong, Z., Than, N. G., Yeo, L., Hernandez-Andrade, E., Conde-Agudelo, A. and Hassan, S. S. (2013) 'Maternal plasma concentrations of angiogenic/antiangiogenic factors in the third trimester of pregnancy to identify the patient at risk for stillbirth at or near term and severe late preeclampsia', *American journal of obstetrics and gynecology,* 208(4), pp. 287.e1-287.e15.

Chakraborty, P. K., Murphy, B., Mustafi, S. B., Dey, A., Xiong, X., Rao, G., Naz, S., Zhang, M., Yang, D., Dhanasekaran, D. N., Bhattacharya, R. and Mukherjee, P. (2018) 'Cystathionine β-synthase regulates mitochondrial morphogenesis in ovarian cancer', *FASEB journal : official publication of the Federation of American Societies for Experimental Biology,* 32(8), pp. 4145-4157.

Chen, D. B., Feng, L., Hodges, J. K., Lechuga, T. J. and Zhang, H. (2017) 'Human trophoblast-derived hydrogen sulfide stimulates placental artery endothelial cell angiogenesis', *Biolology of Reproduction,* 97(3), pp. 478-489.

Chen, Y., Liu, Z. and Xie, X. (2010) 'Hydrogen sulphide attenuates renal and cardiac injury after total hepatic ischemia and reperfusion', *The Journal of surgical research,* 164(2), pp. e305-13.

Chow, L. and Lye, S. J. (1994) 'Expression of the gap junction protein connexin-43 is increased in the human myometrium toward term and with the onset of labor', *American Journal of Obstetrics and Gynecology,* 170(3), pp. 788-95.

Chu, S. Y., Kim, S. Y., Lau, J., Schmid, C. H., Dietz, P. M., Callaghan, W. M. and Curtis, K. M. (2007) 'Maternal obesity and risk of stillbirth: a metaanalysis', *American Journal of Obstetrics and Gynecology,* 197(3), pp. 223-8.

Cindrova-Davies, T., Herrera, E. A., Niu, Y., Kingdom, J., Giussani, D. A. and Burton, G. J. (2013) 'Reduced Cystathionine γ-Lyase and Increased miR-21 Expression Are Associated with Increased Vascular Resistance in Growth-Restricted Pregnancies: Hydrogen Sulfide as a Placental Vasodilator', *The American Journal of Pathology,* 182(4), pp. 1448-1458.

Cindrova-Davies, T., Yung, H.-w., Johns, J., Spasic-Boskovic, O., Korolchuk, S., Jauniaux, E., Burton, G. J. and Charnock-Jones, D. S. (2007) 'Oxidative stress, gene expression and protein changes induced in the human placenta during labor', *The American journal of pathology,* 171(4), pp. 1168-1179.

Craven, C. M., Morgan, T. and Ward, K. (1998) 'Decidual spiral artery remodelling begins before cellular interaction with cytotrophoblasts', *Placenta,* 19(4), pp. 241-52.

Crocker, I. P. (2011) 'Placental Origins of Intrauterine Growth Restriction', in Kay, H.H., Nelson, M. & Wang, Y. (eds.) *The Placenta: From Development to Disease*: Wiley-Blackwell, pp. 237-245.

Crosby, W. M. (1991) 'Studies in fetal malnutrition', *American Journal of Diseases of Children,* 145(8), pp. 871-6.

Cuevasanta, E., Denicola, A., Alvarez, B. and Möller, M. N. (2012) 'Solubility and permeation of hydrogen sulfide in lipid membranes', *PLoS One,* 7(4), pp. e34562.

Cunningham, F., Leveno, K., Bloom, S., Hauth, J., Gilstrap, I. L. and Wenstrom, K. (2005) 'Implantation, embryogenesis, and placental development', *Williams Obstetrics.* 22nd ed: McGraw-Hill, pp. 39–90.

Cunningham, F. G., Cox, S. M., Harstad, T. W., Mason, R. A. and Pritchard, J. A. (1990) 'Chronic renal disease and pregnancy outcome', *American Journal of Obstetrics and Gynecology,* 163(2), pp. 453-9.

d'Emmanuele di Villa Bianca, R., Sorrentino, R., Maffia, P., Mirone, V., Imbimbo, C., Fusco, F., De Palma, R., Ignarro, L. J. and Cirino, G. (2009) 'Hydrogen sulfide as a mediator of human corpus cavernosum smooth-muscle relaxation', *Proceedings of the National Academy of Sciences of the United States of America,* 106(11), pp. 4513-4518.

Demir, B., Demir, S., Pasa, S., Guven, S., Atamer, Y., Atamer, A. and Kocyigit, Y. (2012) 'The role of homocysteine, asymmetric dimethylarginine and nitric oxide in pre-eclampsia', *Journal of Obstetrics and Gynaecology,* 32(6), pp. 525-528.

Denschlag, D., Marculescu, R., Unfried, G., Hefler, L. A., Exner, M., Hashemi, A., Riener, E. K., Keck, C., Tempfer, C. B. and Wagner, O. (2004) 'The size of a microsatellite polymorphism of the haem oxygenase 1 gene is associated with idiopathic recurrent miscarriage', *Molecular human reproduction,* 10(3), pp. 211-4.

Deveraux, Q., Ustrell, V., Pickart, C. and Rechsteiner, M. (1994) 'A 26 S protease subunit that binds ubiquitin conjugates', *Journal of Biological Chemistry,* 269(10), pp. 7059-61.

Díaz-Castro, J., Florido, J., Kajarabille, N., Prados, S., de Paco, C., Ocon, O., Pulido-Moran, M. and Ochoa, J. J. (2015) 'A New Approach to Oxidative Stress and Inflammatory Signaling during Labour in Healthy Mothers and Neonates', *Oxidative Medicine and Cellular Longevity,* 2015, pp. 8.

Dickhout, J. G., Carlisle, R. E., Jerome, D. E., Mohammed-Ali, Z., Jiang, H., Yang, G., Mani, S., Garg, S. K., Banerjee, R., Kaufman, R. J., Maclean, K. N., Wang, R. and Austin, R. C. (2012) 'Integrated stress response modulates cellular redox state via induction of cystathionine γ-lyase: cross-talk between integrated stress response and thiol metabolism', *Journal of Biological Chemistry,* 287(10), pp. 7603-14.

Doctor, B. A., O'Riordan, M. A., Kirchner, H. L., Shah, D. and Hack, M. (2001) 'Perinatal correlates and neonatal outcomes of small for gestational age infants born at term gestation', *American Journal of Obstetrics and Gynecology,* 185(3), pp. 652-9.

Dubova, E. A., Pavlov, K. A., Borovkova, E. I., Bayramova, M. A., Makarov, I. O. and Shchegolev, A. I. (2011) 'Vascular endothelial growth factor and its receptors in the placenta of pregnant women with obesity', *Bulletin of experimental biology and medicine,* 151(2), pp. 253-8.

Duckitt, K. and Harrington, D. (2005) 'Risk factors for pre-eclampsia at antenatal booking: systematic review of controlled studies', *BMJ,* 330(7491), pp. 565.

Dulak, J., Deshane, J., Jozkowicz, A. and Agarwal, A. (2008) 'Heme oxygenase-1 and carbon monoxide in vascular pathobiology: focus on angiogenesis', *Circulation,* 117(2), pp. 231-41.

Duley, L. (2009) 'The global impact of pre-eclampsia and eclampsia', *Seminars in perinatology,* 33(3), pp. 130-7.

Egbor, M., Ansari, T., Morris, N., Green, C. J. and Sibbons, P. D. (2006) 'Morphometric placental villous and vascular abnormalities in early- and late-onset pre-eclampsia with and without fetal growth restriction', *BJOG: An International Journal of Obstetrics & Gynaecology,* 113(5), pp. 580-9.

Ehrenberg, H. M., Mercer, B. M. and Catalano, P. M. (2004) 'The influence of obesity and diabetes on the prevalence of macrosomia', *American Journal of Obstetrics and Gynecology,* 191(3), pp. 964-8.

Elrod, J. W., Calvert, J. W., Morrison, J., Doeller, J. E., Kraus, D. W., Tao, L., Jiao, X., Scalia, R., Kiss, L., Szabo, C., Kimura, H., Chow, C. W. and Lefer, D. J. (2007) 'Hydrogen sulfide attenuates myocardial ischemia-reperfusion injury by preservation of mitochondrial function', *Proceeding of the National Academy of Sciences of the United State of America* 104(39), pp. 15560-5.

Enokido, Y., Suzuki, E., Iwasawa, K., Namekata, K., Okazawa, H. and Kimura, H. (2005) 'Cystathionine beta-synthase, a key enzyme for homocysteine metabolism, is preferentially expressed in the radial glia/astrocyte lineage of developing mouse CNS', *FASEB journal : official publication of the Federation of American Societies for Experimental Biology,* 19(13), pp. 1854-6.

Errington, T. M., Mathur, M., Soderberg, C. K., Denis, A., Perfito, N., Iorns, E. and Nosek, B. A. (2021) 'Investigating the replicability of preclinical cancer biology', *Elife,* 10, pp. e71601.

Esposito, K., Ciotola, M., Schisano, B., Misso, L., Giannetti, G., Ceriello, A. and Giugliano, D. (2006) 'Oxidative stress in the metabolic syndrome', *Journal of endocrinological investigation,* 29(9), pp. 791-5.

Esteve, J. M., Mompo, J., Garcia de la Asuncion, J., Sastre, J., Asensi, M., Boix, J., Vina, J. R., Vina, J. and Pallardo, F. V. (1999) 'Oxidative damage to mitochondrial DNA and glutathione oxidation in apoptosis: studies in vivo and in vitro', *FASEB journal :*

official publication of the Federation of American Societies for Experimental Biology, 13(9), pp. 1055-64.

Farina, A., Sekizawa, A., De Sanctis, P., Purwosunu, Y., Okai, T., Cha, D. H., Kang, J. H., Vicenzi, C., Tempesta, A., Wibowo, N., Valvassori, L. and Rizzo, N. (2008) 'Gene expression in chorionic villous samples at 11 weeks' gestation from women destined to develop preeclampsia', *Prenatal Diagnosis,* 28(10), pp. 956-61.

Faupel-Badger, J. M., Staff, A. C., Thadhani, R., Powe, C. E., Potischman, N., Hoover, R. N. and Troisi, R. (2011) 'Maternal angiogenic profile in pregnancies that remain normotensive', *European journal of obstetrics, gynecology, and reproductive biology,* 158(2), pp. 189-93.

Faxen, M., Nisell, H. and Kublickiene, K. R. (2001) 'Altered mRNA expression of ecNOS and iNOS in myometrium and placenta from women with preeclampsia', *Archives of gynecology and obstetrics,* 265(1), pp. 45-50.

Feng, X., Chen, Y., Zhao, J., Tang, C., Jiang, Z. and Geng, B. (2009) 'Hydrogen sulfide from adipose tissue is a novel insulin resistance regulator', *Biochemical and Biophysical Research Communications,* 380(1), pp. 153-159.

Ferguson, R. E., Carroll, H. P., Harris, A., Maher, E. R., Selby, P. J. and Banks, R. E. (2005) 'Housekeeping proteins: a preliminary study illustrating some limitations as useful references in protein expression studies', *Proteomics,* 5(2), pp. 566-71.

Fernandez-Sanchez, A., Madrigal-Santillan, E., Bautista, M., Esquivel-Soto, J., Morales-Gonzalez, A., Esquivel-Chirino, C., Durante-Montiel, I., Sanchez-Rivera, G., Valadez-Vega, C. and Morales-Gonzalez, J. A. (2011) 'Inflammation, oxidative stress, and obesity', *International journal of molecular sciences,* 12(5), pp. 3117-32.

Flier, J. S., Cook, K. S., Usher, P. and Spiegelman, B. M. (1987) 'Severely impaired adipsin expression in genetic and acquired obesity', *Science,* 237(4813), pp. 405-8.

Fortner, R. T., Pekow, P., Solomon, C. G., Markenson, G. and Chasan-Taber, L. (2009) 'Prepregnancy body mass index, gestational weight gain, and risk of hypertensive pregnancy among Latina women', *American Journal of Obstetrics & Gynecology,* 200(2), pp. 167.e1-167.e7.

Fosang, A. J. and Colbran, R. J. (2015) 'Transparency Is the Key to Quality', *Journal of Biological Chemistry,* 290(50), pp. 29692-4.

Fu, M., Zhang, W., Wu, L., Yang, G., Li, H. and Wang, R. (2012) 'Hydrogen sulfide (H2S) metabolism in mitochondria and its regulatory role in energy production', *Proceedings of National Academy of Sciences of the U S A,* 109(8), pp. 2943-8.

Furne, J., Springfield, J., Koenig, T., DeMaster, E. and Levitt, M. D. (2001) 'Oxidation of hydrogen sulfide and methanethiol to thiosulfate by rat tissues: a specialized function of the colonic mucosa', *Biochemical Pharmacology,* 62(2), pp. 255-9.

Garneau, J. E., Dupuis, M., Villion, M., Romero, D. A., Barrangou, R., Boyaval, P., Fremaux, C., Horvath, P., Magadán, A. H. and Moineau, S. (2010) 'The CRISPR/Cas bacterial immune system cleaves bacteriophage and plasmid DNA', *Nature,* 468(7320), pp. 67-71.

Gazzaniga, J. M. and Burns, T. L. (1993) 'Relationship between diet composition and body fatness, with adjustment for resting energy expenditure and physical activity, in preadolescent children', *The American Journal of Clinical Nutrition,* 58(1), pp. 21-8.

Ge, Y., Konrad, M. A., Matherly, L. H. and Taub, J. W. (2001a) 'Transcriptional regulation of the human cystathionine beta-synthase -1b basal promoter: synergistic transactivation by transcription factors NF-Y and Sp1/Sp3', *The Biochemical journal,* 357(Pt 1), pp. 97-105.

Ge, Y., Matherly, L. H. and Taub, J. W. (2001b) 'Transcriptional Regulation of Cell-specific Expression of the Human Cystathionine β-Synthase Gene by Differential Binding of Sp1/Sp3 to the −1b Promoter', *Journal of Biological Chemistry,* 276(47), pp. 43570-43579.

Geerts, L. and Odendaal, H. J. (2007) 'Severe early onset pre-eclampsia: prognostic value of ultrasound and Doppler assessment', *Journal of Perinatolog,* 27(6), pp. 335-42.

Gemici, B. and Wallace, J. L. (2015) 'Chapter Nine - Anti-inflammatory and Cytoprotective Properties of Hydrogen Sulfide', in Cadenas, E. & Packer, L. (eds.) *Methods in Enzymology*: Academic Press, pp. 169-193.

Genbacev, O., Joslin, R., Damsky, C. H., Polliotti, B. M. and Fisher, S. J. (1996) 'Hypoxia alters early gestation human cytotrophoblast differentiation/invasion in vitro and models the placental defects that occur in preeclampsia', *The Journal of Clinical Investigation,* 97(2), pp. 540-50.

Genbacev, O., Zhou, Y., Ludlow, J. W. and Fisher, S. J. (1997) 'Regulation of Human Placental Development by Oxygen Tension', *Science,* 277(5332), pp. 1669-1672.

Gilda, J. E. and Gomes, A. V. (2013) 'Stain-Free total protein staining is a superior loading control to β-actin for Western blots', *Analytical Biochemistry,* 440(2), pp. 186-8.

Goldenberg, R. L. (2002) 'The management of preterm labor', *Obstetrics and gynecologyl,* 100(5 Pt 1), pp. 1020-37.

Goldman-Wohl, D. and Yagel, S. (2002) 'Regulation of trophoblast invasion: from normal implantation to pre-eclampsia', *Molecular and cellular endocrinology,* 187(1-2), pp. 233-8.

Gomez-Lopez, N., Vega-Sanchez, R., Castillo-Castrejon, M., Romero, R., Cubeiro-Arreola, K. and Vadillo-Ortega, F. (2013) 'Evidence for a role for the adaptive immune response in human term parturition', *American journal of reproductive immunology (New York, N.Y. : 1989),* 69(3), pp. 212-230.

Gong, Q. H., Wang, Q., Pan, L. L., Liu, X. H., Xin, H. and Zhu, Y. Z. (2011) 'S-propargyl-cysteine, a novel hydrogen sulfide-modulated agent, attenuates lipopolysaccharide-induced spatial learning and memory impairment: involvement of TNF signaling and NF-κB pathway in rats', *Brain, Behaviour & Immunity,* 25(1), pp. 110-9.

Grabski, A. C. (2009) 'Advances in preparation of biological extracts for protein purification', *Methods in Enzymology,* 463, pp. 285-303.

Grey, J. F. E., Townley, A. R., Everitt, N. M., Campbell-Ritchie, A. and Wheatley, S. P. (2019) 'A cost-effective, analytical method for measuring metabolic load of mitochondria', *Metabolism Open,* 4, pp. 100020.

Gude, N. M., Roberts, C. T., Kalionis, B. and King, R. G. (2004) 'Growth and function of the normal human placenta', *Thrombosis research,* 114(5-6), pp. 5-6.

Guschin, D. Y., Waite, A. J., Katibah, G. E., Miller, J. C., Holmes, M. C. and Rebar, E. J. (2010) 'A rapid and general assay for monitoring endogenous gene modification', *Methods in Molecular Biology,* 649, pp. 247-56.

Guzmán, M. A., Navarro, M. A., Carnicer, R., Sarría, A. J., Acín, S., Arnal, C., Muniesa, P., Surra, J. C., Arbonés-Mainar, J. M., Maeda, N. and Osada, J. (2006) 'Cystathionine β-synthase is essential for female reproductive function', *Human Molecular Genetics,* 15(21), pp. 3168-3176.

Gygi, S. P., Rochon, Y., Franza, B. R. and Aebersold, R. (1999) 'Correlation between protein and mRNA abundance in yeast', *Molecular and Cellular Biology,* 19(3), pp. 1720-30.

Hannestad, U., Mårtensson, J., Sjödahl, R. and Sörbo, B. (1981) '3-Mercaptolactate cysteine disulfiduria: Biochemical studies on affected and unaffected members of a family', *Biochemical Medicine,* 26(1), pp. 106-114.

Harding, H. P., Zhang, Y., Zeng, H., Novoa, I., Lu, P. D., Calfon, M., Sadri, N., Yun, C., Popko, B., Paules, R., Stojdl, D. F., Bell, J. C., Hettmann, T., Leiden, J. M. and Ron, D. (2003) 'An integrated stress response regulates amino acid metabolism and resistance to oxidative stress', *Molecular Cell,* 11(3), pp. 619-33.

Hauth, J. C., Ewell, M. G., Levine, R. J., Esterlitz, J. R., Sibai, B., Curet, L. B., Catalano, P. M. and Morris, C. D. (2000) 'Pregnancy outcomes in healthy nulliparas who

developed hypertension. Calcium for Preeclampsia Prevention Study Group', *Obstetrics and Gynecology,* 95(1), pp. 24-8.

Hayden, L. J., Franklin, K. J., Roth, S. H. and Moore, G. J. (1989) 'Inhibition of oxytocin-induced but not angiotensin-induced rat uterine contractions following exposure to sodium sulfide', *Life Sciences,* 45(26), pp. 2557-60.

Hecher, K., Spernol, R., Stettner, H. and Szalay, S. (1992) 'Potential for diagnosing imminent risk to appropriate- and small-for-gestational-age fetuses by Doppler sonographic examination of umbilical and cerebral arterial blood flow', *Ultrasound in Obstetrics & Gynecology,* 2(4), pp. 266-71.

Hempstock, J., Jauniaux, E., Greenwold, N. and Burton, G. J. (2003) 'The contribution of placental oxidative stress to early pregnancy failure', *Human Pathology,* 34(12), pp. 1265-75.

Hendrix, N. and Berghella, V. (2008) 'Non-placental causes of intrauterine growth restriction', *Seminnars in Perinatology,* 32(3), pp. 161-5.

Herman, A., Zimerman, A., Arieli, S., Tovbin, Y., Bezer, M., Bukovsky, I. and Panski, M. (2002) 'Down-up sequential separation of the placenta', *Ultrasound in Obstetrics & Gynecology : the official journal of the International Society of Ultrasound in Obstetrics and Gynecology,* 19(3), pp. 278-81.

Hernández-Díaz, S., Toh, S. and Cnattingius, S. (2009) 'Risk of pre-eclampsia in first and subsequent pregnancies: prospective cohort study', *The BMJ,* 338, pp. b2255.

Heslehurst, N., Ells, L. J., Simpson, H., Batterham, A., Wilkinson, J. and Summerbell, C. D. (2007) 'Trends in maternal obesity incidence rates, demographic predictors, and health inequalities in 36, 821 women over a 15-year period', *BJOG: An International Journal of Obstetrics & Gynaecology,* 114(2), pp. 187-194.

Hine, C., Kim, H.-J., Zhu, Y., Harputlugil, E., Longchamp, A., Matos, M. S., Ramadoss, P., Bauerle, K., Brace, L., Asara, J. M., Ozaki, C. K., Cheng, S.-y., Singha, S., Ahn, K. H., Kimmelman, A., Fisher, F. M., Pissios, P., Withers, D. J., Selman, C., Wang, R., Yen, K., Longo, V. D., Cohen, P., Bartke, A., Kopchick, J. J., Miller, R., Hollenberg, A. N. and Mitchell, J. R. (2017) 'Hypothalamic-Pituitary Axis Regulates Hydrogen Sulfide Production', *Cell Metabolism,* 25(6), pp. 1320-1333.e5.

Hogg, K., Price, E. M. and Robinson, W. P. (2014) 'Improved reporting of DNA methylation data derived from studies of the human placenta', *Epigenetics,* 9(3), pp. 333-7.

Holmen, S. L., Vanbrocklin, M. W., Eversole, R. R., Stapleton, S. R. and Ginsberg, L. C. (1995) 'Efficient lipid-mediated transfection of DNA into primary rat hepatocytes', *In Vitro Cellular and Developmental Biolology. Animal,* 31(5), pp. 347-51.

Holwerda, K. M., Bos, E. M., Rajakumar, A., Ris-Stalpers, C., van Pampus, M. G., Timmer, A., Erwich, J. J. H. M., Faas, M. M., van Goor, H. and Lely, A. T. (2012) 'Hydrogen sulfide producing enzymes in pregnancy and preeclampsia', *Placenta,* 33(6), pp. 518-521.

Holwerda, K. M., Burke, S. D., Faas, M. M., Zsengeller, Z., Stillman, I. E., Kang, P. M., van Goor, H., McCurley, A., Jaffe, I. Z., Karumanchi, S. A. and Lely, A. T. (2014) 'Hydrogen sulfide attenuates sFlt1-induced hypertension and renal damage by upregulating vascular endothelial growth factor', *Journal of the American Society of Nephrology : JASN,* 25(4), pp. 717-25.

Holwerda, K. M., Faas, M. M., van Goor, H. and Lely, A. T. (2013) 'Gasotransmitters: A Solution for the Therapeutic Dilemma in Preeclampsia?', *Hypertension,* 62(4), pp. 653-659.

Hosoki, R., Matsuki, N. and Kimura, H. (1997) 'The possible role of hydrogen sulfide as an endogenous smooth muscle relaxant in synergy with nitric oxide', *Biochemical & Biophysical Research Communications,* 237(3), pp. 527-31.

House, J. D., Brosnan, M. E. and Brosnan, J. T. (1997) 'Characterization of homocysteine metabolism in the rat kidney', *The Biochemical journal,* 328 (Pt 1)(Pt 1), pp. 287-292.

Hsiau, T., Maures, T., Waite, K., Yang, J., Kelso, R., Holden, K. and Stoner, R. (2018) 'Inference of CRISPR Edits from Sanger Trace Data', *bioRxiv*, pp. 251082.

Hsu, P. D., Scott, D. A., Weinstein, J. A., Ran, F. A., Konermann, S., Agarwala, V., Li, Y., Fine, E. J., Wu, X., Shalem, O., Cradick, T. J., Marraffini, L. A., Bao, G. and Zhang, F. (2013) 'DNA targeting specificity of RNA-guided Cas9 nucleases', *Nature biotechnology,* 31(9), pp. 827-832.

Hu, F. B., Manson, J. E., Stampfer, M. J., Colditz, G., Liu, S., Solomon, C. G. and Willett, W. C. (2001) 'Diet, lifestyle, and the risk of type 2 diabetes mellitus in women', *New England Journal of Medicine,* 345(11), pp. 790-7.

Hu, L. F., Lu, M., Wu, Z. Y., Wong, P. T. and Bian, J. S. (2009) 'Hydrogen sulfide inhibits rotenone-induced apoptosis via preservation of mitochondrial function', *Molecular Pharmacology,* 75(1), pp. 27-34.

Hu, R., Lu, J., You, X., Zhu, X., Hui, N. and Ni, X. (2011) 'Hydrogen sulfide inhibits the spontaneous and oxytocin-induced contractility of human pregnant myometrium', *Gynecological endocrinology : the official journal of the International Society of Gynecological Endocrinology,* 27(11), pp. 900-4.

Hu, T., Wang, G., Zhu, Z., Huang, Y., Gu, H. and Ni, X. (2015) 'Increased ADAM10 expression in preeclamptic placentas is associated with decreased expression of hydrogen sulfide production enzymes', *Placenta,* 36(8), pp. 947-50.

Hu, T. X., Guo, X., Wang, G., Gao, L., He, P., Xia, Y., Gu, H. and Ni, X. (2017) 'MiR133b is involved in endogenous hydrogen sulfide suppression of sFlt-1 production in human placenta', *Placenta,* 52, pp. 33-40.

Hu, T. X., Wang, G., Guo, X. J., Sun, Q. Q., He, P., Gu, H., Huang, Y., Gao, L. and Ni, X. (2016) 'MiR 20a,-20b and -200c are involved in hydrogen sulfide stimulation of VEGF production in human placental trophoblasts', *Placenta,* 39, pp. 101-10.

Hung, T. H., Skepper, J. N. and Burton, G. J. (2001) 'In Vitro Ischemia-Reperfusion Injury in Term Human Placenta as a Model for Oxidative Stress in Pathological Pregnancies', *The American Journal of Pathology,* 159(3), pp. 1031-43.

Hung, T. H., Skepper, J. N., Charnock-Jones, D. S. and Burton, G. J. (2002) 'Hypoxia-reoxygenation: a potent inducer of apoptotic changes in the human placenta and possible etiological factor in preeclampsia', *Circulation Research,* 90(12), pp. 1274-81.

Illsley, N. P. (2011) 'Placental Metabolism', in Kay, H.H., Nelson, M. & Wang, Y. (eds.) *The Placenta: From development to Disease* Wiley-Blackwell, pp. 50-56.

Irgens, H. U., Reisaeter, L., Irgens, L. M. and Lie, R. T. (2001) 'Long term mortality of mothers and fathers after pre-eclampsia: population based cohort study', *Bmj,* 323(7323), pp. 1213-7.

Irving, J. A., Lysiak, J. J., Graham, C. H., Hearn, S., Han, V. K. and Lala, P. K. (1995) 'Characteristics of trophoblast cells migrating from first trimester chorionic villus explants and propagated in culture', *Placenta,* 16(5), pp. 413-33.

Ishigami, M., Hiraki, K., Umemura, K., Ogasawara, Y., Ishii, K. and Kimura, H. (2009) 'A source of hydrogen sulfide and a mechanism of its release in the brain', *Antioxidants & Redox Signaling,* 11(2), pp. 205-14.

Jarvie, E., Hauguel-de-Mouzon, S., Nelson, S. M., Sattar, N., Catalano, P. M. and Freeman, D. J. (2010) 'Lipotoxicity in obese pregnancy and its potential role in adverse pregnancy outcome and obesity in the offspring', *Clinical Science (London),* 119(3), pp. 123-9.

Jarvie, E. and Ramsay, J. E. (2010) 'Obstetric management of obesity in pregnancy', *SFNM Seminars in Fetal and Neonatal Medicine,* 15(2), pp. 83-88.

Jauniaux, E., Watson, A. L., Hempstock, J., Bao, Y. P., Skepper, J. N. and Burton, G. J. (2000) 'Onset of maternal arterial blood flow and placental oxidative stress. A possible factor in human early pregnancy failure', *The American journal of pathology,* 157(6), pp. 2111-22.

Jin, Z. G., Melaragno, M. G., Liao, D. F., Yan, C., Haendeler, J., Suh, Y. A., Lambeth, J. D. and Berk, B. C. (2000) 'Cyclophilin A is a secreted growth factor induced by oxidative stress', *Circulation Research,* 87(9), pp. 789-96.

Jinek, M., Chylinski, K., Fonfara, I., Hauer, M., Doudna, J. A. and Charpentier, E. (2012) 'A programmable dual-RNA-guided DNA endonuclease in adaptive bacterial immunity', *Science,* 337(6096), pp. 816-21.

Johri, A., Chandra, A. and Flint Beal, M. (2013) 'PGC-1α, mitochondrial dysfunction, and Huntington's disease', *Free Radical Biology & Medicine,* 62, pp. 37-46.

Kaaja, R. (1998) 'Insulin Resistance Syndrome in Preeclampsia', *Seminars in reproductive endocrinology.,* 16(1), pp. 41.

Kabil, O., Zhou, Y. and Banerjee, R. (2006) 'Human cystathionine beta-synthase is a target for sumoylation', *Biochemistry,* 45(45), pp. 13528-36.

Kenchaiah, S., Evans, J. C., Levy, D., Wilson, P. W., Benjamin, E. J., Larson, M. G., Kannel, W. B. and Vasan, R. S. (2002) 'Obesity and the risk of heart failure', *The New England journal of medicine,* 347(5), pp. 305-13.

Kery, V., Bukovska, G. and Kraus, J. P. (1994) 'Transsulfuration depends on heme in addition to pyridoxal 5'-phosphate. Cystathionine beta-synthase is a heme protein', *Journal of Biological Chemistry,* 269(41), pp. 25283-8.

Kery, V., Poneleit, L. and Kraus, J. P. (1998) 'Trypsin cleavage of human cystathionine β-synthase into an evolutionarily conserved active core: structural and functional consequences', *Archives of biochemistry and biophysics,* 355(2), pp. 222-232.

Khan, K. S., Wojdyla, D., Say, L., Gulmezoglu, A. M. and Van Look, P. F. (2006) 'WHO analysis of causes of maternal death: a systematic review', *Lancet,* 367(9516), pp. 1066-74.

Khoury, G. A., Baliban, R. C. and Floudas, C. A. (2011) 'Proteome-wide post-translational modification statistics: frequency analysis and curation of the swiss-prot database', *Scientific reports,* 1, pp. 90.

Khoury, M. J., Erickson, J. D., Cordero, J. F. and McCarthy, B. J. (1988) 'Congenital malformations and intrauterine growth retardation: a population study', *Pediatrics,* 82(1), pp. 83-90.

Kimura, H. (2011) 'Hydrogen sulfide: its production, release and functions', *Amino Acids,* 41(1), pp. 113-121.

Kimura, H. (2014) 'Production and physiological effects of hydrogen sulfide', *Antioxidants & Redox Signaling,* 20(5), pp. 783-93.

Kimura, Y., Goto, Y. and Kimura, H. (2010) 'Hydrogen sulfide increases glutathione production and suppresses oxidative stress in mitochondria', *Antioxidants & Redox Signaling,* 12(1), pp. 1-13.

Kimura, Y. and Kimura, H. (2004) 'Hydrogen sulfide protects neurons from oxidative stress', *FASEB journal : official publication of the Federation of American Societies for Experimental Biology,* 18(10), pp. 1165-7.

Klabunde, R. E. (2004) *Cardiovascular physiology concepts.* 1st edn. Philadelphia: Wolters Kluwer Health/Lippincott Williams & Wilkins, p. 79-88.

Knight, M. (2008) 'Antenatal pulmonary embolism: risk factors, management and outcomes', *BJOG: An International Journal of Obstetrics & Gynaecology,* 115(4), pp. 453-461.

Kohmoto, J., Nakao, A., Stolz, D. B., Kaizu, T., Tsung, A., Ikeda, A., Shimizu, H., Takahashi, T., Tomiyama, K., Sugimoto, R., Choi, A. M., Billiar, T. R., Murase, N. and McCurry, K. R. (2007) 'Carbon monoxide protects rat lung transplants from ischemia-reperfusion injury via a mechanism involving p38 MAPK pathway', *American Journal of Transplantation,* 7(10), pp. 2279-90.

Kokawa, K., Shikone, T. and Nakano, R. (1998) 'Apoptosis in human chorionic villi and decidua during normal embryonic development and spontaneous abortion in the first trimester', *Placenta,* 19(1), pp. 21-6.

Konje, J. C., Huppertz, B., Bell, S. C., Taylor, D. J. and Kaufmann, P. (2003) '3-dimensional colour power angiography for staging human placental development', *Lancet,* 362(9391), pp. 1199-201.

Koussounadis, A., Langdon, S. P., Um, I. H., Harrison, D. J. and Smith, V. A. (2015) 'Relationship between differentially expressed mRNA and mRNA-protein correlations in a xenograft model system', *Scientific reports,* 5, pp. 10775-10775.

Kraus, J. P., Janosik, M., Kozich, V., Mandell, R., Shih, V., Sperandeo, M. P., Sebastio, G., de Franchis, R., Andria, G., Kluijtmans, L. A., Blom, H., Boers, G. H., Gordon, R. B., Kamoun, P., Tsai, M. Y., Kruger, W. D., Koch, H. G., Ohura, T. and Gaustadnes, M. (1999) 'Cystathionine beta-synthase mutations in homocystinuria', *Human Mutation,* 13(5), pp. 362-75.

Kraus, J. P., Oliveriusová, J., Sokolová, J., Kraus, E., Vlček, Č., ́r, de Franchis, R., Maclean, K. N., Bao, L., Bukovská, G. and Patterson, D. (1998) 'The human cystathionine β-synthase (CBS) gene: complete sequence, alternative splicing, and polymorphisms', *Genomics,* 52(3), pp. 312-324.

Kristensen, J., Vestergaard, M., Wisborg, K., Kesmodel, U. and Secher, N. J. (2005) 'Pre-pregnancy weight and the risk of stillbirth and neonatal death', *BJOG: An International Journal of Obstetrics & Gynaecology,* 112(4), pp. 403-8.

Laivuori, H., Kaaja, R., Koistinen, H., Karonen, S. L., Andersson, S., Koivisto, V. and Ylikorkala, O. (2000) 'Leptin during and after preeclamptic or normal pregnancy: its relation to serum insulin and insulin sensitivity', *Metabolism,* 49(2), pp. 259-63.

Langley-Evans, S. C. (2006) 'Developmental programming of health and disease', *The Proceedings of the Nutrition Society,* 65(1), pp. 97-105.

Lanoix, D., St-Pierre, J., Lacasse, A. A., Viau, M., Lafond, J. and Vaillancourt, C. (2012) 'Stability of reference proteins in human placenta: general protein stains are the benchmark', *Placenta,* 33(3), pp. 151-6.

Larsen, T. B., Sørensen, H. T., Gislum, M. and Johnsen, S. P. (2007) 'Maternal smoking, obesity, and risk of venous thromboembolism during pregnancy and the puerperium: a population-based nested case-control study', *Thrombosis Research,* 120(4), pp. 505-9.

Lee, K. J., Shim, S. H., Kang, K. M., Kang, J. H., Park, D. Y., Kim, S. H., Farina, A., Shim, S. S. and Cha, D. H. (2010) 'Global Gene Expression Changes Induced in the Human Placenta during Labor', *Placenta,* 31(8), pp. 698-704.

Lee, M., Schwab, C., Yu, S., McGeer, E. and McGeer, P. L. (2009) 'Astrocytes produce the antiinflammatory and neuroprotective agent hydrogen sulfide', *Neurobiol Aging,* 30(10), pp. 1523-34.

Lefer, D. J. (2007) 'A new gaseous signaling molecule emerges: Cardioprotective role of hydrogen sulfide', *Proceedings of the National Academy of Sciences of the United States of America,* 104(46), pp. 17907-17908.

Leffler, C. W., Nasjletti, A., Yu, C., Johnson, R. A., Fedinec, A. L. and Walker, N. (1999) 'Carbon monoxide and cerebral microvascular tone in newborn pigs', *The American Journal of Physiology* 276(5), pp. H1641-6.

Levonen, A. L., Lapatto, R., Saksela, M. and Raivio, K. O. (2000) 'Human cystathionine gamma-lyase: developmental and in vitro expression of two isoforms', *Biochemical Journal,* 347 Pt 1(Pt 1), pp. 291-5.

Lewis, G., Confidential Enquiries into Maternal Deaths in the United, K., Confidential Enquiry into, M. and Child, H. (2007) *Saving mothers' lives : reviewing maternal deaths to make motherhood safer - 2003-2005 : the seventh report of the Confidential Enquiries into Maternal Deaths in the United Kingdom.* London: CEMACH.

Lewis, G., Drife, J. O., Clutton-Brock, T., Confidential Enquiry into, M. and Child, H. (2004) 'Why mothers die : 2000-2002 : the sixth report of the confidential enquiries into maternal deaths in the United Kingdom'.

Li, N., Chen, L., Muh, R. W. and Li, P. L. (2006) 'Hyperhomocysteinemia associated with decreased renal transsulfuration activity in Dahl S rats', *Hypertension,* 47(6), pp. 1094-100.

Lian, I. A., Langaas, M., Moses, E. and Johansson, Å. (2013) 'Differential gene expression at the maternal-fetal interface in preeclampsia is influenced by gestational age', *PloS one,* 8(7), pp. e69848-e69848.

Lin, C. C., Su, S. J. and River, L. P. (1991) 'Comparison of associated high-risk factors and perinatal outcome between symmetric and asymmetric fetal intrauterine growth retardation', *American Journal of Obstetrics and Gynecology,* 164(6 Pt 1), pp. 1535-41; discussion 1541-2.

Lindhard, A., Bentin-Ley, U., Ravn, V., Islin, H., Hviid, T., Rex, S., Bangsbøll, S. and Sørensen, S. (2002) 'Biochemical evaluation of endometrial function at the time of implantation', *Fertility and Sterility,* 78(2), pp. 221-233.

Linzke, N., Schumacher, A., Woidacki, K., Croy, B. A. and Zenclussen, A. C. (2014) 'Carbon monoxide promotes proliferation of uterine natural killer cells and remodeling of spiral arteries in pregnant hypertensive heme oxygenase-1 mutant mice', *Hypertension,* 63(3), pp. 580-8.

Lithgow, G. J., Driscoll, M. and Phillips, P. (2017) 'A long journey to reproducible results', *Nature,* 548(7668), pp. 387-388.

Liu, J., Wang, X. F., Wang, Y., Wang, H. W. and Liu, Y. (2014) 'The incidence rate, high-risk factors, and short- and long-term adverse outcomes of fetal growth restriction: a report from Mainland China', *Medicine (Baltimore),* 93(27), pp. e210.

Liu, N., Wu, J., Zhang, L., Gao, Z., Sun, Y., Yu, M., Zhao, Y., Dong, S., Lu, F. and Zhang, W. (2017) 'Hydrogen Sulphide modulating mitochondrial morphology to promote mitophagy in endothelial cells under high-glucose and high-palmitate', *Journal of Cellular &Molecular Medicine,* 21(12), pp. 3190-3203.

Liu, W., Xu, C., You, X., Olson, D. M., Chemtob, S., Gao, L. and Ni, X. (2016) 'Hydrogen Sulfide Delays LPS-Induced Preterm Birth in Mice via Anti-Inflammatory Pathways', *PLoS One,* 11(4), pp. e0152838.

Livak, K. J. and Schmittgen, T. D. (2001) 'Analysis of Relative Gene Expression Data Using Real-Time Quantitative PCR and the 2−ΔΔCT Method', *Methods,* 25(4), pp. 402-408.

Lowe, G., Woodward, M., Hillis, G., Rumley, A., Li, Q., Harrap, S., Marre, M., Hamet, P., Patel, A., Poulter, N. and Chalmers, J. (2014) 'Circulating inflammatory markers and the risk of vascular complications and mortality in people with type 2 diabetes and cardiovascular disease or risk factors: the ADVANCE study', *Diabetes,* 63(3), pp. 1115-23.

Lowicka, E. and Beltowski, J. (2007) 'Hydrogen sulfide (H2S) - the third gas of interest for pharmacologists', *Pharmacological reports : PR,* 59(1), pp. 4-24.

Lu, L., Kingdom, J., Burton, G. J. and Cindrova-Davies, T. (2017) 'Placental Stem Villus Arterial Remodeling Associated with Reduced Hydrogen Sulfide Synthesis Contributes to Human Fetal Growth Restriction', *The American Journal of Pathology,* 187(4), pp. 908-920.

Lu, Y., O'Dowd, B. F., Orrego, H. and Israel, Y. (1992) 'Cloning and nucleotide sequence of human liver cDNA encoding for cystathionine gamma-lyase', *Biochemical & Biophys ical Research Communications,* 189(2), pp. 749-58.

Lubchenco, L. O., Hansman, C., Dressler, M. and Boyd, E. (1963) 'Intrauterine growth as estimated from liveborn birth-weight data at 24 to 42 weeks of gestation', *Pediatrics,* 32, pp. 793-800.

Ludwig, D. S., Peterson, K. E. and Gortmaker, S. L. (2001) 'Relation between consumption of sugar-sweetened drinks and childhood obesity: a prospective, observational analysis', *Lancet,* 357(9255), pp. 505-8.

Lyall, F. (2006) 'Mechanisms regulating cytotrophoblast invasion in normal pregnancy and pre-eclampsia', *Australian and New Zealand Journal of Obstetrics and Gynaecology,* 46(4), pp. 266-273.

Lyall, F., Barber, A., Myatt, L., Bulmer, J. N. and Robson, S. C. (2000) 'Hemeoxygenase expression in human placenta and placental bed implies a role in regulation of trophoblast invasion and placental function', *FASEB journal : official publication of the Federation of American Societies for Experimental Biology,* 14(1), pp. 208-19.

Lyall, F. and Belfort, M. A. (2007) *Pre-eclampsia : etiology and clinical practice.* Cambridge: Cambridge University Press.

Lyall, F., Bulmer, J. N., Kelly, H., Duffie, E. and Robson, S. C. (1999) 'Human trophoblast invasion and spiral artery transformation: the role of nitric oxide', *The American journal of pathology,* 154(4), pp. 1105-14.

Lyall, F., Jablonka-Shariff, A., Johnson, R. D., Olson, L. M. and Nelson, D. M. (1998) 'Gene expression of nitric oxide synthase in cultured human term placental trophoblast during in vitro differentiation', *Placenta,* 19(4), pp. 253-60.

Lyall, F., Robson, S. C. and Bulmer, J. N. (2013) 'Spiral artery remodeling and trophoblast invasion in preeclampsia and fetal growth restriction: relationship to clinical outcome', *Hypertension,* 62(6), pp. 1046-54.

Lyall, F., Simpson, H., Bulmer, J. N., Barber, A. and Robson, S. C. (2001) 'Transforming growth factor-beta expression in human placenta and placental bed in third trimester normal pregnancy, preeclampsia, and fetal growth restriction', *The American journal of pathology,* 159(5), pp. 1827-1838.

MacKay, V. L., Li, X., Flory, M. R., Turcott, E., Law, G. L., Serikawa, K. A., Xu, X. L., Lee, H., Goodlett, D. R., Aebersold, R., Zhao, L. P. and Morris, D. R. (2004) 'Gene expression analyzed by high-resolution state array analysis and quantitative proteomics: response of yeast to mating pheromone', *Molecular & cellular proteomics : MCP,* 3(5), pp. 478-89.

Maier, T., Guell, M. and Serrano, L. (2009) 'Correlation of mRNA and protein in complex biological samples', *FEBS letters,* 583(24), pp. 3966-73.

Maines, M. D. (1993) 'Carbon Monoxide: An Emerging Regulator of cGMP in the Brain', *Molecular and Cellular Neurosciences,* 4(5), pp. 389-97.

Makarova, K. S., Haft, D. H., Barrangou, R., Brouns, S. J., Charpentier, E., Horvath, P., Moineau, S., Mojica, F. J., Wolf, Y. I., Yakunin, A. F., van der Oost, J. and Koonin, E. V. (2011) 'Evolution and classification of the CRISPR-Cas systems', *Nature Reviews, Microbiology,* 9(6), pp. 467-77.

Malti, N., Merzouk, H., Merzouk, S. A., Loukidi, B., Karaouzene, N., Malti, A. and Narce, M. (2014) 'Oxidative stress and maternal obesity: feto-placental unit interaction', *Placenta,* 35(6), pp. 411-6.

Many, A. and Roberts, J. M. (1997) 'Increased xanthine oxidase during labour—implications for oxidative stress', *Placenta,* 18(8), pp. 725-726.

Many, A., Schreiber, L., Rosner, S., Lessing, J. B., Eldor, A. and Kupferminc, M. J. (2001) 'Pathologic features of the placenta in women with severe pregnancy complications and thrombophilia', *Obstetrics and Gynecology,* 98(6), pp. 1041-4.

Martín, J. A., Pereda, J., Martínez-López, I., Escrig, R., Miralles, V., Pallardó, F. V., Viña, J. R., Vento, M., Viña, J. and Sastre, J. (2007) 'Oxidative stress as a signal to up-regulate gamma-cystathionase in the fetal-to-neonatal transition in rats', *Cellular & Molecular Biol ogy (Noisy-le-grand),* 53 Suppl, pp. Ol1010-7.

Martin, W. L. and Hutchon, S. P. (2004) 'Mechanism and management of normal labour', *Current Obstetrics & Gynaecology,* 14(5), pp. 301-308.

Matijevic, R., Meekins, J. W., Walkinshaw, S. A., Neilson, J. P. and McFadyen, I. R. (1995) 'Spiral artery blood flow in the central and peripheral areas of the placental bed in the second trimester', *Obstetrics and gynecology,* 86(2), pp. 289-92.

Mattar, F. and Sibai, B. M. (2000) 'Eclampsia. VIII. Risk factors for maternal morbidity', *American Journal of Obstetrics and Gynecology,* 182(2), pp. 307-12.

Mayhew, T. M. (2008) 'Taking Tissue Samples from the Placenta: An Illustration of Principles and Strategies', *Placenta,* 29(1), pp. 1-14.

Maynard, S. E., Min, J. Y., Merchan, J., Lim, K. H., Li, J., Mondal, S., Libermann, T. A., Morgan, J. P., Sellke, F. W., Stillman, I. E., Epstein, F. H., Sukhatme, V. P. and Karumanchi, S. A. (2003) 'Excess placental soluble fms-like tyrosine kinase 1 (sFlt1) may contribute to endothelial dysfunction, hypertension, and proteinuria in preeclampsia', *The Journal of Clinical Investigation,* 111(5), pp. 649-58.

Mazaki-Tovi, S., Romero, R., Vaisbuch, E., Kusanovic, J. P., Erez, O., Gotsch, F., Chaiworapongsa, T., Than, N. G., Kim, S. K., Nhan-Chang, C. L., Jodicke, C., Pacora, P., Yeo, L., Dong, Z., Yoon, B. H., Hassan, S. S. and Mittal, P. (2009) 'Maternal serum adiponectin multimers in preeclampsia', *Journal of perinatal medicine,* 37(4), pp. 349-63.

McCaig, D. and Lyall, F. (2009) 'Heme Oxygenase Expression in Human Placental Villous Tissue in Response to Exposure to in vitro Ischemia-Reperfusion Injury', *Hypertension in Pregnancy,* 28(3), pp. 256-272.

McNamara, J. M. and Kay, H. H. (2011) 'Placental Hormones: Physiology, Disease, and Prenatal Diagnosis', in Kay, H.H., Nelson, M. & Wang, Y. (eds.) *The Placenta: From Development to Disease*: Wiley-Blackwell, pp. 57-65.

Meekins, J. W., Pijnenborg, R., Hanssens, M., McFadyen, I. R. and van Asshe, A. (1994) 'A study of placental bed spiral arteries and trophoblast invasion in normal and severe pre-eclamptic pregnancies', *British Journal of Obstetrics and Gynaecology,* 101(8), pp. 669-74.

Menendez, C., Ordi, J., Ismail, M. R., Ventura, P. J., Aponte, J. J., Kahigwa, E., Font, F. and Alonso, P. L. (2000) 'The impact of placental malaria on gestational age and birth weight', *The Journal of Infectious Diseases,* 181(5), pp. 1740-5.

Mijal, R. S., Holzman, C. B., Rana, S., Karumanchi, S. A., Wang, J. and Sikorskii, A. (2011) 'Midpregnancy levels of angiogenic markers in relation to maternal characteristics', *American Journal of Obstetrics & Gynecology,* 204(3), pp. 244.e1-12.

Mikami, Y., Shibuya, N., Kimura, Y., Nagahara, N., Ogasawara, Y. and Kimura, H. (2011a) 'Thioredoxin and dihydrolipoic acid are required for 3-mercaptopyruvate sulfurtransferase to produce hydrogen sulfide', *Biochemical Journal,* 439(3), pp. 479-85.

Mikami, Y., Shibuya, N., Kimura, Y., Nagahara, N., Yamada, M. and Kimura, H. (2011b) 'Hydrogen sulfide protects the retina from light-induced degeneration by the modulation of Ca2+ influx', *Journal of Biological Chemistry,* 286(45), pp. 39379-86.

Militello, M., Pappalardo, E. M., Ermito, S., Dinatale, A., Cavaliere, A. and Carrara, S. (2009) 'Obstetric management of IUGR', *Journal of Prenatal Medicine,* 3(1), pp. 6-9.

Mislanova, C., Martsenyuk, O., Huppertz, B. and Obolenskaya, M. (2011) 'Placental markers of folate-related metabolism in preeclampsia', *Reproduction,* 142(3), pp. 467-76.

Miyamoto, R., Otsuguro, K.-i., Yamaguchi, S. and Ito, S. (2014) 'Contribution of cysteine aminotransferase and mercaptopyruvate sulfurtransferase to hydrogen sulfide production in peripheral neurons', *Journal of Neurochemistry,* 130(1), pp. 29-40.

Módis, K., Coletta, C., Erdélyi, K., Papapetropoulos, A. and Szabo, C. (2013) 'Intramitochondrial hydrogen sulfide production by 3-mercaptopyruvate sulfurtransferase maintains mitochondrial electron flow and supports cellular bioenergetics', *FASEB journal : official publication of the Federation of American Societies for Experimental Biology,* 27(2), pp. 601-11.

Mongraw-Chaffin, M. L., Cirillo, P. M. and Cohn, B. A. (2010) 'Preeclampsia and cardiovascular disease death: prospective evidence from the child health and development studies cohort', *Hypertension,* 56(1), pp. 166-71.

Murthi, P., Abumaree, M. and Kalionis, B. (2014) 'Analysis of homeobox gene action may reveal novel angiogenic pathways in normal placental vasculature and in clinical pregnancy disorders associated with abnormal placental angiogenesis', *Frontiers in Pharmacology,* 5, pp. 133.

Myatt, L. (1992) 'Control of vascular resistance in the human placenta', *Placenta,* 13(4), pp. 329-41.

Myatt, L., Brewer, A. and Brockman, D. E. (1991) 'The action of nitric oxide in the perfused human fetal-placental circulation', *American journal of obstetrics and gynecology,* 164(2), pp. 687-92.

Myatt, L. and Cui, X. (2004) 'Oxidative stress in the placenta', *Histochem Cell Biol Histochemistry and Cell Biology,* 122(4), pp. 369-382.

Myatt, L., Redman, C. W., Staff, A. C., Hansson, S., Wilson, M. L., Laivuori, H., Poston, L. and Roberts, J. M. (2014) 'Strategy for standardization of preeclampsia research study design', *Hypertension,* 63(6), pp. 1293-301.

Naeye, R. L. (1990) 'Maternal body weight and pregnancy outcome', *The American Journal of Clinical Nutrition,* 52(2), pp. 273-9.

Nagahara, N., Ito, T., Kitamura, H. and Nishino, T. (1998) 'Tissue and subcellular distribution of mercaptopyruvate sulfurtransferase in the rat: confocal laser fluorescence and immunoelectron microscopic studies combined with biochemical analysis', *Histochemistry & Cell Biology,* 110(3), pp. 243-50.

Nagahara, N. and Katayama, A. (2005) 'Post-translational Regulation of Mercaptopyruvate Sulfurtransferase via a Low Redox Potential Cysteine-sulfenate in the Maintenance of Redox Homeostasis', *Journal of Biological Chemistry,* 280(41), pp. 34569-34576.

Nagahara, N. and Nishino, T. (1996) 'Role of amino acid residues in the active site of rat liver mercaptopyruvate sulfurtransferase. CDNA cloning, overexpression, and site-directed mutagenesis', *The Journal of Biological Chemistry,* 271(44), pp. 27395-401.

Nakamura, M., Sekizawa, A., Purwosunu, Y., Okazaki, S., Farina, A., Wibowo, N., Shimizu, H. and Okai, T. (2009) 'Cellular mRNA expressions of anti-oxidant factors in the blood of preeclamptic women', *Prenatal Diagnosis,* 29(7), pp. 691-6.

Nandi, S. S. and Mishra, P. K. (2017) 'H(2)S and homocysteine control a novel feedback regulation of cystathionine beta synthase and cystathionine gamma lyase in cardiomyocytes', *Scientific Reports,* 7(1), pp. 3639.

National Institute, f. H. a., Clinical Excellence (2006) *Obesity : guidance on the prevention, identification, assessment and management of overweight and obesity in adults and children.* London: National Institute for Health and Clinical Excellence.

Newby, D., Cousins, F., Myatt, L. and Lyall, F. (2005) 'Heme oxygenase expression in cultured human trophoblast cells during in vitro differentiation: effects of hypoxia', *Placenta,* 26(2), pp. 201-209.

Ngoc, N. T., Merialdi, M., Abdel-Aleem, H., Carroli, G., Purwar, M., Zavaleta, N., Campódonico, L., Ali, M. M., Hofmeyr, G. J., Mathai, M., Lincetto, O. and Villar, J. (2006) 'Causes of stillbirths and early neonatal deaths: data from 7993 pregnancies in six developing countries', *Bulletin of the World Health Organisation,* 84(9), pp. 699-705.

Niu, W. N., Yadav, P. K., Adamec, J. and Banerjee, R. (2015) 'S-glutathionylation enhances human cystathionine β-synthase activity under oxidative stress conditions', *Antioxidants & Redox Signaling,* 22(5), pp. 350-61.

Norwitz, E. R., Robinson, J. N. and Challis, J. R. (1999) 'The control of labor', *The New England Journal of Medicine,* 341(9), pp. 660-6.

O'Brien, T. E., Ray, J. G. and Chan, W. S. (2003) 'Maternal body mass index and the risk of preeclampsia: a systematic overview', *Epidemiology,* 14(3), pp. 368-74.

Olsen, J. V., Blagoev, B., Gnad, F., Macek, B., Kumar, C., Mortensen, P. and Mann, M. (2006) 'Global, in vivo, and site-specific phosphorylation dynamics in signaling networks', *Cell,* 127(3), pp. 635-48.

Osmers, R. G., Adelmann-Grill, B. C., Rath, W., Stuhlsatz, H. W., Tschesche, H. and Kuhn, W. (1995) 'Biochemical events in cervical ripening dilatation during pregnancy and parturition', *Journal of obstetrics and gynaecology (Tokyo 1995),* 21(2), pp. 185-94.

Ounsted, M., Moar, V. A. and Scott, A. (1985) 'Risk factors associated with small-for-dates and large-for-dates infants', *British Journal of Obstetrics and Gynaecology,* 92(3), pp. 226-32.

Papapetropoulos, A., Pyriochou, A., Altaany, Z., Yang, G., Marazioti, A., Zhou, Z., Jeschke, M. G., Branski, L. K., Herndon, D. N., Wang, R. and Szabo, C. (2009) 'Hydrogen sulfide is an endogenous stimulator of angiogenesis', *Proceedings of the National Academy of Sciences of the United States of America,* 106(51), pp. 21972-7.

Patel, P., Vatish, M., Heptinstall, J., Wang, R. and Carson, R. J. (2009) 'The endogenous production of hydrogen sulphide in intrauterine tissues', *Reproductive Biology and Endocrinology : RB&E,* 7, pp. 10-10.

Peng, H. H., Kao, C. C., Chang, S. D., Chao, A. S., Chang, Y. L., Wang, C. N., Cheng, P. J., Lee, Y. S., Wang, T. H. and Wang, H. S. (2011) 'The effects of labor on differential gene expression in parturient women, placentas, and fetuses at term pregnancy', *The Kaohsiung journal of medical sciences,* 27(11), pp. 494-502.

Pérez-Pérez, R., López, J. A., García-Santos, E., Camafeita, E., Gómez-Serrano, M., Ortega-Delgado, F. J., Ricart, W., Fernández-Real, J. M. and Peral, B. (2012) 'Uncovering suitable reference proteins for expression studies in human adipose tissue with relevance to obesity', *PLoS One,* 7(1), pp. e30326.

Pierro, A. and Eaton, S. (2004) 'Intestinal ischemia reperfusion injury and multisystem organ failure', *Seminars in Pediatric Surgery,* 13(1), pp. 11-7.

Pijnenborg, R. (1994) 'Trophoblast invasion', *Reproductive Medicine Review,* 3(1), pp. 53-73.

Pijnenborg, R., Dixon, G., Robertson, W. and Brosens, I. (1980) 'Trophoblastic invasion of human decidua from 8 to 18 weeks of pregnancy', *Placenta,* 1(1), pp. 3-19.

Pillai-Kastoori, L., Heaton, S., Shiflett, S. D., Roberts, A. C., Solache, A. and Schutz-Geschwender, A. R. (2020) 'Antibody validation for Western blot: By the user, for the user', *The Journal of biological chemistry,* 295(4), pp. 926-939.

Powe, C. E., Levine, R. J. and Karumanchi, S. A. (2011) 'Preeclampsia, a disease of the maternal endothelium: the role of antiangiogenic factors and implications for later cardiovascular disease', *Circulation,* 123(24), pp. 2856-69.

Predmore, B. L., Kondo, K., Bhushan, S., Zlatopolsky, M. A., King, A. L., Aragon, J. P., Grinsfelder, D. B., Condit, M. E. and Lefer, D. J. (2012) 'The polysulfide diallyl trisulfide protects the ischemic myocardium by preservation of endogenous hydrogen sulfide and increasing nitric oxide bioavailability', *American journal of physiology. Heart and circulatory physiology,* 302(11), pp. H2410-8.

Prudova, A., Bauman, Z., Braun, A., Vitvitsky, V., Lu, S. C. and Banerjee, R. (2006) 'S-adenosylmethionine stabilizes cystathionine beta-synthase and modulates redox capacity', *Proceedings of the National Academy of Sciences of the United States of America,* 103(17), pp. 6489-6494.

Qiao, P., Zhao, F., Liu, M., Gao, D., Zhang, H. and Yan, Y. (2017) 'Hydrogen sulfide inhibits mitochondrial fission in neuroblastoma N2a cells through the Drp1/ERK1/2 signaling pathway', *Molecular Medicine Reports,* 16(1), pp. 971-977.

Ramasamy, S., Singh, S., Taniere, P., Langman, M. J. and Eggo, M. C. (2006) 'Sulfide-detoxifying enzymes in the human colon are decreased in cancer and upregulated in differentiation', *American Journal of Physiology. Gastrointestinal & Liver Physiology,* 291(2), pp. G288-96.

Ramlau, J. (1987) 'Use of secondary antibodies for visualization of bound primary reagents in blotting procedures', *ELECTROPHORESIS,* 8.

Rampersad, R., Cervar-Zivkovic, M. and Nelson, D. M. (2011) 'Development and Anatomy of the Human Placenta', *The Placenta: From Development to Disease.*: Wiley-Blackwell, pp. 17-26.

Rasmussen, S., Irgens, L. M. and Dalaker, K. (1999) 'A history of placental dysfunction and risk of placental abruption', *Paediatric and perinatal epidemiology,* 13(1), pp. 9-21.

Redman, C. W. (1991) 'Immunology of preeclampsia', *Seminars in Perinatology,* 15(3), pp. 257-62.

Redman, C. W. (2011) 'Preeclampsia: a multi-stress disorder', *La Revue de medecine interne,* 32 Suppl 1, pp. S41-4.

Renga, B., Mencarelli, A., Migliorati, M., Distrutti, E. and Fiorucci, S. (2009) 'Bile-acid-activated farnesoid X receptor regulates hydrogen sulfide production and hepatic microcirculation', *World Journal of Gastroenterology,* 15(17), pp. 2097-108.

Roberts, D. J. and Post, M. D. (2008) 'The placenta in pre-eclampsia and intrauterine growth restriction', *Journal of clinical pathology.,* 61(12), pp. 1254-60.

Roberts, J. M. and Hubel, C. A. (2009) 'The two stage model of preeclampsia: variations on the theme', *Placenta,* 30 Suppl A, pp. S32-7.

Rodesch, F., Simon, P., Donner, C. and Jauniaux, E. (1992) 'Oxygen measurements in endometrial and trophoblastic tissues during early pregnancy', *Obstetrics & Gynecology,* 80(2), pp. 283-5.

Roper, M. D. and Kraus, J. P. (1992) 'Rat cystathionine β-synthase: Expression of four alternatively spliced isoforms in transfected cultured cells', *Archives of Biochemistry and Biophysics,* 298(2), pp. 514-521.

Rossoni, G., Manfredi, B., Tazzari, V., Sparatore, A., Trivulzio, S., Del Soldato, P. and Berti, F. (2010) 'Activity of a new hydrogen sulfide-releasing aspirin (ACS14) on pathological cardiovascular alterations induced by glutathione depletion in rats', *European Journal of Pharmacology,* 648(1-3), pp. 139-45.

Saben, J., Lindsey, F., Zhong, Y., Thakali, K., Badger, T. M., Andres, A., Gomez-Acevedo, H. and Shankar, K. (2014) 'Maternal obesity is associated with a lipotoxic placental environment', *Placenta,* 35(3), pp. 171-7.

Sander, H., Wallace, S., Plouse, R., Tiwari, S. and Gomes, A. V. (2019) 'Ponceau S waste: Ponceau S staining for total protein normalization', *Analytical Biochemistry,* 575, pp. 44-53.

Sandrim, V. C., Palei, A. C., Metzger, I. F., Gomes, V. A., Cavalli, R. C. and Tanus-Santos, J. E. (2008) 'Nitric oxide formation is inversely related to serum levels of antiangiogenic factors soluble fms-like tyrosine kinase-1 and soluble endogline in preeclampsia', *Hypertension,* 52(2), pp. 402-7.

Sankaran, S. and Kyle, P. M. (2009) 'Aetiology and Pathogenesis of IUGR', *Best Practice & Research Clinical Obstetrics & Gynaecology,* 23(6), pp. 765-777.

Sassoon, D. A., Castro, L. C., Davis, J. L. and Hobel, C. J. (1990) 'Perinatal outcome in triplet versus twin gestations', *Obstetrics and Gynecology,* 75(5), pp. 817-20.

Sattar, N. and Freeman, D. J. (2012) 'Potential mechanisms contributing to gestational diabetes and pre-eclampsia in the obese woman', in Poston, L. & Gillman, M.W. (eds.) *Maternal Obesity*. Cambridge: Cambridge University Press, pp. 45-55.

Schile, A. J., García-Fernández, M. and Steller, H. (2008) 'Regulation of apoptosis by XIAP ubiquitin-ligase activity', *Genes & Development,* 22(16), pp. 2256-66.

Schuhmann, R. A. (1982) 'Placentone structure of the human placenta', *Bibliotheca Anatomica,* (22), pp. 46-57.

Scifres, C. M. and Nelson, D. M. (2009) 'Intrauterine growth restriction, human placental development and trophoblast cell death', *The Journal of physiology,* 587(Pt 14), pp. 3453-8.

Sebire, N. J., Jolly, M., Harris, J. P., Wadsworth, J., Joffe, M., Beard, R. W., Regan, L. and Robinson, S. (2001) 'Maternal obesity and pregnancy outcome: a study of 287,213 pregnancies in London', *International Journal of Obesity and Related Metabolic Disorders,* 25(8), pp. 1175-82.

Sen, N., Paul, B. D., Gadalla, M. M., Mustafa, A. K., Sen, T., Xu, R., Kim, S. and Snyder, S. H. (2012) 'Hydrogen sulfide-linked sulfhydration of NF-κB mediates its antiapoptotic actions', *Molecular Cell,* 45(1), pp. 13-24.

Serkova, N., Bendrick-Peart, J., Alexander, B. and Tissot van Patot, M. C. (2003) 'Metabolite Concentrations in Human Term Placentae and Their Changes Due to Delayed Collection After Delivery', *Placenta,* 24(2), pp. 227-235.

Shen, Y. and Zhu, Y. Z. (2012) 'P56 MiRNA-30 regulates the production of endogenous H2S by Cystathionine gamma-lyase (CSE) in primary cardiac myocytes', *Nitric Oxide,* 27, pp. S37.

Shibuya, N., Mikami, Y., Kimura, Y., Nagahara, N. and Kimura, H. (2009a) 'Vascular endothelium expresses 3-mercaptopyruvate sulfurtransferase and produces hydrogen sulfide', *Journal of Biochemistry,* 146(5), pp. 623-6.

Shibuya, N., Tanaka, M., Yoshida, M., Ogasawara, Y., Togawa, T., Ishii, K. and Kimura, H. (2009b) '3-Mercaptopyruvate sulfurtransferase produces hydrogen sulfide and bound sulfane sulfur in the brain', *Antioxidants & Redox Signaling,* 11(4), pp. 703-14.

Shimomura, I., Funahashi, T., Takahashi, M., Maeda, K., Kotani, K., Nakamura, T., Yamashita, S., Miura, M., Fukuda, Y., Takemura, K., Tokunaga, K. and Matsuzawa, Y. (1996) 'Enhanced expression of PAI-1 in visceral fat: possible contributor to vascular disease in obesity', *Nature Medicine,* 2(7), pp. 800-3.

Sibai, B. M., Hauth, J., Caritis, S., Lindheimer, M. D., MacPherson, C., Klebanoff, M., VanDorsten, J. P., Landon, M., Miodovnik, M., Paul, R., Meis, P., Thurnau, G., Dombrowski, M., Roberts, J. and McNellis, D. (2000) 'Hypertensive disorders in twin versus singleton gestations. National Institute of Child Health and Human Development Network of Maternal-Fetal Medicine Units', *American journal of obstetrics and gynecology,* 182(4), pp. 938-42.

Sibai, B. M., Mercer, B. and Sarinoglu, C. (1991) 'Severe preeclampsia in the second trimester: recurrence risk and long-term prognosis', *Amirecan Journal of Obstetrics & Gynecology,* 165(5 Pt 1), pp. 1408-12.

Sladek, S. M., Regenstein, A. C., Lykins, D. and Roberts, J. M. (1993) 'Nitric oxide synthase activity in pregnant rabbit uterus decreases on the last day of pregnancy', *American journal of obstetrics and gynecology,* 169(5), pp. 1285-91.

Smith , R. (2007) 'Parturition', *New England Journal of Medicine,* 356(3), pp. 271-283.

Snijders, R. J., Sherrod, C., Gosden, C. M. and Nicolaides, K. H. (1993) 'Fetal growth retardation: associated malformations and chromosomal abnormalities', *American Journal of Obstetrics and Gynecology,* 168(2), pp. 547-55.

Solanky, N., Requena Jimenez, A., D'Souza, S. W., Sibley, C. P. and Glazier, J. D. (2010) 'Expression of folate transporters in human placenta and implications for homocysteine metabolism', *Placenta* 31(2), pp. 134-143.

Spranger, J., Kroke, A., Möhlig, M., Hoffmann, K., Bergmann, M. M., Ristow, M., Boeing, H. and Pfeiffer, A. F. (2003) 'Inflammatory cytokines and the risk to develop type 2 diabetes: results of the prospective population-based European Prospective Investigation into Cancer and Nutrition (EPIC)-Potsdam Study', *Diabetes,* 52(3), pp. 812-7.

Srilatha, B., Hu, L., Adaikan, G. P. and Moore, P. K. (2009) 'ORIGINAL RESEARCH-BASIC SCIENCE: Initial Characterization of Hydrogen Sulfide Effects in Female Sexual Function', *The Journal of Sexual Medicine,* 6(7), pp. 1875-1884.

Stadtman, E. R. and Berlett, B. S. (1991) 'Fenton chemistry. Amino acid oxidation', *Journal of Biological Chemistry,* 266(26), pp. 17201-11.

Stelzer, G., Rosen, N., Plaschkes, I., Zimmerman, S., Twik, M., Fishilevich, S., Stein, T. I., Nudel, R., Lieder, I., Mazor, Y., Kaplan, S., Dahary, D., Warshawsky, D., Guan-Golan, Y., Kohn, A., Rappaport, N., Safran, M. and Lancet, D. (2016) 'The GeneCards Suite: From Gene Data Mining to Disease Genome Sequence Analyses', *Current Protocols in Bioinformatics,* 54(1), pp. 1.30.1-1.30.33.

Sugiura, Y., Kashiba, M., Maruyama, K., Hoshikawa, K., Sasaki, R., Saito, K., Kimura, H., Goda, N. and Suematsu, M. (2005) 'Cadmium exposure alters metabolomics of sulfur-containing amino acids in rat testes', *Antioxidants & redox signaling,* 7(5-6), pp. 781-787.

Sun, Q., Collins, R., Huang, S., Holmberg-Schiavone, L., Anand, G. S., Tan, C. H., van-den-Berg, S., Deng, L. W., Moore, P. K., Karlberg, T. and Sivaraman, J. (2009) 'Structural basis for the inhibition mechanism of human cystathionine gamma-lyase, an enzyme responsible for the production of H(2)S', *Journal of Biological Chemistry,* 284(5), pp. 3076-85.

Szabo, C., Coletta, C., Chao, C., Módis, K., Szczesny, B., Papapetropoulos, A. and Hellmich, M. R. (2013) 'Tumor-derived hydrogen sulfide, produced by cystathionine-β-synthase, stimulates bioenergetics, cell proliferation, and angiogenesis in colon cancer', *Proceedings of the National Academy of Sciences of the U S A,* 110(30), pp. 12474-9.

Takizawa, T., Yoshikawa, H., Yamada, M. and Morita, H. (2002) 'Expression of nitric oxide synthase isoforms and detection of nitric oxide in rat placenta', *American Journal of Physiology-Cell Physiology,* 282(4), pp. C762-C767.

Tang, G., Wu, L., Liang, W. and Wang, R. (2005) 'Direct stimulation of K(ATP) channels by exogenous and endogenous hydrogen sulfide in vascular smooth muscle cells', *Molecular Pharmacology,* 68(6), pp. 1757-64.

Tanizawa, K. (2011) 'Production of H2S by 3-mercaptopyruvate sulphurtransferase', *Journal of Biochemistry,* 149(4), pp. 357-9.

Tannetta, D. and Sargent, I. (2013) 'Placental disease and the maternal syndrome of preeclampsia: missing links?', *Current hypertension reports,* 15(6), pp. 590-9.

Taoka, S., Widjaja, L. and Banerjee, R. (1999) 'Assignment of enzymatic functions to specific regions of the PLP-dependent heme protein cystathionine beta-synthase', *Biochemistry,* 38(40), pp. 13155-61.

Teng, H., Wu, B., Zhao, K., Yang, G., Wu, L. and Wang, R. (2013) 'Oxygen-sensitive mitochondrial accumulation of cystathionine β-synthase mediated by Lon protease', *Proceedings of the National Academy of Sciences of the U S A,* 110(31), pp. 12679-84.

Topp, M., Langhoff-Roos, J., Uldall, P. and Kristensen, J. (1996) 'Intrauterine growth and gestational age in preterm infants with cerebral palsy', *Early Human Development,* 44(1), pp. 27-36.

Tranquilli, A. L., Dekker, G., Magee, L., Roberts, J., Sibai, B. M., Steyn, W., Zeeman, G. G. and Brown, M. A. (2014) 'The classification, diagnosis and management of the hypertensive disorders of pregnancy: A revised statement from the ISSHP', *Pregnancy Hypertension,* 4(2), pp. 97-104.

Tripathy, D., Mohanty, P., Dhindsa, S., Syed, T., Ghanim, H., Aljada, A. and Dandona, P. (2003) 'Elevation of free fatty acids induces inflammation and impairs vascular reactivity in healthy subjects', *Diabetes,* 52(12), pp. 2882-7.

Tsuchida, T., Zou, J., Saitoh, T., Kumar, H., Abe, T., Matsuura, Y., Kawai, T. and Akira, S. (2010) 'The ubiquitin ligase TRIM56 regulates innate immune responses to intracellular double-stranded DNA', *Immunity,* 33(5), pp. 765-76.

van Walraven, C., Mamdani, M., Cohn, A., Katib, Y., Walker, M. and Rodger, M. A. (2003) 'Risk of subsequent thromboembolism for patients with pre-eclampsia', *Bmj,* 326(7393), pp. 791-2.

Vandanmagsar, B., Youm, Y. H., Ravussin, A., Galgani, J. E., Stadler, K., Mynatt, R. L., Ravussin, E., Stephens, J. M. and Dixit, V. D. (2011) 'The NLRP3 inflammasome instigates obesity-induced inflammation and insulin resistance', *Nature Medicine,* 17(2), pp. 179-88.

Vandenberg, C. J., Gergely, F., Ong, C. Y., Pace, P., Mallery, D. L., Hiom, K. and Patel, K. J. (2003) 'BRCA1-independent ubiquitination of FANCD2', *Molecular Cell,* 12(1), pp. 247-54.

Vega, G. L. and Grundy, S. M. (2013) 'Metabolic risk susceptibility in men is partially related to adiponectin/leptin ratio', *Journal of Obesity,* 2013, pp. 409679.

Vince, G. S., Starkey, P. M., Austgulen, R., Kwiatkowski, D. and Redman, C. W. (1995) 'Interleukin-6, tumour necrosis factor and soluble tumour necrosis factor receptors in women with pre-eclampsia', *British journal of obstetrics and gynaecology,* 102(1), pp. 20-5.

Vitvitsky, V., Miljkovic, J. L., Bostelaar, T., Adhikari, B., Yadav, P. K., Steiger, A. K., Torregrossa, R., Pluth, M. D., Whiteman, M., Banerjee, R. and Filipovic, M. R. (2018) 'Cytochrome c Reduction by H_2S Potentiates Sulfide Signaling', *ACS chemical biology,* 13(8), pp. 2300-2307.

Waller, D. K., Mills, J. L., Simpson, J. L., Cunningham, G. C., Conley, M. R., Lassman, M. R. and Rhoads, G. G. (1994) 'Are obese women at higher risk for producing malformed offspring?', *American Journal of Obstetrics and Gynecology,* 170(2), pp. 541-8.

Wallstrom, P., Wirfalt, E., Lahmann, P. H., Gullberg, B., Janzon, L. and Berglund, G. (2001) 'Serum concentrations of beta-carotene and alpha-tocopherol are associated with diet, smoking, and general and central adiposity', *The American journal of clinical nutrition,* 73(4), pp. 777-85.

Wang, A., Rana, S. and Karumanchi, S. A. (2009a) 'Preeclampsia: the role of angiogenic factors in its pathogenesis', *Physiology* 24, pp. 147-158.

Wang, C., Du, J., Du, S., Liu, Y., Li, D., Zhu, X. and Ni, X. (2018) 'Endogenous H2S resists mitochondria-mediated apoptosis in the adrenal glands via ATP5A1 S-sulfhydration in male mice', *Molecular and Cellular Endocrinology,* 474, pp. 65-73.

Wang, K., Ahmad, S., Cai, M., Rennie, J., Fujisawa, T., Crispi, F., Baily, J., Miller, M. R., Cudmore, M., Hadoke, P. W., Wang, R., Gratacos, E., Buhimschi, I. A., Buhimschi, C. S. and Ahmed, A. (2013) 'Dysregulation of hydrogen sulfide producing enzyme cystathionine gamma-lyase contributes to maternal hypertension and placental abnormalities in preeclampsia', *Circulation,* 127(25), pp. 2514-22.

Wang, M., Guo, Z. and Wang, S. (2012) 'Cystathionine gamma-lyase expression is regulated by exogenous hydrogen peroxide in the mammalian cells', *Gene Expression,* 15(5-6), pp. 235-41.

Wang, Q., Liu, H. R., Mu, Q., Rose, P. and Zhu, Y. Z. (2009b) 'S-propargyl-cysteine protects both adult rat hearts and neonatal cardiomyocytes from ischemia/hypoxia injury: the contribution of the hydrogen sulfide-mediated pathway', *Journal of Cardiovascular Pharmacology,* 54(2), pp. 139-46.

Wang, R. (2002) 'Two's company, three's a crowd: can H2S be the third endogenous gaseous transmitter?', *FASEB journal : official publication of the Federation of American Societies for Experimental Biology,* 16(13), pp. 1792-1798.

Wang, Y., Beydoun, M. A., Liang, L., Caballero, B. and Kumanyika, S. K. (2008) 'Will all Americans become overweight or obese? estimating the progression and cost of the US obesity epidemic', *Obesity (Silver Spring),* 16(10), pp. 2323-30.

Wang, Y. and Zhao, S. (2010) ' Placental Blood Circulation', *Vascular biology of the placenta*. [San Rafael, Calif.]: Morgan & Claypool Life Sciences

Wang, Y., Zhao, X., Jin, H., Wei, H., Li, W., Bu, D., Tang, X., Ren, Y., Tang, C. and Du, J. (2009c) 'Role of hydrogen sulfide in the development of atherosclerotic lesions in

apolipoprotein E knockout mice', *Arteriosclerosis, Thrombosis,and Vascular Biology,* 29(2), pp. 173-9.

Warkany, J., Monroe, B. B. and Sutherland, B. S. (1961) 'Intrauterine growth retardation', *American journal of diseases of children,* 102(2), pp. 249-279.

Whiteman, M., Gooding, K. M., Whatmore, J. L., Ball, C. I., Mawson, D., Skinner, K., Tooke, J. E. and Shore, A. C. (2010) 'Adiposity is a major determinant of plasma levels of the novel vasodilator hydrogen sulphide', *Diabetologia,* 53(8), pp. 1722-1726.

Whiteman, M., Le Trionnaire, S., Chopra, M., Fox, B. and Whatmore, J. (2011) 'Emerging role of hydrogen sulfide in health and disease: critical appraisal of biomarkers and pharmacological tools', *Clinical Science,* 121(11), pp. 459-488.

WHO (2000) *Obesity : preventing and managing the global epidemic : report of a WHO consultation ; [Consultation on Obesity, 1997 Geneva, Switzerland].* Geneva: World Health Organization.

Wilson, M. J., Lopez, M., Vargas, M., Julian, C., Tellez, W., Rodriguez, A., Bigham, A., Armaza, J. F., Niermeyer, S., Shriver, M., Vargas, E. and Moore, L. G. (2007) 'Greater uterine artery blood flow during pregnancy in multigenerational (Andean) than shorter-term (European) high-altitude residents', *American Journal of Physiology, Regulatory, Integrative and Comparative Physiology,* 293(3), pp. R1313-24.

Wolf, M., Kettyle, E., Sandler, L., Ecker, J. L., Roberts, J. and Thadhani, R. (2001) 'Obesity and preeclampsia: the potential role of inflammation', *Obstetrics and gynecology,* 98(5), pp. 757-62.

Wu, G., Nie, L. and Zhang, W. (2008) 'Integrative analyses of posttranscriptional regulation in the yeast Saccharomyces cerevisiae using transcriptomic and proteomic data', *Current Microbiology,* 57(1), pp. 18-22.

Wu, N., Siow, Y. L. and O, K. (2010) 'Ischemia/reperfusion reduces transcription factor Sp1-mediated cystathionine beta-synthase expression in the kidney', *Journal of Biological Chemistry,* 285(24), pp. 18225-33.

Wyatt, S. M., Kraus, F. T., Roh, C. R., Elchalal, U., Nelson, D. M. and Sadovsky, Y. (2005) 'The correlation between sampling site and gene expression in the term human placenta', *Placenta,* 26(5), pp. 372-9.

Yadav, P. K., Yamada, K., Chiku, T., Koutmos, M. and Banerjee, R. (2013) 'Structure and kinetic analysis of H2S production by human mercaptopyruvate sulfurtransferase', *Journal of Biological Chemistry,* 288(27), pp. 20002-13.

Yallampalli, C., Izumi, H., Byam-Smith, M. and Garfield, R. E. (1994) 'An L-arginine-nitric oxide-cyclic guanosine monophosphate system exists in the uterus and inhibits contractility during pregnancy', *American journal of obstetrics and gynecology,* 170(1 Pt 1), pp. 175-85.

Yang, G., Pei, Y., Cao, Q. and Wang, R. (2012) 'MicroRNA-21 represses human cystathionine gamma-lyase expression by targeting at specificity protein-1 in smooth muscle cells', *Journal of Cellular Physiology,* 227(9), pp. 3192-200.

Yang, G., Wu, L., Jiang, B., Yang, W., Qi, J., Cao, K., Meng, Q., Mustafa, A. K., Mu, W., Zhang, S., Snyder, S. H. and Wang, R. (2008) 'H2S as a physiologic vasorelaxant: hypertension in mice with deletion of cystathionine gamma-lyase', *Science (New York, N.Y.),* 322(5901), pp. 587-90.

Yang, J., Minkler, P., Grove, D., Wang, R., Willard, B., Dweik, R. and Hine, C. (2019) 'Non-enzymatic hydrogen sulfide production from cysteine in blood is catalyzed by iron and vitamin B(6)', *Communications biology,* 2, pp. 194-194.

Yin, P., Zhao, C., Li, Z., Mei, C., Yao, W., Liu, Y., Li, N., Qi, J., Wang, L., Shi, Y., Qiu, S., Fan, J. and Zha, X. (2012) 'Sp1 is involved in regulation of cystathionine γ-lyase gene expression and biological function by PI3K/Akt pathway in human hepatocellular carcinoma cell lines', *Cellular Signalling,* 24(6), pp. 1229-40.

Yinon, Y., Mazkereth, R., Rosentzweig, N., Jarus-Hakak, A., Schiff, E. and Simchen, M. J. (2005) 'Growth restriction as a determinant of outcome in preterm discordant twins', *Obstetrics and Gynecology,* 105(1), pp. 80-4.

You, X.-J., Xu, C., Lu, J.-Q., Zhu, X.-Y., Gao, L., Cui, X.-R., Li, Y., Gu, H. and Ni, X. (2011) 'Expression of Cystathionine β-synthase and Cystathionine γ-lyase in Human Pregnant Myometrium and Their Roles in the Control of Uterine Contractility', *PLOS ONE,* 6(8), pp. e23788.

You, X., Chen, Z., Zhao, H., Xu, C., Liu, W., Sun, Q., He, P., Gu, H. and Ni, X. (2017) 'Endogenous hydrogen sulfide contributes to uterine quiescence during pregnancy', *Reproduction,* 153(5), pp. 535-543.

Yung, H. W., Calabrese, S., Hynx, D., Hemmings, B. A., Cetin, I., Charnock-Jones, D. S. and Burton, G. J. (2008) 'Evidence of placental translation inhibition and endoplasmic reticulum stress in the etiology of human intrauterine growth restriction', *The American journal of pathology,* 173(2), pp. 451-62.

Yung, H. W., Colleoni, F., Atkinson, D., Cook, E., Murray, A. J., Burton, G. J. and Charnock-Jones, D. S. (2014) 'Influence of speed of sample processing on placental energetics and signalling pathways: implications for tissue collection', *Placenta,* 35(2), pp. 103-8.

Yusuf, M., Kwong Huat, B. T., Hsu, A., Whiteman, M., Bhatia, M. and Moore, P. K. (2005) 'Streptozotocin-induced diabetes in the rat is associated with enhanced tissue hydrogen sulfide biosynthesis', *Biochemical and Biophysical Research Communications,* 333(4), pp. 1146-52.

Zanardo, R. C., Brancaleone, V., Distrutti, E., Fiorucci, S., Cirino, G. and Wallace, J. L. (2006) 'Hydrogen sulfide is an endogenous modulator of leukocyte-mediated inflammation', *FASEB journal : official publication of the Federation of American Societies for Experimental Biology,* 20(12), pp. 2118-20.

Zeng, Y., Yi, R. and Cullen, B. R. (2003) 'MicroRNAs and small interfering RNAs can inhibit mRNA expression by similar mechanisms', *Proceedings of the National Academy of Sciences of the U S A,* 100(17), pp. 9779-84.

Zhang, G.-Y., Lu, D., Duan, S.-F., Gao, Y.-R., Liu, S.-Y., Hong, Y., Dong, P.-Z., Chen, Y.-G., Li, T., Wang, D.-Y., Cheng, X.-S., He, F., Wei, J.-S., Li, G.-Y., Zhang, Q.-Y., Wu, D.-D. and Ji, X.-Y. (2018) 'Hydrogen Sulfide Alleviates Lipopolysaccharide-Induced Diaphragm Dysfunction in Rats by Reducing Apoptosis and Inflammation through ROS/MAPK and TLR4/NF-κB Signaling Pathways', *Oxidative medicine and cellular longevity,* 2018, pp. 9647809-9647809.

Zhang, H., Guo, C., Zhang, A., Fan, Y., Gu, T., Wu, D., Sparatore, A. and Wang, C. (2012) 'Effect of S-aspirin, a novel hydrogen-sulfide-releasing aspirin (ACS14), on atherosclerosis in apoE-deficient mice', *European Journal of Pharmacology,* 697(1), pp. 106-116.

Zhang, L., Yang, G., Tang, G., Wu, L. and Wang, R. (2011) 'Rat pancreatic level of cystathionine γ-lyase is regulated by glucose level via specificity protein 1 (SP1) phosphorylation', *Diabetologia,* 54(10), pp. 2615-25.

Zhang, X., Zuo, X., Yang, B., Li, Z., Xue, Y., Zhou, Y., Huang, J., Zhao, X., Zhou, J., Yan, Y., Zhang, H., Guo, P., Sun, H., Guo, L., Zhang, Y. and Fu, X. D. (2014) 'MicroRNA directly enhances mitochondrial translation during muscle differentiation', *Cell,* 158(3), pp. 607-19.

Zhao, P., Huang, X., Wang, Z.-y., Qiu, Z.-x., Han, Y.-f., Lu, H.-l., Kim, Y.-c. and Xu, W.-x. (2009) 'Dual effect of exogenous hydrogen sulfide on the spontaneous contraction of gastric smooth muscle in guinea-pig', *European Journal of Pharmacology,* 616(1), pp. 223-228.

Zhao, W., Ndisang, J. F. and Wang, R. (2003) 'Modulation of endogenous production of H2S in rat tissues', *Canadian Journal of Physiology and Pharmacology,* 81(9), pp. 848-53.

Zhao, W., Zhang, J., Lu, Y. and Wang, R. (2001) 'The vasorelaxant effect of H(2)S as a novel endogenous gaseous K(ATP) channel opener', *The EMBO journal,* 20(21), pp. 6008-16.

Zhong, Z., Sassi, M., Heaton, S., Koch, S., De Block, G., Conlon, D., Lochead, J., Dreja, H., Munro, M., Solache, A. and Hamilton, B. (2018) 'Large-scale use of knockout validation to confirm antibody specificity', *The Journal of Immunology,* 200(1 Supplement), pp. 120.18.